The Use of Metal and Metal Oxide Nanoparticles Against Biofilms

Jyoti Tejpal

Thesis submitted to De Montfort University in partial fulfilment of the requirements for the degree of Doctor of Philosophy

De Montfort University

June 2016

Acknowledgements

I would like to express my sincere gratitude to my supervisors, Dr Katie Laird, Dr Richard Cross and Professor Richard Jenkins. Their guidance and encouragement has made this thesis possible.

A special thanks to all the microbiology team, Karen Stones, Abdul Razaaq and Richard Smith; for always being so supportive. Karen, a huge thank you to you for all your generous care and encouragement throughout this process. I would also like to show my appreciation to Rachel Armitage, David Armitage and Liz O'Brien for all their assistance with the SEM and CLSM, Unmesh Desai and Nazmin Juma for the use of the spectroscopy equipment and their expertise.

I am very grateful to my friends Kate Riley and Ruth Reid, whose invaluable friendship has made this journey enjoyable and smoother; I will thoroughly miss all our lunch time catch ups.

Thanks go to all my family for giving me motivation throughout. This PhD would have not been possible without the blessings of my Dad and Mum who have always stood by me throughout this entire journey; your encouragement, love and support has led me to where I am today. Bhavin, words cannot describe my appreciation for everything you have done for me. A huge thank you for believing in me and giving me unfailing love and support throughout this PhD; I couldn't have done this without you.

Abstract

Introduction:
The persistence of biofilms in hospital settings are associated with Healthcare Associated Infections (HCAI), causing increased morbidity, mortality and healthcare costs. The resistance of biofilms against commonly used hospital disinfectants has been well reported. Metal and metal oxide nanoparticles (NP) such as silver (Ag), copper (Cu), zinc oxide (ZnO) and copper oxide (CuO) exhibit antimicrobial properties against various pathogens.

Methods:
Biofilm formation of *Pseudomonas aeruginosa* and *Staphylococcus aureus* in a Centre for Disease Control (CDC) biofilm reactor and a 96 well plate was compared. A three stage approach including Minimum Biofilm Reduction Concentration (MBRC), R^2 values and $\log_{(10)}$ reductions was used to assess the efficacy of Ag and ZnO NPs both alone and in combination against *P. aeruginosa* and *S. aureus* biofilms. Atomic Absorption Spectroscopy (AAS), Scanning Electron Microscopy (SEM) and Confocal Laser Scanning Microscopy (CLSM) was used to further assess the antimicrobial ability of the metal and metal oxide NPs. The prevention of *P. aeruginosa* and *S. aureus* adherence on Ag and ZnO thin film coating on silicon (Si) surfaces was also investigated, as well as *icaC*, *ebpS* and *fnbB* gene expression in *S. aureus* biofilms.

Results:
The CDC biofilm reactor demonstrated to be the most effective method for *P. aeruginosa* and *S. aureus* biofilm production in comparison to 96 well plates, with lower standard errors of the mean (SE) and higher replicability. Individual MBRC of ZnO and Ag NPs in suspension were 256 and 50 µg/ml for *P. aeruginosa* and 16 and 50 µg/ml for *S. aureus* respectively. The concentrations in combination were reduced by at least a half, with concentrations of 32/25 µg/ml of ZnO/Ag NPs in suspension resulting in a significant ($p \leq 0.05$) reduction of 3.77 $\log_{(10)}$ against *P. aeruginosa* biofilms and 8/12 µg/ml of ZnO/Ag NPs in suspension resulted in a 3.91 $\log_{(10)}$ ($p \leq 0.05$) against *S. aureus* biofilms. Both combinations showed an additive effect. Time point analysis confirmed that a 24 hour treatment is vital for any significant ($p \leq 0.05$) antimicrobial activity. AAS data suggested that the Ag^+ ions quenched Zn^{2+} ions, therefore the antimicrobial efficacy of the combination is mainly due to Ag^+ ions. Damage of the biofilms from Ag and ZnO NPs was observed in the SEM imaging and energy dispersive X-ray (EDX) analysis confirmed the adherence of Zn and Ag within the biofilms. CLSM imaging showed dead (red) cells of *P. aeruginosa* and *S. aureus* biofilms throughout the depth of the biofilm. *P. aeruginosa* formation was reduced by 1.41 $\log_{(10)}$ and 1.43 $\log_{(10)}$ on Ag and ZnO thin film coatings respectively. For *S. aureus*, a reduction of 1.82 $\log_{(10)}$ and 1.65 $\log_{(10)}$ was obtained for Ag and ZnO coating respectively. Only low levels of ribonucleic acid (RNA) were achieved so no further gene analysis could occur.

Conclusion:
Reductions of ≥ 3 $\log_{(10)}$ were observed for *P. aeruginosa* and *S. aureus* biofilm treatment with ZnO/Ag NP suspensions. It can be concluded that the ZnO/Ag NP suspensions had greater antimicrobial activity than Ag and ZnO coated surfaces owing to large concentrations of Ag^+ and Zn^{2+} ions acting upon the biofilms. The slower release of ions from coated surfaces suggest an inadequate concentration of ions in the media, which are therefore unable to prevent biofilm formation as rapidly as NP suspensions, however provide a sustained release of ions over time. The results from this investigation propose that Ag and ZnO NPs in suspension could be a potential alternative to disinfectants for use in nosocomial environments against *P. aeruginosa* and *S. aureus* biofilms.

Contents

Notation

agr	Accessory Gene Regulator
A. baumannii	*Acinetobacter baumannii*
AHL	Acylated Homoserine Lactone
ATP	Adenosine Triphosphate
Al	Aluminium
ASTM	American Society for Testing and Materials
ARHAI	Antimicrobial Resistance and Healthcare Associated Infection
AAS	Atomic Absorption Spectroscopy
AI	Autoinducer
B. cereus	*Bacillus cereus*
B. subtilis	*Bacillus subtilis*
Bap	Biofilm associated proteins
BSA	Bovine Serum Albumin
B. cepacia	*Burkholderia cepacia*
CaO	Calcium Oxide
C. albicans	*Candida albicans*
CN	Carbonitrile
CDC	Centre for Disease Control
C. difficile	*Clostridium difficile*
cfu	Colony Forming Units
cDNA	Complementary Deoxyribonucleic Acid
CLSM	Confocal Laser Scanning Microscopy
Cu	Copper
CuO	Copper Oxide
$\mathbf{R^2}$	Correlation Coefficient
DNA	Deoxyribonucleic acid
ECFA	Eco-friendly Cleaning Agent
ebpS	Elastin Binding Protein gene
e-beam	Electron-beam
EDX	Energy Dispersive X-ray
ECAP	Equal Channel Angular Pressing
E. coli	*Escherichia coli*
eDNA	Extracellular Deoxyribonucleic Acid
EPS	Extracellular Polymeric Substances
FIC	Factorial Inhibition Concentration
fnbA	Fibronectin Binding Protein A gene
fnbB	Fibronectin Binding Protein B gene
FnbP	Fibronectin Binding Proteins
Au	Gold
HCAI	Healthcare Associated Infections
HICPAC	Healthcare Infection Control Practices Advisory Committee

H_2O_2	Hydrogen peroxide
HI	Hydrophobicity Index
ICP-MS	Inductively Coupled Plasma Mass Spectroscopy
ICU	Intensive Care Unit
icaC	Interceullular Adhesin C gene
Fe_2O_3	Iron Oxide
K. pneumoniae	*Klebsiella pneumoniae*
LPS	Lipopolysaccharide
LN_2	Liquid Nitrogen
L. monocytogenes	*Listeria monocytogenes*
$MgCl_2$	Magnesium Chloride
MgO	Magnesium Oxide
mRNA	Messenger Ribonucleic Acid
MRSA	Methicillin Resistant *Staphylococcus aureus*
MRSE	Methicillin Resistant *Staphylococcus epidermidis*
MSSA	Methicillin susceptible *S. aureus*
MSCRAMM	Microbial Surface Components Recognising Adhesive Matrix Molecules
MTP	Microtitre Plate
MBC	Minimum Bacterial Concentrations
MBRC	Minimum Biofilm Reduction Concentration
MIC	Minimum Inhibitory Concentration
NF	Nanofiltration
NP	Nanoparticles
NHS	National Health Service
NiO	Nickel Oxide
NA	Nutrient Agar
NB	Nutrient Broth
PBS	Phosphate Buffered Saline
PVP	Poly-(*N*-vinyl-pyrrolidone)
PC	Polycarbonate
PCR	Polymerase Chain Reaction
PNAG	Poly-N-acetyl-β-(1-6)-glucosamine
PIA	Polysaccharide Intercellular Adhesin
PTFE	Polytetrafluoroethylene
PVC	Polyvinyl Chloride
P. aeruginosa	*Pseudomonas aeruginosa*
P. protogens	*Pseudomonas protogens*
P. putida	Pseudomonas putida
qPCR	Quantitative Polymerase Chain Reaction
QAC	Quaternary Ammonium Compounds
QS	Quorum Sensing
QS	Quorum Sensing
RF	Radio Frequency

ROS	Reactive Oxygen Species
RO	Reverse-osmosis
RNA	Ribonucleic Acid
SEM	Scanning Electron Microscopy
Si	Silicon
SiO_2	Silicon Dioxide
Ag	Silver
$AgNO_3$	Silver Nitrate
Ag_2O	Silver Oxide
NaDCC	Sodium Dichloroisocyanurate
SDS	Sodium Dodecyl Sulphate
NaOH	Sodium Hydroxide
SACAR	Special Advisory Committee on Antimicrobial Resistance
SS	Stainless steel
SE	Standard Error of the Mean
S. aureus	*Staphylococcus aureus*
S. epidermidis	*Staphylococcus epidermidis*
Ti	Titanium
TiO_2	Titanium Dioxide
TSB	Tryptone Soya Broth
UV	Ultraviolet
VISA	Vancomycin intermediate *S. aureus*
VRE	Vancomycin Resistant *Enterococcus*
WHO	World Health Organisation
Zn	Zinc
ZnO	Zinc Oxide
ZOI	Zone of Inhibition

Chapter 1

Chapter 1: Introduction

The World Health Organisation (WHO) defines Healthcare Associated Infections (HCAIs) as infections that develop in patients after 48 hours of hospitalisation or when they reside at a healthcare facility. The infection, however, should not have been present or incubating when the patient was admitted. Infections occurring within four weeks after discharge are also considered as a HCAI (World Health Organization, 2002). HCAIs have become an increasing problem over the last decade leading to an increase in medical costs, patient stays in hospital, morbidity and mortality (Hensley & Monson, 2015). The increase in HCAI correlates with the improved capability of bacteria to withstand and adapt to harsh environments i.e. in the vicinity of antimicrobial agents in the form of a biofilm, making the environment a continuous reservoir for pathogens (Abreu *et al.*, 2013).

S. aureus and *P. aeruginosa* are included in the top five pathogens responsible for HCAIs, and are the cause of 15.6 and 7.5% of HCAIs respectively (Rutala & Weber, 2014). Both *S. aureus* and *P. aeruginosa* are commonly isolated nosocomial pathogens that have the ability to form biofilm related infections by colonising on central venous catheters (Pérez-Zárate *et al.*, 2015), lower respiratory tract infections from contaminated ventilators (Humphreys *et al.*, 2010), and urinary tract infections from catheters (Barbadoro *et al.*, 2015). The ubiquitous bacterium *P. aeruginosa* is present in the environment, requiring minimal conditions to survive and can adapt to a range of environmental stresses (Gaynes & Edwards, 2005). *P. aeruginosa* mainly resides in humid environments, and in a hospital setting, including areas such as taps and sinks (Blanc *et al.*, 2016). *S. aureus* colonises on the skin or nares of healthy individuals and is also a common cause of nosocomial infections and indwelling medical device related infections (Hensley & Monson, 2015). Methicillin resistant *S. aureus* (MRSA) still remains a major cause of HCAIs since it was reported fifty years ago, only after two years of methicillin usage (Jevons, 1961).

The residence of bacteria on hospital surfaces and transmission *via* the hands of healthcare workers can potentially cause HCAIs (Dancer *et al.*, 2009; Pittet *et al.*, 2006). Claro *et al.* (2015) found that the most contaminated surface within hospitals were the toilet door handles and bedside lockers with 7.97 colony forming units (cfu)/cm^2 and 7.34 cfu/cm^2 respectively. As stated by the Healthcare Infection Control Practices Advisory Committee (HICPAC) and the CDC, non-critical medical equipment should be disinfected routinely when it has visibly been soiled (Centre for Disease Control, 2008). Contaminated non-critical medical equipment including stethoscopes can be a cause of cross contamination as it can transfer organisms between patients and an examiner if not cleaned. *S. aureus*, *P. aeruginosa*, vancomycin resistant *Enterococcus* (VRE), and *Clostridium difficile* are among those bacterium that have been isolated from stethoscopes (O'Flaherty & Fenelon, 2015).

Biocide tolerance can be acquired when it is used at lower concentrations than stated by manufacturers, accidently diluted more than required, organic matter interferes with its activity, or when it is utilised at an incorrect pH and temperature (Condell *et al.*, 2012). Often one key factor overlooked in many disinfectant related studies is the ability of bacteria to construct a biofilm, shielding them from environmental stress, including antimicrobials.

The judicious use of antimicrobials is detrimental for managing bacterial resistance. Currently disinfectants used in hospitals contain active ingredients such as alcohols, sodium hypochlorite, hydrogen peroxide (H_2O_2) and quaternary ammonium compounds (QAC) (Rutala & Weber, 2016; Wessels & Ingmer, 2013). The susceptibility of *P. aeruginosa* and *Burkholderia cepacia* biofilms against chlorine dioxide was reduced in multispecies biofilms in comparison to monospecies biofilms (Behnke & Camper, 2012), similar to the findings by Behnke *et. al* (2011), whereby a multispecies biofilm of *P. aeruginosa* and *B. cepacia* had greater resistance to sodium hypochlorite in comparison to a monospecies biofilm. *S. aureus* biofilms had ten up to >100 times reduced susceptibility to chlorhexidine (Xing *et al.*, 2012) whereas *Staphylococcus epidermidis* treatment with chlorhexidine showed a 16 fold increase in minimum inhibitory concentration

(MIC) for biofilms in comparison to planktonic cells (Karpanen *et al.*, 2008). The antimicrobial activity of household bleach, a sodium dichloroisocyanurate (NaDCC) based disinfectant and eco-friendly cleaning agent (EFCA) was determined against four *S. aureus* strains. Bleach and NaDCC showed a > 5 $\log_{(10)}$ reduction in suspension, whereas only a <3 $\log_{(10)}$ reduction occurred on surfaces (Adukwu *et al.*, 2015). Kotb *et al.* (2015) showed that MRSA had no susceptibility to 3% H_2O_2. Furthermore, *P. aeruginosa* showed resistance to triclosan (de Abreu *et al.*, 2014), possibly due to multidrug efflux systems to eliminate the biocide (Chuanchuen *et al.*, 2003). All these studies suggest that alternatives for antimicrobials are required to overcome this resistance and prevent biofilm formation particularly in the healthcare sector.

In recent years, metal and metal oxide nanoparticles (NPs) have gained significant attention as antimicrobials, including silver (Ag) (Hanh *et al.*, 2016), copper (Cu) (Kruk *et al.*, 2015), copper oxide (CuO) (Ren *et al.*, 2009), zinc oxide (ZnO) (Abdulkareem *et al.*, 2015) and titanium dioxide (TiO_2) (Combarros *et al.*, 2016). NPs tend to have enhanced antimicrobial characteristics in comparison to the bulk material as they are smaller in size and have an increased surface area to volume ratio (Arakha *et al.*, 2015).

Research conducted on the efficacy of metal and metal oxide NPs against biofilms is limited. Ag NPs have shown to have antimicrobial activity against *Escherichia coli*, *P. aeruginosa* and *S. aureus* with a MIC of 14.38, 6.74 and 14.38 µg/ml respectively (Guzman *et al.*, 2012), similar MICs of 1 ppm were found by Song *et al.* (2006) and Sondi *et al.* (2004) at 10 ppm. A zone of inhibition (ZOI) of 22 ± 1.8 mm for *P. aeruginosa* was observed against 25 µg/ml of ZnO NPs (Jayaseelan *et al.*, 2012). An agar well diffusion method gave a ZOI of 19 and 16 mm for *S. aureus* and *E. coli* respectively after treatment with ZnO NPs (Ambika & Sundrarajan, 2015). The green synthesis of ZnO NPs using *Trifolium pratense* flower extract demonstrated that ZnO NPs gave a larger antimicrobial effect against *P. aeruginosa* in comparison to gentamicin with a ZOI of 20 and 13 mm at a concentration of 256 µg/ml (Dobrucka & Długaszewska, 2016). The antimicrobial effect of nanocrystalline CuO on woven and non-woven fabrics against *S. aureus*

and *E. coli* was established, with ZOI of 15 and 16 mm for *E. coli* and 21 and 20 mm for *S. aureus* for woven and non-woven fabrics respectively (Subramanian *et al.*, 2014).

With the high costs associated with HCAIs and the inadequacy of many commonly utilised disinfectants, against either resistant bacterial species or biofilms, further investigation into novel antimicrobials for use as disinfectants is required. A disinfectant should aim to be effective against bacteria that are a common cause of outbreaks and HCAIs (Rutala & Weber, 2016), whilst considering their efficacy against biofilms in the environment and potential future resistance. Although there has been substantial research into the antimicrobial effect of NPs on bacteria, the majority of the research has focussed on their efficacy against vegetative cells and not biofilms. This study aims to fill this gap in the knowledge and establish the efficacy of metal and metal oxide NPs on both the treatment and prevention of *P. aeruginosa* and *S. aureus* biofilms. Thus, going some way to establish whether metal based nanotechnology could be a feasible option for disinfectant development against HCAIs.

Chapter 2

Chapter 2: Literature Review

2.1 S. aureus

S. aureus is an opportunistic Gram-positive coccus is globally established as one of most common microorganisms liable for nosocomial infections (Sarkar *et al.*, 2016). *S. aureus* commonly colonises on human skin of healthy individuals (Otto, 2010), however its access to the body can lead to disease formation such as skin and soft tissue infections, septic arthritis, osteomyelitis, endocarditis, bacteraemia, sepsis and pneumonia (Kim *et al.*, 2012; David & Daum, 2010). The emergence of *S. aureus* mutations has led to the persistence of *S. aureus* derived infections. *S. aureus* mutations, which are predominantly resistant to the majority of β-lactam antibiotics, are known as MRSA. MRSA is difficult to eliminate and results in high numbers of morbidity and mortality (de Kraker *et al.*, 2011). MRSA is often present as a biofilm in hospitals which results in prolonged permanence of the bacteria (Sakoulas *et al.*, 2006; Vickery *et al.*, 2012; Wagenvoort *et al.*, 2000). It has the capability of surviving on hospital surfaces for several weeks and can be transmitted to patients indirectly or directly, for instance, through contaminated hands or gloves of the healthcare workers (Huang *et al.*, 2006; Weber & Rutala, 2013; Wagenvoort *et al.*, 2000; Vickery *et al.*, 2012; Kramer *et al.*, 2006).

Furthermore, *S. aureus* has the ability to adhere to indwelling medical devices *via* immediate interaction with its polymer surface or indirectly, by creating connections to human matrix proteins once they have covered the indwelling device. This is then followed by proliferation *via* the production of an extracellular matrix, leading to intercellular aggregation. The matrix of staphylococci, also known as the "slime" layer, contain many secreted polymers including exopolysaccharides, teichoic acids, and specific and DNA (deoxyribonucleic acid) from lysed cells (Otto, 2008).

Death certificates mentioning MRSA have reduced by 20% between 2011 and 2012. However, out of the 292 deaths noted in 2012, 13% were due to the organism itself. Furthermore, MRSA death rates increase with age (Office for National Statistics, 2013). Between 2014 and 2015, 801 cases of MRSA were reported by the English National Health Service (NHS) Acute Trusts, which is a 7.1% reduction from 2013/2014 where 862 cases were noted. There was an overall reduction of 82% from the number of cases from 2007/2008 (4,451 cases). It should be noted that even though the number of MRSA cases over the years has decreased, the decline rate has slowed down over time. For instance, a 22% reduction of cases between 2009/2010 and 2010/2011, compared with a 7.1% reduction between 2013/2014 and 2014/2015 (Public Health England, 2015a). Although there has been a drop in the morbidity and mortality rates of MRSA, it still poses a high risk to immunocomprised patients.

Cuervo *et al.* (2016) found that out the of the 579 cases of MRSA bacteraemia studied, 231 (39.9%) was present in patients ≥75 years of age, with the cause unknown. Out of 68 staphylococcal bacteraemia instances, over half were due to MRSA, although the resistance in the 22 cases that were over 70 years of age was not certain (Malani *et al.*, 2008). This is in compliance with studies by Bader (2006) and Big and Malani (2010), who also observed methicillin resistance in patients over 60 and 80 with resistance of 56 and 60% respectively. The resemblance of clones between older and younger patients implies frequent clonal exchange within hospitals and healthcare facilities, especially due to regular hospital admissions with the elderly population.

Three outbreaks of MRSA were traced in the UK; whereby whole genome sequencing was used to identify the cause of the outbreaks (Lindsay, 2014). Whole genome sequencing enables the comparison of clinical isolates with reference sequences to study the evolution of isolates, down to differences in single nucleotides (Young *et al.*, 2012). It provides important information about the spreading of isolates and the way they have evolved (Lindsay, 2013). Two out of the three outbreaks involved the MRSA CC22 SCC*mec*IV clone. Firstly, the NHS Foundation Trust in

Cambridge reported eleven colonised infants and another baby that had developed bacteraemia, this led to the unit's closure for nine days. The isolates derived from two patients with bacteraemia that were placed in adjacent beds for six days (Köser *et al.*, 2012). Secondly, The Oxford University Hospitals NHS Trust in Oxfordshire had two outbreaks between July and October 2011. An intensive care unit (ICU) was identified with seven carriers, alongside a bacteraemia and colonisation occurrence in the ICU two months after (Eyre *et al.*, 2012). Thirdly, in 2011 at The Rosie Hospital in the Cambridge University NHS Foundation Trust, 12 infants were colonised with MRSA in a 6-month period. Whole genome sequencing was used to identify that the MRSA was carried by a member of the hospital staff, which lead to the outbreak (Harris *et al.*, 2013). The recurring MRSA cases in hospitals and its risk to patients, colonisation on healthcare staff and surfaces suggests that MRSA still resides in high numbers in hospital environments and alternative disinfection methods may need to be considered.

2.2 P. aeruginosa

P. aeruginosa is of concern within the healthcare sector as it is accountable for a range of acute and chronic infections for instance bacteraemia, pneumonia, urinary tract infections (Dosler & Karaaslan, 2014) and cystic fibrosis (Winstanley *et al.*, 2016). *P. aeruginosa* infections can be acquired in the community, however, the majority of *P. aeruginosa* infections are obtained in a healthcare environment, particularly in immunosuppressed patients and vulnerable patients in ICU. Infections derived from *P. aeruginosa* can lead to mortality and morbidity, even with the various therapeutic choices available for treatment due to the emerging resistance of *P. aeruginosa* against antibiotics including quinolones (Jiang *et al.*, 2014), carbapenams (Wang et al., 2016a) and aminoglycosides such as tobramycin (Wu et al., 2015a). The severity and potential of *P. aeruginosa* infections and the problems related to multidrug resistant strains of *P.*

aeruginosa means that it is fundamental to find effective strategies to prevent their growth and prevalence.

P. aeruginosa residing in the reservoirs of healthcare environments poses a serious health risk (Kerr & Snelling, 2009). *P. aeruginosa* can be found in the hospital environment usually in moist environments (Loveday *et al.*, 2014) including taps and tap water (Walker *et al.*, 2013), potable water systems (Eckmanns *et al.*, 2008), water from drinking fountains (Costa *et al.*, 2015), sinks, showers and toilets (Breathnach *et al.*, 2012) as well as nebulisers for home treatment of cystic fibrosis (Blau *et al.*, 2007). There are various reasons as to why *P. aeruginosa* can survive in a hospital environment. Firstly, it is highly resistant to disinfectants including biguanides and QAC due to multidrug efflux pumps. It can form a biofilm on various inanimate surfaces, which adds to its resistance to disinfectants in addition to making its physical removal problematic (Kerr & Snelling, 2009).

In January 2012, three premature babies died following a pseudomonas outbreak in Royal Jubilee Maternity Hospital in Belfast in the neonatal ICU. Prior to this, there was another outbreak in December 2011 in the Altnagelvin Hospital in Londonderry, where another baby died due to a Pseudomonas infection; however, this was due to a different strain (Wise, 2012). A study by Walker *et al.* (2013) further investigated the outbreak in Northern Ireland to see whether *P. aeruginosa* was colonised within the neonatal unit taps and if the waterborne isolates matched with the patient isolates. When 30 taps and eight flow straighteners were grouped and dismantled into 494 components, the greatest counts of *P. aeruginosa* were obtained from the flow straighteners (52, 033 cfu/ml), metal support collars (71, 970 cfu/ml) and the tap bodies (634 cfu/ml) surrounding the two parts. Biofilms of *P. aeruginosa* were mostly found in flow straighteners and its components. These were identified as the likely source of infection, highlighting that water outlets in healthcare systems need to be monitored extensively to reduce contamination.

The overall occurrence of *Pseudomonas* spp. bacteraemia in England, Wales and Northern Ireland was 6.2 per 100, 000 population in 2014, showing an 11% decline from 2007 with a value of 6.9/100, 000. *Pseudomonas* spp. was the most prevalent in England with a value of 6.4/100, 000, followed by Northern Ireland (4.1) and Wales (3.1). A greater reduction has been noted in the *Pseudomonas* spp. bacteraemia in Wales and Northern Ireland with decreased rates of infection by 36% and 26% respectively in comparison to England over the last five years which only had a 6% decrease in the infection rate between 2010 and 2014 (Public Health England, 2015b).

Cases of *P. aeruginosa* infection in vulnerable patients has been reported for many years (Ayliffe *et al.*, 1974). *P. aeruginosa* is often associated with hospital water reservoirs and after four pre-term babies died in Northern Ireland in 2011/2012 (Walker & Moore, 2014), specific guidelines of *P. aeruginosa* and water quality in augmented care units was released by the Department of Health in 2012/2013 (Department of Health, 2012). *P. aeruginosa* is readily present in the environment, especially at hand wash stations and water outlets and is a still a major concern within the hospital environment (Trautmann *et al.*, 2005; Trautmann *et al.*, 2006; Trautmann *et al.*, 2009; Crivaro *et al.*, 2009; Jefferies *et al.*, 2012). The recurring outbreaks of *P. aeruginosa* in hospitals over recent years highlights the issues that are faced within healthcare environments in terms of reducing contamination from this bacterium, in particular, due to its ability to form biofilms. Alternative disinfection methods to tackle this problem need to be considered.

2.3 Biofilms

Biofilms are a structured community of bacterial cells enclosed in a self-derived matrix that attach to biotic and abiotic surfaces including living tissues, industrial surfaces, indwelling devices such as catheters, waterlines of dental units, cardiac pacemakers, and contact lenses (Donlan, 2002; Donlan, 2001). The adherence of planktonic cells to an abiotic surface leads to the formation of sessile aggregates, surrounded by an extracellular polymeric substances (EPS) matrix, that acts

as a barrier (Feng *et al.*, 2015; Bjarnsholt, 2013). The EPS matrix is comprised of polysaccharides, proteins, extracellular DNA (eDNA) and lipids (Flemming *et al.*, 2007). The bond between bacterial cells and the substratum is enhanced by the EPS and it protects the colony from any stress in the environment (Donlan, 2002). Dense networks are then formed by secondary colonisers. Dispersion of cells from the cell community can either spread to form new biofilms or thrive as planktonic cells (Sun *et al.*, 2013).

Biofilms can be an accumulation of either single species or multispecies of bacteria surrounded by an extracellular polymeric matrix (Pereira *et al.*, 2016) though it is the sessile form that is problematic in numerous industries, particularly in the healthcare sector such as hospitals where patients are at a high risk of infection (Pérez-Zárate *et al.*, 2015). Sessile cells, mainly present in the inner layers of the biofilm and have slower metabolic and growth rates, hence reducing the efficacy of antimicrobials (de Oliveira *et al.*, 2012). The EPS acts as an adsorbent, lowering the concentration of antimicrobials able to diffuse to the bottom of the biofilm (Davenport *et al.*, 2014). Sessile cells differentiate from planktonic cells as they have the ability to express specific protection factors in order to protect the biofilm (Gilbert *et al.*, 2002). However, bacteria in biofilms are up to 1000-fold more resistant to antimicrobials in comparison to their planktonic counterparts (Liao & Sauer, 2012). In addition to this, properties that biofilms possess such as high stress tolerance, antibiotic resistance and resistance against other biocides (Rendueles *et al.*, 2013) makes it challenging to treat biofilms with antibiotics and antimicrobial agents (Murugan *et al.*, 2016).

2.4 Biofilm Formation

Biofilm formation occurs in a four stage process as shown in Figure 2.1: adhesion of bacteria to a surface, microcolony formation, maturation of the biofilm, and finally dispersion, whereby the cells detach from the biofilm to colonise elsewhere (Abdallah *et al.*, 2014).

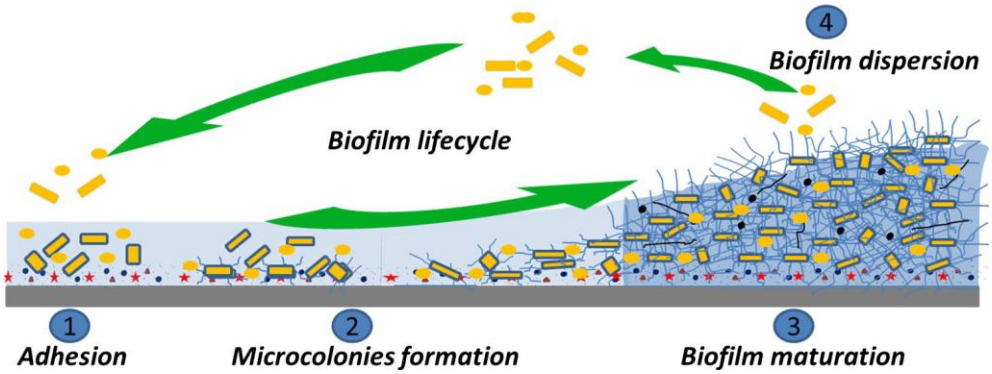

Figure 2.1: The four stage process of biofilm formation adapted from Abdallah *et al.* (2014).

2.4.1 Adhesion

Cell attachment to a substrate is vital for biofilm formation, it is reversible and aided by physical, chemical and biological interactions (Renner & Weibel, 2011). The adhesion process is highly influenced by the physicochemical property of the bacterial cell surface (Ferreira *et al.*, 2010). Forces such as Lifshitz-van der Waals, Lewis acid-base, and electrostatic interactions all aid in bacterial adhesion when bacteria are in close proximity to a substrate (Meireles *et al.*, 2015; Habimana *et al.*, 2014). These imposed forces enable reversible adhesion onto the surface (Karatan & Watnick, 2009). If repulsive forces exceed the attractive forces, bacterial cells can detach from the surface and revert back to their planktonic state (Garrett *et al.*, 2008). Motile bacteria can feel the drag on the motor of their flagella due to the substratum interactions with the bacterial appendage, initiating gene expression required in biofilm formation (Karatan & Watnick, 2009). This is followed by repression of flagella synthesis, so that motility is prevented (Karatan & Watnick, 2009).

Apart from physicochemical properties of bacterial cells, the chemical composition and physical properties of a substrate influence bacterial adhesion (Bayoudh *et al.*, 2006). Typically, most surfaces can be favourable substrates for biofilm formation such as plastic, glass, metal, wood and food products. Factors such as texture, i.e. the roughness and smoothness of a surface

(Donlan, 2002), surface charge (Ferreira *et al.*, 2010), pH, temperature (Nilsson *et al.*, 2011), nutrient composition of the pre-conditioning solution (Donlan, 2002; Gerstel & Romling, 2001), and organic matter, all influence the adhesion of cells to abiotic surfaces (Geng & Henry, 2011). These environmental conditions can alter the substrata and bacterial surface properties, affecting the adherence of bacteria to abiotic surfaces (Abdallah *et al.*, 2014). Sinde and Carballo (2000) demonstrated that *Salmonella* sp. and *Listeria monocytogenes* have enhanced adhesion to hydrophobic surfaces in comparison to hydrophilic surfaces as attachment was the greatest on polytetrafluorethylene (PTFE) being the most hydrophobic, followed by rubber and stainless steel (SS), which was the most hydrophilic with values of 78.7, 37.3 and 8.1 cfu mm^{-2} for *Salmonella* ES3 respectively and 668.0, 601.5 and 312.3 cfu mm^{-2} for *L. monocytogenes* ES15 respectively.

The conditioning layer consists of organic and inorganic particles and is the base on which biofilms develop. The gravitational force or movement of flow allows particles present in the bulk fluid to settle onto the substrate forming part of the conditioning layer, altering the substrata, making it easier for bacteria accessibility. Interactions that occur between the conditioning layer and substrate can change the surface charge, potential and tensions. The substrate supplies anchorage and nutrients allowing for bacterial growth (Garrett *et al.*, 2008). The nature of conditioning films vary according to the environment the substrate surface is surrounded by (Lorite *et al.*, 2011).

The conversion from a reversible to an irreversible attachment is a result of the change from weak interactions between the bacteria and the substrate to permanent bonding with the EPS (Stoodley *et al.*, 2002b). Irreversible attachment makes biofilms challenging to remove due to strong shear forces or chemical breakdown of the attachment forces having to be overcome using enzymes, surfactants, detergents, sanitisers (Sinde & Carballo, 2000) or heat (Augustin *et al.*, 2004; Maukonen *et al.*, 2003; Sinde & Carballo, 2000). Even though biofilms are made up of non-motile cells, some biofilm forming species require motility for growth or cell attachment to a substrate (Abee *et al.*, 2011). The initial stage of attachment in *P. aeruginosa* biofilm formation involves

reversible tethering through the flagella, whereby the bacteria position themselves in an orientation where their long axes is perpendicular to the substrate. This is followed by semi-permanent attachment in a horizontal position (Conrad *et al.*, 2011).

S. aureus on the other hand is a non-flagellated bacterium (Kaito & Sekimizu, 2007). Biofilm associated proteins (Bap) aid in initial attachment and biofilm formation in *S. aureus* on biotic and abiotic surfaces (Latasa *et al.*, 2006). All Bap positive *S. aureus* isolates tested by Cucarella *et al.* (2001) produced strong and adherent biofilms. Microbial Surface Components Recognizing Adhesive Matrix Molecules (MSCRAMM) in *S. aureus* also mediate initial cell attachment to an abiotic or biotic surface *via* ionic or hydrophobic interactions (Heilmann, 2011).

2.4.2 Microcolony Formation and Biofilm Maturation

During microcolony formation and biofilm formation, cells begin to replicate and adhesion that was reversible, becomes irreversible due to the secretion of EPS that constitute the biofilm matrix (Flemming & Wingender, 2010). The EPS enables the attachment of bacteria to a surface and to each other (Steinberg & Kolodkin-Gal, 2015). Biofilms mature to form an enclosed biofilm structure where the cells grow in a sessile form in heterogeneous complex-enclosed microcolonies, contained in an EPS matrix, with an efficient network of water channels (Dunne, 2002; Davey & O'Toole, 2000). This matrix forms a scaffold to stabilise this 3D biofilm structure (Dunne, 2002).

P. aeruginosa biofilms develop a mushroom-like structure comprising of microcolonies in the stalk and cap, with structural integrity provided by Pel and Psl polysaccharides and eDNA (Yang *et al.*, 2009a; Barken *et al.*, 2008; Yang *et al.*, 2011a). In *S. aureus* biofilms, the polymer poly-N-acetyl-β-(1-6)-glucosamine (PNAG) (also known as polysaccharide intercellular adhesin (PIA)) is predominant in the *S. aureus* EPS matrix and plays an important role in *S. aureus* biofilm morphology. A weak PNAG producing *S. aureus* strain will have a simple morphology, similar

to that of a young biofilm, whereas a strong PNAG producing *S. aureus* strain will form a compact biofilm with mushroom like colonies with channels (Jefferson, 2004). PNAG facilitates biofilm formation and helps in providing resistance to antimicrobials (Ganeshnarayan *et al.*, 2009).

Quorum sensing (QS) is a bacterial cell-to-cell communication mechanism by which signalling molecules, known as autoinducers (AI), are released and detected (Rutherford & Bassler, 2012; Mund *et al.*, 2016). *P. aeruginosa* has the Las and Rhl QS systems, both of which are acylated homoserine lactone (AHL) based (De Kievit, 2009). Genes encoding for extracellular proteases such as elastase are activated by the LasR system (Park *et al.*, 2014). During QS, transcription of the *pel* operon in *P. aeruginosa* encodes for proteins that are necessary for the formation of glucose rich exopolysaccharide (Sakuragi & Kolter, 2007). The AI peptide-based QS system in *S. aureus* is encoded by the accessory gene regulator (*agr*) locus (Boles & Horswill, 2008), which is involved in biofilm structuring (Periasamy *et al.*, 2012).

2.4.3 Dispersion

Biofilms are dynamic structures as the sessile cells can detach from the biofilm matrix and revert back to their planktonic state to undergo the dispersion process (Kaplan, 2010; Sauer *et al.*, 2002). Active dispersal is triggered though a regulated procedure, whereas passive dispersion can occur due to external forces such as fluid shear and abrasion. Biofilm dispersal can be a result of variation in environmental factors such as nutrient availability and oxygen depletion, regardless of whether this would have a positive or negative impact on the biofilm (Kaplan, 2010) which leads to the expression of genes necessary for dispersion (McDougald *et al.*, 2011). Factors such as an increase in fluid shear (Stoodley *et al.*, 2002a), internal biofilm processes, endogenous enzymatic degradation, EPS release or surface binding proteins release (Kaplan *et al.*, 2004, Kaplan *et al.*, 2003) as well as variation in nutrient levels (Schleheck *et al.*, 2009) can all lead to biofilm detachment.

An example of this is demonstrated by *P. aeruginosa* biofilm production as they have the ability to disperse when there is a rapid increase in the nutrients succinate, glutamate and glucose. A ~80, 72 and 54% reduction in surface-associated biofilm biomass was observed in the presence of succinate, glutamate and glucose respectively (Sauer *et al.*, 2004). An escalation in nutrient levels, hence carbon levels, led to increased flagella expression and a decreased pilus expression, enabling twitching motility in dispersed cells (Sauer *et al.*, 2004). A decrease in nutrient levels produced a 90% reduction of *P. aeruginosa* PA01 biofilm cells (Hunt *et al.*, 2004). In this case, detachment was a result of starvation. Dispersal enables cells to colonise in areas of plentiful nutrients when nutrients are limited, allowing bacteria to survive, resulting in the expansion of the bacterial community (Wood *et al.*, 2011; Karatan & Watnick, 2009). In *P. aeruginosa*, detachment is first triggered in the centre of the caps (Harmsen *et al.*, 2010). This leads to the formation of a fluid filled cavity within the cap, enabling the planktonic cells to be seen (Sauer *et al.*, 2002). As the cavity enlarges, the planktonic cells are released and form new biofilms elsewhere (Boles *et al.*, 2005; Sauer *et al.*, 2002). In *S. aureus* biofilms, glucose depletion is also known to encourage biofilm disassembly. Under normal growth conditions of biofilms, i.e. in the presence of glucose, the *agr* QS system remains repressed *via* the excretion of acidic metabolites generating a low pH. Depletion of glucose levels in the environment reactivates the *agr* system, leading to matrix degrading enzyme production as well as surfactants, resulting in biofilm breakdown (Boles & Horswill, 2008). The *agr* locus positively regulates various protease expressions, encouraging the dispersion of *S. aureus* biofilms (Boles & Horswill, 2008).

2.5 Biofilms in a Clinical Setting

In 2011, the occurrence of HCAIs was 6.4% in the English NHS hospitals (Health Protection Agency, 2012). HCAIs cost the NHS around £1 billion per annum (National Audit Office, 2009; National Patient Safety Agency, 2004). Antimicrobial resistance is a major problem in the health care services, as fewer antimicrobials are being introduced into the market and at the same time,

pathogenic microorganisms are becoming increasingly resistant to the common antimicrobials (World Health Organisation, 2014).

Over the last 10 years, various schemes have been established in the UK to promote antimicrobial stewardship and to address the issue of antimicrobial resistance (Cooke *et al.*, 2014). This involves evidence-based standard setting, education and communication as well as audits of practice. These methods are fundamental to the control of antimicrobial resistance (Cooke *et al.*, 2010). Campaigns such as Essential Steps to Safe, Clean Care: Reducing Healthcare-Associated Infections (Department of Health, 2006), Saving Lives (Department of Health, 2007), The Special Advisory Committee on Antimicrobial Resistance (SACAR) Antimicrobial Framework (SACAR, 2007), *C. difficile* Infection: How to deal with the problem (Department of Health and the Health Protection Agency, 2008), Clean, Safe Care: Reducing Infections and Saving Lives (Department of Health, 2008a), The Health and Social Care Act 2008, Code of Practice (Department of Health, 2008b), Start SMART then FOCUS (Department of Health Advisory Committee on antimicrobial resistance and healthcare associated infection (ARHAI), 2011), the UK Five-Year Antimicrobial Resistance Strategy (Department of Health, 2013) and regional programs such as 'Hand in Hand' in 2007 in the East Midlands region all aim to increase awareness of antimicrobial resistance and improve infection control (Newitt *et al.*, 2015).

S. aureus, *E. coli*, *P. aeruginosa*, *Acinetobacter baumannii* are examples of bacterial strains that form biofilms on clinical surfaces and medical devices. They are resistant to well-known eradication techniques such as desiccation, antibiotic treatment and nutrient deprivation (Gaddy & Actis, 2009). One reason for this could be due to bacteria in the deeper layers of the biofilm having reduced metabolic and growth rates, therefore, they are more resistant to antimicrobials. Furthermore, biofilms' high cell density lowers the efficacy of antimicrobials, the extracellular polymers comprising the matrix act as adsorbents preventing the interaction of the antimicrobial with the biofilm cells as well as lowering the penetration of the bactericidal agent into the cell hindering inactivation. Physiological variations between planktonic and sessile cells and the

expression of specific protection factors by sessile cells make them more difficult to target (Gilbert *et al.*, 2002). Biofilms remain unaffected by the host immune response which allows further growth and infection regardless of the antibiotic treatments utilised (Gaddy & Actis, 2009; Rogers *et al.*, 2010). A particular concern is the persistence of biofilms on indwelling medical devices, which act as a continuous source of infection (Richards & Melander, 2009). The extent of this problem is seen worldwide, for instance, a total of 1834 patients over the age of 18 were admitted to eleven ICUs in a tertiary care hospital in North India (Kumar *et al.*, 2014). The use of indwelling devices and HCAIs had a predominant link as 27% of the patients surveyed had a medical device and out of the 129 HCAIs noted, 35% were related to indwelling devices, 18% were from ventilated patients, 4% were due to patients with a urinary catheter, and 15% were from patients with a central venous catheter (Kumar *et al.*, 2014).

The residence of biofilms on dry surfaces have been reported by many studies (Vickery *et al.*, 2012; Espinal *et al.*, 2012). A terminal cleaning procedure was carried out in a 16 bed ICU ward by cleaning with a neutral detergent first, and then disinfecting with 500 ppm chlorine (Vickery *et al.*, 2012). Despite terminal cleaning, SEM imaging confirmed the presence of MRSA on the venetian blind cord, curtain and mattress bay. The production of a thin film of water due to surface condensation could be the reason for biofilm formation even on dry surfaces. Alternatively, the relative humidity in ICUs could be adequate for biofilm formation on ICU surfaces. Following the formation of the biofilm, the EPS surrounds the biofilm, guarding it from disinfectants (Vickery *et al.*, 2012). Espinal *et al.* (2012) found that the survival time of *A. baumannii* on hospital dry surfaces was higher for biofilm forming strains in comparison to the non-biofilm forming ones with 36 and 15 day survival respectively. These studies suggest that biofilms on dry surfaces in hospital environments act as a reservoir for the initiation of infections in patients.

Vancomycin intermediate *S. aureus* (VISA) have thick cell walls and the ability to readily form dense biofilms (Howden *et al.*, 2014). Methicillin susceptible *S. aureus* (MSSA) 25923, MRSA ATCC 33591, and VISA was obtained from a patient suffering with endocarditis that was treated

with vancomycin. All three strains survived on vinyl flooring and formica for a minimum of 40 days, whereas VISA survived for over 45 days (Zarpellon *et al.*, 2015). All three strains were highly hydrophobic with a hydrophobicity index (HI) values of above 50% (Zarpellon *et al.*, 2015). Bacterial hydrophobicity can encourage colonisation, permanence and dissemination of pathogens in healthcare settings (Di Ciccio *et al.*, 2015). Rougher surfaces have been known to harbour bacteria in comparison to smoother surfaces as demonstrated by Huang *et al.* (2006). MRSA has been shown to survive for nine days, 11 days and over 12 days on a cloth curtain, plastic patient chart, and a laminated table top respectively, suggesting that rougher surfaces encourage biofilm growth (Huang *et al.*, 2006). Tajeddin *et al.* (2016) established the contamination rate of the hands of healthcare workers and environmental surfaces in ICUs, *A. baumannii* (1.4 and 16.5% respectively), *S. aureus* (5.9 and 8.1% respectively), *S. epidermidis* (20.9 and 18.7% respectively) and *Enterococcus* spp. (1 and 1.3% respectively) were the most frequently isolated bacteria. Results showed that the oxygen masks from patients, bed linens and ventilators were the most contaminated surfaces (Tajeddin *et al.*, 2016). *P. aeruginosa* in a biofilm form enables the persistence of *P. aeruginosa* for lengthy periods in hospital water systems, leading to nosocomial infections. Out of 11 hospitals examined, 82% of hospital water systems were positive for *P. aeruginosa* (Baghal Asghari *et al.*, 2013).

2.6 Disinfectant Resistance

The growth phase of the planktonic bacteria is vital when investigating biocide susceptibility. Clinical isolates of MRSA and *P. aeruginosa* biofilms were grown on discs made of SS, Teflon and polyethylene, and treated with the most commonly used disinfectants, Anticide Bac-50, MediHex-4 and Mediscrub containing the antimicrobial compounds benzalkonium chloride (1% w/v), chlorhexidine gluconate (4% w/v) and Triclosan (1% w/v). For MRSA and *P. aeruginosa* planktonic cells, the minimum bactericidal concentrations (MBC) were 100 to 1000 fold and ten

to 100 fold lower than the manufacturer's recommended concentration for MRSA and *P. aeruginosa* respectively. However, the biocides were unable to kill bacteria in the biofilm at the concentrations suggested by the manufacturer, 0-11% and up to 80% of MRSA and *P. aeruginosa* cell viability was noted respectively post treatment (Smith & Hunter, 2008), demonstrating that bacteria attached to a surface in the form of a biofilm in a hospital environment are less susceptible to the antimicrobial in comparison to their planktonic counterparts (Lewis, 2001; Mah & O'Toole, 2001; Gilbert *et al.*, 2002). A lower susceptibility of *P. aeruginosa* biofilms to chlorhexidine was exhibited with an MIC of <145 µg/ml in comparison to its planktonic counterpart (Bonez *et al.*, 2013), similar to the findings by Totè *et al.* (2010) showing only a 40% decrease in *P. aeruginosa* biofilm viability. The increased resistance of microorganisms to commonly used antimicrobials in hospitals is concerning especially due to the virulence factors exhibited by biofilms. Therefore, further research is required in order to find new and novel antimicrobials. In addition, when assessing the efficacy of antimicrobials, their ability to penetrate biofilms should also be determined. There is also another factor that needs to be considered; the impact of multispecies biofilms.

When biofilms are present in a multispecies form, they possess improved protective characteristics in comparison to monospecies biofilms. When single or four species of marine bacterial biofilms composed of *Microbacterium phyllosphaerae*, *Shewanella japonica*, *Dokdonia donghaensis*, and *Acinetobacter lwoffii* were exposed to 1,700 µg/ml of H_2O_2 or 20 µg/ml of tetracycline, mixed species biofilm increased in biomass by >167% in comparison to single isolates (Burmølle *et al.*, 2006). This may be due to mixed species biofilms reducing the permeability and diffusion of the antimicrobials (Burmølle *et al.*, 2006). Multispecies biofilms comprising of organisms found in drinking water, as well as opportunistic pathogens exhibited greater chlorine resistance in comparison to planktonic cells and monospecies biofilms (Schwering *et al.*, 2013). Planktonic cells of *Bradyrhizobium* sp. B1-1, *Methylobacterium isbiliense* MWI-1, *Mycobacterium* sp. MWI-2, *Sediminibacterium* sp. C0-3, *Novosphingobium*

subterraneum FH-D, *Sphingomonas* sp. FH-G, *Blastomonas natatoria* FH-J, *Variovorax* sp. A2-1, *Cupriavidus respiraculi* A3-2, *Kocuria rhizophila* C0-6 and the opportunistic pathogenic strains *E. coli* MEC-8, *Enterobacter cloacae* MTC-21, *P. aeruginosa* PAE-1 and *Stenotrophomonas maltophilia* FH-W1 were all eliminated at chlorine concentrations of 0.2-5.0 mg l^{-1}. However, higher chlorine concentrations between 1.6-40 fold, was needed to remove their biofilms. Approximately 70% of biofilms were unaffected by 5.0 mg l^{-1} of chlorine. An average of ~700–1100 mg l^{-1} of chlorine was needed to eradicate pathogens within the biofilm, which is 50-300 fold greater than the concentration required for single species biofilms (Schwering *et al.*, 2013).

Lee *et al.* (2014b) investigated the spatial and relative species distribution of a multispecies biofilm consisting of *P. aeruginosa* PA01, *Pseudomonas protegens* Pf-5 and *Klebsiella pneumoniae* KP-1. Various resistance levels were seen with monospecies biofilms of these microorganisms towards 10 µg ml^{-1} tobramycin and 0.1 % w/v sodium dodecyl sulphate (SDS). Monospecies biofilms of PA01, Pf-5 and KP-1 showed a reduction in biovolume of 33.6 ± 14.0%, 8.8 ± 2.3% and 37.2 ± 8.4% respectively when treated with tobramycin whereas in a multispecies biofilm, a reduction of 7.6 ± 7.0% was noted. With SDS treatment, the biovolume of *P. protegens* Pf-5, *P. aeruginosa* PA01 and *K. pneumoniae* KP-1 biofilms were reduced by 61.9 ± 8.8%, 9.7 ± 2.3% and 15.9 ± 2.0% respectively. Treatment of the multispecies biofilm with SDS exhibited resistance with a biovolume reduction of 11.5 ± 4.2% only, similar to tobramycin. Interestingly, when a mixed community of planktonic cells of the three strains were grown and treated with 10 µg ml^{-1} tobramycin, only the tobramycin resistance strain Pf-5 survived, showing that community resistance is only observed in biofilms, where the extracellular matrix and the unique spatial arrangement of the biofilm can exhibit these effects (Lee *et al.*, 2014b).

Due to most biofilms naturally existing as a multispecies biofilm (Yang *et al.*, 2011b), it is vital that when novel antimicrobials are designed, that they are able to have an inhibitory effect on the

biofilm as a whole and not just individual species due to the resistance exhibited by multispecies biofilms in comparison to monospecies biofilms.

2.7 NPs as Antimicrobial Agents

The ability to produce particulates of any shape or size has led nanotechnology researchers to assess new strategies for the use of NPs as biocidal agents (Janaki *et al.*, 2015). It is known that antibiotics can eliminate approximately six different disease causing microorganisms, whereas nanomaterials have bactericidal properties against at least 650 cell types (Sungkaworn *et al.*, 2007). Metal NPs are versatile in that they have properties such as catalytical, magnetic, electronic, optical as well as antimicrobial (Ingle *et al.*, 2008; Durán *et al.*, 2005), wound-healing and anti-inflammatory benefits (Taylor *et al.*, 2005). Therefore, metal and metal oxide NPs may be an effective alternative to current antimicrobials that have been rendered ineffective against resistant bacteria.

The individual characteristics, potency and spectra of activity of metal NPs and their derivatives such as Ag, silver oxide (Ag_2O), CuO, Cu, gold (Au), titanium (Ti), TiO_2, zinc (Zn), ZnO, calcium oxide (CaO) and magnesium oxide (MgO) have made them ideal candidates for antimicrobial agents (Dizaj *et al.*, 2014). The properties of metal NPs completely differ from their metal counterparts due to the surface/volume ratio of the NPs being greater as their size decreases (Rai & Bai, 2011; Buzea *et al.*, 2007). There is ongoing research into the mechanisms by which NPs act to exert an antimicrobial effect, however, the current proposed mechanisms are: a) free metal ion toxicity derived as a result of dissolution of the metal/metal oxide NPs' surface and b) oxidative stress exerted due to reactive oxygen species (ROS) formed from the NPs surface (Besinis *et al.*, 2014).

Ag NPs are the most commonly used inorganic metal NPs for antimicrobial agents (Zinjarde, 2012). The antifungal (Jo *et al.*, 2009), anti-viral (Rogers *et al.*, 2008), anti-inflammatory (Nadworny *et al.*, 2008), and anti-angiogenic (Gurunathan *et al.*, 2009) properties make Ag NPs

ideal for antimicrobial use. Furthermore, Ag NPs are non-toxic to the human body at low concentrations. Ag additives are safe, cost effective and long lasting, therefore, have been used in polymers, paints and textiles (Yuan Gao & Cranston, 2008; Appendini & Hotchkiss, 2002). Published studies have also shown that Ag NPs have lower toxicity in comparison to other disinfectants, making them suitable for use for a range of applications (Marambio-Jones & Hoek, 2010) such as burn treatments (Parikh, 2005; Ulkür *et al.*, 2005), the reduction of bacterial colonisation on medical devices such as catheters (Rupp *et al.*, 2004; Samuel & Guggenbichler, 2004), antimicrobial textile fabrics (Yuranova *et al.*, 2003; Jeong *et al.*, 2005) and water disinfection treatment (Chou *et al.*, 2005).

ZnO NPs are considered to have low toxicity and to be safe when in close proximity with human skin, making them ideal for usage in the textiles industry and also for surfaces in contact with humans (Liu *et al.*, 2014; Saraf, 2013). ZnO is commonly used for a range of cosmetics, sunscreens, toothpastes, food colouring, paints as well as coatings for vitamin supplements (Yu & Li, 2011). Bacterial growth requires Zn in small quantities for DNA synthesis, transcription and translations, however, in excessive concentrations; it can be toxic to bacterial cells (Blindauer *et al.*, 2001).

Cu NPs possess unique chemical, biological and physical characteristics and bactericidal properties in addition to being inexpensive to prepare, making it a popular candidate for antimicrobial use (Ahamed *et al.*, 2014; Wu *et al.*, 2002; Usman *et al.*, 2013). Cu is utilised as an antimicrobial due to its bactericidal properties against fungi and bacteria, and that it shares similar properties to other expensive noble metals with antimicrobial properties such as Au and Ag (Usman *et al.*, 2013). The advantages of utilising CuO as an antimicrobial agent is that it can be readily mixed with polymers and has stable physical and chemical properties. CuO is an example of highly ionic metal oxide NP, which can be developed to have a large surface area and various crystal morphologies (Stoimenov *et al.*, 2002).

2.8 Antimicrobial Efficacy of NPs

Mirzajani *et al.* (2011) tested the antimicrobial efficacy of Ag NPs against *S. aureus* PTCC1431. Results demonstrated that 4 µg/ml of Ag NPs showed complete inhibition of bacteria (Mirzajani *et al.*, 2011). A two hour treatment of the biofilms with 100 nM of Ag NPs gave a 95% and 98% reduction of *P. aeruginosa* and *S. epidermidis* biofilms respectively, whereas 50 nM Ag NPs reduced the biofilm of both microorganisms by 50% (Kalishwaralal *et al.*, 2010).

Antimicrobial efficacy is impacted by the shapes and sizes of NPs. *E. coli* was almost completely reduced at 1 µg of Ag truncated triangular nanoplates, whereas, lower antimicrobial efficacy was exhibited by spherical, rod-shaped and Ag^+ (in the form of silver nitrate ($AgNO_3$)) (Pal *et al.*, 2007). The high-atom-density surface of the triangular nanoplates is thought to be the cause of biocidal activity (Pal *et al.*, 2007). Bera *et al.* (2014) reported that 1.5 nm Ag NPs gave an MIC of 1.5 µg/ml for *S. epidermidis*, *P. aeruginosa* and *E. coli*, whereas 40 nm triangular Ag NPs gave an MIC of 3.90 µg/ml for *P. aeruginosa* and *E. coli* and 7.81 µg/ml for *S. epidermidis*. Ag NPs at 1.5 nm can penetrate directly though the cell membrane owing to their small size. The antimicrobial efficacy of ZnO ultrafine powder (> 1µm), ZnO NPs (8 nm), and ZnO nanopowder (50-70 nm) against *S. aureus* was assessed. ZnO nanopowder and ultrafine powder showed only a *circa* 50 % reduction, 8 nm ZnO NPs (1mM) showed over a 95% reduction, whilst 50-70nm ZnO NPs (5 mM) only showed a 40-50% reduction, suggesting that smaller sized NPs have greater antimicrobial efficacy than larger ones (Jones *et al.*, 2008), similar to the findings of Bera *et al.* (2014).

The antimicrobial activity of ZnO (19.89 ± 1.43 nm), CuO (29.11 ± 1.61 nm) and Fe_2O_3 (35.16 ± 1.47 nm) NPs was tested against *E. coli*, *P. aeruginosa*, *B. subtilis* and *S. aureus* (Azam *et al.*, 2012a). MBC values for ZnO, CuO and Fe_2O_3 against *E. coli* were 18, 25 and 65 µg/ml respectively, 14, 28 and 120 µg/ml against *P. aeruginosa* respectively; 12, 20 and 78 µg/ml respectively against *B. subtilis* and 16, 22, and 80 µg/ml against *S. aureus* respectively, suggesting

the enhanced efficacy of metal oxide NPs against Gram-positives with decreasing particle size. This correlates with findings by Premanathan *et al.* (2011) whereby strains of *E. coli*, *S. aureus* and *P. aeruginosa* were treated with ZnO NPs, and the MICs observed were 500, 125 and 500 µg/ml respectively. Lee *et al.* (2014a) reported that ZnO NPs (<50nm) treatment lowered virulence factor expression and inhibited *P. aeruginosa* biofilm formation by over 95% on a polystyrene surface at a concentration of 1 mM, whilst Feris *et al.* (2010) found the MICs of ZnO NPs (<13 nm) were >4.25 mM against *P. aeruginosa*. The efficacy of crystalline flower shaped ZnO nanostructures was determined, with an MIC of 25 mg/l against *S. aureus* and *E. coli* (Mohan Kumar *et al.*, 2013). This suggests that the ZnO NP toxicity to bacterial cells varies according to the concentration, bacterial species and particle size (Ma *et al.*, 2013).

The complete inhibition of *P. aeruginosa*, *S. aureus* (Oxford), epidemic MRSA (EMRSA)-16 and *S. epidermidis* SE-51 was observed after exposure to 1000 µg/ml of CuO NPs over 4 hours (Ren *et al.*, 2009). The antimicrobial efficacy of CuO NPs (23 nm) and its MIC was determined against various bacteria such as *E. coli*, *P. aeruginosa* and *S. aureus*, with MICs of 31.25, 125 and 62.5 µg/ml respectively (Ahamed *et al.*, 2014). Padil and Černik (2013) found CuO NP (4.8 nm) MIC values of 103 and 120 µg/ml were effective against *E. coli* and *S. aureus* respectively. Azam *et al.* (2012b) also reported MICs of 103 and 120 µg/ml for *E. coli* and *S. aureus* respectively although the CuO NP size was larger at 20 nm. Most published research has been based on the antimicrobial activity of metal and metal oxide NPs against planktonic cultures. Due to the continuing occurrence of biofilm related infections and the well-known antimicrobial properties of metal and metal oxide NPs, further research needs to be focussed towards the anti-biofilm properties of metal and metal oxide NPs.

2.9 Modes of Action of NPs

Different metal/metal oxide NPs act upon bacterial cells *via* different pathways as shown in Figure 2.2.

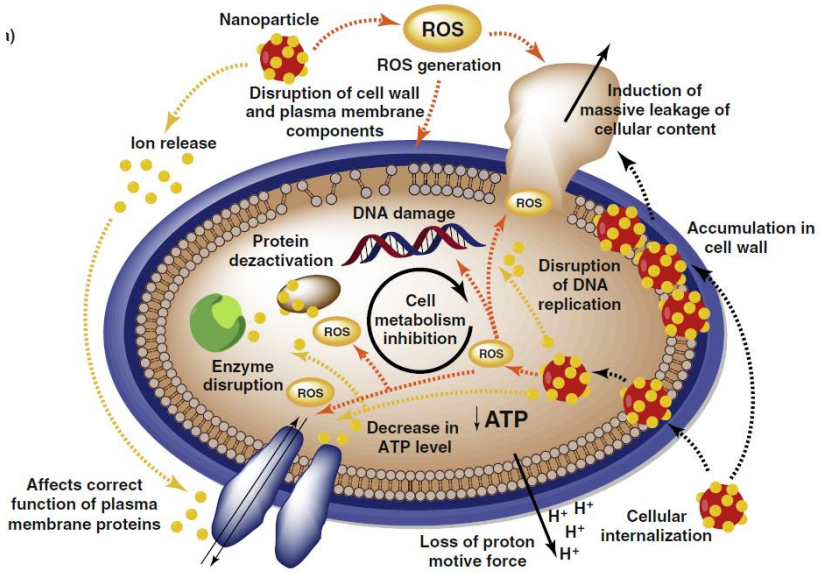

Figure 2.2: Modes of action of metal/metal oxide NPs adapted from Wyszogrodzka *et al.* (2016).

One of the mechanisms by which Ag NPs destroy bacterial cells is *via* damage to the bacterial outer membrane of the cell (Lok *et al.*, 2006). Many studies have reported the formation of pits when Ag NPs accumulate on the membrane of the bacteria, followed by fragmentation of the membrane (Ansari *et al.*, 2014a; Sondi & Salopek-Sondi, 2004; Li *et al.*, 2010; Rajesh *et al.*, 2014). The interaction of Ag with bacterial membranes containing sulfur can lead to inhibition of proteins and membrane bound enzymes, disrupting metabolic processes (Pal *et al.*, 2007; Holt & Bard, 2005). Ag NP treatment also causes intracellular leakage of cell contents (Rajesh *et al.*, 2014). Ag NPs can penetrate to the cytoplasm, interacting with elements containing phosphorous e.g. DNA (Yuan *et al.*, 2013; Morones *et al.*, 2005; Bondarenko *et al.*, 2013), hindering replication. In the cytoplasm, ROS can be formed from Ag NPs as described in numerous studies,

with smaller NPs forming more ROS (Bae *et al.*, 2011; Ivask *et al.*, 2014; Bondarenko *et al.*, 2013; Ansari *et al.*, 2014a) due to smaller NPs being able to reach the cytoplasm more efficiently than larger NPs (Durán *et al.*, 2015).

Although Ag NPs have shown to exert antimicrobial activity directly, research has also suggested the importance of Ag^{+} ions released from Ag NPs (Marambio-Jones & Hoek, 2010; Reidy *et al.*, 2013; Manke *et al.*, 2013; Rajeshkumar & Malarkodi, 2014; Dos Santos *et al.*, 2014). Ag NPs can rupture bacterial cell membranes directly, however, it is the Ag^{+} form that results in increased permeability of membranes, cellular contents leakage, interruption of DNA replication and de-energisation of bacterial cells. Samberg *et al.* (2011) suggested that a synergistic effect between the Ag^{+} ions binding to the cell wall, their uptake, and accumulation in the cell is what exerts the antimicrobial effect.

One proposed mechanism by which ZnO exerts its antimicrobial properties is *via* the production ROS such as of H_2O_2, O_2^{-},$^1O_2$ and ·OH on the surface of the NPs (Zhang *et al.*, 2008). Brayner *et al.* (2006) and Huang *et al.* (2008) have also reported the internalisation of ZnO NPs. Electrostatic forces between the ZnO NPs and the bacterial cell membrane encourage contact between the two and formation of ROS close to membrane results in an antimicrobial effect (Zhang *et al.*, 2008). The release of Zn^{2+} ions from ZnO NPs leads to an increased intracellular concentration of Zn^{2+}, resulting in an over generation of ROS within the cell leading to plasma membrane leakage, mitochondria dysfunction and cell death (Wang *et al.*, 2014a).

CuO NPs also generate ROS species producing $\cdot O2^{-}$, which interacts with the outer wall of the bacterial cell. The free radical species can then enter the cell, disrupting the inner contents, leading to cell deformation and leakage (Hassan *et al.*, 2012). Perelshtein *et al.* (2009) suggested that the antimicrobial efficacy of CuO NP was due to the NP itself. However, Aruoja *et al.* (2009) and Mortimer *et al.* (2010) demonstrated that the toxicity of CuO NPs is due to Cu^{2+} ions.

2.10 Conclusion

Extensive research has been carried out on novel ways by which biofilm formation can be controlled, yet antimicrobial biofilm resistance still remains an issue within the clinical arena. Problems such as cross contamination, infections derived from nosocomial pathogens and disease associated with biofilm formation on medical equipment have yet to be fully addressed. The requirement for novel agents that can overcome the resistance of bacterial biofilms to current antimicrobials is of paramount importance. The majority of currently published research has focussed on metal/metal oxide NPs as antimicrobials against planktonic cells rather than biofilms. However, bacteria commonly reside in a biofilm form rather than planktonic state, and most available antimicrobial agents are only effective at concentrations that inhibit planktonic cells, hence their inefficacy at decontaminating healthcare environments. Metal and metal oxide NPs could be a potential agent with antimicrobial promise against biofilms.

2.11 Scope of this Work

Aim:

This study aims to determine the antimicrobial efficacy of metal and metal oxide NPs against *P. aeruginosa* and *S. aureus* biofilms.

Objectives:

- To establish the best method for biofilm formation that can replicate biofilms in hospital and healthcare arenas.
- To investigate the inhibitory effect of metal and metal oxide NP suspensions alone and in combination against biofilms of *S. aureus* and *P. aeruginosa*.
- To determine the effect of thin film coating of metal and metal oxide NPs on the formation of *S. aureus* and *P. aeruginosa* biofilms.
- To assess the gene expression of *S. aureus* metal and metal oxide NPs treated biofilms.

Chapter 3

Chapter 3: *In vitro* Biofilm Formation

3.1 Introduction

Biofilms can be defined as a community of microorganisms adhered to a biotic or abiotic surface. Biofilm formation is a multistep process where bacterial cells undergo adhesion to a surface which is initially reversible. However, extracellular matrix production consisting of polysaccharides, protein and DNA, enables a stronger cell attachment, which eventually becomes irreversible (Sauer, 2003; Stoodley *et al.*, 2002b).

Biofilm production is highly reliant on the experimental conditions (Reisner *et al.*, 2006; Hancock *et al.*, 2011). Methods used to assess biofilm formation *in vitro* can be standardised poorly, therefore, it can be challenging when data in the published literature is compared. Moreover, what one study defines as a strong biofilm producer may differ considerably from another study (Skyberg *et al.*, 2007; Naves *et al.*, 2008).

Published research has used various methods to form biofilms *in vitro*, each posing different advantages and disadvantages. For instance, static biofilm methods such as microtiter plates (MTP) are compact and can hold a number of samples so replicates can be obtained rapidly with low costs (Campbell *et al.*, 2003). Conversely, flow systems such as the CDC biofilm reactor enable biofilm formation on surfaces including SS and plastics e.g. polycarbonate (PC). These materials are readily found in a healthcare environment and are a common substrate for biofilm formation (Smith & Hunter, 2008).

3.1.1 In vitro *Biofilm Model Systems*

3.1.1.1 MTP

MTP based systems are commonly used to assess biofilms (Toté *et al.*, 2008; Uppuluri *et al.*, 2009; Silva *et al.*, 2010). Most commonly, 96 well plates are used whereby biofilms are formed on the walls of the MTP plates on in the bottom of the wells. Alternatively, they are grown on coupon surfaces which are then placed in the wells of a 6, 12 or 24 well MTP (Heersink & Goeres, 2003). The plates are inoculated with organisms, incubated for 24 to 48 hours followed by a crystal violet assay used to determine the biomass of the biofilm (Crémet *et al.*, 2013; Moreira *et al.*, 2013). This method was first outlined by Christensen *et al.* (1985). Such systems are known as closed or batch reactor-like systems, as there is no fresh flow of nutrients in and out of the plates throughout the course of the experiment (Heersink & Goeres, 2003). Therefore, the environmental conditions of the well alter as the experiment proceeds, as nutrients deplete and signalling molecules accumulate. In order to avoid such changes in conditions, the culture media needs to be replenished (Coenye & Nelis, 2010).

MTP based models have many advantages as they are usually simple to operate, cost effective due to only minimal volumes or reagents required and numerous tests can be undertaken simultaneously (Sandberg *et al.*, 2008; Stepanović *et al.*, 2000; Pitts *et al.*, 2003; Knezevic & Petrovic, 2008). They are, therefore, ideal to use for screening of antimicrobials against biofilms (Niu & Gilbert, 2004). These systems have been widely utilised for screening the antimicrobial and anti-biofilm properties of many antibiotics and disinfectants (Tremblay *et al.*, 2014; Abbanat *et al.*, 2014; Perumal *et al.*, 2014). MTP based models can allow in depth assessments of the biofilm formation on modified, coated and impregnated materials different stages of formation (Mowat *et al.*, 2007; Imamura *et al.*, 2008; De Prijck *et al.*, 2010, 2007; Chandra *et al.*, 2001). The MTP system also enables researchers to alter various conditions such as growth media,

incubation temperature, humidity, shear stress and O_2 and CO_2 levels (Krom *et al.* 2007; Stepanović *et al.* 2003).

Even though the crystal violet assay is laborious, it is commonly used for studying biofilm formation. The process itself is lengthy and hard to standardise (Crémet *et al.*, 2013). Many published studies have used this method, although the number of washing steps, washing conditions (i.e. automation, and use of buffer or water for washing) and the time of crystal violet staining differs as well as its concentration (Chavant *et al.*, 2007; Naves *et al.*, 2008; Reisner *et al.*, 2006; Skyberg *et al.*, 2007; Wang *et al.*, 2009). This method primarily measures biomass rather than the biofilm cell viability (Crémet *et al.*, 2013).

Flow displacement systems contrast to MTP based systems as they are "open" systems. In flow systems, growth media containing nutrients are continuously or semi-continuously introduced into the system and waste products are eliminated (Heersink & Goeres, 2003; Busscher & Van Der Mei, 2006).

3.1.1.2 Flow Systems

The CDC biofilm reactor is a continuous flow system which involves a glass vessel with a polyethylene top containing eight holes to place polypropylene rods, which are perpendicular to the rotating baffle in the middle of the glass vessel (Buckingham-Meyer *et al.*, 2007; Donlan *et al.*, 2004; Goeres *et al.*, 2005). Three removable coupons can be placed in each rod on which the biofilms are formed (Donlan *et al.*, 2004; Goeres *et al.*, 2005). Each coupon is 12.7 mm in diameter with a 2.52 cm^2 surface area. The coupons can be made from various materials, such as PC, mild steel, SS and polyvinyl chloride (PVC), vinyl, glass etc. depending on the purpose of the assay and the bacteria (Macià *et al.*, 2014). The glass reactor is joined to a flask containing sterile broth pumped through the system *via* a peristaltic pump to provide a continuous source of

fresh nutrients to the biofilm. Bacteria are inoculated into the CDC biofilm reactor and biofilms then form on the coupons. A magnetic stirrer in the centre of the vessel rotates the nutrients, enabling high shear conditions for the biofilm to grow (Macià *et al.*, 2014). Previous studies have demonstrated the reliability of the CDC biofilm reactor for the formation of biofilms across a wide range of organisms such as *Pseudomonas putida* (Thuptimdang *et al.*, 2015), *S. epidermidis* (Paredes *et al.*, 2012) and *P. aeruginosa* (Nagant *et al.*, 2013). A total of 24 'identical' biofilms can be grown on coupons at once and enumerated. This system is ideal to study the growth of the biofilm over longer periods of time (Honraet *et al.*, 2005; Nailis *et al.*, 2009), the antimicrobial effect of coated materials (Agostinho *et al.*, 2009) and evaluation of disinfection methods and cleaning procedures (Buckingham-Meyer *et al.*, 2007; Hadi *et al.*, 2010). The CDC biofilm reactor has a large capacity of 500-1000 ml, therefore testing the efficacy of antimicrobials in the CDC biofilm reactor can be costly due to the large volumes of media required (Coenye & Nelis, 2010). Recently, the CDC biofilm reactor was used to test the efficacy of sodium hypochlorite, a commonly used disinfectant, on dry surface biofilms of *S. aureus*. A 7 $\log_{(10)}$ kill was observed, with a reduction in biomass. However, CLSM demonstrated the persistence of *S. aureus* cells (Almatroudi *et al.*, 2016). The CDC biofilm reactor is well established for its ability to produce *P. aeruginosa* biofilms under conditions of high shear and continuous flow and is used by the American Society for Testing and Materials (ASTM E2562) (Coenye & Nelis, 2010; American Society for Testing and Materials, 2012). An illustration of the CDC biofilm reactor is shown in Figure 3.1.

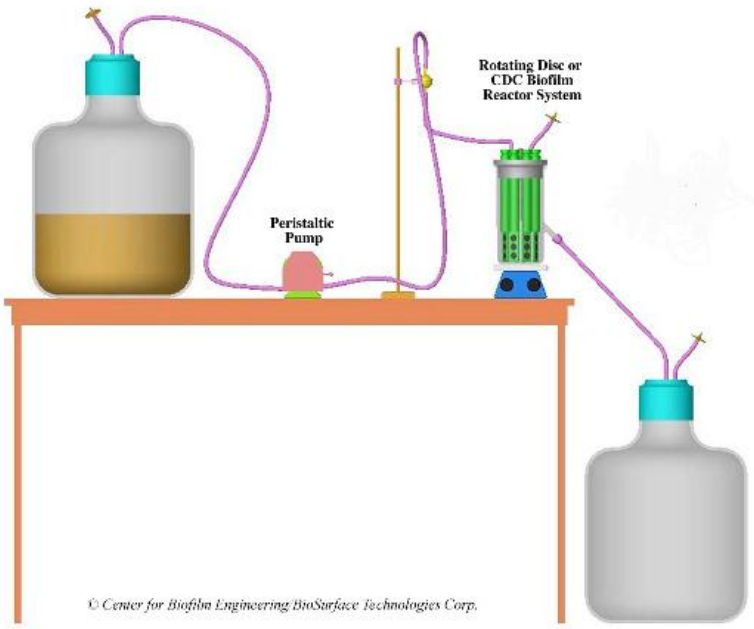

Figure 3.1: Setup of a CDC biofilm reactor (BioSurface Technologies Corporation, 2010)

Other flow systems include a drip flow reactor, which is a plug flow reactor where biofilms grow in conditions of low shear in close proximity to the air/liquid interface (Goeres *et al.*, 2009). Biofilms grown using the drip-flow method have been previously used to analyse: the effect of powdered brushing on biofilm plaque removal (Adams *et al.*, 2002); to evaluate the reduction of *S. epidermidis* biofilm formation by bacteriophages (Curtin & Donlan, 2006); and to investigate the efficacy of a range of disinfectants (Stewart *et al.*, 2001; Buckingham-Meyer *et al.*, 2007).

3.1.1.3 Rotating Disc Reactor

The rotating disc reactor includes a Teflon disc which holds 6 x 12.7 mm diameter coupons. A magnetic stirring bar at the bottom of the rotating disc allows the disc to rotate, creating a liquid surface shear on the coupons. The disc that holds the coupons is put in a reactor vessel and growth media (in the absence or presence of an antimicrobial) is distributed throughout the vessel whilst the disc is rotating (Buckingham-Meyer *et al.*, 2003). The rotating disc reactor has been utilised

to investigate many properties of biofilms such as the cohesive strength of *P. aeruginosa* and *S. epidermidis* biofilms (Aggarwal *et al.*, 2010), resistance of *P. aeruginosa* to heavy metals (Teitzel & Parsek, 2003) and multispecies biofilm interactions (Komlos *et al.*, 2005).

3.1.2 Comparison of in Vitro *Biofilm Models*

Often *in vitro* biofilm formation methods can be modified to suit the needs of a study. Bacterial contaminants in commercial fuel ethanol production facilities are usually present as a multispecies biofilm under laboratory conditions (Rich *et al.*, 2011). Rich *et al.* (2011) assessed the ability of the pure cultures to form monospecies biofilms using a modified method by Gross *et al.* (2007) and their susceptibility to virginiamycin. In this assay, 96 well MTP contained 96-pin replicator lids, which were exposed to plates containing medium, encouraging biofilm growth. Crystal violet was then used to analyse the biomass that adhered to the pin. The MTP based method was advantageous as it allows simultaneous assays of different bacterial species under a range of conditions. Furthermore, this assay is less labour intensive as set-up time, data analysis, as well as cleaning-up is also reduced. MTP based assays require less media and in this particular study, antibiotics, therefore more cost effective (Rich *et al.*, 2011). Skinner-Nemec *et al.* (2007) studied multispecies biofilms of bacterial contaminants in commercial fuel ethanol production facilities, but in a CDC biofilm reactor. This method permits precise biofilm growth measurements and regulation of parameters, though only one organism can be assayed at a time (Rich *et al.*, 2011).

The crystal violet assay and the CDC biofilm reactor can be used in conjunction with each other to test the efficacy of antimicrobials. A CDC biofilm reactor was used to grow biofilms of *P. aeruginosa* ATCC 25619 on polytetrafluoroethylene coupons and subjected to commercial surgical equipment disinfectants. The biofilms were hydrolysed and the crystal violet assay and a commercially available protein assay were used to detect the remaining biofilm. Sodium hydroxide (NaOH) at a concentration of 1% gave the highest reduction of 77.3%, whereas Tween

20 gave the lowest reduction of 18.7%. No significant difference was found in between the results obtained for the percentage reduction values acquired for crystal violet or the protein assay, thus suggesting that the crystal violet assay is an appropriate method to use for the detection of remaining biofilms after treatment (Hadi *et al.*, 2010).

In conclusion, there are various methods that can be used to investigate biofilm formation, each having its advantages and disadvantages. Biofilms are a concern in the healthcare sector, due to increasing antimicrobial resistance. Methods to replicate these biofilms *in vitro* for further study are vital in order to assess their structure and formation to develop antimicrobials for prevention and elimination of biofilms. Furthermore, the study of biofilm formation on various surfaces is of paramount importance as the topography and chemical composition of a surface can also affect the adherence of a biofilm *in vitro*.

3.1.3 Aims and Objectives

Aim:

The aim of this investigation was to determine which method of biofilm formation is most appropriate for forming biofilms of *P. aeruginosa* and *S. aureus* for the assessment of metal/metal oxide NPs as antimicrobials.

Objectives:

- To compare a static and a flow system for the formation of *P. aeruginosa* and *S. aureus* biofilms.
- To evaluate *P. aeruginosa* and *S. aureus* biofilm formation by measurement of protein.
- To compare the surface topography of *P. aeruginosa* and *S. aureus* biofilms using SEM.

3.2 Methods

3.2.1 Culture Methods and Microorganisms

The test organisms used were *P. aeruginosa* NCTC 6749 and *S. aureus* ATCC 6538. All culture media was acquired from Oxoid Ltd. (Hampshire, UK) unless otherwise stated.

Strains were stored on beads (Technical Service Consultant Ltd., Lancashire, UK) at -80°C. Cetrimide agar (CM0579) for *P. aeruginosa* and Mannitol salt agar (CM0085) for *S. aureus* was used to phenotypically determine the organisms.

Organisms were grown on Nutrient agar (NA) (CM0003) and then 1 colony per 10 ml of Nutrient broth (NB) (CM0001) was grown aerobically for 24 hours at 37 °C. NA was used to culture the bacteria for viable count enumeration.

3.2.2 Biofilm Formation in 96 Well Plates

Aliquots of 200 µl of a 24-hour culture of either *P. aeruginosa* or *S. aureus* were plated into 96 well plates and incubated in a rotating incubator (Innova 44, New Brunswick Scientific, Stevenage, UK) at 37°C for 10 days at 100 rpm. The wells were replenished at 5 and 9 days with 200 µl of sterile NB. Planktonic bacteria were removed by washing plates twice with phosphate buffered saline (PBS, BR0014G). The cells were then fixed with 200 µl of ethanol for 10 minutes (mins), stained with 50 µl of 0.1 % crystal violet for 15 mins, washed three times with PBS and dried. Aliquots of 200 µl of 10 % (v/v) glacial acetic acid were then added to each well in order to solubilise the crystal violet and the absorbance was read at 595 nm using a micro plate reader (Molecular Devices Thermo Max Microplate Reader, Berkshire, UK)(Christensen *et al.*, 1985).

The procedure was repeated but with replenishment of the broth occurring daily.

3.2.3 Biofilm Formation in a CDC Biofilm Reactor

3.2.3.1 Batch Phase

PC and SS coupons were placed in CDC biofilm reactor (CBR 90, Biosurface Technologies Corporation, Montana, USA) containing 500 ml of NB and 1 ml of an overnight culture of either *P. aeruginosa* or *S. aureus*. The CDC biofilm reactor was then placed on a stirring plate (125 rpm) and incubated at room temperature for 24 hours.

3.2.3.2 Continuous Flow

After 24 hours in batch phase, a continuous flow of NB medium was passed through the CDC biofilm reactor at a flow rate of 11.7 ± 0.2 ml/min for *P. aeruginosa* and *S. aureus* for 24 hours. The flow rate was maintained using a peristaltic pump (120S Watson Marlow Pumps, Cornwall, UK).

The flow rate was calculated using the following equation:

$$\text{Flow rate} = \text{CDC Biofilm Reactor Volume} / \text{Residence Time}$$

The CDC biofilm reactor volume is approximately 350 ml once the rods and baffles are assembled. The residence time for *P. aeruginosa* and *S. aureus* is 30 mins (BioSurface Technologies Corporation, 2010; Barber *et al.*, 2015).

3.2.3.3 Validation of Removal of Biofilms from Coupons

Biofilms were formed on PC (RD128-PC, Biosurface Technologies, Montana, USA) or SS (RD128-316P, Biosurface Technologies, Montana, USA) coupons in the CDC biofilm reactor.

The biofilm was physically removed using a glass rod by scraping one surface of sample in a circular motion for 5 seconds each and placing the scraped cells into 9 ml of PBS. This was repeated 5 times. The surface of the coupon was then rinsed with 1 ml of PBS and added to the 9ml of PBS containing the cells. The solution was then homogenised (Ultra-Turrax T25, IKA-Labortechnik, Staufen im Breisgau, Germany) at 20,500 rpm for 30 seconds. The solution was spread plated and incubated at 37°C for 24 hours. Alternatively, the coupon was stomached for 1 min in 1 ml of PBS and the resulting solution was spread plated and incubated at 37°C for 24 hours. Colonies were then enumerated.

The homogenising probe was cleaned between samples by rinsing for 30 seconds at 20,500 rpm in sterile water, followed by a rinse at 20,500 rpm for 15 seconds in 70% ethanol, then immersed in ethanol for 1 min and rinsed with sterile water at 20,500 rpm for 30 seconds.

3.2.4 Protein Assay

Protein standards were prepared in 10% v/v NaOH using bovine serum albumin (BSA, A9056, Sigma Aldrich, Dorset, UK) at the following doubling concentrations: 0, 0.156, 0.313, 0.625, 1.25, 2.5, 5 and 10 mg/ml. Aliquots of 5 µl of protein standard were added to 96 well plates. Aliquots of 250 µl of Bradford reagent (B6916, Sigma Aldrich, Dorset, UK) was then added to each of the wells and thoroughly mixed for 30 seconds. Samples were then incubated at room temperature for 10 mins and absorbance read at 595 nm using a microplate reader.

Aliquots (200 µl) of a 24 hour culture of either *P. aeruginosa or S. aureus* were placed in 96 well plates and incubated in a rotating incubator at 100 rpm at 37°C for 10 days. The wells were replenished daily with 200 µl of NB. The wells were then washed with PBS to remove any planktonic bacteria and 250 µl of Bradford reagent added and mixed for 30 seconds, incubated at room temperature for 10 mins and the absorbance was then read at 595 nm using a microplate reader (Spectramax Plus 384, Molecular Devices, Berkshire, UK).

3.2.5 Depth and Topography of P. aeruginosa and S. aureus Biofilms

A PC coupon was cut in half and then placed back together into the hole of the CDC biofilm reactor rod to form a divide by which the biofilm thickness can be measured. Biofilms of *S. aureus* and *P. aeruginosa* were formed in the CDC biofilm reactor as per method described in Sections 3.2.3.1 and 3.2.3.2 The coupons were then removed and cut using a scalpel along the divide in the coupon made. Samples were then washed with PBS and fixed with 95 % ethanol for viewing under the SEM (Evo HD 15 Carl Zeiss, Cambridge, UK). The samples were pre-coated with a 15 nm coating of gold (Q150RS, Quorum Technologies, East Sussex, UK). The thickness of the biofilm was determined. To view the topography of the biofilm, biofilms *S. aureus* and *P. aeruginosa* were formed in the CDC biofilm reactor as per method described in Method 3.2.3.1 and 3.2.3.2 on PC coupons, washed with PBS and fixed with 95% ethanol.

3.2.6 Statistical Analysis

Statistical analysis was undertaken to observe if there was a significant difference in *P. aeruginosa* and *S. aureus* biofilm formation on PC and SS coupons, and between the absorbance obtained for *P. aeruginosa* and *S. aureus* biofilms over 10 days when the broth in the MTP assays was replenished at 5 and 9 days and daily. IBM SPSS Statistics Version 20 for Windows was used for all statistical analysis tests with the significance value set at $p \leq 0.05$. Assumption of normality was tested using Kolmogorov-Smirnov test if sample sizes were ≥50 or the Shapiro-Wilcox test used if samples were <50. For non-parametric data, a Kruskal Wallis test was used to analyse significant differences between more than two group means or a Mann-Whitney U test for two means. An example of Mann-Whitney U output can be found in Appendix I.

All investigations were carried out in triplicate on at least two separate occasions.

3.3 Results

3.3.1 Biofilm Formation in 96 well plates

When no replenishment of broth was conducted, evaporation of the nutrients occurred in the rotating incubator, leaving a residue in the wells. This therefore caused an increased absorbance of the crystal violet in the dried wells, creating invalid data, large variations and SE. The broth was replenished at 5 and 9 days due to the evaporation. Between day 1 and 3 of biofilm formation, no visible biofilms could be seen in the 96 well plates.

When biofilms were replenished at 5 and 9 days, the highest biofilm formation ($p \leq 0.05$) was seen at day 9 (1.57 au) for *S. aureus* biofilm formation in comparison to day 4 when biofilm formation was the lowest (0.26 au) (Figure 3.2). For *P. aeruginosa* biofilms, the highest biofilm formation was at day 8 (3.26 au) ($p \leq 0.05$) in comparison to day 4 (0.63 au) (Figure 3.2). A significant drop ($p \leq 0.05$) in biofilm formation occurred at day 6 (0.45 au) for *S. aureus* biofilms in comparison to day 5 (0.94 au). A significant ($p \leq 0.05$) decrease in absorbance for *P. aeruginosa* biofilms was observed at day 4 (0.63 au) and 10 (2.09 au). *P. aeruginosa* biofilms generally gave a higher absorbance in comparison to *S. aureus* biofilms (Figure 3.2).

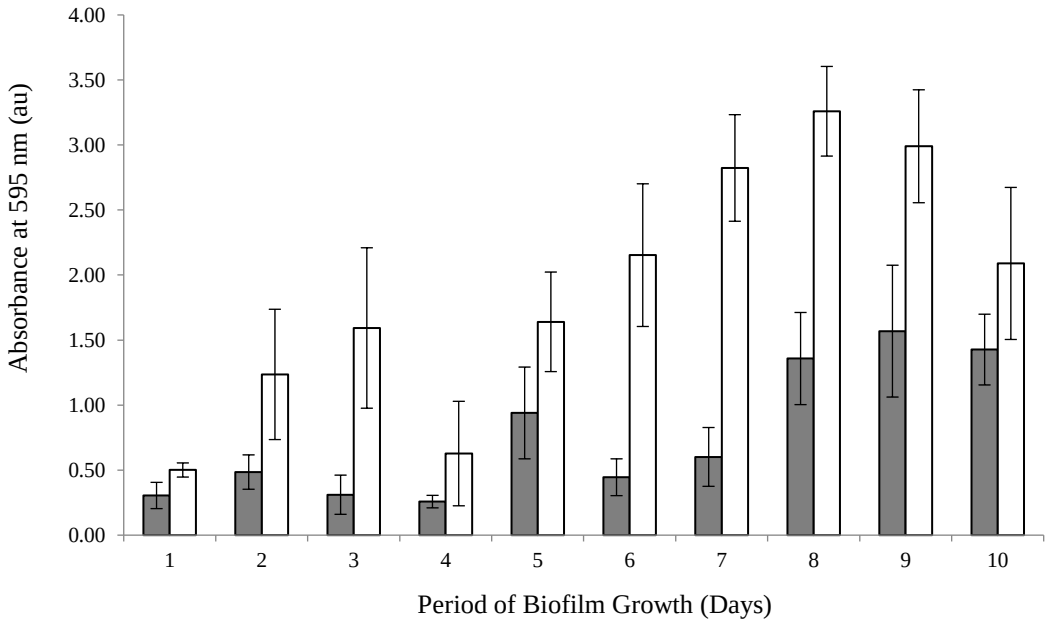

Figure 3.2: Comparison of biofilms for *S. aureus* and *P. aeruginosa* using 96 well plate method when broth was replenished at 5 and 9 days (n=6 ± SE) *S. aureus* *P. aeruginosa*

When broth was replenished daily, biofilm formation for *S. aureus* was the highest at day 9 (1.66 au) ($p \leq 0.05$) in comparison to day 4 (0.25 au), when *S. aureus* biofilm formation was the lowest (Figure 3.3). *P. aeruginosa* biofilm formation was the highest at day 3 (2.04 au) and 9 (2.00 au) in comparison to day 5, where there was a significant ($p \leq 0.05$) decrease in biofilm formation. A significant ($p \leq 0.05$) reduction in biofilm formation occurred at day 4 and 10 for *S. aureus* with absorbance readings of 0.25 au and 1.19 au respectively (Figure 3.3). For *P. aeruginosa* biofilms, there was a significant ($p \leq 0.05$) drop at days 4, 7 and 10 with absorbance values of 0.98, 1.02 and 1.44 au respectively (Figure 3.3).

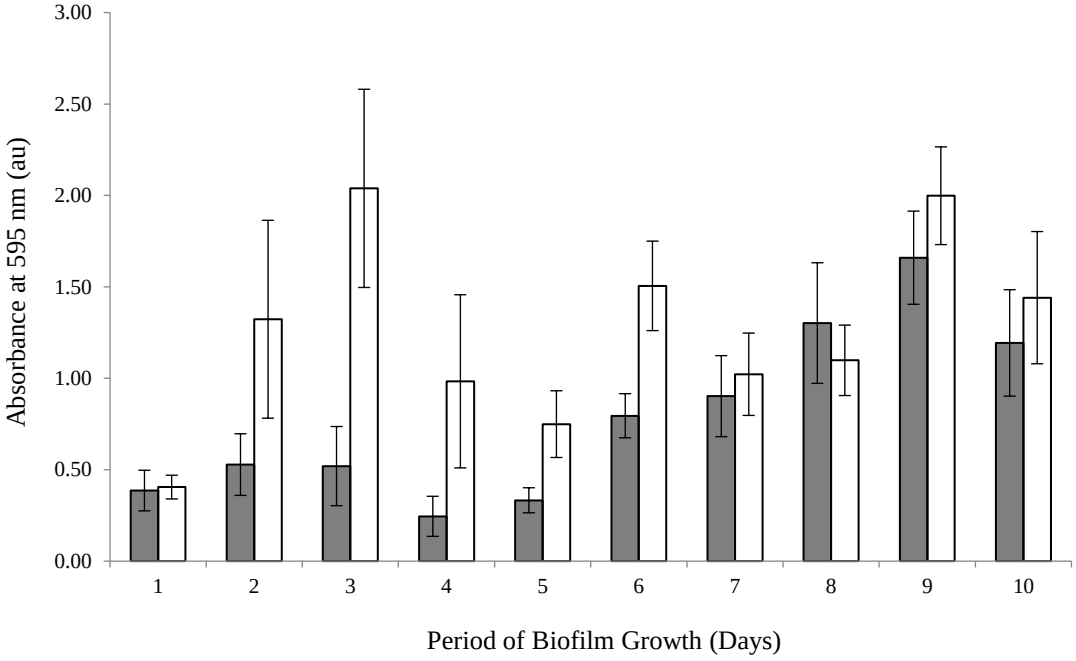

Figure 3.3: Comparison of biofilms for *S. aureus* and *P. aeruginosa* using 96 well plate method when broth was replenished daily (n=6 ± SE) *S. aureus* *P. aeruginosa*

3.3.2 Protein Assay Using the Bradford Reagent

The highest absorbance for a *P. aeruginosa* biofilm was observed for day 8 (0.36 au), with a significant ($p \leq 0.05$) increase from day 3 (0.07 au), where the lowest absorbance was obtained. Overall the protein content per well increased over 10 days (Figure 3.4). A significant ($p \leq 0.05$) decrease in absorbance was seen between day 8 (0.36 au) and 10 (day 0.25 au), and day 4 (0.26 au) and 6 (0.17 au). When the absorbance values were converted into concentration of protein, a protein concentration of 0.005 mg/ml was determined for *P. aeruginosa* at day 8 only, as all other concentrations were below the limit of detection of the standard curve.

A minimal change in absorbance was noted over the first 8 days for *S. aureus* biofilms, with a significant ($p \leq 0.05$) increase at day 9 (0.36 au) and 10 (0.47 au) (Figure 3.5) from day 7 (0.07 au), where a slight increase in absorbance was noted. When the absorbance values were converted into protein content, values of 0.13 mg/ml and 0.28 mg/ml were only found at 9 and 10 days only. For days 1-8, no values could be calculated due to the limit of detection.

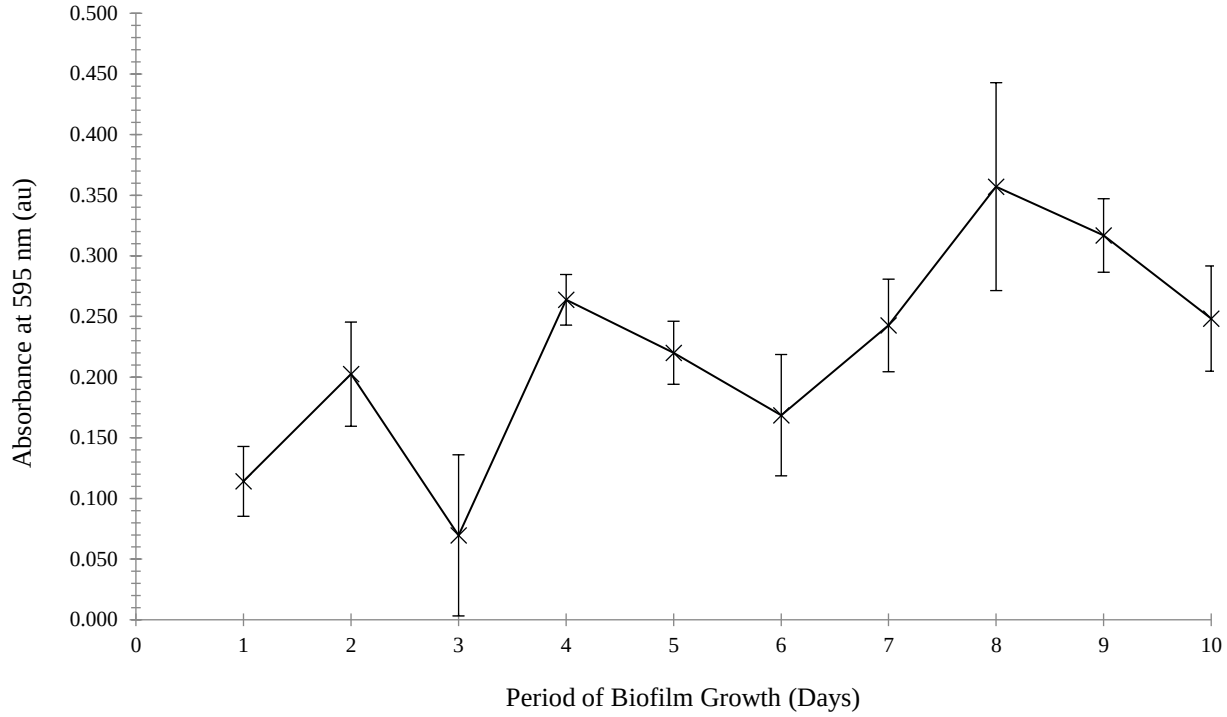

Figure 3.4: Protein assay using Bradford Reagent to quantify protein content of *P. aeruginosa* biofilm between 1 to 10 days (n=6 ± SE).

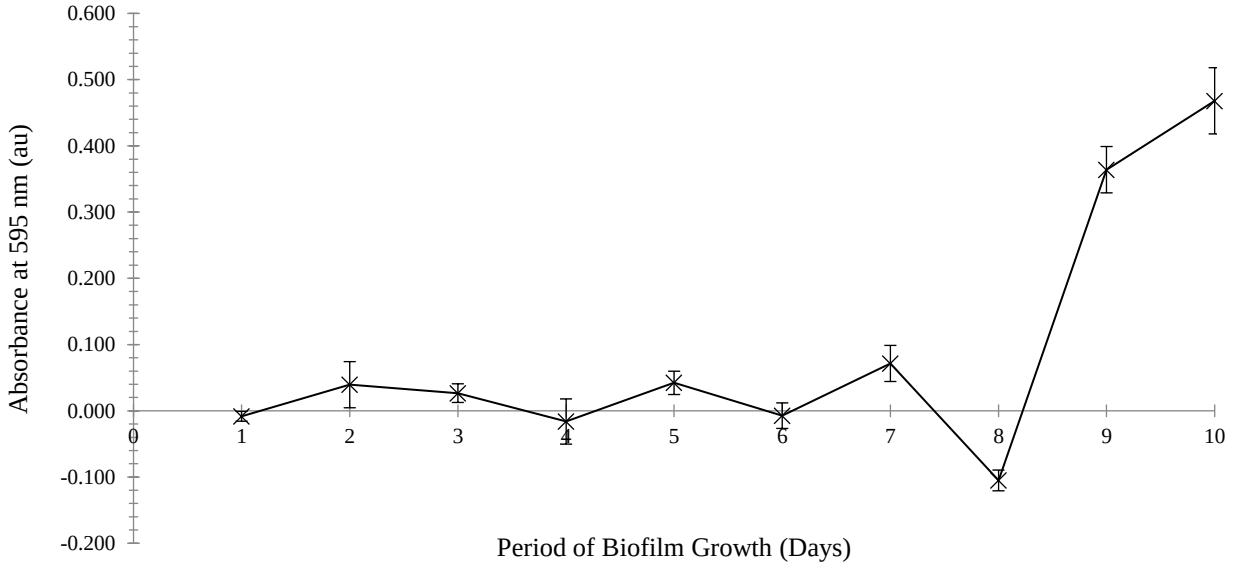

Figure 3.5: Protein assay using Bradford reagent to quantify protein content of *S. aureus* biofilm between 1 to 10 days (n=6 ± SE).

3.3.3 Biofilm Formation in the CDC Biofilm Reactor

Stomaching removed 6.05 ± 0.03 $\log_{(10)}$ and 6.12 ± 0.12 $\log_{(10)}$ from *S. aureus* biofilms on PC and SS coupons respectively, and 6.56 ± 0.18 $\log_{(10)}$ and 6.04 ± 0.10 $\log_{(10)}$ from *P. aeruginosa* biofilms from PC and SS coupons respectively.

Scraping removed 7.86 ± 0.19 and 7.85 ± 0.17 $\log_{(10)}$ cfu/ml from *P. aeruginosa* biofilms on PC and SS coupons respectively, and 7.09 ± 0.05 and 7.06 ± 0.04 $\log_{(10)}$ cfu/ml from *S. aureus* biofilms on PC and SS coupons respectively (Figure 3.6). There was no significant difference ($p > 0.05$) between the quantity of biofilm formed on PC and SS coupons for *S. aureus* or *P. aeruginosa*, however *P. aeruginosa* did form the most biofilm on both surfaces in comparison to *S. aureus*.

However, there was a difference of ~1 $\log_{(10)}$ between the $\log_{(10)}$ cfu/ml counts using scraping and stomaching. Hereafter, only scraping was utilised to enumerate the samples.

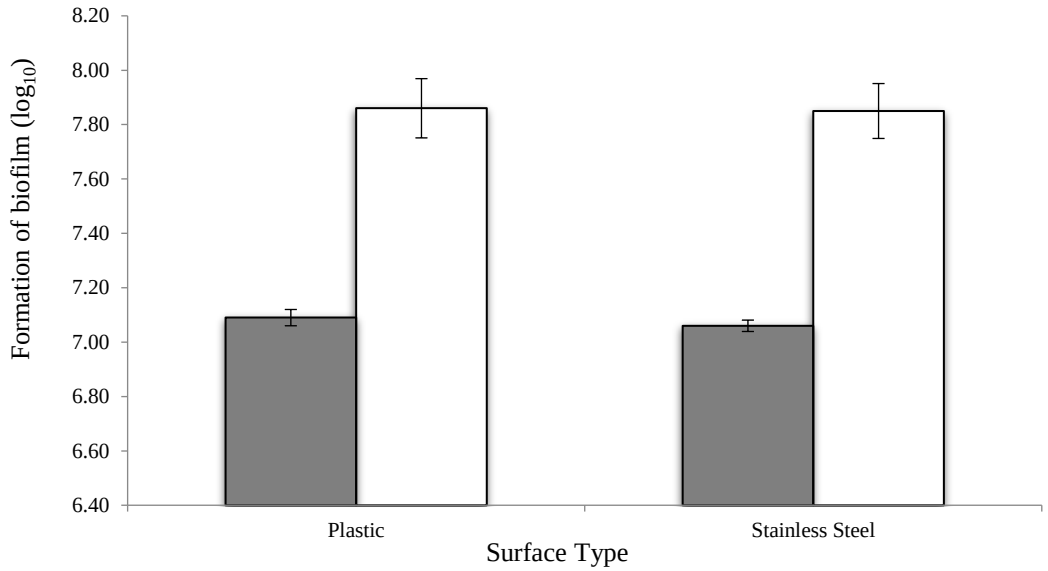

Figure 3.6: Comparison of $\log_{(10)}$ cfu/ml of *S. aureus* and *P. aeruginosa* biofilms formed on PC and SS coupons (n=6 ± SE) *S. aureus* *P. aeruginosa*

3.3.4 Depth and Topography of S. aureus *and* P. aeruginosa *Biofilms*

SEM images obtained after growth of a biofilm on PC coupons (Figure 3.7) show *S. aureus* (Figure 3.7a) and *P. aeruginosa* (Figure 3.7b) embedded in a layer of EPS. Greater magnification shows the cocci cells of *S. aureus* agglomerated together (Figure 3.7a). In Figure 3.7b, a *P. aeruginosa* biofilm can be seen across the surface of the coupon. Figure 3.7e and 3.7f show the depth of *S. aureus* and *P. aeruginosa* biofilm respectively. *S. aureus* biofilm thickness ranged between 18 to 19 µm and *P. aeruginosa* biofilm thickness was ~ 7 µm.

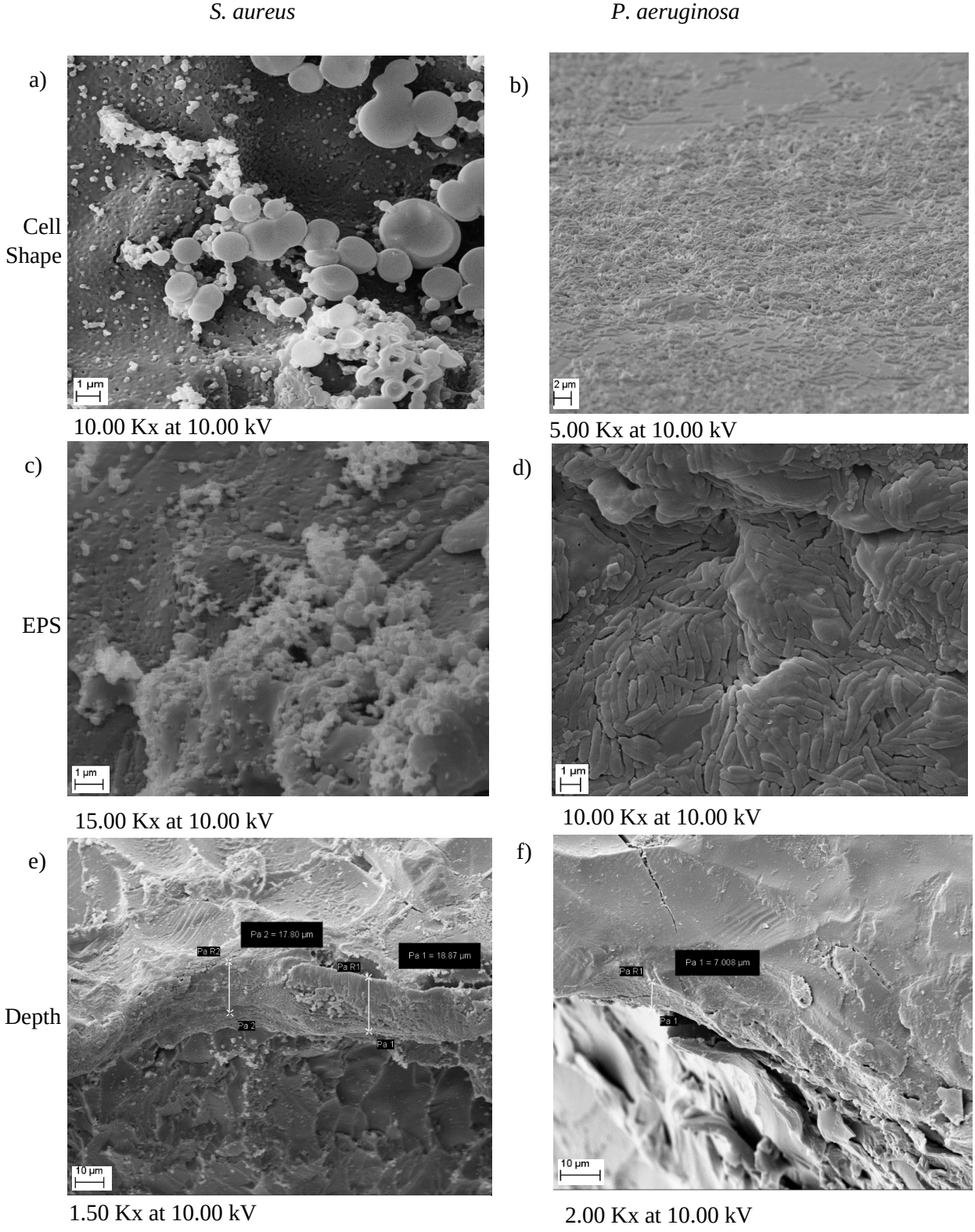

Figure 3.7: SEM images showing the individual cells in the biofilm, EPS formation, topography and depth of 48 hour biofilms of *P. aeruginosa* and *S. aureus* formed in the CDC biofilm reactor on PC coupons; a) *S. aureus* biofilm, b) *P. aeruginosa* biofilm, c) *S. aureus* cells surrounded by EPS, d) *P. aeruginosa* cells surrounded by EPS, e) cross section of an *S. aureus* biofilm and f) cross section of a *P. aeruginosa* biofilm.

3.4 Discussion

Hospital acquired infections cause high morbidity and mortality, and can be costly to treat. The presence of bacteria on inanimate surfaces in hospitals can encourage infections due to the transmission from the environment to immunocomprised patients (Hu *et al.*, 2015). It is, therefore, important to use *in vitro* methods to study biofilms in depth in order to be able to understand their growth process, persistence in the environment and the prevention of infections. The high-throughput biofilm screening MTP methods, and the low costs associated, facilitate the process of identifying genes that are crucial for production of surface-attached biomass in growth medium (Pitts *et al.*, 2003). MTP based methods are also suitable for the mass screening of anti-biofilm compounds by quantifying the reduction in the surface attached biomass post treatment (Pitts *et al.*, 2003; Jakobsen *et al.*, 2012). Flow systems such as the CDC biofilm reactor mimic conditions that a biofilm would experience in nature such as shear forces and a renewable nutrients, therefore forming biofilms that are comparable to those found in the environment (Williams & Bloebaum, 2010). In this study, two methods were used to quantify and compare biofilm formation in a 96 well plate assay and the CDC biofilm reactor flow system.

3.4.1 Biofilm Formation in 96 Well Plates

When using the 96 well plate assay without the replenishment of nutrients, the wells were found to dry out, leaving a residue of broth and the cells. As a result, during the crystal violet assay, darker wells were seen for those that had dried out giving highly variable absorbance values. Biofilm growth for *P. aeruginosa* and *S. aureus* was assessed by replenishing nutrients at 5 and 9 days as it was around those days that the wells were observed to dry out. The wells were also replenished daily to observe whether there was any difference in growth. Furthermore, for biofilm formation at day 1 and 2, no visible biofilm was seen whereas between day 3 and 10, a biofilm

was observed at the bottom and the walls of the wells. Often the crystal violet dye adhered to the dried NB in the wells, giving an absorbance reading is not representative of biofilm growth (Figure 3.2 and 3.3).

Biofilm replenishment at 5 and 9 days (Figure 3.2) show that the greatest biofilm formation was at day 9 (1.57 au) and day 8 (3.26 au) for *S. aureus* and *P. aeruginosa* respectively. When replenished daily (Figure 3.3), the highest growth for *S. aureus* was again at day 9 (1.66 au), similar to the results in Figure 3.2, whereas the highest growth for *P. aeruginosa* was at day 3 (2.04 au) and 9 (2.00 au) (Figure 3.3). Both Figure 3.2 and 3.3 are similar in that the biofilm formation was the highest at day 8/9 for *P. aeruginosa* and day 9 for *S. aureus*. The rise and fall in biofilm formation was initially thought to be a result of broth replenishment at 5 and 9 days (Figure 3.2). However, when the broth in the wells were replenished daily, a similar 'up down' pattern was observed (Figure 3.3). Due to the large SE obtained using the MTP method, conclusions about biofilm formation cannot be drawn without any further investigation.

The protein assay was carried out in conjunction with biofilm formation in 96 well plates to measure secreted extracellular protein and cells that have lysed 'naturally' in the biofilm over the 10 days of growth. For *S. aureus* biofilms, an increase in protein concentrations is only seen at day 9 (0.36 au) and 10 (0.47 au), whereas between days 1 to 8, the absorbance levels were found to be below 0.1 au (Figure 3.5). This correlates to the large absorbance values obtained at day 9 (1.57, 1.66 au) and 10 (1.43, 1.19 au) for *S. aureus* biofilms when the broth was replenished at 5 and 9 days and daily (Figure 3.2 and 3.3). A large absorbance is also seen for day 8 for *S. aureus* in Figure 3.2 (1.36 au) and 3.3 (1.30 au), however, a negative protein value was seen for day 8 for *S. aureus* in Figure 3.5. A limitation of nutrients present in the wells could limit growth, thus the amount of protein produced.

Previous studies have shown that when the 96 well plates were used to determine biofilm formation over time, the crystal violet assay was inappropriate for *P. aeruginosa* biofilm biomass

quantification as large standard deviations were seen between experiments and data (Peeters *et al.*, 2008). Absorbance values reported for *P. aeruginosa* strains were much lower than that of the absorbance values obtained for the other species tested, even though a 0.5% crystal violet concentration were used throughout. This could be due to the inadequate fixing of *P. aeruginosa* biofilms due to the large quantities of water present in the slime layer of *P. aeruginosa* biofilms (Peeters *et al.*, 2008). Similar findings were observed in the present research as large SE in biofilm formation of both organisms, particularly *P. aeruginosa* were also seen when the broth was replenished daily and at 5 and 9 days (Figure 3.2 and 3.3). The ability of *S. aureus* and *P. aeruginosa* to form exopolysaccharides may have also influenced the protein assay results, again large SE were observed, particularly in Figure 3.4.

During initial biofilm growth, reversible attachment occurs, therefore washing wells with PBS or water could mean that cells are being washed out from the wells. For *P. aeruginosa*, absorbance for Bradford reagent increased overtime, with a drop at 3, 6 and 10 days (Figure 3.4). Biofilm growth varies over the 10 days of incubation that were studied therefore, it would be expected that changes in the presence of protein would also do so (Figure 3.2, 3.3, 3.4 and 3.5). Lutskiy *et al.* (2015) used a 96 well plate method to measure early stage of biofilm formation of *Klebsiella oxytoca* on reverse-osmosis (RO) and nanofiltration (NF) polyamide membranes under static conditions. The incubation period between 5 to 10 hours was critical for biofilm development as during this period, the growth accelerated the most, beyond this time period the biofilm growth resulted in a daily 'up down' pattern in the growth curve (Lutskiy *et al.*, 2015), similar to the results obtained in Figure 3.3 and 3.4. Moreover, there is a possibility that after a certain time, possibly around day 9 and 10 (Figure 3.2 and 3.3), there was a limitation of nutrients within the biofilm due to an increase in cells; therefore, dispersion lowered the overall biofilm biomass, hence giving the irregular pattern observed in Figure 3.3 and 3.4.

A study by Oja *et al.* (2014) monitored the biofilm development of *S. aureus* ATCC 25923, using a static method. Glass coupons were placed on agar covered with filter paper, and growth of

biofilms was monitored over 48 hours using the crystal violet assay and viable counts. In the first 2 hours, no significant change in the viable counts occurred. However, there was a steady increase in the viable counts between 4 and 24 hours with values of 7.36 ± 0.03 log cfu/cm^3 and 8.23 ± 0.62 log cfu/cm^3 respectively (Oja *et al.*, 2014). Static biofilm formation methods are useful for analysis of established biofilms and monitoring the early stages of biofilm development, such as adhesion on different substrates (Oja *et al.*, 2014). MTP based assays enable high throughput assays and multiplexing, meaning several organisms can be treated with several treatments simultaneously (Coenye & Nelis, 2010).

3.4.2 CDC Biofilm Reactor

P. aeruginosa and *S. aureus* formed biofilms of 7.86 and 7.09 $\log_{10}$ cfu/ml on PC coupons, and 7.85 and 7.06 $\log_{10}$ cfu/ml on SS coupons respectively (Figure 3.6). There was no significant difference ($p > 0.05$) found between the two surfaces for either microorganism with very low SE values of 0.12 and 0.11 for *P. aeruginosa* biofilms on PC coupons and SS coupons respectively and 0.03 and 0.02 for *S. aureus* biofilms for PC and SS coupons respectively. When compared to the data collected from the 96 well plates, the SE ranged from 0.05 to 0.51 and 0.34 to 0.62 for *S. aureus* and *P. aeruginosa* biofilms respectively during 5 and 9 day replenishment (Figure 3.2) and 0.07 to 0.33 and 0.18 to 0.19 for *S. aureus* and *P. aeruginosa* biofilms respectively for daily replenishment (Figure 3.3). Thus, the low SE and reproducibility of data indicates that the CDC biofilm reactor is a more reliable method of producing biofilms for quantification purposes.

In the CDC biofilm reactor, biofilm formation on both PC and SS coupon surfaces were tested, whereas adhesion to polystyrene surfaces only could be tested in 96 well plates. An advantage of the CDC biofilm reactor is that biofilms can be formed on various surface materials in a coupon form. Materials such as SS are readily found in medical devices and healthcare associated environments, therefore, results from a CDC reactor would replicate hospital environments more

accurately (Liu & Zhao, 2005; Wilks *et al.*, 2005). The use of crystal violet in the MTP assays for measuring absorbance only gives a semi-quantitative measure of the amount of biofilm formed. This absorbance gives no indication of the activity of the biofilm nor the bactericidal effects of the anti-biofilm agent, however, it assesses the destruction of the biofilm (Pitts *et al.*, 2003).

The production of a dense biofilm structure for *P. aeruginosa* and *S. aureus* biofilms when formed in a CDC biofilm reactor can be seen in Figure 3.7e and 3.7f. The EPS can be seen surrounding the embedded cells in Figure 3.7c and 3.7d. The EPS forms a barrier around the cells that the antimicrobial has to overcome to be effective. The thickness and maturity of these biofilms poses a challenge to antimicrobials, it is, therefore, essential to ensure the antimicrobial penetrates the biofilm completely in order to exert its antimicrobial effect. Shen *et al.* (2011) suggested that the maturity of a biofilm and its age should be accounted for when comparing the antimicrobial efficacy of disinfectants. Multispecies biofilms from plaque bacteria increased in thickness from 57 µm to 201 µm between 2 days to 12 weeks respectively (Shen *et al.*, 2011). When exposed to 1, 3 and 10 mins of 2% chlorhexidine, the proportion of non-viable cells was higher in the younger biofilms compared with mature biofilms, indicating that nutrient limited biofilms in their mature stages of growth have greater resistance against disinfectants (Shen *et al.*, 2011). The depth of *P. aeruginosa* and *S. aureus* biofilms obtained in the SEM images (Figure 3.7e and f) were between 18 to 19 µm and ~7 µm for *S. aureus* and *P. aeruginosa* biofilms respectively, therefore not as high as seen in the study by Shen *et al.* (2011). However, the biofilms in the CDC biofilm reactor were grown over 48 hours with plentiful nutrients. The morphology and structure between biofilms of 48 hours and 12 weeks with nutrient limited conditions are likely to differ greatly.

Stimulating the same growth conditions for biofilms that the natural environment provides is complicated in a lab setting. The CDC biofilm reactor offers reliable, repetitive and realistic conditions for biofilms to develop, where they can express their natural phenotype (Williams & Bloebaum, 2010). The CDC biofilm reactor has been extensively used to form hydrated biofilms that are well adhered and statistically reproducible on 24 coupons (Goeres *et al.*, 2005; Hadi *et*

al., 2010). Almatroudi *et al.* (2015) developed a method that was reproducible in producing dehydrated *S. aureus* biofilms, comparable to those formed on dry hospital clinical surfaces in ICUs for disinfectant testing. *S. aureus* ATCC 25923 biofilms grown on PC coupons in a CDC biofilm were dehydrated using alternating cycles of dehydration for 12 days. Multi-layered biofilms were surrounded by dense EPS containing 10^7 cfu/coupon. Biofilms formed in the CDC biofilm reactor were with 30.74 ± 2.1 µm thick whereas biofilms on clinical surfaces were between 24 and 47 µm. The coefficient of variation within each run was 9.5% and between each run was 10.1% suggesting that this model is appropriate to replicate clinical biofilms as well as being user friendly and cost effective (Almatroudi *et al.*, 2015). The biofilms of *S. aureus* formed *in vitro* in this chapter ranged between 18 to 19 µm, which in comparison to the work by Almatroudi *et al.* (2015), is thinner.

The *in vitro* method chosen to form biofilms can affect biofilm growth, and characteristics such as cell density of biofilm growth can vary depending on the chosen method. For these reasons, the results obtained from 96 well plates and CDC biofilm reactor are not directly comparable. The crystal violet assay was used to assess biofilms of *P. putida* KT2440 at various stages of growth in 96 well plates (Thuptimdang *et al.*, 2015). Biofilm formation at 12 hours and 48 hours were 6 and 5 times higher than the formation at 6 hours under static conditions. The CDC biofilm reactor was used to study the growth of *P. putida* KT2440 biofilms under dynamic conditions and the total carbohydrate content was measured. The biofilms at 30 hours and 48 hours were 2 and 3 times greater respectively in comparison to 12 hours under dynamic conditions. This variation in growth could be due the different *in vitro* methods used to determine biofilm growth. The total carbohydrate assay solely measures the carbohydrate content in the EPS of the biofilm, as opposed to the crystal violet assay that measures the total biomass from the EPS, live and dead cells combined (Thuptimdang *et al.*, 2015). *S. epidermidis* ATCC 12228 was unable to form biofilms in 96 well plate models using the crystal violet assay, whereas formed biofilms readily in flow cells (Dice *et al.*, 2009). This illustrates that biofilm growth cannot be solely determined from 96

well plate methods as this is a less robust system in comparison to the CDC biofilm reactor. Similar observations were made during this study whereby when *P. aeruginosa* (7.86 and 7.85 $\log_{(10)}$ cfu/ml on PC and SS coupons respectively) and *S. aureus* (7.09 and 7.06 $\log_{(10)}$ cfu/ml on PC and SS coupons respectively) biofilms were produced in the CDC biofilm reactor (Figure 3.6), analysis of biofilm topography and depth could be assessed (Figure 3.7e and f).

3.4.3 Conclusion

In conclusion, after the comparison of the 96 well plate and CDC biofilm reactor methods for biofilm formation, an understanding of the advantages and disadvantages of both methods has been obtained allowing for an informed approach to studying biofilms related to HCAIs. The crystal violet assay allows for high throughput screening thus being ideal for the initial screening of antimicrobials, although the semi-quantitative data produced only gives an indication of efficacy and can be highly variable thus not suitable for in depth analysis of antimicrobials effects against biofilms. However, the CDC biofilm reactor provides a quantitative method that can go further than the 96 well assays in replicating environmental conditions, the data generated is also reproducible with low SE. With the increasing resistance to antimicrobials, and the demand for novel antimicrobials, gaining a better insight into the formation of biofilms for efficacy testing is essential.

Chapter 4

Chapter 4: Metals in a Suspension

4.1 Introduction

4.1.1 Metal and Metal Oxide NPs as Antimicrobials

Multidrug resistant bacteria are a major concern in the healthcare arena due to infectious diseases commonly being the reason for mortality. This has arisen due to the broad use and misuse of antibacterial drugs (Chen *et al.*, 2014). Furthermore, the environment serves as a reservoir for microorganisms, and although there are various disinfectants available on the market, they have moderate or insufficient disinfection capabilities (Pitten *et al.*, 2003). The effective management of bacterial infections and the development of alternative means to tackle antibiotic and disinfectant resistance are vital to control and prevent persister cells residing in biofilms, the spread of HCAIs and cross-resistance (Simões *et al.*, 2007).

Alternative antimicrobial candidates that bacteria have limited resistance to include metal and metal oxide NPs, including Ag (Sotiriou & Pratsinis, 2010), Cu (Yoon *et al.*, 2007), CuO (Ren *et al.*, 2009), Cu_2O (Ren *et al.*, 2009) and ZnO (Liu *et al.*, 2009). NPs are typically less than 100 nm in size; their small size and high surface to volume ratio allows for close interactions with the bacterial cell, increasing their efficacy as an antimicrobial (Allaker, 2010; Morones *et al.*, 2005). Inorganic antimicrobial agents including metal and metal oxides are favourable for antimicrobial use due to their stability in comparison to organic compounds (Sawai, 2003; Sondi & Salopek-Sondi, 2004).

4.1.2 The Antimicrobial Efficacy of Metal/Metal Oxide NPs

Over 90% of bacteria are known to live in biofilms (Toole *et al.*, 2000), which enable them to reside on surfaces, and build protection mechanisms to prevent eradication by commercial antimicrobials and disinfectants at working concentrations. Yet, the majority of studies published on the antimicrobial efficacy of metal/metal oxide NPs are based on planktonic cells. In order to combat HCAIs, it is essential to assess new novel antimicrobials such as metal/metal oxide NPs against biofilms.

Over the last few decades, with the aid of nanoscience and nanotechnology, metal and metal oxide NPs such as Ag, Cu and CuO NPs have been utilised for their antimicrobial properties (Pandiyarajan *et al.*, 2013). The antimicrobial efficacy of Ag^{+} and Cu^{2+} ions have been extensively used for treatment of burn wounds, dental applications and catheters (Kim *et al.*, 2007). CuO nanostructures are widely used due to their sensory (Umar *et al.*, 2009), catalytic (Yang *et al.*, 2010), optical (Yu *et al.*, 2004) and antimicrobial (Azam *et al.*, 2012a) applications.

S. aureus, *K. pneumoniae* (Hanh *et al.*, 2016), *E. coli* and *P. aeruginosa* (Logeswari *et al.*, 2015) are all examples of bacterial species that have shown susceptibility to Ag NPs. The antimicrobial properties of Ag^{+} ions and Ag based antimicrobial agents against various bacterial species make them ideal for use in the medical industry (Furno *et al.*, 2004; Prakash *et al.*, 2013). Ag is usually in the form of a nitrate when exhibiting an antimicrobial activity, however, when Ag NPs are used, there is an increase in surface area, resulting in greater antimicrobial activity (Ahmed *et al.*, 2015). Ag NPs are known to work on bacterial cells by causing cell lysis or growth prevention through many modes of action (Kim *et al.*, 2007; Prabhu & Poulose, 2012). For instance, Ag can bind with thiol groups, inactivating enzymes (Feng *et al.*, 2000; Chen & Schluesener, 2008).

The antimicrobial effect of Ag NPs (concentrations ranging from 0.0976 to 100 µg/ml), Ag nanorods and Ag nanoplates against *S. aureus* ATCC 51153 and *E. coli* ATCC 35218 was investigated (Sadeghi *et al.*, 2012). Ag nanoplates, Ag nanorods and Ag NPs exhibited growth

inhibition zones of 9 and 4 mm, 6 and 3 mm and 2 and 1 mm for *S. aureus* and *E. coli* respectively. Ag nanoplates had the largest surface area and greatest antimicrobial efficacy, highlighting the importance of surface area on antimicrobial activity. A 2 $\log_{(10)}$ reduction was observed by Velázques-Velázquez *et al.* (2015) when commercial dressings containing 250 ppm of Ag NPs (9.3 ± 1.1 nm) were used against *P. aeruginosa*. Park *et al.* (2013) compared the antimicrobial efficacy of 10 mg/l Ag NPs and 1.0 mg/l Ag^+ ions against biofilms of *P. aeruginosa* PA01. In two day old *P. aeruginosa* biofilms grown on glass coupons, the Ag^+ ions resulted in more than a 2 $\log_{(10)}$ reduction after a 150 mins, whereas only a 0.3 $\log_{(10)}$ reduction was observed with a 150 min exposure to Ag NPs, suggesting the antimicrobial effect was predominantly due to Ag^+ ions, possibly due to lower penetration of Ag NPs into the biofilm. An MIC of 12.5 µg/ml of spherical shaped Ag NPs against both *P. aeruginosa* and *E. coli* after 24 hours was reported by Mohan *et al.* (2014). Bae *et al.* (2010) and Choi and Hu *et al.* (2008) have shown that Ag NPs give higher toxicity to bacteria than Ag^+ ions, contrasting with findings from Park *et al.* (2013), however, factors such as surface coatings (El Badawy *et al.*, 2011), variation in particle sizes (Choi & Hu, 2008) and ionic ratios (Bae *et al.*, 2010) could have contributed.

Lee *et al.* (2014a) studied the effect of ZnO NPs (<50 nm) against *P. aeruginosa* PA01, *E. coli* 0157:H7 (ATCC 43895), MSSA (ATCC 6538) and MRSA (ATCC BAA-1707). *P. aeruginosa* biofilm growth was inhibited on a polystyrene surface at 1 mM by more than 95%. The reduction in optical density showed that biofilms of MSSA, MRSA and *E. coli* 0157:H7 were inhibited at 5mM of ZnO NPs (Lee *et al.*, 2014a). This correlates with findings by Ragupathi *et al.* (2011) where a 5 mM colloidal suspension of ZnO NPs with an average diameter of 12 nm showed a 95% growth inhibition of a range of hospital and community acquired MRSA strains and MSSA. Jones *et al.* (2008) compared the effect of ZnO ultrafine powder (>1 µm), ZnO NP (mean particle size 8 nm) and ZnO nanopowder (mean particle size 50-70 nm) to test their antimicrobial activity against *S. aureus* RN6390. A *ca* 50% reduction in growth rates of *S. aureus* RN6390 was observed for ZnO ultrafine powder and ZnO nanopowder, which had larger particle sizes in comparison to

ZnO NPs. ZnO NPs showed a 99% growth reduction in a colloidal suspension at 2 mM, demonstrating that smaller particle sizes have an enhance antimicrobial effect. Emami-Karvani and Chehrazi (2012) reported the ZnO NPs MIC values of *E. coli* and *S. aureus* were 1 and 0.5 mg/ml respectively. ZOI of 29 and 19 mm for *S. aureus* and *E. coli* were observed respectively for 10 mg/ml of ZnO NPs, suggesting the enhanced effectivity of ZnO NPs against Gram-positive bacteria.

CuO NPs with a particle size ranging between 15-30 nm were assessed for their antimicrobial efficacy against vegetative cultures of *P. aeruginosa* BS3, *Bacillus circulens* BP2, *E. coli* and *S. aureus* at concentrations of 1, 2.5 and 4 mg/ml (Das *et al.*, 2013). A concentration of 1 mg/ml and 4 mg/ml showed inhibition of *E. coli* after 9 hours and 3 hours respectively. All concentrations tested against *S. aureus* showed inhibition at 6 hours, while *Bacillus cereus* was inhibited at all concentrations after 12 hours. Notably, a significant decrease of *P. aeruginosa* growth was shown after a 4 hour treatment with 4 mg/ml of CuO NPs (Das *et al.*, 2013). Gram-negative bacteria have between 3-20 fold less negatively charged peptidoglycans, therefore are less susceptible to positively charged antimicrobials (Kawahara *et al.*, 2000).

Many studies have shown MIC concentrations of CuO NPs between a range of 31.25 to 120 µg/ml (Padil & Černík, 2013; Ahamed *et al.*, 2014; Azam *et al.*, 2012b). Azam *et al.* (2012b) and Padil and Černik (2013) determined the MIC of CuO NPs as 120 µg/ml and 103 µg/ml against *S. aureus* and *E. coli* respectively; Azam *et al.* (2012b) used particle sizes of 20 nm, whereas Padil and Černik (2013) used particle sizes of 4.8 nm. Ahamed *et al.* (2014) determined the MIC of CuO NPs (23 nm) as 31.25 µg/ml against *E. coli*, which is lower than the those found by Azam *et al.* (2012b) and Padil and Černik (2013). Smaller particle sizes have shown to have enhanced antimicrobial efficacy (Jones *et al.*, 2008), however a lower MIC value was obtained by Ahamed *et al.* (2014), even though Azam *et al.* (2012b) and Padil and Černik (2013) used a larger CuO NP particle size.

4.1.3 Antimicrobial Action of Metals in Synergy

Synergistic approaches are widely used when developing antimicrobials because they often have positive clinical implications and can lower the occurrence of resistance, especially with multidrug resistance being an ongoing problem (Cassone & Otvos, 2010; Anantharaman *et al.*, 2010; Sueke *et al.*, 2010; Worthington & Melander, 2013). The combination of two antimicrobials are only effective if there are no antagonistic interactions present between components resulting in a reduced antimicrobial effect of one or both components in the presence of each other. Furthermore, additivity or synergy can lower the concentrations of toxic ions required to inhibit bacterial cells, thus reducing potential adverse side effects (Walkenhorst *et al.*, 2014). Prior studies have reported the use of metals in combination with another antimicrobial such as Ag^{+} ions with *Menthapiperita* essential oil (Ahmad *et al.*, 2014), Ag NPs with amoxicillin (Jyoti *et al.*, 2015; Fayaz *et al.*, 2010) or banana peel extract (Ibrahim, 2015), resulting in a greater inhibitory effect at lower concentrations than using the metal NPs alone.

It is important to consider the impact of NPs on humans and the environment. For instance, the toxicity of Ag NPs has been investigated in humans and have shown to exhibit cytotoxic behaviour even in low concentrations, which can affect the physiology of eukaryotic cells, preventing replication as well as damaging the morphology of the structure, leading to the loss of vital cell functions (Arora *et al.*, 2008; Shin *et al.*, 2007). Furthermore, the impregnation of Ag NPs in clothes and washing systems can mean that the NPs can leach into the environment during washing, harming beneficial bacteria that are essential for the environment, and can endanger organisms in the lakes and streams (Impellitteri *et al.*, 2009). When investigating the antimicrobial efficacy of metal NPs, it is vital to minimise the toxic effects of the metal NPs to humans and the environment by keeping the concentrations low, or considering synergism with other metal/metal oxide NPs.

Jafari *et al.* (2011) studied the antibacterial efficacy of mono metallic nanocrystals Ag, ZnO and composite nanocrystals of Ag/ZnO in combination, with MICs for ZnO of 512, 256, 128 and 64

µg/ml for *B. subtilis*, *S. aureus* and *P. aeruginosa*, *S. galinarium* and *E. coli* respectively. The MIC for Ag NPs for *S. aureus*, *E. coli*, were 1024 and 2048 µg/ml respectively and >4096 µg/ml for *S. galinarium*, *B. subtilis* and *P. aeruginosa*. However, the MIC for Ag/ZnO NPs in a composite nanocrystal for *S. galinarium*, *E. coli*, *P. aeruginosa*, *S. aureus* and *B. subtilis* was 32, 32, 64, 128 and 128 µg/ml respectively. Lower MICs were found by Egger *et al.* (2009) when a range of microorganisms including *E. coli* and *S. aureus* were tested for their susceptibility to Ag-Si nanocomposites. MIC values ranging between 62.5 and 500 µg/ml (containing 12.5 to 100 µg/ml of pure Ag) were obtained for Ag-Si nanocomposites. The MICs were higher when compared to $AgNO_3$ and silver zeolite as they both dissolve readily, releasing Ag^+ rapidly, therefore, the effect is instant but short lived. Ag^+ in the nanocomposite is released slower, providing a sustained release (Egger *et al.*, 2009; Kumar *et al.*, 2005). Ag/silicon dioxide (SiO_2) samples provided reductions of >5.06, >5.17 and >4.54 $\log_{(10)}$ for *E. coli*, *S. aureus* and *C. albicans* respectively (Mukha *et al.*, 2010). The efficacy of MgO and nisin (an antibacterial peptide) in synergy was observed by Jin and He (2011). In contrast, Vidic *et al.* (2013) reported that 80% of *E. coli* cells remained viable after a 24 hour treatment with ZnO-MgO in combination, showing inefficacy of synergy, whereas a complete inhibition of *B. subtilis* at 1 mg/ml was noted, suggesting a greater affinity of ZnMgO to Gram-positive cell walls. Ag-Au alloy NPs in combination with penicillin G and piperacillin against *S. aureus* gave an increase in ZOI surface area by 193.8% (Bahrami *et al.*, 2014).

4.1.4 Mechanisms of Action of Metal/Metal Oxide NPs

Metal/metal oxide NP vary in the way they exert their antimicrobial effect such as ROS formation, oxidative stress, lipid peroxidation, damage to the cell wall, release of metal ion and particle-cell interactions (Djurišić *et al.*, 2015). A proposed mechanism of action of Ag NPs (Ag^0 metallic and Ag^+ ions) against biofilms is *via* interference and/or regulation of exopolysaccharide. For instance, in *P. aeruginosa*, the exopolysaccharide production is controlled by a gene cluster of 15 genes

(Matsukawa & Greenberg, 2004), and the inhibition of proteins *via* Ag NPs hinder exopolysaccharide synthesis. Ionisation of Ag NPs to form Ag^+ ions interact with the protein and enzyme thiol groups (i.e. cysteine) of the bacteria increasing cell damage (Velázquez-Velázquez *et al.*, 2015). Ag NPs have a greater capability than elemental Ag for attaching or penetrating into bacterial membranes, and therefore accumulate inside bacterial cells enabling a sustained release of Ag^+ ions within the cell (Ansari *et al.*, 2013, Ansari *et al.*, 2014b; Rai *et al.*, 2009). Ag NPs are also thought to hinder the QS process through gene activation/inactivation, preventing the QS system working efficiently and reducing biofilm (Majik & Parvatkar, 2014). The resistance of Ag NPs to mature biofilms can be due to various factors. Firstly, bacterial cells in mature biofilms are usually in the stationary phase and are likely to be less susceptible to antimicrobial agents (Anderl *et al.*, 2003). Secondly, dead cells in the outer layers of the mature biofilms can act as a source of nutrients to encourage growth in the deeper layers of the biofilm (Ito *et al.*, 2009).

Cell membrane disruption by CuO causes cell enzyme malfunction, as they are able to pass through the cell membranes of bacteria directly (Ren *et al.*, 2009). The Cu^{2+} ions released can bind with bacterial DNA, resulting in damage to its helical structure by initiating cross linking among the nucleic acid strands, hindering replication (Pandiyarajan *et al.*, 2013). Additionally, Cu^{2+} ions released from the NPs can attach to the negatively charged cell wall of the bacteria, causing rupturing, inducing protein denaturation and cell death (Sondi & Salopek-Sondi, 2004).

Zn^{2+} is an crucial trace element required for bacterial growth (Gielda & DiRita, 2012), yet higher concentrations of Zn^{2+} can exhibit toxicity against bacterial cells (Jones *et al.*, 2008). ZnO as an antimicrobial is known to inhibit the attachment and viability of microorganisms on nosocomial surfaces (Yamamoto *et al.*, 2001; Brayner *et al.*, 2006). The release of Zn^{2+} from ZnO NPs and the generation of ROS results in inhibition of bacterial species (Sirelkhatim *et al.*, 2015) such as *S. aureus, E. coli* and *L. monocytogenes* at concentrations between 5 and 8 mM of ZnO (Firouzabadi *et al.*, 2014). However, Premanathan *et al.* (2011) reported MICs for ZnO of 500, 500 and 125 µg/ml for *E. coli*, *P. aeruginosa* and *S. aureus* respectively. Various mechanisms of

action of ZnO have been proposed. For instance, ZnO NPs are able to interact with membrane lipids, hindering the structure of the membrane, reducing membrane integrity, causing malfunction and eventually bacterial cell death (Krishnamoorthy *et al.*, 2012; Zhang *et al.*, 2007). ZnO also has the ability to penetrate inside the bacteria at a nanoscale level leading to the formation of toxic oxygen radicals, causing DNA, cell membrane or cell protein damage and ultimately bacterial growth inhibition and cell death (Applerot *et al.*, 2009; Irzh *et al.*, 2010; Makhluf *et al.*, 2005; Zhang *et al.*, 2007).

4.1.5 Conclusion

As a result of the ever-increasing issue of resistance to disinfectant and antimicrobials, there is a constant need for novel antimicrobials. Many studies have focussed on the efficacy of metal/ metal oxide NPs on vegetative cells and have shown significant reductions as described above. With the lack of knowledge in the differences in disinfectant efficacy between planktonic and sessile cells, and their phenotypic variation, this is an area that needs further investigation. Antimicrobials that are effective against planktonic cultures will not necessarily have the same efficacy on biofilms. Currently, there are no European standards in place for the efficacy of biocides on biofilms comprised of Gram-negative organisms (Perumal *et al.*, 2014). BS EN 13697:2001 is the European Standard for chemical disinfectants and antiseptics that disinfection products need to comply to (British Standards Institute, 2001), however this mainly focusses on vegetative cells. Future standards need to clarify the efficacy of disinfectants on biofilms, to ensure their efficacy in a laboratory is comparable to a clinical setting (Lindsay & von Holy, 2006). The promising antimicrobial efficacy of metal/metal oxide NPs against a wide variety of bacterial species maybe a potential solution to the issue of antimicrobial resistance in biofilms.

4.1.6 Aims and Objectives

Aim:

The aim of this investigation was to establish the antimicrobial properties of Ag, CuO and ZnO suspensions against mature biofilms of *P. aeruginosa* and *S. aureus.*

Objectives:

- To determine the MBRC of Ag, ZnO and CuO against *P. aeruginosa* and *S. aureus* biofilms.
- To investigate possible synergistic relationships between metal and metal oxide NPs against *P. aeruginosa* and *S. aureus* biofilms using the checkerboard method.
- To assess the effects of metal and metal oxide NPs on *P. aeruginosa* and *S. aureus* biofilms using SEM and CLSM.

4.2 Methods

4.2.1 Particle Size Distribution

Ag nanopowder <100 nm particle size (576832), ZnO nanopowder <50nm particle size (677450) and CuO nanopowder (copper (ii) oxide) <50 nm (544868) were all purchased from Sigma Aldrich (Dorset, UK).

The distribution of particle size of Ag NPs and ZnO NPs within the batch was measured using zeta sizer (Nanobrook Omni Zeta Sizer, New York, USA). Aliquots of 2 ml of 1 mM potassium nitrate (KNO_3) was used to dissolve ~1mg of Ag or ZnO NP sample and left to stand for 15 mins before the particle size distribution was measured in the zeta sizer at 659 nm.

4.2.2 Neutralisation of Metal/Metal Oxide NPs

4.2.2.1 Neutraliser Content

One gram of sodium thioglycollate (S/7140, FSA Laboratories) and 1.46g of sodium thiosulphate (S/7420, FSA Laboratories) was added to one litre of distilled water. All neutraliser tests were based on BS EN 1276:2009 (E).

4.2.2.2 Neutraliser Toxicity

A bacterial count of 10^3 cfu/ml of either *P. aeruginosa* or *S. aureus* was prepared from a 24 hour culture. A solution of 8 ml of neutraliser, 1 ml of sterile water and 1 ml of bacterial suspension was left to stand for 5 mins ± 10 seconds at 20°C ± 1°C. The suspension was then vortexed and 0.1 ml was spread plated onto NA and incubated at 37°C for 24 hours. The neutraliser was deemed

as non-toxic if the $\log_{(10)}$ cfu/ml was identical to the $\log_{(10)}$ cfu/ml with the samples that were not exposed to the neutraliser.

4.2.2.3 Neutraliser Method Validation

A bacterial count of between 10^2 cfu/ml and 10^3 cfu/ml of either *P. aeruginosa* NCTC 6749 or *S. aureus* ATCC 6538 was prepared from a 24 hour culture. A volume of 2 ml of the highest concentration of each of the three metal and metal oxide NP suspensions were added to 1 ml of sterile water and 8 ml of neutraliser and left to stand for 5 mins ± 10 seconds at 20°C ± 1°C. After 5 mins, 1.0 ml of the previously prepared inoculum was added to the tube and left to stand for 30 mins ± 1 min at 20°C ± 1°C. Aliquots of 0.1 ml of the sample was plated and incubated at 37°C ± 2°C for 24 hours and then enumerated. Validity of the neutraliser was based on whether the $\log_{(10)}$ cfu/ml were similar to those of non-neutralised samples post treatment with metal or metal oxide NP suspensions.

4.2.3 Culture Methods and Microorganisms

The test organisms used were *P. aeruginosa* NCTC 6749 and *S. aureus* ATCC 6538. All culture media was acquired from Oxoid Ltd. unless otherwise stated. Clinical strains of MRSA NCTC 12497 and *P. aeruginosa* MG756624Z were obtained from a skin lesion and a sputum sample from a cystic fibrosis patient respectively.

Strains were stored on beads at -80°C. Cetrimide agar for *P. aeruginosa* and Mannitol salt agar for *S. aureus* was used to phenotypically determine the organisms.

Organisms were grown on NA and then 1 colony per 10 ml of NB was grown aerobically for 24 hours at 37 °C. NA was used to culture the bacteria for viable count enumeration.

4.2.4 Determination of MBRC Using 96 well Plates

A 24 hour culture of *P. aeruginosa* or *S. aureus* in NB was prepared and placed in a rotating incubator at 100 rpm at 37°C. Aliquots of 200 µl of culture was then transferred into 96 well plates and incubated in rotating incubator at 37°C for 9 days for *S. aureus* and *P. aeruginosa*. The wells were replenished daily with 200 µl of broth. The plates were washed twice with PBS to remove any planktonic bacteria. The metal/metal oxide NP suspensions at doubling concentrations of metal and metal oxide NP suspension; Ag from 3 to 6400 µg/ml, ZnO; 1 to 1,024 µg/ml and CuO; 20 to 10,000 µg/ml were sonicated for 10 mins. Aliquots of 200 µl of each suspension was added to the wells and placed in the rotating incubator for 24 hours at 100 rpm at room temperature. A crystal violet assay was carried out as per Method 3.2.2 and the absorbance was read at 595 nm.

4.2.5 MBRC Determination Using a CDC Biofilm Reactor

P. aeruginosa or *S. aureus* biofilms were grown according to Method 3.2.3.1 and 3.2.3.2 using PC coupons only.

4.2.5.1 Sampling

PC coupons were removed from the CDC biofilm reactor and placed in 2 ml of doubling concentrations of metal and metal oxide NP suspension as stated in Method 4.2.4 and placed in a rotating incubator for 24 hours at 100 rpm at room temperature. Metal and metal oxide NP suspensions were sonicated for 10 mins prior to usage. Coupons in sterile water were used as controls. The coupons were then placed in 8 ml of neutraliser at 20°C for 5 mins. The samples were enumerated as per Method 3.2.3.3, spread plated, incubated at 37°C for 24 hours. The MBRC was termed as the lowest concentration of metal and metal oxide NP suspensions required

to provide a ≥3 $\log_{(10)}$ reduction (Dosunmu *et al.*, 2015; Gomes *et al.*, 2012). The correlation between metal and metal oxide NP concentrations for Ag, CuO and ZnO up to and including the MBRC was plotted against the $\log_{(10)}$ cfu/ml and the R^2 (correlation coefficient) was determined.

4.2.6 Metal and Metal Oxide Combination Treatment in a CDC Biofilm Reactor

PC coupons were removed from the CDC biofilm reactor and placed in 2 ml of the following concentrations of metal and metal oxide NP suspension combinations of ZnO and Ag respectively: 8 and 12 µg/ml, 8 and 25 µg/ml, 8 and 50 µg/ml, 8 and 100 µg/ml, 16 and 12 µg/ml, 16 and 25, 16 and 50 µg/ml, 16 and 100 µg/ml, 32 and 12 µg/ml, 32 and 25 µg/ml, 32 and 50 µg/ml, 32 and 100 µg/ml, 64 and 12 µg/ml, 64 and 25 µg/ml, 64 and 50 µg/ml, 64 and 100 µg/ml. Metal and metal oxide NP suspensions were sonicated for 10 mins prior to usage. The samples were placed in a rotating incubator for 24 hours at 100 rpm (room temperature) and coupons were then placed in 8ml of neutraliser at 20°C for 5 mins. The biofilm was enumerated as per Method 3.2.3.3, spread plated and incubated at 37°C. Coupons in sterile water were used for the controls. The factorial inhibitory concentration (FIC) was then calculated. The FIC was calculated using the following equation:

$$\Sigma FIC = FIC_{ZnO} + FIC_{Ag} = (C_{ZnO}/MIC_{ZnO}) + (C_{Ag}/MIC_{Ag})$$

where MIC_{ZnO} and MIC_{Ag} are the MICs of ZnO and Ag alone, and C_{ZnO} and C_{Ag} are the concentrations of Ag and ZnO in combination.

An FIC value of ≤0.5 = synergy, >0.5 to ≤1.0 = additivity, >1 to ≤4.0 = indifference and >4.0 = antagonistic. The most effective combination of ZnO/Ag NP suspensions was tested against a clinical strain of MRSA and against *P. aeruginosa.*

4.2.7 Polymicrobial Biofilms in a CDC Biofilm Reactor

Biofilms were formed in the CDC biofilm reactor as per Method 3.2.3.1 and 3.2.3.2 however; the reactor was inoculated with 1 ml of overnight culture of *P. aeruginosa* and a 1 ml of overnight culture of *S. aureus* simultaneously. Metal and metal oxide NP suspensions were sonicated for 10 mins prior to usage. Coupons in sterile water were used as a control. The coupons were then placed in a suspension of 32/25 µg/ml of ZnO/Ag suspension for 24 hours in a rotating incubator at 100 rpm (room temperature) and then enumerated as per Method 3.2.3.3.

4.2.8 Time Point Analysis in a CDC Biofilm Reactor

Biofilms of *P. aeruginosa* and *S. aureus* were grown on PC coupons in the CDC biofilm reactor as per Method 3.2.3.1 and 3.2.3.2. Metal and metal oxide NP suspensions were sonicated for 10 mins. The coupons were individually placed in 2 ml of 8/12 µg/ml of ZnO/Ag suspensions for *S. aureus* biofilms and 32/25 µg/ml of ZnO/Ag suspensions for *P. aeruginosa* biofilms in a rotating incubator at 100 rpm (room temperature) for 24 hours. Coupons in sterile water were used for the controls. The coupons were removed from the metal and metal oxide NP suspensions at 1, 2, 4, 6, 8 and 24 hours, neutralised as per Method 4.2.5.1, enumerated as per Method 3.2.3.3, spread plated and incubated at 37°C for 24 hours.

4.2.9 AAS

Universals containing 10ml of all combination suspensions of ZnO/Ag: 8/12, 8/25, 8/50, 8/100, 16/12, 16/25, 16/50, 16/100, 32/12, 35/25, 32/50, 32/100, 64/12, 64/25, 64/50 and 64/100 µg/ml and individual suspension of Ag: 12, 25, 50 and 100 µg/ml and ZnO: 8, 16, 32 and 64 µg/ml were placed in a rotating incubator at room temperature for 24 hours at 100 rpm. The metal and metal oxide NP suspensions were pelleted by centrifugation at 4000 rpm for 1 hour and the supernatant

was used to measure the concentration of ions present using Atomic Absorption Spectroscopy (AAS) (PerkinElmer, AA2DD, Beaconsfield, UK) with a hollow cathode Ag and Zn lamp. The concentration of Ag^+ ions was determined using a standard curve.

4.2.10 SEM and EDX

Biofilms of *P. aeruginosa* and *S. aureus* were grown on PC coupons in the biofilm reactor as per Method 3.2.3.1 and 3.2.3.2. Metal and metal oxide NP suspensions were sonicated for 10 mins prior to usage. *P. aeruginosa* biofilms were treated for 24 hours in 2 ml of 32/25 µg/ml ZnO/Ag NP suspensions and *S. aureus* biofilms were treated with 2 ml of 8/12 µg/ml of ZnO/Ag NP suspensions. PC coupons in sterile water was used for the controls. PC coupons were washed with PBS and fixed with 95% ethanol for 10 mins at room temperature. PC coupons were then mounted onto aluminium stubs and coated with 15 nm of gold in a gold coater (Quorum Q150 RS, East Sussex, UK), ready for imaging. Biofilms were visualised using SEM (Evo HD15 Carlzeiss, Jena, Germany). EDX analysis was performed (EDX software X-max 80mm^2, Oxford Instruments, Oxfordshire, UK).

4.2.11 CLSM

Biofilms of *P. aeruginosa* and *S. aureus* were grown in the CDC biofilm reactor on PC coupons as per Method 3.2.3.1 and 3.2.3.2. *P. aeruginosa* biofilms were treated with 32/25 µg/ml of ZnO/Ag suspensions whereas *S. aureus* biofilms were treated with 8/12 µg/ml of ZnO/Ag suspensions for 24 hours. Coupons in sterile water were used as controls. After 24 hours, the coupons were washed and placed in a 24 well plate with 2 ml of PBS, enough to cover the surface of the coupon. The coupons were then stained with 6 µl of a 1:1 ratio of SYTO® 9 and propidium iodide mixture (Live/dead® BacLight™ Bacterial Viability Kit, Life Technologies, Oregon,

USA) and incubated at room temperature in the dark for 15 mins. After incubation, the coupons were removed from the plate and placed in a new 24 well µ-plate (Ibidi, Martinsried, Germany) alongside 50 µl of the solution from the previous plate to keep the coupon moist. The propidium iodide and SYTO 9 was excited at 476 and 488 nm respectively, between the green emission (500-530 nm) and red emission (600-709 nm). The intact biofilms were observed using the Leica DMIRE2 (Wetzler, Germany) confocal microscope using the oil immersion lens. The Leica Microsystems Confocal Software V 2.61 Build 1537 was used to analyse the images.

4.2.12 Statistical Analysis

Assumption of normality was tested using Kolmogorov-Smirnov test if sample sizes were ≥50 or Shapiro-Wilcox test if samples were <50. For non-parametric data, the Kruskal Wallis test was used and well as the Mann-Whitney U test. Significance was set at $p \leq 0.05$.

All investigations were carried out in triplicate on at least two separate occasions.

4.3 Results

4.3.1 Particle Size Distribution

The particle size distribution curves showed that the ZnO particle sizes are between 45 to 60 nm and Ag particle sizes are between 100 to 120 nm (Figure 4.1).

a)

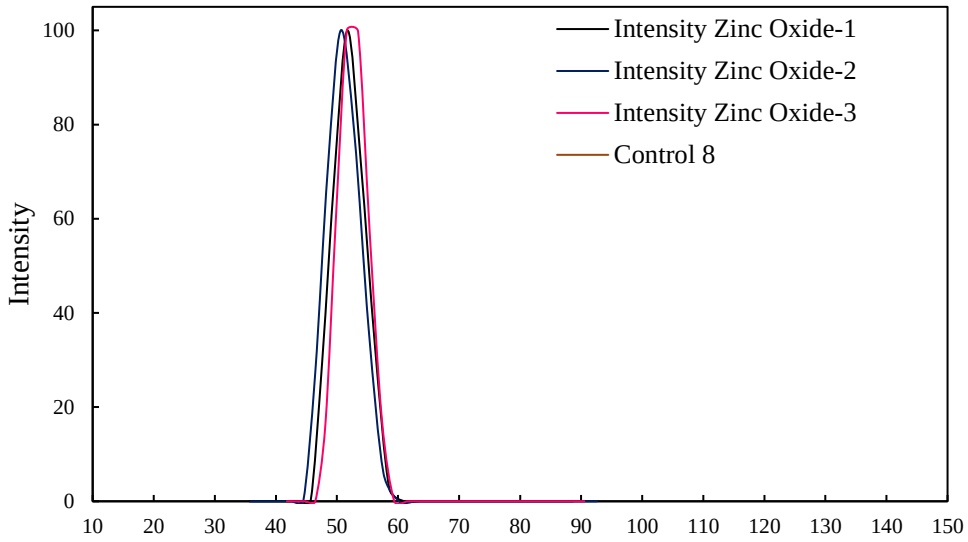

b)

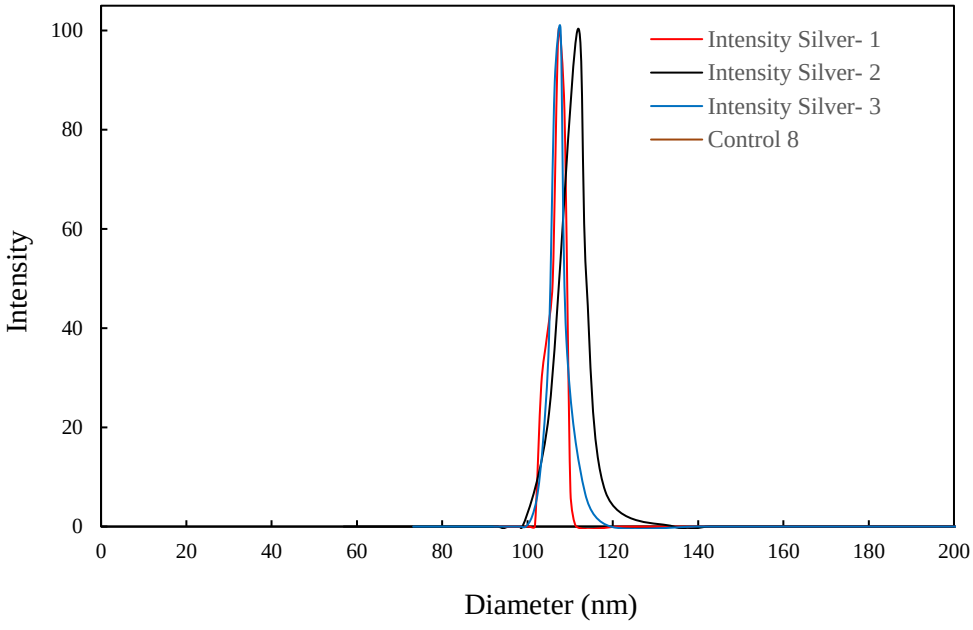

Figure 4.1: Particle size distribution of a) ZnO NPs and b) Ag NPs.

4.3.2 MBRC and R^2 Correlations

Initially, 96 well plates were used to screen metal/metal oxide NP suspensions individually in the concentrations stated in Method 4.2.4. However, due to the large variation in SE, for example 0.22, 0.43 and 0.27 for CuO NPs (20 µg/ml), Ag NPs (3 µg/ml) and ZnO NPs (1 µg/ml) respectively for *P. aeruginosa* (data not shown), and the absorbance (data not shown), the data was disregarded. The agglomeration of Ag NPs in the suspensions left a residue even after washing the wells with PBS, which was hard to eliminate without hindering the actual biofilm formed. The irregularity in the data is consistent with the data obtained in Chapter 3. Henceforth, only the CDC biofilm reactor was used to determine the MBRC. MBRC was termed as the lowest concentration of metal and metal oxide NP suspensions required to provide a ≥ 3 $\log_{(10)}$ reduction (Dosunmu *et al.*, 2015; Gomes *et al.*, 2012) (Table 4.1).

A threshold of ≥ 3 $\log_{(10)}$ reduction was set in order to consider a metal/metal oxide NP suspension as having the potential for development as an antimicrobial. The lowest MBRC required to treat *S. aureus* biofilms was 16 µg/ml of ZnO NPs with a significant reduction ($p \leq 0.05$) from that of the controls of 3.61 $\log_{(10)}$. For *P. aeruginosa*, the MBRC was 50 µg/ml of Ag with a significant reduction ($p \leq 0.05$) from that of the controls of 3.42 $\log_{(10)}$. CuO NPs showed a higher MBRC of 160 µg/ml for *S. aureus* in comparison to the MBRCs observed for ZnO and Ag (Table 4.1). An MBRC of 200 µg/ml of CuO NPs for *P. aeruginosa* biofilms was observed, and a lower R^2 value (0.85) in comparison to ZnO and Ag, therefore, CuO NPs were not taken forward for further investigations. Untreated control PC coupons formed biofilms of 8.16 ± 0.02 $\log_{(10)}$ and 7.38 ± 0.01 $\log_{(10)}$ for *P. aeruginosa* and *S. aureus* respectively (Table 4.1). The R^2 value was determined by plotting the $\log_{(10)}$cfu/ml against a range of concentrations up to the MBRC and assessing the correlation between the two. The R^2 values show the strength of the relationship between the $\log_{(10)}$ cfu/ml and the concentration of the metal/metal oxide NPs. For *P. aeruginosa*, the highest R_2 value was observed for ZnO (0.99) and Ag (0.96). For *S. aureus*, CuO (0.97) and ZnO (0.95) showed the highest R^2 values (Table 4.1, Figure 4.2 and 4.3).

Table 4.1: The MBRC values for metal/metal oxide NPs against *P. aeruginosa* and *S. aureus* biofilms and their correlation coefficients (n=6 ± SE).

	P. aeruginosa MBRC (µg/ml)	*P. aeruginosa* R^2	$Log_{(10)}$ Reduction	*S. aureus* MBRC (µg/ml)	*S. aureus* R^2	$Log_{(10)}$ Reduction
ZnO	256	0.99	3.52 ± 0.03	16	0.95	3.61 ± 0.02
Ag	50	0.96	3.42 ± 0.02	50	0.80	3.65 ± 0.02
CuO	200	0.85	3.39 ± 0.03	160	0.97	3.61 ± 0.01

a)

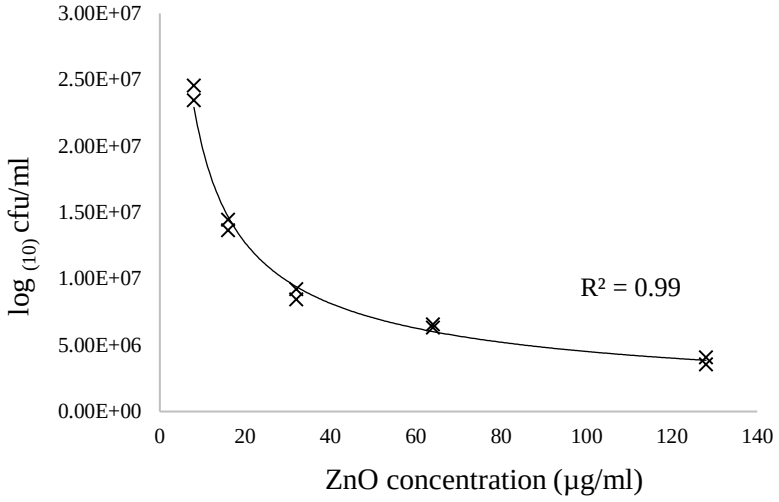

b)

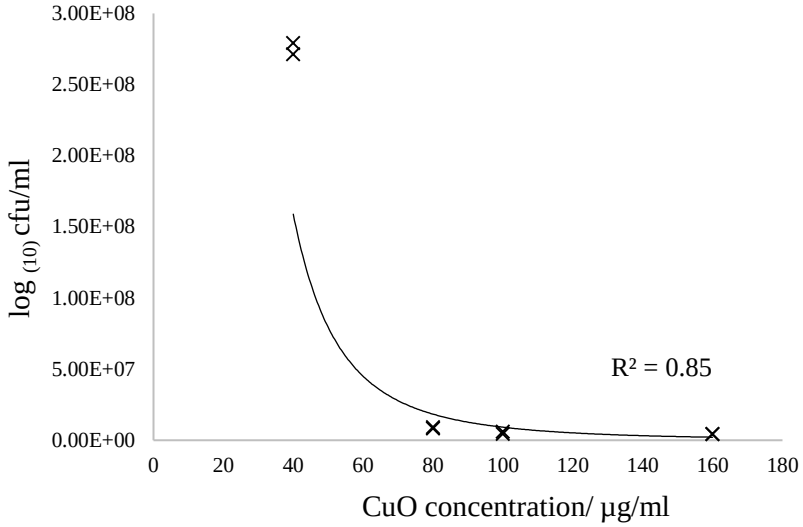

c)

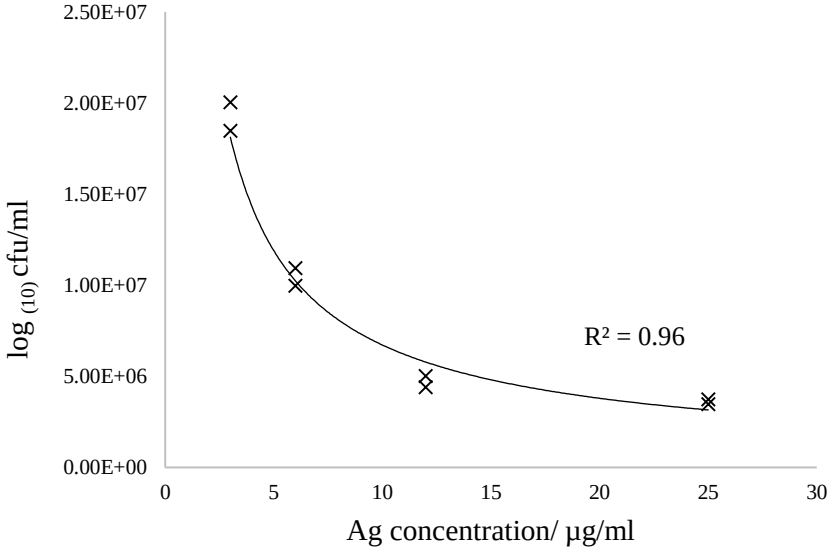

Figure 4.2: Correlation between the $\log_{(10)}$ cfu/ml and metal NP concentration for *P. aeruginosa* biofilms.

a)

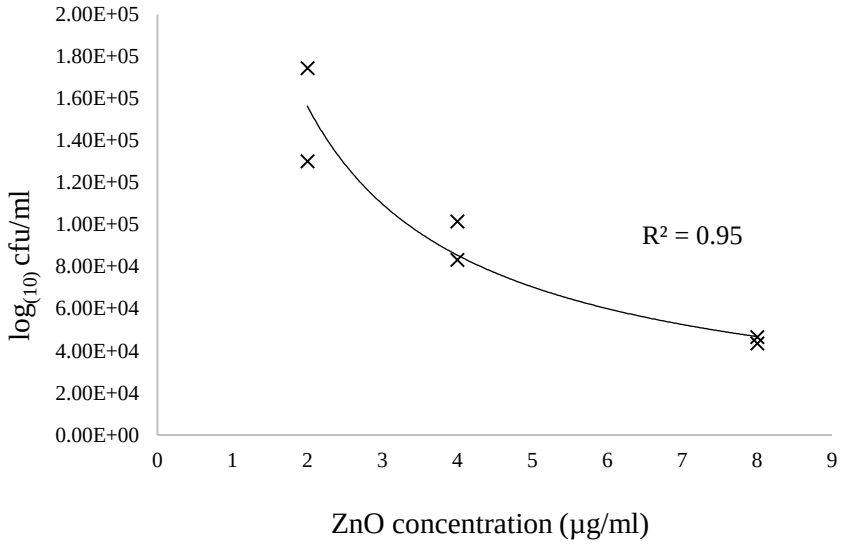

b)

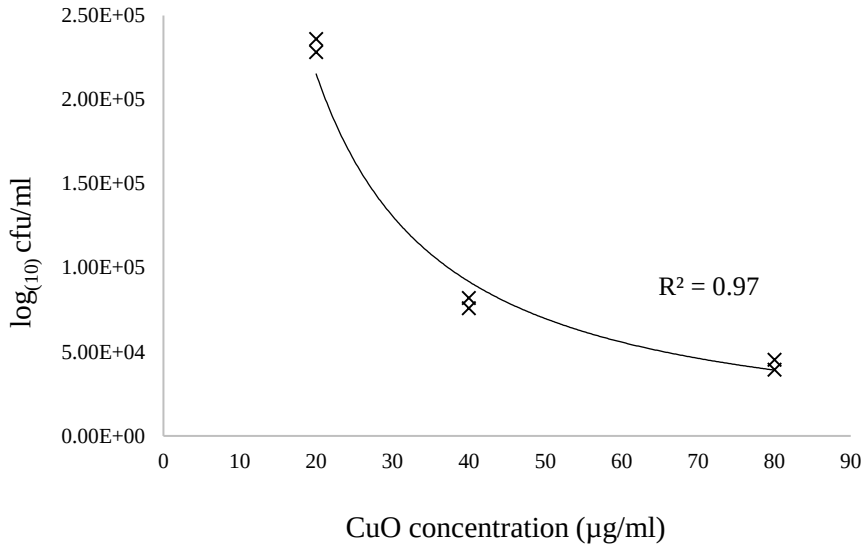

c)

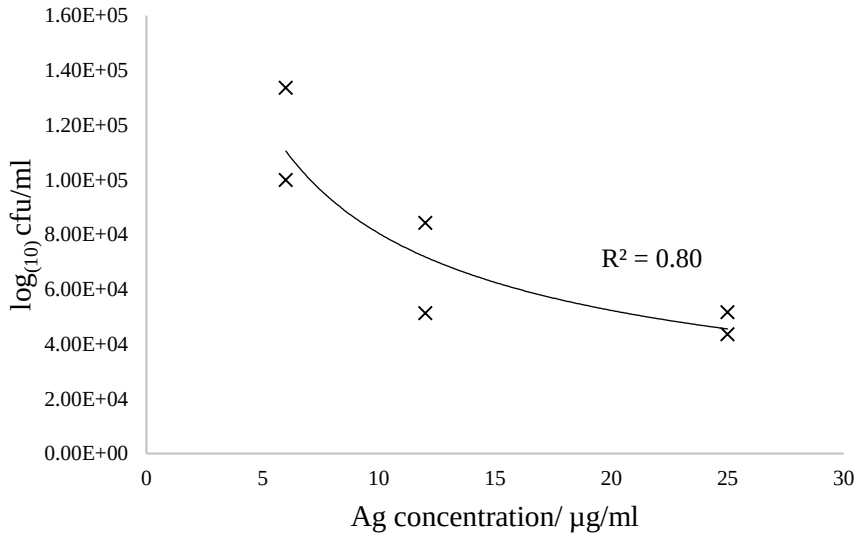

Figure 4.3: Correlation between the $\log_{(10)}$ cfu/ml and metal NP concentration for *S. aureus* biofilms.

4.3.3 Fractional Inhibitory Concentration (FIC) and Combination of Ag and ZnO NP Suspensions

A combination of metal and metal oxide NP suspension was deemed effective if there was a ≥3 $\log_{(10)}$ (99.9 %) reduction in the cfu/ml in comparison to untreated samples. A concentration of 32/25 µg/ml of ZnO/Ag NP suspension respectively was the selected concentration to treat a biofilm of *P. aeruginosa.* This was the lowest concentration of ZnO and Ag NP combinations required to exhibit an antibacterial effect, giving a ≥3 $\log_{(10)}$ (3.77 $\log_{(10)}$) reduction ($p \leq 0.05$), with an additive effect (Table 4.2a), compared with a ZnO (256 µg/ml) and Ag (50 µg/ml) NP suspension when used alone (Table 4.1). For *S. aureus*, 8/12 µg/ml of ZnO/Ag NP suspension was the combination with the lowest concentration of ZnO and Ag NPs suspensions required to give a ≥3 $\log_{(10)}$ (3.91 $\log_{(10)}$) reduction ($p \leq 0.05$) and an additive effect (Table 4.2b), compared with a ZnO (16 µg/ml) and Ag (50 µg/ml) NP suspension when used alone (Table 4.1). Although an additive effect was seen for combinations of 32/25 µg/ml against *P. aeruginosa* and 8/12 µg/ml against *S. aureus* of ZnO/Ag NP suspensions, reductions in biofilms counts were still above the 3 $\log_{(10)}$ threshold. Both combinations gave a significant ($p \leq 0.05$) reduction for *S. aureus* and *P. aeruginosa* biofilms.

Combinations of 8/12 µg/ml and 32/25 µg/ml of ZnO/Ag NP suspensions were also effective against clinical strains of MRSA and *P. aeruginosa* giving a significant ($p \leq 0.05$) reduction of approximately 4 $\log_{(10)}$ (99.99%) (Table 4.3) compared with the controls of 8.42 $\log_{(10)}$ and 8.43 $\log_{(10)}$ for *S. aureus* and *P. aeruginosa* respectively. When a polymicrobial biofilm of *P. aeruginosa* and *S. aureus* was treated with 32/25 µg/ml of ZnO/Ag suspensions, a $\log_{(10)}$ reduction of 3.77 $\log_{(10)}$ and 3.74 $\log_{(10)}$ was noted for *P. aeruginosa* and *S. aureus* biofilms respectively ($p \leq 0.05$).

Table 4.2: Checkerboard showing the FIC relationship and the $\log_{(10)}$ reduction for concentrations of ZnO and Ag in combination that were effective in inhibiting a) *P. aeruginosa* (8.36 $\log_{(10)}$) and b) *S. aureus* (7.43 $\log_{(10)}$) biofilm growth (n=6 ± SE).

a)

Ag (µg/ml) \ ZnO (µg/ml)	8	16	32	64
12				Syn 3.46 ± 0.03
25			Add 3.77 ± 0.01	
50				
100	Add 3.72 ± 0.03			Add 3.51 ± 0.06

b)

Ag (µg/ml) \ ZnO (µg/ml)	8	16	32	64
12	Add 3.91± 0.01		Add 3.77± 0.04	Ant 3.75± 0.05
25	Add 3.88± 0.03		Add 3.77± 0.07	Ant 3.70± 0.04
50	Add 3.67± 0.04	Add 3.77± 0.05	Add 3.75± 0.05	Ant 3.68± 0.07
100	Add 3.86± 0.04	Add 3.73± 0.05	Ant 3.71± 0.03	Ant 3.67± 0.05

Table 4.3: MBRC and $\log_{(10)}$ reductions of *P. aeruginosa* type and clinical strains and *S. aureus* type and clinical strains (n=6 ± SE).

Organism	MBRC of ZnO/Ag NP suspension (µg/ml)	Control ($\log_{(10)}$)	Reduction ($\log_{(10)}$)
P. aeruginosa NCTC 6749	35/25	8.36	3.77 ± 0.01
P. aeruginosa (clinical isolate)	32/25	8.43	3.69 ± 0.02
S. aureus ATCC 6538	8/12	7.43	3.91 ± 0.01
MRSA (clinical isolate)	8/12	8.42	3.81 ± 0.04

4.3.4 Time Point Assay

The results in Table 4.4 shows that a 24 hour treatment is required to achieve a ≥3 $\log_{(10)}$ reduction, before this time point, there is limited reductions in the biofilms. There is a significant difference in biofilm between 1– 8 and 24 hours for *P. aeruginosa* and *S. aureus* ($p \leq 0.05$).

Table 4.4: A 24 hour time point assay for the treatment of *P. aeruginosa* (8.27 $\log_{(10)}$) and *S. aureus* (7.43 ± 0.02 $\log_{(10)}$) biofilms with 32/25 µg/ml and 8/12 µg/ml of ZnO/Ag suspensions respectively (n=6 ± SE).

Hours	*P. aeruginosa* Reduction ($\log_{(10)}$)	*S. aureus* Reduction ($\log_{(10)}$)
1	0.08 ± 0.01	0.05± 0.01
2	0.13 ± 0.01	0.05 ± 0.01
4	0.15 ± 0.01	0.12 ± 0.01
6	0.20 ± 0.01	0.15 ± 0.01
8	0.18 ± 0.01	0.15 ± 0.01
24	3.30 ± 0.02	3.75 ± 0.02

4.3.5 AAS for Ion Release from Metal and Metal Oxide NP Suspensions.

Table 4.5 shows that levels of ZnO above ≥32 µg/ml with low levels of Ag ≤16 µg/ml, or high levels of Ag ≥50 µg/ml with low levels of ZnO ≤16 µg/ml, result in the quenching of Zn^{2+} ions. For example, at individual concentrations of 8 and 50 µg/ml for ZnO and Ag NP suspensions respectively, there are 1.98 and 0.71 mg/l of ions present respectively, however, when there is a ZnO/Ag NP combination suspension of 8/50 µg/mL, there are 1.30 and 0.45 mg/l of Zn^{2+} and Ag^{+} ions respectively. For concentrations of 64/100 µg/ml and 64/50 µg/ml of ZnO/Ag NPs suspension, quenching of both Ag and ZnO occurs (Table 4.5).

Table 4.5: Ion release from Ag and ZnO both in combination and alone.

Ag (mg/l)	ZnO (mg/l)	Ag^+ (mg/l)	Zn^{2+} (mg/l)	Ag^+ in ZnO/Ag suspension (mg/l)	Zn^{2+} in ZnO/Ag suspension (mg/l)	Relationship between Ag^+ and Zn^{2+}
12	8	0.18	1.98	1.61	2.51	Increase in Ag^+/Zn^{2+}
12	16	0.18	2.97	0.89	2.91	Increase in Ag^+
12	32	0.18	3.58	0.35	0.93	Ag^+ quenches Zn^{2+}
12	64	0.18	4.18	0.59	2.24	Ag^+ quenches Zn^{2+}
25	8	0.39	1.98	0.68	1.12	Ag^+ quenches Zn^{2+}
25	16	0.39	2.97	0.26	3.47	No difference
25	32	0.39	3.58	0.50	4.67	Increase in Zn^{2+}
25	64	0.39	4.18	0.43	2.28	Ag^+ quenches Zn^{2+}
50	8	0.71	1.98	0.45	1.30	Ag^+ quenches Zn^{2+}
50	16	0.71	2.97	0.91	3.14	No difference
50	32	0.71	3.58	0.76	2.75	Ag^+ quenches Zn^{2+}
50	64	0.71	4.18	0.66	2.68	Ag^+ quenches Zn^{2+}
100	8	1.35	1.98	0.89	0.85	Ag^+/Zn^{2+} quench each other
100	16	1.35	2.97	1.87	3.22	No difference
100	32	1.35	3.58	1.98	1.66	Ag^+ quenches Zn^{2+}
100	64	1.35	4.18	0.72	3.13	Ag^+/Zn^{2+} quench each other

* A reduction $\geq 3 \log_{(10)}$ was noted for ZnO/Ag NP suspensions at concentrations of 12/16 and 25/16 µg/ml for *S. aureus* and 12/8, 50/8, 12/16 and 25/16 µg/ml for *P. aeruginosa*

4.3.6 SEM and EDX Imaging

Untreated *S. aureus* biofilms show island like biofilm clusters with distinct cocci cells (Figure 4.4a). Similarly, the untreated *P. aeruginosa* biofilms are uniform across the surface and distinct rod shaped cells can be observed (Figure 4.4b). Whereas, the treated biofilms of *P. aeruginosa* and *S. aureus* show clear fragmentation and cells appear to have disintegrated (Figure 4.4c and 4.4d). EDX images show the presence of Ag and ZnO in the treated *S. aureus* and *P. aeruginosa* biofilm (Figure 4.4e, f, g and h).

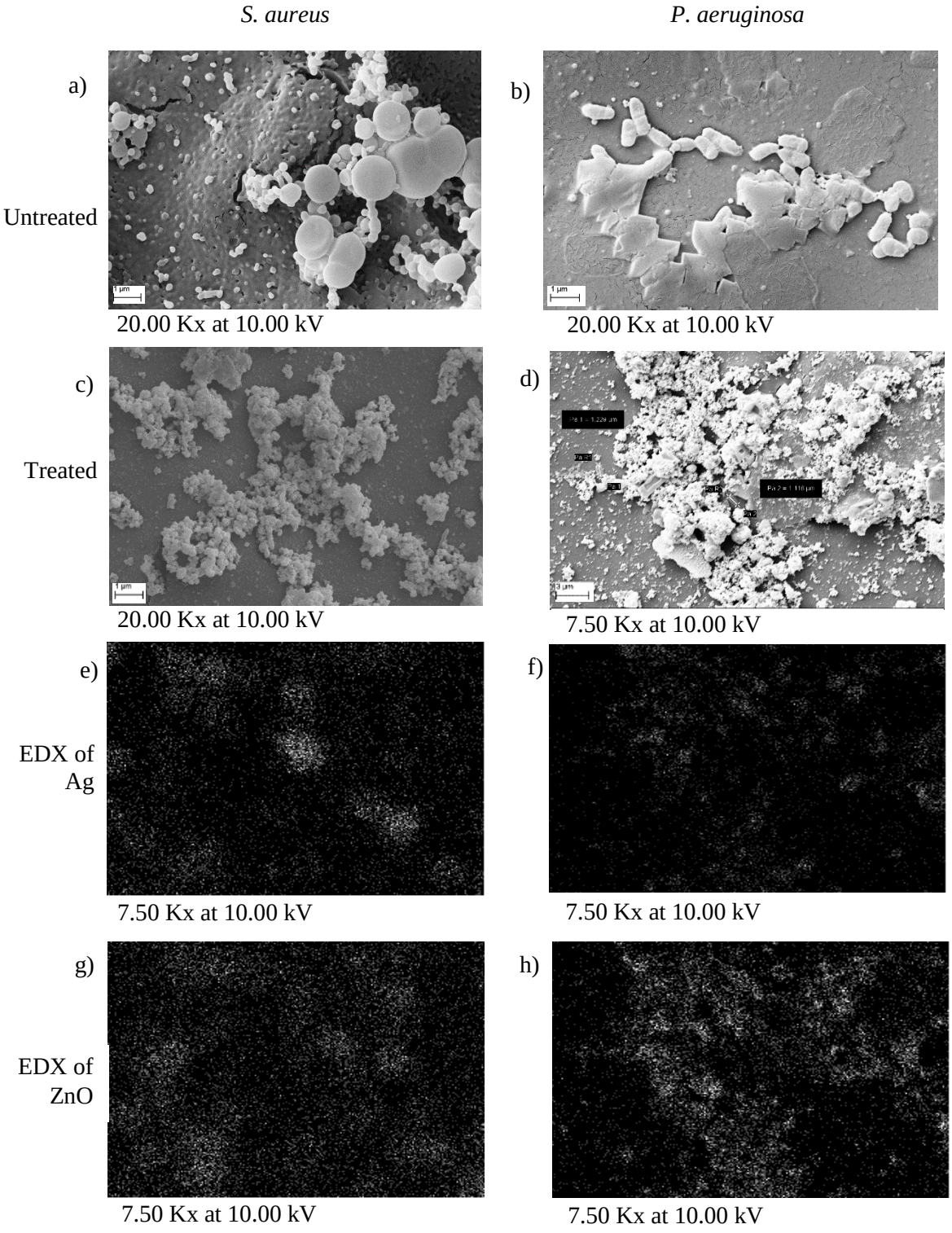

Figure 4.4: SEM/EDX images showing *S. aureus* and *P. aeruginosa* 24 hour biofilms on PC coupons formed in the CDC biofilm reactor treated with ZnO/Ag NP suspensions; a) Untreated *S. aureus* biofilm, b) Untreated *P. aeruginosa* biofilm, c) *S. aureus* biofilm treated with 8/12 µg/ml of ZnO/Ag NPs, d) *P. aeruginosa* biofilm treated with 32/25 µg/ml of ZnO/Ag NPs, e) EDX image showing the presence of Ag in the *S. aureus* biofilm, f) EDX image showing the presence of Ag in the *P. aeruginosa* biofilm, g) EDX image showing the presence of Zn in the *S. aureus* biofilm and h) EDX image showing the presence of Zn in the *P. aeruginosa* biofilm.

4.3.7 CLSM

Figure 4.5 shows the top, middle and bottom portions of *S. aureus* and *P. aeruginosa* biofilms after treatment with 8/12 μg/ml and 32/25 μg/ml of ZnO/Ag NPs suspension respectively. Dead (red) portions of biofilms for both organisms were observed throughout the biofilms, suggesting that ZnO/Ag NP suspensions have penetrated the depth of the biofilm (Figure 4.5a, b, c, d, e and f). In contrast, the untreated biofilms are predominantly live (green) with a denser distribution of cells (Figure 4.5g and 4.5h).

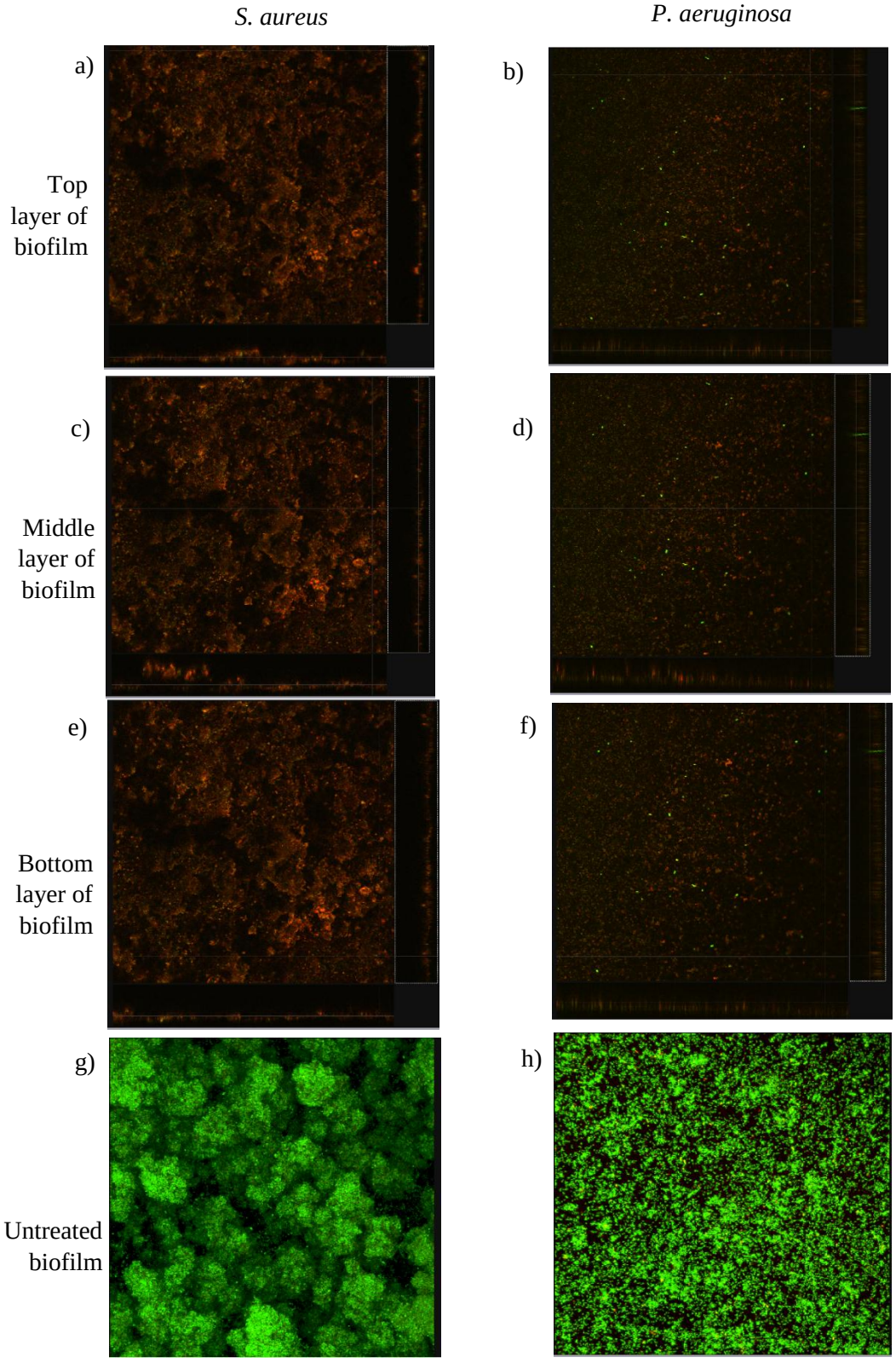

Figure 4.5: Live/dead assays of the top, middle and bottom layers of *S. aureus* and *P. aeruginosa* biofilms treated for 24 hours with suspensions of 8/12 and 32/25 µg/ml ZnO/Ag NP respectively.

4.4 Discussion

Antimicrobials used in clinical settings do not always adequately remove biofilms due to the inefficacy of stated disinfectant concentrations by manufacturers and incorrect contact times, thus highlighting the antimicrobial resistance of biofilms (Rutala & Weber, 2016; Wong *et al.*, 2010). The growth of HCAI organisms growing on surfaces in a biofilm form poses problems within the healthcare arena due to cells within a biofilm being more virulent (Wand *et al.*, 2012; Naves *et al.*, 2008), thus having greater resistance to disinfectants.

Nanomaterials such as metal/metal oxide NPs may be a substitute to conventional antimicrobials as they can impregnate bacterial cells and ion release from NPs which can hinder metabolic processes and damage the cell (Seil & Webster, 2012; Hsueh *et al.*, 2015). Moreover, their high surface area to volume ratio owing to their small size enables higher reactivity and strong particle-cell interactions with biological entities, which is otherwise not observed in the bulk form for same material (Jo *et al.*, 2015).

4.4.1 Treatment of **S. aureus** *and* **P. aeruginosa** *Biofilms With Metal and Metal Oxide NP Suspensions*

In this study, a novel three step approach was used to determine the appropriate metal/metal oxide NPs and concentrations required to inhibit biofilms in order to start developing a metal/metal oxide NP based antimicrobial, using the MBRC (screening individual metal/metal oxide NPs using the CDC Biofilm Reactor, Table 4.1), R^2 values (Figure 4.2 and 4.3) and MBRC ($\log_{(10)}$ reductions of combinations of metal/metal oxide NPs using a CDC biofilm reactor) (Table 4.2a and b). The majority of other studies reported in the published literature rely only on viable counts (Bailón-Sánchez *et al.*, 2014; Gupta *et al.*, 2013) or absorbance values (Kovaleva *et al.*, 2010; Moreno *et al.*, 2015). These studies generally are only related to vegetative cells, however, due to the complex nature of a biofilm community, relying on just one method to determine the

appropriate antimicrobial concentration for use against biofilms may not be sufficient, an example of this is the large SE associated with the 96 well plate method. There was considerable variation in the data when using the 96 well plate method, making it only suitable for mass screening of metals/metal oxide NPs and giving an indication of the MBRCs had it have been successful, therefore one approach of screening for biofilms is not appropriate. Consequently, using a combination of data and methods to determine not only the concentration at which a biofilm is reduced with individual metal/metal oxide NPs, but also in combination, whilst also taking into consideration the R^2 value, allows for a predictable inhibitory behaviour of the metals and demonstrates the closeness of the values to the line of best fit, describing a linear relationship of the inhibitory effect of the metal concentrations below that of the MBRC (Figure 4.2 and 4.3). Sessile cells are surrounded by EPS, and persister cells embedded within the biofilm make biofilms more tolerant to antimicrobials in comparison to their planktonic counterparts (Yang *et al.*, 2015; Spoering & Lewis, 2001), whereas planktonic cells are unbound, having greater interactions with disinfectants. Therefore, it is often difficult to compare inhibitory concentrations of vegetative cells with biofilm cells. When developing an antimicrobial or disinfectant, a precise dose would be mandatory. R^2 value further reinforces the strength the relationship between the $\log_{(10)}$ cfu/ml and the concentrations of NPs. A greater R^2 value suggests a strong linear relationship.

After taking into consideration the R^2 value and the $\log_{(10)}$ reductions, the selected metals for both organisms were Ag and ZnO (Table 4.1). Ag and ZnO NPs were chosen for assessment of efficacy in combination due to the low MBRC of ZnO (16 µg/ml) and linear R^2 value (0.95) (Figure 4.3a), giving a reduction of 3.61 $\log_{(10)}$ for *S. aureus* biofilms (Table 4.1). Similarly, a linear R^2 value was observed for ZnO for *P. aeruginosa* (0.99) (Figure 4.2a) with an MBRC of 256 µg/ml and a reduction of 3.52 $\log_{(10)}$ (Table 4.1), compared to a slightly lower MBRC of CuO (200 µg/ml) but a lower, more unstable R^2 value of 0.85 (Table 4.1). Ag NPs were chosen due to the low MBRC of 50 µg/ml (Table 4.1) and stable R^2 value against *P. aeruginosa* (0.96) (Figure 4.2c) and *S.*

aureus (0.80) (Figure 4.3c), with reductions of 3.42 and 3.65 $\log_{(10)}$ for *P. aeruginosa* and *S. aureus* respectively (Table 4.1). Furthermore, the MBRC of Ag (50 μg/ml) is much lower than the MBRC of CuO (200 μg/ml) for *P. aeruginosa*, therefore a smaller concentration is required for a ≥3 $\log_{(10)}$ reduction. Although the R^2 value is lower for Ag (0.80) than CuO (0.97) for *S. aureus*, there is only a difference of 0.17 between the values. Similar to *P. aeruginosa*, the MBRC of Ag (50 μg/ml) is considerably lower than CuO (160 μg/ml) for *S. aureus* (Table 4.1). After all these factors were taken into account, Ag and ZnO NPs seemed reasonable to use in combination for antimicrobial activity and were carried forward for further investigation.

4.4.2 Efficacy of Metal/Metal Oxide NPs

Durairaj *et al.* (2012) showed a reduction in *P. aeruginosa* isolates at 50 μg/ml when added in the lag phase of growth, giving 100% inhibition. A complete inhibition of *S. aureus* was reported when exposed to 50 ppm of poly-(*N*-vinyl-pyrrolidone) (PVP) stabilised Ag NPs (Cho *et al.*, 2005). Studies by Cho *et al.* (2005) and Durairaj *et al.* (2012) were conducted on vegetative cells, whereas 50 μg/ml of Ag NP in this investigation have been proven to be effective on biofilms (Table 4.1). Rahim and Mohammad (2015) determined the MIC of Ag NPs against clinical MRSA isolates to be 100 μg/ml, and MICs of ZnO NPs against *P. aeruginosa* were between 150 to 158 μg/ml (Hassani Sangani *et al.*, 2015). However, ZnO NPs in the study by Hassani Sangani *et al.* (2015) have a particle size of 20 nm in comparison to the 50 nm ZnO NPs used in this study with an MBRC of 256 μg/ml for *P. aeruginosa* when used individually and 32 μg/ml in combination (Table 4.1). The particle size could have an effect on the antimicrobial efficacy of NPs as demonstrated by Yamamoto *et al.* (2001), whereby increasing particles sizes of ZnO powders from 0.1 to 0.8 μm increased its antimicrobial efficacy against *S. aureus* and *E. coli*, however, further investigation would need to be undertaken with a range of sizes in order to confirm this. Most of the published studies have used methods such as microdilution assays (Durairaj *et al.*,

2012; Abdel Rahim & Ali Mohamed, 2015) to determine the MIC; combining correlations and $\log_{(10)}$ reductions in the published literature is an approach that has not yet been used for analysing the effect of metal/metal oxide NPs suspension against biofilms.

The toxic effects of metal and metal oxide NPs need to be taken into consideration before the development of a metal or metal oxide NP containing product. For instance, exposure of high concentrations of Ag in the air can result in breathing problems, as well as lung and throat irritation. Skin contact with Ag can result in mild allergic reactions like rashes, swelling and even inflammation (Ray *et al.*, 2009). If a product was to be developed containing a metal/metal oxide NP combination, there is greater practicality to use the same combination for all types of organisms regardless of whether they are Gram-negative or Gram-positive.

The acceptance criteria for disinfectants require a minimum of a 4 $\log_{(10)}$ kill in ≤5 mins (British Standards Institute, 2001). The combinations of Ag and ZnO (Table 4.3) or individual usage of Ag, ZnO and CuO (Table 4.1) have shown reductions between *ca.* 3 to 4 $\log_{(10)}$ but over 24 hours. Even though biofilms are problematic in many industries, standard efficacy testing of disinfectants only accounts for planktonic cells (Ali *et al.*, 2006; Toté *et al.*, 2010), it is important to take this into account when comparing the efficacy of antimicrobial products for biofilms. Lower $\log_{(10)}$ reductions may be observed during this study as the efficacy of metal/metal oxide NPs were assessed against *P. aeruginosa* and *S. aureus* biofilms, with reductions of 3.77 and 3.69 $\log_{(10)}$ for *P. aeruginosa* type and clinical strain respectively using 32/25 µg/ml of ZnO/Ag NPs and 3.91 and 3.81 $\log_{(10)}$ reductions for *S. aureus* type and clinical strain respectively with 8/12 µg/ml of ZnO/Ag NPs (Table 4.3). This demonstrates that using combinations for both *S. aureus* and *P. aeruginosa* biofilms has promising antimicrobial characteristics for further development, especially due to the closeness of the reductions for the acceptance criteria for disinfectants, even though the efficacy testing was against biofilms.

Sessile cells are highly resistant and eradication of biofilms using suggested concentrations of disinfectants is challenging, therefore increased concentrations, treatment times and even mechanical disruption can be required to remove a biofilm (Rajdev *et al.*, 2015). When planktonic and biofilm cultures of *Acinetobacter* spp., *K. pneumoniae* and *P. aeruginosa* were treated with working concentrations of H_2O_2 and H_2O_2 based formulations, MICs were between 0.5 to 20 mM H_2O_2, whereby biofilms showed up to 266 fold more resistance (Perumal *et al.*, 2014). Four *Candida* spp. and two *E. coli* strains exhibited resistance to sodium hypochlorite, H_2O_2, ethanol and iodine. MICs were >10 fold higher at 5 min and 24 hour treatments in comparison to planktonic cells (Leung *et al.*, 2012). This could be owing to barriers in penetration, reduced accumulation of biocides, as well as adaptation and selective pressure. Notably, the MIC values of iodine and H_2O_2 treatment for the adhesion and biofilm phases exceeded the commercially available concentration of 1% and 3% respectively (Leung *et al.*, 2012). Similarly, *C. albicans* strains in a biofilm form were found to be 8-fold more resistant to chlorhexidine than *C. albicans* in a planktonic state, showing the inefficacy of clinically utilised disinfectants (Lamfon *et al.*, 2004). This suggests that even though biocides may be effective against planktonic cells, they may not necessary eradicate biofilms too, thus unsuccessful in preventing HCAIs derived from biofilms (Smith & Hunter, 2008).

4.4.3 Synergistic Combination of Ag and ZnO

It is noteworthy that even though antagonism is expressed as seen is Table 4.2b, a ≥ 3 $\log_{(10)}$ reduction is observed for all the concentrations that have shown to work. This is seen mainly in the higher concentration combinations such as 32/100, 64/12, 64/25, 64/50 and 64/100 µg/ml for *S. aureus* biofilms. This suggests that even though one metal/metal oxide NP may be hindering the effect of the other, the other metal NP may be in excess, therefore exerting the antimicrobial effect alone. For example, at 32/100 µg/ml of ZnO/Ag NPs respectively, the Ag may be in excess,

therefore overall the Ag^+ ions are exerting the antimicrobial effect, whereas at 64/12 µg/ml, the ZnO NPs may be in excess.

In a study by Liu *et al.* (2016), an antagonistic effect was seen for ZnO NPs on the toxicity of Cu NPs, due to the occurrence of interactions between dissolved and particulates of Cu and Zn (Liu *et al.*, 2016). The individual susceptibility of *Photobacterium phosphoreum*, a commonly used organism for bioluminescence inhibitions assays, to metal oxide NPs was tested (Wang *et al.*, 2014b). The synergistic effect of ZnO, α-Fe_2O_3, γ-Fe_2O_3, Fe_2O_3 and nickel oxide (NiO) NPs were tested. ZnO antimicrobial efficacy was a result of dissolved Zn^{2+} ions, whereas the Fe-oxides and NiO antimicrobial effect was due to particle specific toxicity. The interactions between Zn^{2+} ions and are other NPs present in the suspension gave an antagonistic effect. This was confirmed when the concentration of Zn^{2+} ions was measured in individual ZnO NP suspensions and ZnO NPs mixed with other NPs, showing the Zn^{2+} ion concentration was higher in individual ZnO NP suspensions in comparison to when in combination with other NPs. Nanomaterials tend to have a greater adsorption capacity in comparison to other materials due to their high surface area to volume ratio (Liu *et al.*, 2005). Due to the high surface energy of NPs, ions have an affinity for the NPs, therefore, it is likely that dissolved Zn^{2+} ions from the ZnO NPs adsorb onto the surface of other NPs in the suspension, reducing the overall ion concentration. In this case, Zn^{2+} ions are absorbed by Fe-oxides and NiO NPs, reducing the overall Zn^{2+} ion concentration. Zn^{2+} dissolved in the individual ZnO suspensions can adhere to the bacterial cell surface which is negatively charged, resulting in an antimicrobial effect. This reduction in available ions in mixed NP suspensions could be the reason for an antagonistic effect in combination suspensions (Wang *et al.*, 2014b).

The ion release from combinations of ZnO/Ag NPs and individually was investigated in this study using AAS (Table 4.5). After analysis of results in Table 4.5, high levels of ZnO (≥32 µg/ml) in combination with low levels of Ag (≤16 µg/ml) or high levels of Ag (≥50 µg/ml) with low levels of ZnO (≤16 µg/ml) have led to quenching of Zn^{2+} ions, suggesting the antimicrobial

effect is mainly due to Ag^+ ions. However, reductions ≥3 $log_{(10)}$, were observed for *P. aeruginosa* and *S. aureus* (Table 4.2a and b), showing the antimicrobial efficacy of the lower combined concentrations. The pH of the suspension was monitored throughout the study and remained stable at pH 7. For ZnO/Ag NP suspensions in combinations of 64/50 µg/ml, quenching of Zn^{2+} is observed, where individually 50 µg/ml and 64 µg/ml of Ag and ZnO NP released 0.71 and 4.18 g/l ions respectively, whereas in combination, 0.66 and 2.68 mg/l of ions were released respectively. Both Ag^+ and Zn^{2+} ions quenched eachother for 64/100 µg/ml of ZnO/Ag NPs, as individually 100 µg/ml and 64 µg/ml of Ag and ZnO respectively released 1.35 and 4.18 g/l ions respectively, whereas in combination, 0.72 and 3.13 mg/l ions were released respectively (Table 4.5). Thus, synergistic relationships between the metal/metal oxide NPs were not observed, additive effects mainly occurred (Table 4.2a and b). This may suggest that both Ag and ZnO NPs works *via* different mechanisms and one is influencing more damage than the other.

Talari *et al.* (2012) evaluated the antimicrobial efficacy of Ag doped ZnO NPs against *E. coli* and *S. aureus*. The MIC of the NPs, decreased from 80 to 40 µg/ml and 160 to 100 µg/ml for *E. coli* and *S. aureus* respectively as the concentration of Ag increases from ratios of 0.00 to 0.10. This could be due to the combined effect of increased attachment of the Ag doped ZnO NPs to the bacterial cell surface, releasing Ag^+ ions and the production of H_2O_2 from ZnO NPs, leading to a synergistic antimicrobial action.

Yıldırım *et al.* (2013) observed the substitution of Ag^+ ions into Zn^{2+} sites in the ZnO lattice. An increased concentration of Ag results in increased occupancy of Ag^+ ions in the Zn sites. Some results in Table 4.5 correlate with these findings, showing that higher Ag concentrations between 50 to 100 µg/ml in combination results in a reduction in Ag^+ ions, endorsing the fact that antimicrobial efficacy here could be mainly due to Zn^{2+} ions, but contrasting with the hypothesis that a high and low combination of Ag and ZnO NPs result in quenching of Zn^{2+} ions. For example, this is seen in the decrease in Ag^+ ions in 8/100 µg/ml of ZnO/Ag NP suspension,

whereby the initial Ag^{+} ion concentrations were 1.35 mg/l for 100 µg/ml and in combination, decreased to 0.89 mg/l for 8/100 µg/ml. However, this was not seen for 16/50, 8/50, and 16/100 µg/ml. Studies have also reported that pure Ag NPs had limited antimicrobial efficacy due to the agglomeration of Ag NPs into Ag clusters, reducing particle/cell interactions (Lok *et al.*, 2007; Liu *et al.*, 2010; Samberg *et al.*, 2011). In addition, the ability of the transition metal Ag to form ligands with Zn^{2+} ions could explain the reasons behind the low concentrations of available Zn^{2+} ions to interact with the bacterial cells.

Another possible explanation may be that metal oxide NPs and the ions released into the aqueous media undergo three main processes which are 1) dissolution, 2) adsorption and 3) hydrolysis as seen in Figure 4.6 (Wang *et al.*, 2016b).

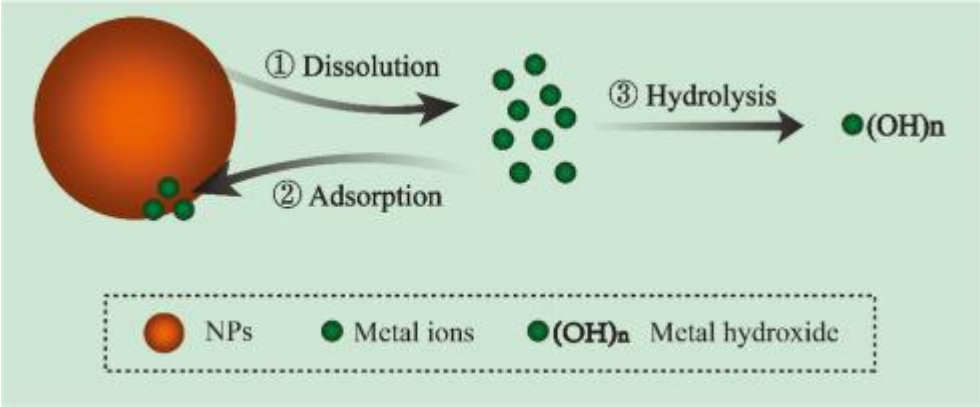

Figure 4.6: The processes of dissolution, adsorption and hydrolysis in metal NP suspensions adapted from Wang *et al.* (2016b).

The concentration of metal ions released from the NPs depends on dissolution and adsorption. In the suspension, dissolution and adsorption occur simultaneously, and eventually reach equilibrium. Metal ions are more likely to dissolve at lower concentrations and the concentration of metal ions increase at lower particle concentrations. With an increase in the metal NP concentration, a larger concentration of metal ions tends to get adsorbed onto the NPs, leading to a decrease in the availability of the metal ions, which explains the reduction of metal ions in CuO NPs at concentrations higher than 180 µg/ml (Wang *et al.*, 2016b). Furthermore, the dissolved

metal ions in the aqueous suspension can also pass through the hydrolysis process, forming insoluble complexes of metal hydroxides (Wang *et al.*, 2016b).

For *P. aeruginosa*, the concentrations that gave a ≥ 3 $\log_{(10)}$ reduction were 8/100, 32/25, 64/12 and 64/100 µg/ml of ZnO/Ag respectively (Table 4.2a). For *S. aureus*, all the tested concentrations gave a reduction ≥ 3 $\log_{(10)}$ (Table 4.2b) apart from 16/12 and 16/25 µg/ml of ZnO/Ag respectively, which were also found to be ineffective in *P. aeruginosa* too (Table 4.2a). The chosen combinations of ZnO/Ag NPs respectively were 32/25 µg/ml for *P. aeruginosa* and 8/12 µg/ml for *S. aureus*. A 8/12 µg/ml combination of ZnO/Ag NP suspension respectively was the lowest combination tested against *S. aureus* biofilms which was found to give a significant reduction ($p \leq 0.05$) of 3.91 $\log_{(10)}$, lowering the MBRC of the metal/metal oxide NPs to that of when used individually (16 µg/ml for ZnO and 50 µg/ml for Ag). For *P. aeruginosa*, the MBRC of Ag and ZnO when used alone was 50 and 256 µg/ml respectively whereas a combination of 32/25 µg/ml of ZnO/Ag gave a significant reduction ($p \leq 0.05$) of 3.77 $\log_{(10)}$. These results are similar to findings from Ghosh *et al.* (2012), where Ag/ZnO nanohybrids were tested against *S. aureus* and *E. coli*. Results demonstrated that MICs of 100 µg/ml of ZnO and 46 µg/ml Ag for *S. aureus* and 127 µg/ml of ZnO and 37 µg/ml of Ag was required for *E. coli* individually. However, in combination, Ag/ZnO nanohybrids at MICs of 23, 18, 10 and 7 µg/ml for was required for *S. aureus* and 35, 25, 20 and 12 µg/ml for *E. coli* with Ag concentrations of 0.97, 3.79, 6.63 and 9.10% respectively, demonstrating a synergistic effect of the nanohybrids. Moreover, ZnO/Ag nanohybrids showed greater ZOI in comparison to Ag and ZnO individually, suggesting hybrids may be preferable for the treatment of both Gram-negative and Gram-positive bacteria (Ghosh *et al.*, 2012; Akhil *et al.*, 2015).

Clinical strains of *S. aureus* and *P. aeruginosa* biofilms in this study were also significantly reduced ($p \leq 0.05$) by 3.81 and 3.69 $\log_{(10)}$ respectively. When *P. aeruginosa* and *S. aureus* biofilms were treated with Ag NPs, a 90% reduction was observed for both biofilms at concentrations of 0.5 µg/ml and 0.7 µg/ml respectively (Gurunathan *et al.*, 2014). Ag NPs at a

concentration of 2 µg/ml gave reductions of 73.7 and 66.3% when tested against *P. aeruginosa* and *S. aureus* biofilms respectively (Kora & Sashidhar, 2014). Both of these studies used MTP based models to find the most effective concentration for the inhibition of *P. aeruginosa* and *S. aureus* biofilms. Lower concentrations of Ag NPs were required by Kora and Sashidar (2014) and Gurunathan (2014) for an antimicrobial effect in comparison to the Ag MBRC concentrations found in this Chapter, i.e. 50 µg/ml individually and 12 and 25 µg/ml in the ZnO/Ag combination for *S. aureus* and *P. aeruginosa* respectively, this may be due to the methodology used.

The reduction in the Ag and ZnO NP concentrations in combination could be due to the utilisation of multiple antimicrobial mechanisms. It is the ion form of Ag that is known to exhibit the antimicrobial effect as opposed to the NP (Durán *et al.*, 2010). Electrostatic interactions of the ions to the negatively charged cell surface of the bacteria can produce free radicals, changing the permeability of the cell, resulting in leaking to intercellular contents (Durán *et al.*, 2015). Ag^+ ions react with the thiol groups of proteins, inactivating the bacteria (Durán *et al.*, 2010). Ag NPs or Ag^+ ions can hinder the respiratory chain in the mitochondria of the bacteria, leading to cell death (Durán *et al.*, 2015). The ability of ribosomes to translate messenger ribonucleic acid (mRNA) into vital proteins is hindered by Ag^+ ions (Kwakye-Awuah *et al.*, 2008; Park *et al.*, 2009). The release of Zn^{2+} ions from ZnO contribute to their antimicrobial efficacy (Pasquet *et al.*, 2014). Other studies have reported that ROS species released from the surface of ZnO react with H^+ ions, producing H_2O_2 that can penetrate the cell membrane, eliminating the bacteria (Fang *et al.*, 2015). The surface area of ZnO affects the generation of H_2O_2 - the greater the surface area the more ROS produced (Ohira *et al.*, 2008). If the NPs are smaller than the pore size of bacteria, they can cross the barrier of the cell directly (Jadhav *et al.*, 2011). Often the antimicrobial activity of metal oxide NPs is on the surface, whereby they bind to the protein thiol group in the cell wall, reducing cell permeability and resulting in cell lysis (Zhang & Chen, 2009). It may be these modes of action for Ag and ZnO NPs in combination that are exerting their antimicrobial effect against *P. aeruginosa* and *S. aureus* biofilms in this study.

Ansari *et al.* (2015) demonstrated the efficacy of Ag NPs against MRSA and methicillin resistant *S. epidermidis* (MRSE) isolated from wounds in a tertiary care hospital. The MIC determined to be within the range of 11.25-45 µg/ml. At 50 µg/ml, complete biofilm reduction was seen. This is comparable to when Ag NPs were used alone to treat biofilms of *P. aeruginosa* and *S. aureus*, where 50 µg/ml resulted in a ≥ 3 $\log_{(10)}$ reduction (Table 4.1). Ansari *et al.* (2015) used the Congo Red method to test the effect of Ag NPs by visually assessing the presence and absence of dry crystalline black colonies which indicates the synthesis of glycocalyx matrix. The CDC biofilm reactor produces thick mature biofilms due to the continuous nutrients supply (Figure 3.7a-f). Due to the biofilms being treated after 48 hours of formation in this investigation, it would be expected that a larger concentration of antimicrobials would be required in comparison to planktonic cultures. The EPS which surrounds and encases the biofilm cell community constructs 90 % of the biofilm, providing it with protection, often making detergents ineffective (Fux *et al.*, 2005; Hadi *et al.*, 2010; Vickery *et al.*, 2004).

4.4.4 Time Point Assay

The time needed in order to exhibit an antimicrobial effect by the metal NPs was investigated at 1, 2, 4, 6, 8 and 24 hours. For *S. aureus*, between 1 and 8 hours, there was a reduction of 19.79% ($p > 0.05$), between 1 and 24 hours, there was a 99.98% reduction ($p \leq 0.05$) (Table 4.4). Similar reductions between 1-8 hours was also observed for *P. aeruginosa* whereby between 1 and 8 hours, there was a reduction of 21.08% ($p > 0.05$), and between 1 and 24 hours, there was a 99.94% reduction ($p \leq 0.05$) (Table 4.4). This data signifies the importance of a 24 hour metal/metal oxide NP treatment against mature biofilm for both organisms (Table 4.4). Pourmand *et al.* (2013) used a time kill assay to show the antimicrobial activity of Ag NPs against *Legionella pneumophila* vegetative cells with an MIC of 30 µg/ml at 4°C and 25°C for 24 hours. There were no viable cells at 24 hours at 4°C, at 25°C though 1.2×10^5 to 5.5×10^5 cfu/ml were detected, suggesting

temperature affects antimicrobial efficacy. Between 0 to 8 hours, there was a reduction of *ca.* 2.5 $\log_{(10)}$ cfu/ml. A time kill assay was used to test Ag NPs at concentrations of 0.0, 6.25, 12.5, 25.0 and 50.0 mM against vegetative cells of *Streptococcus pyogenes*, *E. coli* O157:H7 and multidrug resistant *P. aeruginosa* over 24 hours (Lara *et al.*, 2009). At 50.0 mM, total inhibition was achieved for all three strains. Even though 6.25 mM was below the MIC/MBC range, the bacterial growth was still lower at 24 hours in comparison to the control. At 24 hours, there was a 99.7%, 95.7 and 92.8% reduction in *S. pyogenes*, *E. coli* and *P. aeruginosa* respectively (Lara *et al.*, 2009).

4.4.5 SEM, EDX and CLSM

SEM images showed diminished biofilms of *P. aeruginosa* and *S. aureus* after a 24 hour treatment (Figure 4.4c and d). This is evident in *P. aeruginosa* biofilm (Figure 4.4b) where the cells are in close proximity to each other, whereas in Figure 4.4d, only the remains of the biofilm are observed. In *S. aureus* biofilm samples without treatment, it is clear that the cells are intact and have smooth surfaces (Figure 4.4a). However, with the treated biofilms, smaller number of cells can be seen with rougher cell edges showing that the ZnO/Ag NP combination (Figure 4.4c), most likely in the ion form, are disrupting the cells. EDX analysis has shown the presence of Ag and ZnO in the *P. aeruginosa* (Figure 4.4f and h) and *S. aureus* biofilm (Figure 4.4e and g), suggesting impregnation of some of the metal/metal oxide NPs into the biofilm or adsorption of the NPs onto the surface of the cell, thereby slowly releasing ions. Similar findings were seen by Ansari *et al.* (2015) when biofilms of clinical strains of *S. aureus* were treated with Ag NPs between 5 to 10 nm. SEM images showed similar patterns, i.e. distortion of cell integrity and reduction of surface coverage. Moreover, a study by Kostenko *et al.* (2010) showed that nanocrystalline Ag has antibiofilm activity against *P. aeruginosa.* SEM demonstrated a reduced surface coverage of *P. aeruginosa*. CLSM imaging confirmed the antimicrobial efficacy of ZnO/Ag NPs, with cell death

occurring throughout the depth of the biofilm, suggesting that inhibition was not just on the surface of the biofilm (Figure 4.5a-f).

Ag NPs were found on the cell membrane surface and inside the bacterial cell after their exposure to *E. coli* cells, where the former hindered permeability and the latter led to DNA damage (Morones *et al.*, 2005). Alongside ion release from metal/metal oxide NPs, these could be two other ways by which antimicrobial activity was exerted in the present study. Ag NPs on the surface of ZnO in a ZnO/Ag nanohybrid were shown to have a slight electro positive charge (Ghosh *et al.*, 2012). At pH 7.4, the dissociation of excess carboxylic acid groups on the bacterial cell surface lead to a negative charge (Morones *et al.*, 2005; Sondi & Salopek-Sondi, 2004). Interaction between the cell wall surface and the Ag NP causes electrostatic attraction between the two oppositely charged species, therefore Ag NPs in the hybrid adhere onto the *E. coli* cell wall surface preferentially than ZnO NPs (Ghosh *et al.*, 2012). Eventually, the Ag NPs interact with the cell membrane, increasing permeability and entering the cell, resulting in cell death (Yang *et al.*, 2009b). In comparison to *E. coli*, *S. aureus* cell surface has a lesser negative charge, therefore less susceptible to the Ag^+ ions. OH· signals were detected for pure ZnO, which were not present for ZnO/Ag hybrids, suggesting that OH· formation is quenched by Ag. This proposes that the antimicrobial effect on *S. aureus* is due to a physical attack of the ZnO/Ag hybrid on the cell wall, rather than the OH· radicals (Applerot *et al.*, 2009; Li *et al.*, 2011; Lipovsky *et al.*, 2009). This supports the AAS data (Table 4.5) showing that the Ag^+ ions are predominantly responsible for the antimicrobial effect, due to the electrostatic attraction described by Ghosh *et al.* (2012). Gram-positive *P. aeruginosa* was found to be less susceptible in comparison to *S. aureus* in the present study, however, NP suspensions were used here whereas nanohybrids were used by Ghosh *et al.* (2012), this could explain the variation seen between studies in terms of ion release.

4.4.6 Conclusion

A three step approach was used to determine a suitable combination of NPs against HCAI associated biofilms by: 1) using the MBRC of individual metal/metal oxide NPs against *P. aeruginosa* and *S. aureus* biofilms, 2) R^2 values and 3) $\log_{(10)}$ reductions of ZnO/Ag NP suspensions in combination. A reduction of ≥ 3 $\log_{(10)}$ within the acceptance criteria set in this study was mandatory. This approach has not been used to date in the published literature to assess the efficacy of metal and metal oxide NPs against biofilms. Moreover, the antimicrobial effect of metal/metal oxide NPs against biofilms *per se* has not been studied in depth, and there is limited published research on the synergistic effect of metal/metal oxide NPs against biofilms. A reduction of *ca.* 3.5 $\log_{(10)}$ after 24 hours for metal/metal oxide NPs against biofilms is promising due to biofilms being harder to eradicate in comparison to vegetative cells. With the ongoing issue of antimicrobial resistance, the combination of ZnO/Ag NP suspensions could provide an alternative to conventional disinfectants that are often ineffective against biofilms.

Chapter 5

Chapter 5: Antimicrobial Coatings

5.1 Introduction

The transfer of pathogens from an infected to susceptible patients is usually due to cross contamination from the hands of healthcare personnel. Contaminated hospital surfaces, hospital equipment, water and air can also be a cause of transmission both directly or indirectly (Randle *et al.*, 2010).

Surfaces can be a source of contamination in hospitals, consequently having an impact on endemic transmission of HCAIs (Otter *et al.*, 2011). In particular, those surrounding patients have a greater chance of contamination in comparison to other surfaces within a hospital (Huslage *et al.*, 2010; Hayden *et al.*, 2008). Hospital pathogens can survive on dry surfaces for lengthy time periods. In specific, *S. aureus* can survive between 7 days to >12 months (Wagenvoort *et al.*, 2000) and *P. aeruginosa* can survive between 6 hours to 16 months (Otter *et al.*, 2013). Biofilms enable bacteria to survive on dry surfaces for lengthy periods without a source of nutrients (Yezli & Otter, 2012; Vickery *et al.*, 2012).

Recently, "no touch" methods of disinfection have been encouraged to decrease the occurrence of contamination of surfaces in hospital rooms, including emission of ultraviolet (UV) light and aerosolized/vaporised H_2O_2 (Rutala & Weber, 2011). However, there are limitations associated with these techniques as patients and healthcare personnel have to be removed from the room prior to cleaning, these systems are more suitable for terminal cleaning (Rutala & Weber, 2011). High costs associated with room decontamination and the increase in the time taken for room turnover make commercially available disinfection methods such as H_2O_2 and chlorine based products unfavourable to use (Doan *et al.*, 2012). Routine and terminal cleaning is often

inadequate, due to less than 50% of room surfaces in hospitals being thoroughly disinfected when cleaned with chemical germicides (Carling *et al.*, 2008; Goodman *et al.*, 2008).

An example of a self-disinfecting product is Surfacine (Surfacine Development Company, Tyngsborough, MA), used for disinfecting hospital surfaces. It utilises the water soluble antimicrobial silver iodide in a surface immobilised coating, which is modified with polyhexamethylene biguanide. Surfacine is capable of chemically recognising and interacting with the lipid bilayer of the bacterial cell membrane *via* electrostatic interaction (Rutala & Weber, 2001). It can be applied to abiotic surfaces *via* dipping, brushing or spraying without having to previously treat surfaces. A 3.3 to 4.3 $\log_{(10)}$ kill and a 2.2 to 4.8 $\log_{(10)}$ kill has been achieved against *S. aureus* and *P. aeruginosa* respectively (Brady *et al.*, 2003). It has also been shown to reduce MRSA and VRE by >3 $\log_{(10)}$ (Rutala & Weber, 2001).

The antimicrobial effect of NPs comprising of a combination of $AgNO_3$ and TiO_2 coated onto surgical masks were tested against *E. coli* ATCC 25922 and *S. aureus* ATCC 25923 with doubling dilutions of NPs from 1/2 to 1/1024. A 100% reduction in viable *E. coli* and *S. aureus* was observed after a 48 hour incubation of masks treated with NP dilutions of 1/128 and 1/512 for *E. coli* and *S. aureus* respectively (Li *et al.*, 2006). However, for the untreated mask, there was an increase in viable counts by 25% and 50% of *E. coli* and *S. aureus* respectively. Li *et al.* (2006) proposed that the NPs caused damage to the bacterial enzymes or plasma membrane, impairment of the metabolic pathways and leakage of the cytoplasmic matter.

Cu-coated or impregnated surfaces are often utilised in healthcare environments due to their promising antimicrobial properties. Cu toilet seats showed a 94-98% reduction in cfu of microorganisms including MSSA, MRSA, VRE, *C. difficile* and coliform bacteria (Casey *et al.*, 2010). Marais *et al.* (2010) showed that Cu coated desks, trolleys, tops of cupboards and window sills, led to a 1-2 $\log_{(10)}$ reduction in mean cfu. A 37% reduction was observed in the total aerobic bacteria on Cu light switches, push plates and door knobs (Mikolay *et al.*, 2010).

Bacterial adhesion can be influenced by physico-chemical factors such as the bacterial cell surface and substratum surface (Bayoudh *et al.*, 2008). Attachment is also affected by environmental factors such as temperature and pH, surface properties such as hydrophobicity and characteristics of the microorganism itself such as the presence of flagella and motility (Di Bonaventura *et al.*, 2008), as well as the topographical features of a surface (Mitik-Dineva *et al.*, 2008, 2009; Truong *et al.*, 2009; Ivanova *et al.*, 2010). Equal channel angular pressing (ECAP) of Ti surfaces, a technique used to increase the strength of material *via* a nanoscale grain structure, led to a greater anchoring of *S. aureus* CIP 65.8 and *P. aeruginosa* ATCC 9025 cells onto ECAP-modified Ti in comparison to un-modified Ti (Truong *et al.*, 2010; Valiev *et al.*, 2008). A biofilm thickness of approximately 3.5 µm and 6 µm was observed for *P. aeruginosa* and *S. aureus* respectively in comparison an unmodified surface of between 2.5 to 3 µm for *P. aeruginosa* and *S. aureus*. Increased cell adhesion could be due to a greater surface area and defects in the surface such as edges and corner sites exposed, enabling greater adherence (Truong *et al.*, 2010). Generally hydrophobic bacteria adhere better to hydrophobic surfaces (Katsikogianni & Missirlis, 2004). The hydrophobicity of *P. aeruginosa* cells means that they adhered better to the hydrophobic ECAP-modified Ti surface, which is in conjunction with studies by Li and Logan (2004) and Vadillo-Rodríguez *et al.* (2004) (Truong *et al.*, 2010). Similar findings were observed by Bohinc *et al.* (2016) when the effect of surface roughness on bacterial adhesion was investigated. A comparison between an untreated 304C SS disc, and a 3D polished, brushed, grinded and electro polished AISI 304 stainless surface was made. The 3D surface had the lowest roughness with a value of 25.20 nm, and the highest was obtained from the ground surface with a value of 986 nm. *L. monocytogenes* ŽM 520 and *P. aeruginosa* ŽM 517 adhered the most to the 3C and the grinded SS surface, which had the roughest surface. *S. aureus* ŽMJ 72 and *P. aeruginosa* ŽMJ 87 both being hydrophobic adhered best to SS, the most hydrophobic surfaces (Bohinc *et al.*, 2016).

Wojcieszak *et al.* (2015) found that *E. coli* and *S. aureus* suspensions were reduced to 0 cfu/ml after a 2 hour short term contact with Cu-Ti thin film. The homogenous thin film is able to provide

a constant ion release over time. Bacteria attaching to a cell surface produce slime as a protection mechanism from the environment (Oliveira & Cunha, 2008), therefore, release of Cu^{2+} ions from Cu coatings prevent adhesion and colonisation, which is a favourable property of coatings. The effect of ZnO polyurethane coating was tested for its efficacy on *E. coli* and *B. subtilis* (El Saeed *et al.*, 2015). A range of loading levels between 0.1-2 wt. % were investigated. A 2 wt. % showed the a 100 % inhibition on both bacteria, owing to Zn^{2+} release from the ZnO powder, penetration of the NPs and production of H_2O_2 from the ZnO nanopowder (Heinlaan *et al.*, 2008; Brayner *et al.*, 2006).

Eight strains of bacteria were studied by Li and Logan (2004) including three *E. coli* strains, two *P. aeruginosa* strains and two *B. cepacia* strains, each differed in their lipopolysaccharide (LPS) length, exopolysaccharide content, and adhesion properties respectively. *B. subtilis* is a well-studied Gram-positive strain that lacks LPS, therefore used as a reference. Their adherence to 11 glass and metal oxide surfaces was determined. Adhesion increased along with the LPS length of the three *E. coli* strains. *P. aeruginosa* PDO300 is an over producer of EPS, therefore, had enhanced adherence in comparison to *P. aeruginosa* PA01. *B. cepacia* G4 adhered better in comparison to its non-adhesive mutant Env435 strain. *B. subtilis* 7003 does not contain LPS thus it adhered less to the eleven surfaces in comparison to the other eight strains studied.

Published research has shown that various factors affect the formation of a biofilm and its properties. In a study by Chen *et al.* (2005), a microencapsulation technique was used to assess the adhesive properties of biofouling deposits on surfaces of a glass test stud. The biofilm of *Pseudomonas flourescens* from the pipe's inner surface was detached using a T-shaped probe, and the force applied on the biofilm was noted. The adhesive strength of the biofilm was dependant on the age of the biofilm, presence of nutrients, suspended cell concentration, bulk fluid pH, fluid velocity and surface roughness of the substratum. Increasing the fluid velocity by 0.6, 1.0 and 1.6 m/s and the glucose concentration from 15 to 30 mg/l, the biofilm adhesive strength also increased from ~0.13–0.60, 0.28–0.79 and 0.51–1.0 J/m^2 respectively. When the

glucose concentration was increased to 45 mg/l, the mean adhesive strength reduced from 0.60 to 0.07, 0.79 to 0.28 and 1.0 to 0.30. This indicates that higher nutrient availability can increase the adhesive strength, although an excess of nutrients can reduce the adhesiveness (Chen *et al.*, 2005).

Research by Oh *et al.* (2009) demonstrated that increased roughness of a substrate encourages bacterial adherence. Biofilm formation by *P. aeruginosa* ATCC 27853 was assessed on sheets of steel, aluminium, rubber and polypropylene, which form parts of washing machines. Thickest *P. aeruginosa* biofilms were formed on polypropylene with a depth of 806.65 ± 181.12 nm whereas the thinnest biofilms were formed on steel with a value of 487.63 ± 144.34 nm. Polypropylene had the greatest surface roughness in comparison to steel. Rough valleys present on the polypropylene surface gave polypropylene the most roughness in comparison to steel with roughness at the micronanometer level (Oh *et al.*, 2009).

The use of antimicrobial coatings is increasing within the healthcare arena due to them reducing the rates of infection by preventing cross contamination between surfaces and healthcare personnel/patients as well as bacterial persistence in the environment. Reductions in bioburden in hospitals have been reported when metal and metal oxide coatings have been implemented, thus potentially resulting in safer hospital surfaces. Investigating factors affecting adhesion onto metal surfaces and how they can impact on its antimicrobial efficacy could be helpful in understanding the mechanisms by which antimicrobial coatings exhibit an antimicrobial action.

5.1.1 Aims and Objectives

Aim:

The aim of this investigation was to establish the antimicrobial properties of thin film coatings of Ag and ZnO on a Si substrate in preventing biofilm formation of *P. aeruginosa* and *S. aureus*.

Objectives:

- To determine the most robust method for thin film coating of Si substrates with Ag and ZnO to withstand the testing environment in NB.
- To establish the antimicrobial efficacy of Ag and ZnO thin film coatings.
- To assess the effects of thin film coating of Si substrates with Ag and ZnO on the biofilm formation of *P. aeruginosa* and *S. aureus* using SEM.

5.2 Method

5.2.1 Thermal Evaporation

Evaporation is a widely-used technique for the deposition of thin films, whereby the material source is heated to a high temperature in vacuum either by thermal or electron-beam (e-beam) methods; e-beam evaporation is utilised primarily for refractory materials and is beyond the scope of this thesis, hence only thermal evaporation will be discussed briefly here.

Deposition *via* this method is achieved when the material in question is vapour transported to a substrate where it condenses to form a thin film. To initiate this process, current is passed through a heating element/crucible holding the source material until the resistive heating causes the material to evaporate (or sublimate). The heating element/crucible is usually tungsten or molybdenum. A high vacuum (i.e. usually < $1x10^{-6}$ Torr) is required to minimise collisions of source atoms with background species/contaminants and to ensure that the mean free path of atoms in the chamber is greater than the distance between the source and the substrate. In this work, thin films of Ag 99.999% pure (Advent Research Materials, Oxford, UK), and ZnO 99.999% pure (Advent Research Materials, Oxford, UK) were deposited using an Edwards 306 evaporation system and a tungsten heating element and whose thickness was monitored precisely using a quartz balance (Edwards FTMZ, Boc Edwards, Crawley, UK). Figure 5.1 shows an image of the thermal evaporator. Substrates were cleaned following the procedure outline (Appendix II) and placed into the evaporation chamber. The system was then pumped down to < 5 $x10^{6}$ Torr prior to the application of current. Once the desired thickness was reached, the process was halted and the samples left to cool for ~ 1 hour before removal. A schematic diagram of a thermal evaporator is shown in Figure 5.1.

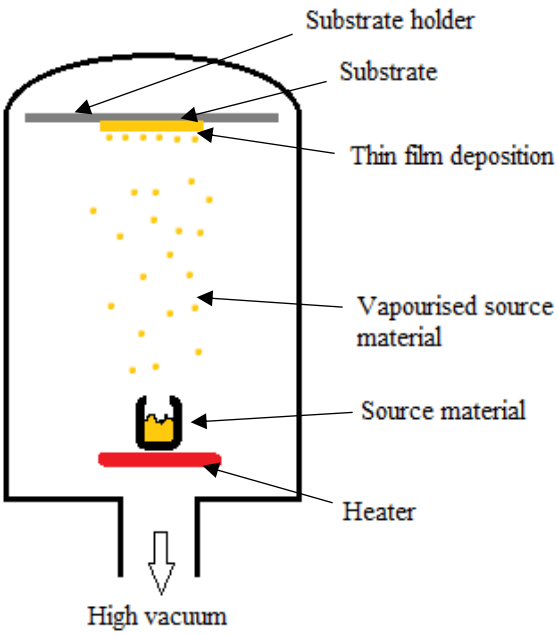

Figure 5.1: A schematic diagram of a thermal evaporator adapted from Hivatec Laboratory (2016).

5.2.2 Sputtering

Thin films of Ti and ZnO were sputtered using the Nordiko Ltd. 1500 RF sputterer (Hampshire, UK). Radio Frequency (RF) magnetron sputtering is method of ion-sputtering. In RF magnetron sputtering deposition, collisions between background electrons, accelerated by an RF field, and the sputtering gas (argon), leads to various dissociative reactions and at steady state, a plasma is formed between the Ti (99.993%-99.995%, Kurt J. Lesker, East Sussex, UK) or ZnO (99.993%-99.995%, Kurt J. Lesker, East Sussex, UK) sputtering target and substrate holder. The magnetic field below the target traps electrons close to the target increasing the sputtering yield. Some ions accelerate towards the target due to the voltage drop between the plasma body and the target electrode; this is known as the plasma sheath. The ion bombardment of the target leads to the release of target species as well as secondary electrons. Atoms released from the target move towards the substrate form a thin film. Figure 5.2 shows a schematic diagram of a RF sputtering system utilised in this study.

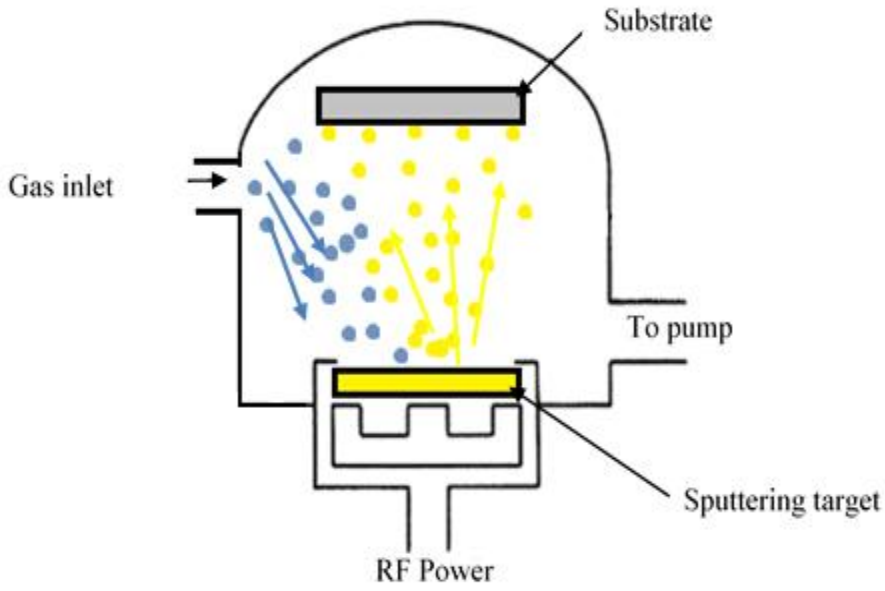

Figure 5.2: A schematic diagram of a RF sputtering system adapted from Yoshino *et al.* (2000)

5.2.3 Aluminium (Al) Evaporation

PC coupons were plasma cleaned (PT 7100, Bio-Rad, Hemel Hempstead, UK) with oxygen and thin films of aluminium (Al) (Advent Research Materials, Oxford, UK) were deposited as per Method 5.2.1. The coupons were then annealed at 150°C in an oven (Harbour Freight, California, USA) to further aid the adhesion of the coating on the surface. Coating was tested in NB and scraped with a glass rod to observe the strength of adherence and observed whether the coating was being removed visually.

5.2.4 ZnO Coating on PC Coupons

Ti was first sputtered onto the PC coupon to aid adhesion. ZnO thin films were then sputtered onto 10 x 10 mm Si substrates at room temperature using RF sputtering at 150 W at ~6nm/min. The Ti target (99.993%-99.995%, Kurt J. Lesker, East Sussex, UK) and ZnO target (99.993%-

99.995%, Kurt J. Lesker, East Sussex, UK) substrate distance was 7 cm and the chamber pressure maintained at 8 x 10^{-6} Torr, with the flow rates of argon (99.999 maintained *via* mass flow controllers). The thickness of the Ti and Ag/ZnO coating were 20 and 100 nm respectively. For Ag coating, Ti was again sputtered onto the PC coupon to aid adhesion. Thin films of Ag were deposited as per Method 5.2.1.

5.2.5 Efficacy Testing of Coating

Coated samples were placed into NB for 24 hours. The coated surface of the coupons was scraped with a glass rod to observe the adherence of the coating. Visual observations were made to ascertain if there was any degree of peeling whilst in the NB or during scraping of the surface of the sample.

5.2.6 Culture Methods and Microorganisms

The test organisms used were *P. aeruginosa* NCTC 6749 and *S. aureus* ATCC 6538. All culture media was acquired from Oxoid Ltd. unless otherwise stated.

Strains were stored on beads at -80°C. Cetrimide agar for *P. aeruginosa* and Mannitol salt agar for *S. aureus* was used to phenotypically determine the organisms.

Organisms were grown on NA and then 1 colony per 10 ml of NB was grown aerobically for 24 hours at 37 °C. NA was used to culture the bacteria for viable count enumeration.

5.2.7 Effect of Ag and ZnO Coating Over Time

The Ag and ZnO coated Si substrates were placed in the rods of the CDC biofilm reactor, containing 500 ml of NB. Biofilms of *P. aeruginosa* and *S. aureus* were formed in the CDC biofilm reactor as per Method 3.2.3.1 and 3.2.3.2. Once the continuous flow was added, samples

were taken at 2, 4, 6, 8, 24 and 48 hours and enumerated as per Method 3.2.3.3. Uncoated Si samples were used for the controls.

5.2.8 SEM

Ag and ZnO coated Si substrates were attached onto the rods of the CDC biofilm reactor. Biofilms of *P. aeruginosa* and *S. aureus* were grown for 48 hours as per Method 3.2.3.1 and 3.2.3.2, washed with PBS and fixed with 95% ethanol for 10 mins at room temperature. The samples were then mounted onto aluminium stubs, ready for imaging. Biofilms were visualised using SEM.

5.2.9 Statistical Analysis

Assumption of normality was tested using Kolmogorov-Smirnov test if sample sizes were ≥50 or Shapiro-Wilcox test if samples were <50. For non-parametric data, a Kruskal Wallis test was used and well as Mann-Whitney U test. Significance was set at $p \leq 0.05$.

All investigations were carried out in triplicate on at least two separate occasions.

5.3 Results

Al was used to test the efficacy of various coating methods prior to testing. Initially, PC coupons were plasma cleaned, and thin films were evaporated followed by annealing to strengthen the adhesion of the film onto the substrate. However, the Al coating in NB over 24 hours had partially dissolved (Figure 5.3a), and when the surface of the PC was scraped with a glass rod, the coating was easily detached from the surface. Thus, due to the strong formation of thin films with better adhesion than thermal evaporation, RF sputtering was used instead. All Si substrates were coated with a thin film of Ti to aid adhesion. ZnO thin films were formed using RF sputtering. However, due to the costs that would incur in buying an Ag target, the Ag thin films were thermal evaporated, followed by annealing. The detachment of coating seen in Figure 5.3 was prevented by the Ti adhesion layer.

a) b)

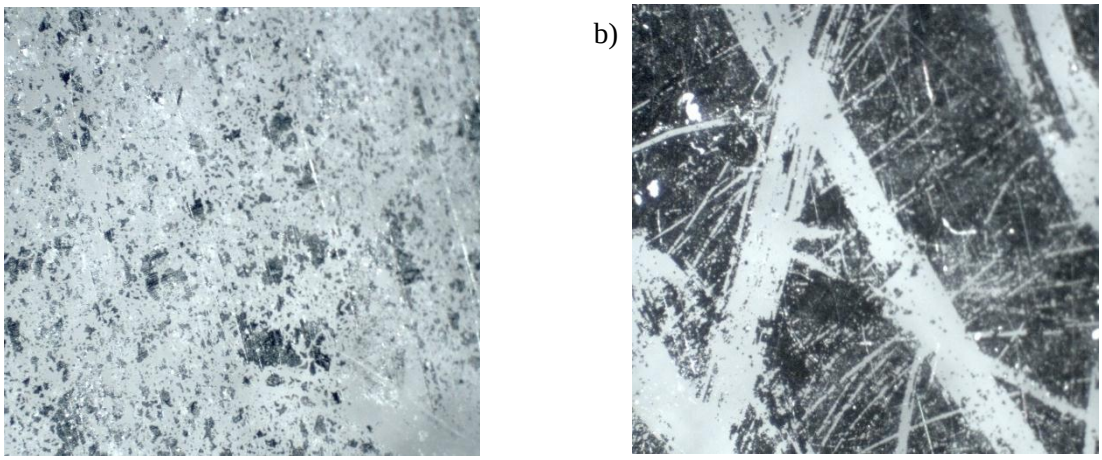

Figure 5.3: a) image of dissolved Al coating in water and b) image of removed Al coating when scraping.

5.3.1 Ag and ZnO Coating Overtime

The anti-adhesive properties of Ag and ZnO biofilms increased over 48 hours against both *P. aeruginosa* and *S. aureus* from little or no reduction in the first 24 hours, to a significant ($p \leq 0.05$) reduction of 1.41 $\log_{(10)}$ and 1.43 $\log_{(10)}$ for Ag and ZnO respectively against *S. aureus* and 1.82 $\log_{(10)}$ and 1.65 $\log_{(10)}$ for Ag and ZnO respectively against *P. aeruginosa* at 48 hours (Table 5.1). No significant differences were noted between the controls and Ag and ZnO coating at 2, 4, 6, 8 and 24 hours for *P. aeruginosa* and *S. aureus* ($p > 0.05$)

Table 5.1: The $\log_{(10)}$ reduction of *P. aeruginosa* and *S. aureus* biofilms on coated Ag and ZnO surfaces over 48 hours (n=6 ± SE).

	P. aeruginosa			*S. aureus*		
Hours/h	Control Si	Ag coating	ZnO coating	Control Si	Ag coating	ZnO coating
2	3.36 ± 0.04	0.11 ± 0.05	0.07 ± 0.03	3.37 ± 0.03	-0.01 ± 0.03	0.05 ± 0.04
4	3.53 ± 0.02	-0.03 ± 0.02	-0.09 ± 0.02	3.68 ± 0.01	0.09 ± 0.02	0.07 ± 0.03
6	3.74 ± 0.02	0.04 ± 0.01	0.02 ± 0.02	3.80 ± 0.02	0.03 ± 0.02	0.01 ± 0.02
8	3.82 ± 0.02	-0.04 ± 0.01	-0.01 ± 0.01	4.00 ± 0.02	0.05 ± 0.01	0.02 ± 0.01
24	7.07 ± 0.02	0.21 ± 0.01	0.28 ± 0.02	5.94 ± 0.02	0.27 ± 0.02	0.10 ± 0.01
48	8.12 ± 0.01	1.41 ± 0.01	1.43 ± 0.01	7.42 ± 0.01	1.82 ± 0.03	1.65 ± 0.02

5.3.2 SEM of **P. aeruginosa** *and* **S. aureus** *Biofilms on Ag and ZnO Thin Film Coatings*

The SEM images obtained after a 48 hour growth of *P. aeruginosa* and *S. aureus* biofilms on Ag and ZnO thin film coating (Figure 5.4) show that visible growth can be seen on the antimicrobial surfaces in Figure 5.4a, b, c and d. These images do not differ greatly from the growth observed on the control samples in Figure 5.4e and f. The cocci shape and rod shape of *S. aureus* and *P. aeruginosa* can be seen clearly without any visible damage.

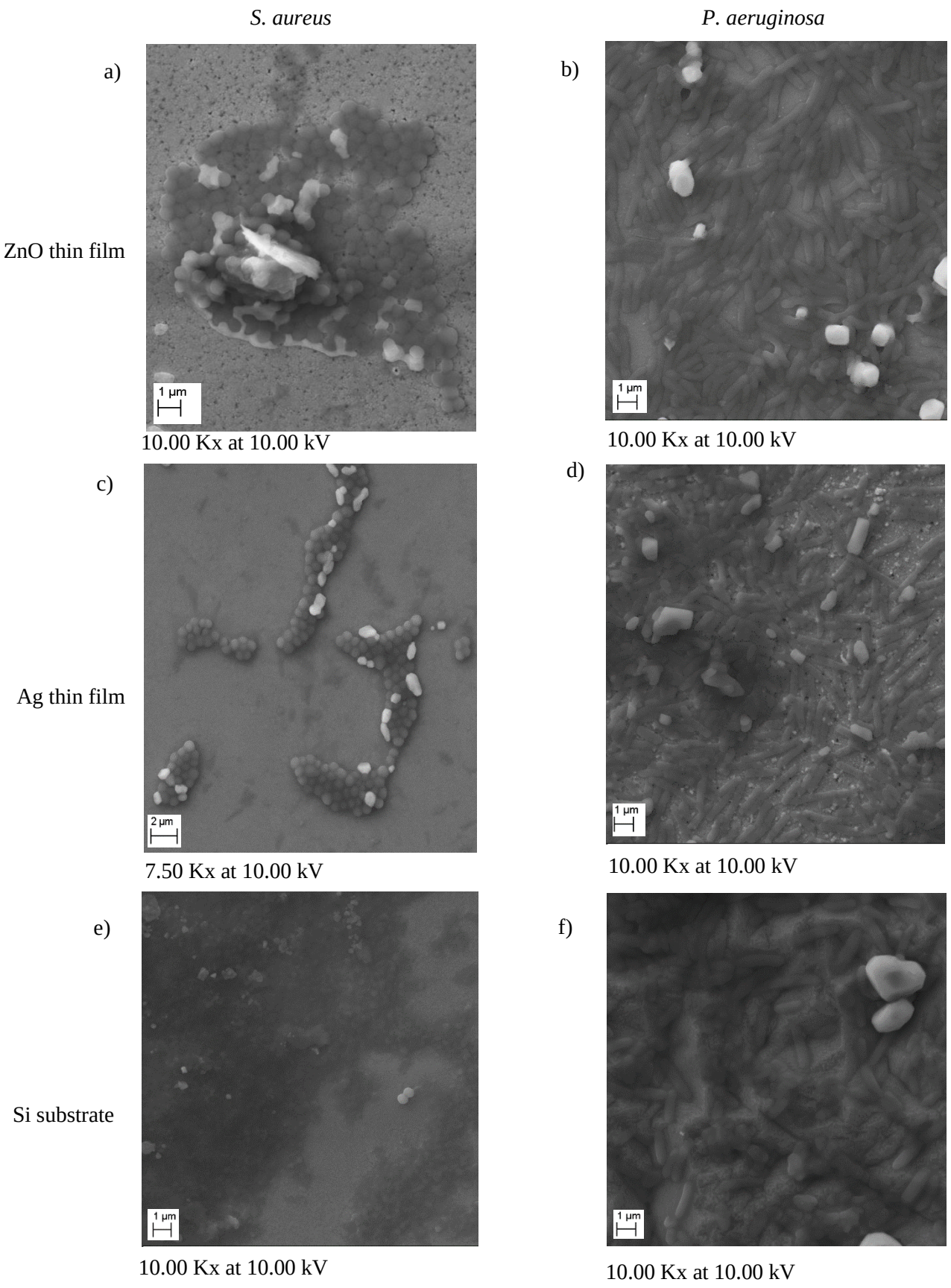

Figure 5.4: SEM images showing *S. aureus* and *P. aeruginosa* biofilm formation on Ag and ZnO thin films in comparison to Si substrates a) *S. aureus* biofilm on ZnO thin film, b) *P. aeruginosa* biofilm on ZnO thin film, c) *S. aureus* biofilm on Ag thin film, d) *P. aeruginosa* biofilm on Ag thin film, e) *S. aureus* biofilm on Si substrate, and f) *P. aeruginosa* biofilm on Si substrate.

5.4 Discussion

Previous studies have shown that contact with environmental surfaces carry the same degree of risk as touching an infected patient directly. A study by Stiefel *et al.* (2011) showed that there was only a 5% difference between the presence of MRSA on the gloved hands of healthcare workers that had direct contact with the patient (45%) and the environmental surface (40%). Similarly, a study by Guerrero *et al.* (2012) showed that 50% of healthcare personnel showed the presence of *C. difficile* on their gloved hands either after direct contact with the patient or environmental surfaces. It is noteworthy that healthcare personnel with direct contact with patients exhibited better hand hygiene compliance (80%) in comparison to those in contact with environmental surfaces (50%), illustrating that contamination from environmental surfaces has a greater chance to persist for longer and therefore, is more likely to be the main source for further transmission (Randle *et al.*, 2010).

Daily cleaning/disinfection ensures that the surroundings of the patient remain visibly clean in order to control environmental burden. At patient discharge, terminal cleaning is performed to certify that the clinical area is thoroughly disinfected, ready for the next patient. Unfortunately, even after terminal cleaning and disinfection, environmental sampling has shown that surfaces are still contaminated with nosocomial pathogens (Goldenberg *et al.*, 2012; Boyce *et al.*, 2008; Otter *et al.*, 2007; French *et al.*, 2004; Morter *et al.*, 2011). A study by Manian *et al.* (2011) showed that 27% of rooms after 4 rounds of bleach disinfection stayed contaminated with *A. baumannii* or MRSA, demonstrating that even numerous rounds of bleach disinfection is insufficient for disinfection. Furthermore, norovirus ribonucleic acid (RNA) resided on 43% of surfaces post one round of bleach treatment, and two rounds of bleach treatment left 16% of surfaces still contaminated. Disinfectants used in hospitals and bleach have shown to have antimicrobial activity *in vitro*, therefore theoretically, disinfection alone has the ability to eliminate contamination. The underlying issue for continuation of contamination could be due to inadequate distribution of the disinfectant across a surface and its contact time with the

contaminated area (Otter *et al.*, 2013). Self-disinfecting surfaces - i.e. coating with an antimicrobial agent - could potentially address this issue by preventing adhesion of microorganisms to its surface.

5.4.1 Thin Film Coating

Coatings are designed to limit microorganism adhesion in the initial stages of biofilm growth and potentially prevent its contiguous formation. Si samples coated with Ag and ZnO thin films were assessed for their ability to prevent the formation of *P. aeruginosa* and *S. aureus* biofilms (Table 5.1). For *P. aeruginosa*, ZnO thin films gave the largest reduction of 96.28% followed by Ag thin films with 96.13%. For *S. aureus*, the largest reduction was achieved using Ag followed by ZnO with reductions of 98.47% and 97.78% respectively in comparison to the uncoated Si substrates (Table 5.1). A slightly larger reduction was observed for the Ag and ZnO coatings for *S. aureus*. This could be due to the structural differences between Gram-negative and Gram-positive bacteria cell structures. The cell wall in Gram-negative bacteria contains an inner membrane with efflux proteins, peptidoglycan, and a double layered outer envelope made up of an outer membrane and LPS (Sheldon, 2005). Hydrophilic porin channels in the outer membrane manage the passage of solutes and prevent access of hydrophilic biocides (Lambert, 2002). Gram-positive bacteria however, are known to be more permeable to biocides due to the absence of an outer membrane (Brown *et al.*, 2015). Even though statistically significant ($p \leq 0.05$) $\log_{(10)}$ reductions were observed on Ag and ZnO coated substrates after 48 hours (Table 5.1), the results do not show ≥ 3 $\log_{(10)}$ reduction, there may be some promise in metal/metal oxide thin film coatings because they did prevent further formation of biofilms over time and thus had some limiting factor. An explanation for the metal and metal oxide based coatings not being effective in the first 24 hours may be because there was inadequate release of ions from the coatings, giving rise to insufficient ion concentration in the surrounding media to prevent adhesion. However, at 48 hours, the

increase in ion release over time shows better antimicrobial efficacy (Table 5.1). In order to confirm this, the release rates of ions from Ag and ZnO coated surfaces overtime need to be further investigated using techniques such as inductively coupled plasma mass spectroscopy (ICP-MS). Other studies have shown that 24 hours is sufficient to reduce biofilm formation, with Ag coating reducing *P. aeruginosa* biofilms by 13-fold (DeVasConCellos *et al.*, 2012). Li and Logan (2004) suggested that hydrophobicity of *P. aeruginosa* and the positive charge of metal oxide surfaces could promote the adhesion of negatively charged bacterial species. Due to the ZnO coating having a positive charge of Zn^{2+}, this could be a possible explanation for the adherence of *P. aeruginosa* to ZnO coated surfaces, further confirmed by the denseness of *P. aeruginosa* biofilms seen in Figure 5.4b and d.

Stranak *et al.* (2011) tested the antimicrobial efficacy of Ti-Cu thin films formed by three different methods of plasma-assisted magnetron sputtering. Growth inhibition of *S. epidermidis* ATCC 35985 and *S. aureus* ATCC 25923 cells in a planktonic form occurred within the first 24 to 96 hours, showing a high diffusion of Cu^{2+} ions into the media. However, the effect of Ti-Cu thin film coating was limited for biofilms of *S. aureus* and *S. epidermidis.* In general, *S. aureus* was more susceptible to the Ti-Cu films than *S. epidermidis*. There was a 3 $\log_{(10)}$ reduction of *S. epidermidis* over 10 days whereas there was total inhibition of *S. aureus* in 4 days was seen after exposure to Cu. On the 10^{th} day, persisting *S. aureus* biofilm cells re-grew, possibly owing to the low concentration of Cu ions after absorption of the initial Cu ions by the initially seeded bacteria (Stranak *et al.*, 2011). In the present work, a 48 hour biofilm of *S. aureus* and *P. aeruginosa* was reduced, suggesting that the ion concentration was sufficient to result in a significant ($p \leq 0.05$) reduction in comparison to 24 hours. Even though statistically there is a significant reduction, the reductions are very low for *P. aeruginosa* (1.41 and 1.43 $\log_{(10)}$ for Ag and ZnO coating respectively) and *S. aureus* (1.82 and 1.65 $\log_{(10)}$ for Ag and ZnO coating respectively) when compared to the controls (Table 5.1). The presence of persister cells may be the reason for biofilm growth even after 48 hours. The initially adhered bacteria may have been killed due to the uptake

of ions, resulting in low availability of ions for bacteria formed at a later stage (Stranak *et al.*, 2011). However, this cannot be confirmed here as AAS data has not obtained for ion leaching overtime. Moreover, factors such as QS may upregulate relevant genes, particularly those involved in encoding for virulence factors (Beceiro *et al.*, 2013).

The anti-adhesive effect of ZnO nanorod substrates and ZnO sputtered substrates for the adhesion prevention of *P. aeruginosa* and *S. epidermidis* in comparison to glass as a reference was tested previously (Jansson *et al.*, 2012). *P. aeruginosa* showed a 2.5 and 1.7 fold greater reduction in cells on ZnO nanorod and ZnO sputtered surfaces respectively in comparison to glass substrates and *S. epidermidis* showed a ~20 and 30 fold greater reduction on ZnO sputtered and nanorod substrates respectively in comparison to a glass surface (Jansson *et al.*, 2012). This difference in anti-adhesive properties of ZnO nanorod and sputtered substrates against both bacteria could be due to the variance in the cell wall structures of Gram-negative and Gram-positive bacteria e.g. the presence of an outer wall in Gram-negative bacteria (Silhavy *et al.*, 2010). Cell wall structure differences may cause the ZnO nanorods to have different electrostatic and van der Waals interactions, thereby, affecting the adhesion of the biofilms. ZnO nanorods could be exerting an antimicrobial effect by piercing into *S. epidermidis* cells, leading to membrane integrity loss and cell death (Jansson *et al.*, 2012). Flagella formation is required by *P. aeruginosa* to bind to a surface. Twitching motility of *P. aeruginosa* enables it to form mature biofilm structures with a slime layer (O'Toole & Kolter, 1998), which could be strong enough to overcome the antimicrobial effects of ZnO nanorods.

Growth of *E. coli* ATCC 25922 biofilms on ZnO thin films on Si substrates has been investigated previously using disk diffusion and the CDC biofilm reactor (Gittard *et al.*, 2009). The cell density was $13.16 \pm 9.44 \times 10^6$ cfu/cm^2 and $6.28 \pm 3.52 \times 10^6$ cfu/cm^2 on uncoated Si and ZnO thin films respectively over a 48 hour growth period in the CDC biofilm reactor (Gittard *et al.*, 2009), similar antimicrobial properties of ZnO coatings were also observed in other studies (Zhou *et al.*, 2005; Szunyogová *et al.*, 2007; Fang *et al.*, 2015). *E. coli* grew on both coated and uncoated substrates

but more than 50% reduction in cell density was observed on the ZnO coating in comparison to Si surface. No change in growth reduction was seen on an uncoated surface in dark conditions or with constant fluorescent light, suggesting light is not required for antimicrobial activity (Gittard *et al.*, 2009). The leaching of Zn^{2+} ions from the surface of the coating could be providing the antimicrobial activity (Szunyogová *et al.*, 2007). In the present investigation, lower reductions were found, however, the method of *in vitro* testing could have had an effect on the results acquired. Jansson *et al.* (2012) used optical density to semi-quantify biofilm formation, and Stranak *et al.* (2011) used 24 well plates to form the biofilm to obtain cfu/ml, whereas the CDC biofilm reactor is a reliable real life replica of biofilm formation. The differences in reductions obtained could be due to the chosen *in vitro* biofilm formation method.

The adhesion of *S. epidermidis* IE186 and 1457 to Ag-Ti carbonitrile (Ag-TiCN) antimicrobial coatings has been assessed previously in the literature (Carvalho *et al.*, 2013). Three ratios of Ag/Ti concentrations were tested with increasing concentration of Ag with 0, 10 and 15%. As the concentration of Ag increases, the roughness of the *S. epidermidis* biofilm reduces. Only a <2 $\log_{(10)}$ difference was seen between the TiCN coatings with and without Ag. Increase in Ag concentration in TiCN coated surfaces was shown to promote biofilm formation of *S. epidermidis* strains at 24 hours, which is unexpected due to the well-known antimicrobial properties of Ag (Carvalho *et al.*, 2013). This could be due to minimal levels of Ag^{+} released from the surface of the coating which are insufficient to result in an antimicrobial effect on the bacterial cells. A similar phenomenon may perhaps be occurring in this study whereby Ag is encouraging biofilm formation. Alternatively, the initial biofilm adhesion could have been prevented due to the antimicrobial properties of the Ag and ZnO coating and their ion release; but due to the formation of slime layers as well as the initiation of QS factors in the biofilm, the antimicrobial effect of the coating is overcome. The formation of conditioning layers could be the reason for the low $\log_{(10)}$ reductions observed in this study, as the adhesion of macromolecules such as proteins can change the adhesion properties on the substrate, thus favouring attachment (Lorite *et al.*, 2011; Lejeune,

2003). An example of this are surfaces coated with quaternary ammonium salts, which have an antimicrobial effect prior to conditional layer deposition (Tiller *et al.*, 2001; Melo *et al.*, 2011). Furthermore, the continuous flow of nutrients and rotation in the biofilm reactor aids biofilm growth and the biofilm community may be able to overcome the stress exerted by ions.

5.4.2 Conclusion

Antimicrobial surfaces aim to reduce bacterial adhesion on a surface in the initial stages of biofilm growth in order to prevent the formation of mature biofilms, which are then difficult to eradicate. Although Ag and ZnO have demonstrated their efficacy in suspensions post biofilm formation, in this investigation they have shown limited antimicrobial properties as a thin film coating. In order for metals/metal oxides in a coated form to have potential as a self-disinfecting surface within a healthcare setting, further development is required. The inhibition of bacterial adherence is partly dependent on the physicochemical properties of the substrate as well as the properties of the pathogen, therefore it is important to understand the underlying mechanisms of action that bring about the beneficial effects.

Chapter 6

Chapter 6: Gene Expression in *S. aureus* Biofilms

6.1 Introduction

Reducing the spread of HCAIs is the responsibility of the HICPAC, through providing advice on ensuring valid procedures are undertaken to clean and disinfect environmental surfaces, eliminating nosocomial pathogens such as *S. aureus* (Umscheid *et al.*, 2010). Planktonic cells have lower resistance to antimicrobials in comparison to cells embedded within a biofilm (Kim & Rhee, 2016). Bacterial biofilms express virulence factors in response to antimicrobials, antibiotics or disinfectants, exhibiting resistance (Gaddy & Actis, 2009; Wroblewska *et al.*, 2008).

Biofilms have four main stages of biofilm formation including formation of planktonic cells, reversible and irreversible adhesion, maturation and finally dispersion (Monds & O'Toole, 2009), which occur dynamically during the process of biofilm formation. Gene expression regulates the phenotypes associated to each stage of biofilm formation. Initially, flagella are used by bacteria to move towards a surface. Irreversible attachment requires the flagella genes to be repressed, and adhesion proteins such as curli, pilli and type I fimbriae to be expressed as motility is no longer required as the bacteria are in a fixed position on the attached substrate (Lazazzera, 2005; Prüß *et al.*, 2006). Irreversible attachment to a surface results in the genes of exopolysaccharide biosynthesis to be expressed, which enable the construction of mature biofilms. For instance, *alg8*, *pelF* and *pslA* are genes required for the synthesis of three exopolysaccharides (alginate, Psl and Pel) essential for *P. aeruginosa* biofilm development (Ghafoor *et al.*, 2011; Prüß *et al.*, 2006; Colvin *et al.*, 2012).

6.1.1 S. aureus *Biofilm Forming Genes*

Adhesion is a vital step in biofilm formation on tissues and abiotic surfaces which is aided by adhesins in the family of MSCRAMM, present in Gram-positive bacteria (Tenover *et al.*, 2006). After adhesion, bacteria multiply forming a multi-layered structure, leading to PIA production (Götz, 2002). PIA is a polysaccharide composed of poly-β(1-6)-*N*-acetylglucosamine, involved in the bacterial aggregation (Arciola *et al.*, 2015). The products of the intercellular adhesin (*ica)* locus synthesise PIA, mainly *via* the enzyme *N*-acetylglucosaminyltransferase, which is encoded by *icaA* (Mack *et al.*, 2006). MSCRAMMs are proteins that are anchored on the cell surface of bacteria and can bind to the extracellular matrix as well as the hosts' plasma components (Tenover *et al.*, 2006). They are mainly covalently bound to the peptidoglycan in the bacterial cell wall and can identify more than one host extracellular matrix factors, such as: collagen (encoded by the *cna* gene); fibronectin binding proteins A and B *(*encoded by the *fnbA* and *fnbB* gene); elastin binding protein (encoded by the *ebpS* gene);fibrogen (encoded by the *fib* gene); bone sialoprotein (encoded by the *bbp* gene); laminin (encoded by the *eno* gene) and clumping factors A and B (encoded by the *clfA* and *clfB* gene)(Seo *et al.*, 2008; Zuniga *et al.*, 2015). All these proteins have the same signal for secretion and for anchoring onto the cell wall (Atshan *et al.*, 2013). The *ica* ADBC operon encoded by the *ica* gene are proteins required for PIA synthesis as well as capsular polysaccharide/adhesion (PS/A), which are vital in staphylococci (Chaieb *et al.*, 2005). The proteins *icaA*, *icaC* and *icaD* are found in the membrane, whereas *icaB* is usually present in the supernatant of the culture and deacylates PIA when it adheres to a cell surface. The activity of *N*-acetylglucosamine transferase activity is increased by the co-expression of *icaD* and *icaC* (Arciola *et al.*, 2006). The function of the gene *icaB* is to encode for an extracellular protein, however its function is yet unclear. The gene *icaC* encodes for a membrane protein which is known to have receptor function for polysaccharides (Atshan *et al.*, 2013).

The *ica* operon is known to be vital for *S. aureus* biofilm formation (Mack *et al.*, 2006), however O'Neill *et al.* (2007) showed that deleting the *ica* genes did not affect biofilm formation in some

MRSA strains. Bap is a cell wall surface protein that is also important in intercellular adhesion and biofilm growth (Cucarella *et al.*, 2001).

IcaC is a transmembrane protein that is mainly involved in translocation and elongation of the polysaccharide, which is essential for PIA synthesis (Rohde *et al.*, 2010). Beenken *et al.* (2004) and Vandecasteele *et al.* (2003) showed that *icaC* gene has highest expression in the icaADBC operon. A study by Mirzaee *et al.* (2014) examined 63 MRSA isolates for the presence of *icaADBC* genes using a polymerase chain reaction (PCR) approach. All MRSA isolates had *icaD* and *icaC* genes, whereas there was a prevalence of 60.3% and 51% of *icaA* and *icaB* respectively in all the isolates. In contrast, a study by Yazdani *et al.* (2006) noted the presence of *icaA* in all the *S. aureus* strains tested. The expression of *ica* can be influenced by environmental factors such as glucose, temperature, osmolarity and its growth in anaerobic environments (Kim *et al.*, 2008; Beenken *et al.*, 2004). A study by Szczuka *et al.* (2013) found that 23% of the MRSA strains tested did not show the presence of *icaA* and *bap* genes. However, they did form a biofilm, showing that MRSA biofilms do form without the presence of *icaA*, demonstrating the formation of *ica*-independent biofilms, coinciding with findings of O'Neill *et al.* (2008), Izano *et al.* (2008) and O'Neill *et al.* (2007).

The *ebpS* gene encodes for the *S. aureus* binding protein that controls attachment to host cells by binding to elastin (Nakakido *et al.*, 2014). The *ebpS* gene is conserved by *S. aureus*, which could explain the importance of the gene. The N-terminal region of EbpS can bind to Zn^{2+}, resulting in local conformational alterations in the structure of the EbpS protein. In an EbpS deficient strain, growth rates had reduced, suggesting that EbpS is vital in biofilm formation regulation and vital for infections derived from staphylococcal species (Nakakido *et al.*, 2014). The inhibition of binding of EbpS to Zn^{2+} could be a potential target for therapeutical agents in preventing *S. aureus* infections (Nakakido *et al.*, 2014).

Fibronectin binding proteins (FnbPs) are multifunctional and encourage bacterial attachment to fibronectin, elastin and fibrinogen (McCourt *et al.*, 2014). In a study by Cha *et al.* (2013), MRSA biofilm forming strains showed increased expression of the *fnbB* gene compared with the non-biofilm forming strains with values of 74.4% and 45.0% respectively. Furthermore, in order to determine the presence of FnbA and FnbB on the cell surface of *S. aureus* strain LAC, ligand affinity blotting with biotin-labelled fibronectin was used to analyse cell wall extracts from cultures in the stationary phase (McCourt *et al.*, 2014). Two reactive bands were observed for fibronectin-binding protein A (FnBPA) and fibronectin-binding protein B (FnBPB) but not for LACΔ*fnbAfnbB*, *fnbA* and *fnbB* deficient *S. aureus* USA300 isolate LAC, suggesting the presence of FnBPs on the cell surface of bacteria during the stationary phase (McCourt *et al.*, 2014). In addition to this, bacteria were able to adhere to fibronectin during the stationary phase and is dependent on FnbP expression. FnbPs promote accumulation of cells as well as the attachment phase of biofilms (McCourt *et al.*, 2014). Similar findings were observed by Lei *et al.* (2011), showing that FnbPs mediate primary cell attachment and biofilm accumulation in *S. aureus* CC30 strain MW2.

One approach that can be used to test the antimicrobial efficacy of antimicrobial agents is to measure the change in gene expression associated with biofilm formation and virulence factors, before and after treatment with an antimicrobial agent. This knowledge could be beneficial as the up and down regulation of biofilm forming genes in a biofilm due to treatment with an antimicrobial agent can be used as a target for novel antimicrobial agents.

6.1.2 Aims and Objectives

Aim:

The aim of this investigation was to determine the change in gene expression of *ebpS, icaC* and *fnbB* of mature *S. aureus* biofilms caused by treatment with 8/12 µg/ml of ZnO/Ag NP suspensions, *via* quantitative PCR (qPCR).

Objectives:

- To determine the best biofilm forming method to obtain the required quantity of RNA.
- To assess the difference in gene expression in *S. aureus* biofilm forming genes with and without treatment with 8/12 µg/ml of ZnO/Ag NP suspensions.

6.2 Methods

6.2.1 Sample Collection

6.2.1.1 Biofilm formation in CDC biofilm reactor

Biofilms of *S. aureus* were grown in the CDC biofilm reactor as per Method 3.2.3.1 and 3.2.3.2. A 24 hour culture of *S. aureus* grown in tryptone soya broth (TSB) was used. Samples were treated for 48 hours with 8/12 µg/ml of ZnO/Ag NP suspension. Treated and untreated control samples were taken at 0, 12, 24 and 48 hours by scraping the surface of the 6 PC coupons per sample (Method 3.2.3.3) into 1.5 ml of PBS and freezing the samples in liquid nitrogen (LN_2) for RNA extraction. Control samples were placed in sterile water over 48 hours.

6.2.1.2 Biofilm formation in 6 well plates

Aliquots of 5ml of a 24 hour culture of *S. aureus* were added to a 6 well plate and incubated statically for 48 hours at 37°C. After the formation of a 48 hour biofilm, the biofilms were treated with 8/12 µg/ml of ZnO/Ag NP suspension. Sterile water was added for the control wells. At 0, 12, 24 and 48 hours, control and treated samples were collected by removing the media, and rinsing the biofilms twice with PBS. PBS (200µl) was then added to each well and the biofilms removed by scraping. The agitated biofilm cells were then placed into a 2ml Eppendorf tube and frozen in LN_2 prior to RNA extraction.

6.2.1.3 Biofilm formation in Eppendorf Tubes

A 24 hour culture of *S. aureus* was grown in TSB broth. Eppendorf tubes containing 1.5ml of PBS were inoculated with the 24 hour culture and incubated at 37°C (rotating incubator) for 48

hours. The tubes were rinsed with PBS, leaving the remaining adhered biofilm. At 0, 12 and 48 hours, aliquots of 1.5 ml of PBS was then added to the Eppendorf tubes and sonicated in an ice bath for 3 mins to disrupt the biofilm. The samples were then frozen in LN_2 for RNA extraction at stored at -80 °C.

6.2.2 PCR

PCR amplification was performed containing Go-Taq 5 x Colourless Flexi Buffer (Promega, Wisconsin, USA), 10µl; $MgCl_2$ solution (Promega, Wisconsin, USA), 4µl; dNTP mix 10 mM (Promega, Wisconsin, USA), 1 µl; specific upstream primer (Integrated DNA Technologies, Coralville, USA), 1 µl; specific downstream primer (Integrated DNA Technologies, Coralville, USA), 1 µl; Go Taq Flexi polymerase (Promega, Wisconsin, USA), 0.25 µl; template DNA, 1 µl to make up to 50 µl per reaction with nuclease free water (Promega, Wisconsin, USA). The conditions for the Thermocycler PCR (PIKO 24, Thermo Fisher Scientific, Loughborough, UK) consisted of denaturing at 95°C for 30 seconds, annealing at 55°C for 30 seconds and extension at 72°C for 1 min.

6.2.3 Gel Electrophoresis

A 2% agarose gel (Sigma Aldrich, Dorset, UK) was prepared using the Sybr® Safe DNA gel stain in 1 x TAE (Invitrogen, Eugene, USA) and left to set in a gel tank (FHU6 Fisher Scientific, Loughborough, UK) with a well comb. The gel tank was topped up with 0.5 X TAE running buffer (40 mM Tris (pH 7.6), 20 mM acetic acid and 1 mM EDTA). In each well, 5 µl of blue/orange loading dye with 5 µl of PCR product was added. A benchtop ladder 1 kb DNA (Promega, Wisconsin, USA) was added alongside the PCR product. The electrophoresis was run

at 90V for 45 mins and the gel was visualised under ultraviolet transillumination using the Gel Doc™ EZ Imager (Bio-Rad, Hemel Hempstead, UK).

6.2.4 RNA Extraction and Purification

The extraction was undertaken as per the instructions in the RNeasy mini kit (Qiagen, Valencia, USA). Products were kept on ice throughout the extraction process to avoid degradation. In brief, samples stored at 4°C were defrosted on ice. The bacteria were harvested to form a pellet by using a 4°C chilled centrifuge (Heraeus Fresco 21, Thermo Electron Corporation, Massachusetts, USA) at 5000 x *g* for 5 mins and supernatant decanted. Buffer RLT was added and the pellet was resuspended. Acid wash beads were used to disrupt the cells in a TissueLyser (Retsch, Hope Valley, UK) for 5 mins at maximum speed. Ethanol (70%) was added and the lysate was transferred to an RNeasy spin column with a collection tube and centrifuged for 15 seconds at 8000 x *g*. Buffer RW1 was added and centrifuged for 15 seconds at 8000 x *g*. Buffer RPE was added and centrifuged at 15 seconds at 8000 x *g* and then added once again and centrifuged at 2 mins at 8000 x *g*. The RNeasy column was placed in a new collection tube and centrifuged at full speed for 1 min. The RNeasy spin column was placed in a new 1.5 ml collection tube and with 30-50 µl of RNase-free water was added and centrifuged at 8000 x *g*.

6.2.5 RNA Quantification

The RNA was quantified using the Nanodrop (Nanodrop Lite Spectrophotometer, Thermo Fisher Scientific, Loughborough, UK). The product was run on an agarose gel (Sybr® Safe DNA gel stain in 1 x TAE, Invitrogen, Massachusetts, USA) at 90 volts for 25 mins in a gel tank to observe the presence of RNA. To purify the RNA, Turbo DNase (Thermo Fisher Scientific, Loughborough) was used and quantified against using the Nanodrop.

6.2.6 Synthesis of cDNA

cDNA was synthesised using the iScript Select cDNA synthesis kit (Bio-Rad, Hemel Hempstead, UK). cDNA synthesis was performed using 5 x iScript reaction mix-4 µl, iScript reverse transcriptase- 1µl, nuclease-free water and RNA template (100 fg to 1 µg total RNA) to make up a final volume of 20 µl. The protocol used to perform the reverse transcriptase process was 25°C for 5 mins, 42°C for 30 mins, 85°C for 5 mins and held at 4°C.

6.2.7 qPCR Assay

Fragments of *ebpS, icaC, fnbB* and *16S* (Integrated DNA Technologies, Coralville, USA) were amplified with the SensiFAST™ SYBR Hi-ROX Kit (Bioline, London, UK) following the manufacturer's protocol.

Table 6.1: Primer sequence and annealing temperatures

Genes	Nucleotide primer sequence (5'-3')	Annealing Temperature (°C)
*ebp*S	5'-GGT GCA GCT GGT GCA ATG GGT GT-3'	64.8
	5'-GCT GCG CCT CCA GCC AAA CCT-3'	65.5
*ica*C	5'-TTG CAA ATC GTG GGT ATG TGT-3'	55.0
	5'-CTT GGG TAT TTG CAC GCA TT-3'	54.1
fnbB	5'-ACG CTC AAG GCG ACG GCA AAG-3'	63.0
	5'-ACC TTC TGC ATG ACC TTC TGC ACC T-3'	62.3
16S	5'-GGG ACC CGC ACA AGC GGT GG-3'	66.4
	5'-GGG TTG CGC TCG TTG CGG GA-3'	65.9

PCR amplification was performed using the following protocol: SensiFAST™ SYBR Hi-ROX (2x), 5µl; forward primer (10 µM), 0.1 µl; reverse primer (10µM), 0.1 µl; as well as template and RNase free water to make up to 10 µl final volume.

The programme for the qPCR (PIKOREAL 96 Real-time PCR system, Thermo Fisher Scientific) protocol for the SensiFAST™ SYBR Hi-ROX Kit consisted of 1 cycle of 95℃ for 2 mins (polymerase activation), and 40 cycles of 95℃ for 5 seconds (denaturation), annealing temperature of specific primer (annealing) (Table 6.1) and 72°C for 5-20 seconds (extension).

6.3 Results and Discussion

6.3.1 Biofilm Formation and RNA extraction

Despite a number of studies reporting the expression of biofilm genes in *S. aureus* biofilms (Dunman *et al.*, 2001; Resch *et al.*, 2005; Beenken *et al.*, 2004), little is known regarding the effect of metal and metal oxide NPs on biofilm forming genes.

Acquiring and quantifying mRNA from biofilms is fundamental in understanding the molecular mechanisms of gene expression involved in biofilm formation and maturation on surfaces such as medical devices (França *et al.*, 2011). However, the successful completion of RNA based analysis methods are based on the yield, purity and integrity of RNA (Bustin *et al.*, 2005; Nolan *et al.*, 2006). It is also important to understand that the RNA quality and quantity is based in the RNA extraction methods used (Nour *et al.*, 2010; Rump *et al.*, 2010).

The genes *ebpS, icaC, fnbB* are all biofilm forming genes, known to be expressed the most during *S. aureus* biofilm formation (Atshan *et al.*, 2013), hence were chosen for this study along with *16S* as a reference gene. An agarose electrophoresis gel to show the presence of *icaC, ebpS, fnbB* and reference gene *16S* in *S. aureus* is shown in Figure 6.1. The gene *icaC* is not seen in the image, possibly due the melting temperature set on the PCR for the annealing step. The annealing temperature is vital in PCR as the set temperature allows PCR primers to anneal to their complementary targets (Integrated DNA Technologies, 2011). Atshan *et al.* (2013) demonstrated that after 48 hours, there was an up-regulation of *fnbA, fnbB, clfB, ebpS* and *icaC* in *S. aureus* biofilms with an increase between 7.2-21.1, 14.5-17.8, 2.4-2.8, 25.9-45.1 and 91.4-239 fold respectively between four *S. aureus* isolates. The genes *fnbA, fnbB, icaC* and *ebpS* showed the highest up regulation.

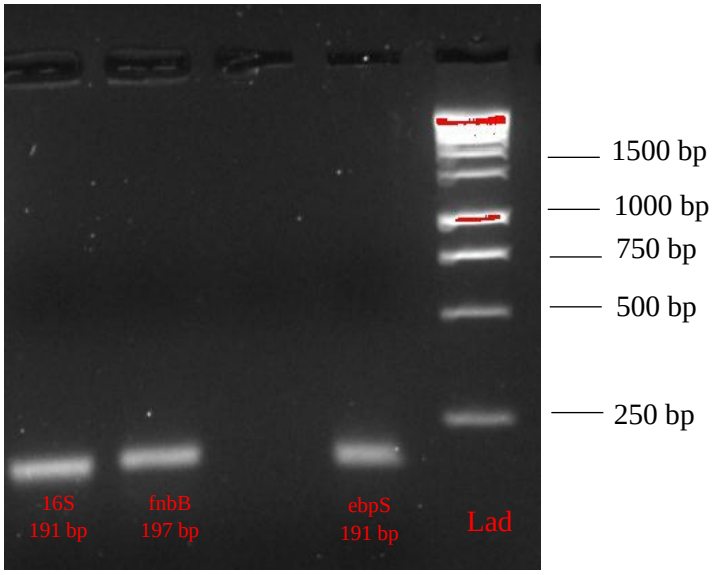

Figure 6.1: Agarose gel electrophoresis of the amplified *S. aureus ebpS, fnbB* and *16S* reference gene

Resch *et al.* (2005) compared planktonic and biofilm cells and found highest expression of *ica* genes between 6 and 8 hours of biofilm development. This contradicts the finding by Atshan *et al.* (2013), who reported that expression of *ica* genes were relatively low between 6 and 12 hours. Furthermore, Vandecasteele *et al.* (2003) found that the ica operon mainly functioned in the initial growth phase of the biofilm as opposed to maturation, whereas Atshan *et al.* (2013) showed that these genes were expressed higher during the 48 hours of growth. Szczuka *et al.* (2013) demonstrated that 76% of the *S. aureus* strains tested all produced slime and carried the *ica*A gene. However, studies by Peacock *et al.* (2002) and Rohde *et al.* (2007) showed that all *S. aureus* strains possess the *ica* genes. *S. aureus* cells isolated from orthodontic appliances were investigated for their ability to adhere to polystyrene and dental alloys (Merghni *et al.*, 2016). Amongst the strains tested, 94% were positive for *ica*A and *ica*D (Merghni *et al.*, 2016), whereas a study by Aricola *et al.* (2001) that showed 60.86% of *S. aureus* strains isolated from catheters were positive for *ica*A and *ica*D. These differences could be due to a factors such as environmental stimuli, nature of the strain and growth media resulting in differences in gene expressions of biofilms (Beloin *et al.*, 2006).

Various methods of biofilm formation were investigated to determine the most effective method to obtain the largest quantity of RNA when quantified on Nanodrop spectrometer. RNA values for treated samples formed in the CDC biofilm reactor, 6 well plates and Eppendorf tubes at 12, 24 and 48 hours ranged between 0.8 to 26.5 ng/µl, and the control samples ranged between 0.9 to 47.4 ng/µl. Regardless of the formation method used, large variations were observed within the samples taken at each time point and their replicates. Even though higher values (47.4 ng/µl) was obtained for some samples, no band was observed on an agarose gel. Treated biofilm samples at 24 hours for instance, values of 4.6 and 0.8 ng/µl, 2.8 and 16.68 ng/µl, and 1.2 and 15.9 ng/µl were obtained for biofilms formed in the CDC biofilm reactor, Eppendorf tubes and 6 well plates respectively. Similar variation was observed throughout. The inconsistency in values, small quantities of RNA, and poor quality of RNA obtained meant methods after RNA extraction (Method 6.2.4) to qPCR (Method 6.2.7) were not performed. The lower the initial sample concentration, the lower the RNA yield (Nour *et al.*, 2010), therefore taking this into account, a conclusion was drawn that scraping the PC coupons with a glass rod to remove biofilm did not provide an adequate quantity of cells to extract RNA from, even though two rods containing three PC each were used. The variation in RNA quantity from biofilms formed in Eppendorf tubes and in 6 well plates, meant these methods were not appropriate for RNA extraction. If processes after RNA extraction were commenced, it would be likely to prove unsuccessful as RNA yield is lost through each stage. A gel electrophoresis to show RNA integrity in *S. aureus* biofilms formed in a CDC biofilm reactor is shown in Figure 6.2. The presence of RNA was only seen for the control sample at 12 hours and 24 hours, and a sample treated with 8/12 µg/ml of ZnO/Ag NP suspension for 48 hours (Figure 6.2). No RNA was seen for all the treated and control samples tested. The low quantities of RNA in conjunction with the smeared appearance observed in Figure 6.2 could suggest that some of the RNA may have been degraded. If sufficient quantities of ribosomal RNA were present, smears would have been observed with two bands. However, a smeared appearance solely could suggest degradation or contamination with chromosomal DNA.

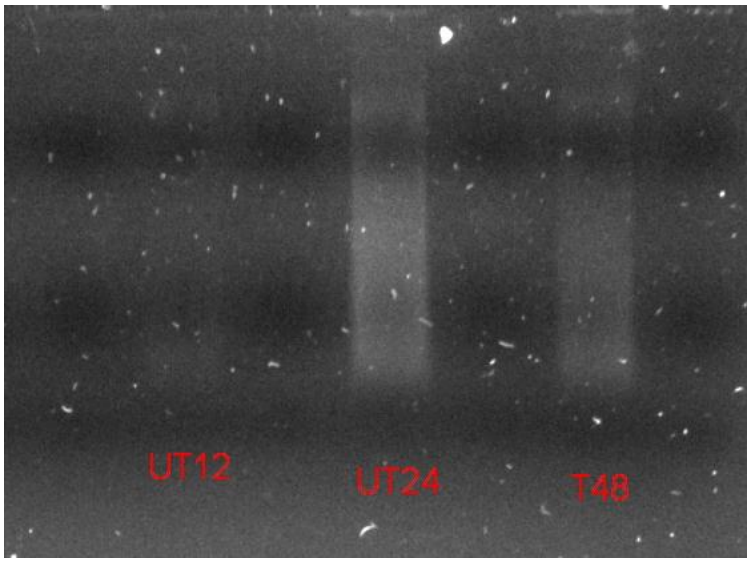

Figure 6.2: Gel electrophoresis showing the presence of RNA post RNA extraction of treated (8/12 µg/ml of ZnO/Ag NP suspension) and control biofilms of *S. aureus* in a CDC biofilm reactor.

There are a few reasons that could be proposed for the low yields or lack of the presence of RNA in some of the samples. Firstly, high cell densities within biofilm mean increased external protein concentrations and polysaccharide contents, which could interfere with the RNA extraction process (França *et al.*, 2011). RLT buffer provided in the RNA extraction kit was used for cell lysis prior to RNA extraction. RLT buffer contains guanidine thiocyanate, which is used for protein degradation. Phenol is known to promote greater cell lysis than using acid wash beads and a TissueLyser (França *et al.*, 2011). Furthermore, the presence of the extracellular matrix can hinder cell lysis and RNA extraction. Even after RNA purification, the RNA can still contain inhibitory substances (Santiago-Vázquez *et al.*, 2006; Junttila *et al.*, 2009). Furthermore, the use of sonication for cell lysis can also lead to degradation of the RNA, even though it was performed in an ice bath.

Atshan *et al.* (2012) used four Gram-positive strains (MSSA ATCC 35556 and ATCC 29278, MRSA ATCC 700698, *S. epidermidis*) and two Gram-negative bacteria (*P. aeruginosa* and *E.*

coli) for the RNA extraction procedure. Five commercially available extraction kits tested were the RNeasy Mini Kit (as used in this chapter), NucleoSpin RNAII (Macherey-Nagel, Germany), InnuREP RNA Mini (Jena, Germany), Trizol (Invitrogen) and MasterPure RNA Purification Kits (EPICENTRE Biotechnologies)(Rump *et al.*, 2010). Apart from Trizol and MasterPure kits, the other three kits utilises a spin-column comprising of silica membranes technology. Trizol and Master Pure kits on the other hand use a protocol rather than a column to purify the RNA and retain the small RNA molecules that usually get washed out in methods using spin columns (Rump *et al.*, 2010). RNA extraction using commercial kits was compared to using a boiling method containing an addition of hot phenol incubation step (Atshan *et al.*, 2012). Low quantities and integrity of RNA were obtained using the commercial kits, possibly due to inadequate lysis of the bacterial cells embedded in the dense structure of the biofilm (Atshan *et al.*, 2012). Physiological characteristics such as the cell wall which can obstruct cell lysis, in turn affecting the release of RNA (Ludwig & Schleifer, 2000). Higher yields were achieved with an additional hot phenol incubation step instead of using bead mill or enzyme. When an additional phenol step was used with the RNeasy Mini Kit, RNA with greater integrity was produced which did not need further purification. Although the phenol method can be time consuming and require more biochemical reagents, the highest RNA integrity was obtained using this method (Atshan *et al.*, 2012). Heat degradation can affect the RNA yield (Sung *et al.*, 2003) which could be another reason for such low RNA recovery in the present investigation.

MSCRAMMs found on the surface of *S. aureus* aid in adhering *S. aureus* to components in the extracellular matrix of the host organism (Vazquez *et al.*, 2011). These components assist in biofilm formation alongside the PIA producing *ica* operon (Mirzaee *et al.*, 2014). A total of 22 *S. aureus* strains obtained from hospitalised infants were examined for the presence of *mecA* as well as *clfA, clfB, fnbA, fnbB, fib, eno, cna, ebpS* and *bbp via* PCR (Ghasemian *et al.*, 2015). The gene *mecA* is used as a standard for determining resistance as it is found in all MRSA strains (Elhassan *et al.*, 2015). All isolates expressed *clfAB* and the occurrence of *fnbA, fnbB, fib, eno, cna, ebpS*

and *bbp* was 63%, 6%, 50%, 59%, 82%, 63%, 9% and 0% respectively (Ghasemian *et al.*, 2015). Being aware of the gene expression in biofilm can aid in targeting certain genes for therapeutic purposes for treatment (Ghasemian *et al.*, 2015).

6.3.2 Gene Expression Analysis Using qPCR

The small quantities of RNA recovered from *S. aureus* biofilms meant that qPCR was unable to be performed. After determining the antimicrobial effect of a combination of metal and metal oxide NP suspensions in Chapter 4, it would be expected that there would be a downregulation of *icaC, ebpS* and *fnbB*. This would be due to the prevention of the biofilm being formed in the presence of this antimicrobial, therefore preventing the biofilm genes from being expressed. Published research on the effect of metal NP suspensions on biofilms is limited, therefore it would be beneficial to investigate this further for future disinfectant development which could be utilised in healthcare arenas. Radzig *et al.* (2013) determined the antimicrobial activity of Ag NPs (8.3 nm) against planktonic cells and biofilms of Gram-negative bacteria including *E. coli* AB1157, *P. aeruginosa* PA01 and *Serratia proteamaculans* 94. Concentrations of 4-5, 10 and 10-20 µg/ml of Ag NPs were required to decrease the bacterial mass of biofilms of *E. coli, P. aeruginosa* and *S. proteamaculans* respectively. The viability of *E. coli* cells within the biofilm was lessened with Ag NP concentrations over 100-150 µg/ml (Radzig *et al.*, 2013). *E. coli* strains containing mutated genes that repair DNA with oxidative lesions (*mutY, mutS, mutM, mutt, nth*) were found to be less resistant to Ag NPs in comparison to the wild type strains, suggesting that these genes are vital in the repairing of damaged DNA caused by Ag NPs (Radzig *et al.*, 2013). Even though there is limited research on the effect of metal/metal oxide NP suspensions on biofilms, the study by Radzig *et al.* (2013) shows the antimicrobial potential of Ag NPs.

Baker *et al.* (2010) demonstrated that excess Cu represses expression of Sae and Agr, two of the main global virulence gene regulators, as well as the protein Eap, therefore, preventing *S. aureus*

biofilm formation. Eap is an extracellular protein that is vital for biofilm formation in low iron conditions. Accessory gene regulator protein D (*agrD*), sensor histidine kinase (*SaeS*) and response regulator SaeR (*SaeR*) were downregulated with a fold change of -2.17, -2.00 and -2.01 respectively (Baker *et al.*, 2010). The *agr* locus represses cell wall associated protein expression and induces expression of exoproteins after exponential growth. The *saeRS* locus induces exoprotein expression as well as α-hemolysin and protein A (Bronner *et al.*, 2004). On the contrary, heavy metals at low, sub toxic concentrations can actually induce biofilm formation (Perrin *et al.*, 2009). After exposure of *S. epidermidis* ATCC 35984 to 1.56 and 3.13 µM of cadmium, qPCR showed an upregulation of *atlE, embp, aap, icaA* and *icaB* which could be due to the fact that cells are in a dormant state in biofilms (Wu *et al.*, 2015b).

Motile bacteria use flagella to move onto a substrate (Belas, 2014). For irreversible adhesion, flagella forming genes are repressed and expression of adhesion proteins including curli, pilli, and type I fimbriae occur (Lazazzera, 2005; Prüß *et al.*, 2006). Expression and repression of genes occur at the relevant stage of biofilm formation they are involved in. Thuptimdang *et al.* (2015) studied the gene expressions of *alg8* and *csgA* in *P. putida* ATCC 47054 biofilms at various stages of maturity and the effect of Ag NPs on its biofilm. Curli is a protein that is important in bacterial surface adhesion, and six proteins that are encoded by the operons *csgBA* and *csgFEDG* are involved in curli production (Saldaña *et al.*, 2009). The *csgA* gene in *P. putida* is a vital subunit for curli, therefore would be expected to be expressed highly during irreversible phases of biofilm growth (Prüß *et al.*, 2006). The gene *alg8* encodes for the alginate biosynthesis protein, that is vital in *P. putida* KT2440 for polysaccharide production to form the biofilm structure (Thuptimdang *et al.*, 2015). It would be expected that *alg8* expression would be higher in mature biofilms due to polysaccharide production. The expressions of *csgA* and *alg8* were greater between 6 and 12 hours during the early development of the biofilm and 12 and 30 hours where metabolic activity would be the highest. When the EPS of *P. putida* biofilms were removed, the

biofilms were more susceptible to Ag NPs, highlighting the importance of EPS in biofilm resistance against Ag NPs (Thuptimdang *et al.*, 2015).

6.3.3 Conclusion

Due to difference in gene expression and protein production between planktonic and sessile cells (Beenken *et al.*, 2004; Brady *et al.*, 2006; Resch *et al.*, 2006), producing an antimicrobial agent suitable for use for both modes of growth can be challenging. However, with the promising data obtained in Chapter 4 on ZnO/Ag NPs suspension, using such combination suspensions could be a step closer to resolving the issues currently encountered with biofilm formation in the healthcare sector. In addition, prior to analysis of gene expression, it is essential to determine the stage of biofilm growth at which genes are expressed, therefore it would be beneficial to do a qPCR at various stages of biofilm formation overtime to determine the highest expression of *icaC*, *ebpS* and *fnbB* and then observe the effect of treatment with NP suspensions on the gene expression. Although qPCR was not utilised in this chapter, the effect of metal/metal oxide NP suspensions on biofilms and the pathways for inhibition they utilise were considered. An attempt was made to focus on gene expression of *S. aureus* biofilms post treatment with a combination of ZnO/Ag NPs in suspension, exploring a range of methods for obtaining RNA. For future research, a change in the RNA extraction kits or even inclusion of extra steps such a phenol extraction could prove successful.

Chapter 7

Chapter 7: Discussion

7.1 To establish the best method for biofilm formation that can replicate biofilms in hospital and healthcare arenas.

In vitro methods of biofilm formation enable scientists to replicate bacterial biofilms to be studied in depth, possibly enabling the testing of potential novel antimicrobial agents to overcome the problem of antimicrobial resistance faced by the healthcare arena. A comparison between the CDC biofilm reactor and the 96 well plate method was investigated in Chapter 3, concluding that the CDC biofilm reactor was the most reliable and replicable method to use for initially forming the biofilms, and further utilising this method to treat biofilms with metal and metal oxide NP suspensions. Lower SE were obtained for the CDC biofilm reactor (0.02-0.11) (Figure 3.6) in comparison to the microtiter method when the broth was replenished at 5 and 9 days and daily with SE ranging from 0.05 to 0.62; and 0.07 to 0.54 respectively (Figure 3.2 and 3.3). High SE were also observed in Bradford protein assays carried out in the 96 well plates (Figure 3.4 and 3.5). SEM images further confirmed the 'stacked' morphology of biofilms formed in the CDC biofilm reactor (Figure 3.7 a-d). Moreover, the CDC biofilm reactor provided a quantitative method as opposed to the microtiter method which gave semi-quantitative data. Absorbance readings were affected by the crystal violet dye in the crystal violet assay due to the adhesion of the dye to components of the biofilm such as the EPS. This gave a higher absorbance in certain wells, giving a large SE (Figure 3.2 and 3.3).

When screening metal/metal oxide suspensions for MBRCs, initially the 96 well plate assay was used. The 96 well plate method was beneficial when mass screening numerous concentrations of metal and metal oxide NP suspensions to give an indication of the MBRC, however, due to the large variations in data and SE, the suspensions were rescreened in the CDC biofilm reactor

(Table 4.1). The variation in biofilm formation was reported by Leuck *et al.* (2014), biofilms of *E. faecalis* varied and formed minimal biofilms in 96 well plates, even when different media was tested. This study supports the findings of Chapter 3 and 4, whereby screening was unreliable using the MTP based assays for Bradford protein assays and biofilm formation (Figure 3.2-3.5). When 6 well plates were used for producing 48 hour biofilms for RNA extraction, minimal and non-visible biofilms of *S. aureus* formed, even though the biofilm forming properties of *S. aureus* ATCC 6538 in 96 well plates and 6 well plates have been well reported previously (Park *et al.*, 2012; Latimer *et al.*, 2012; Atshan *et al.*, 2013). O'Toole (2011) proposed that as MTP based assays use static and batch-growth conditions, mature biofilms comparable to those produced in continuous flow systems cannot be formed.

7.2 To investigate the inhibitory effect of metal and metal oxide NP suspensions in combination against biofilms of S. aureus *and* P. aeruginosa.

Many studies have shown the efficacy of metal and metal oxides, against biofilms and planktonic cells from a range of organisms. Sharma *et al.* (2015) reported an MIC of 25 µg/ml of Ag ($AgNO_3$), and an MIC of ZnO NPs between ~80 to 280 µg/ml against a range of Gram-positive and Gram-negative (Shah *et al.*, 2016). Most published research has focussed on obtaining an MIC for NPs against biofilms, however, in the present work, a three staged approach was used to assess the efficacy of antimicrobials against biofilms to determine the most effective combination of NPs. This approach consists of determination of the a) MBRC (Ag, ZnO and CuO individually), b) R^2 value between the $\log_{(10)}$ reductions and individual concentration range (Ag, ZnO and CuO) tested and c) MBRC of ZnO/Ag combined against *P. aeruginosa* and *S. aureus* biofilms. The strong linear relationship and high R^2 values of ZnO and Ag NPs (Table 4.1) indicate their potential as an antimicrobial.

Biofilms are dynamic structures with their structure changing over time, this can lead to bacterial resistance to disinfectants, antibiotics and sterilisation procedures (Bandeira *et al.*, 2015), and can result in bacterial survival on dry surfaces in hospitals (Almatroudi *et al.*, 2015). Vegetative bacterial cells have shown antimicrobial susceptibility to metal and metal oxide NPs, suggesting that their antimicrobial properties can be used to combat issues faced by the healthcare arena with biofilm resistance (Abdulkareem *et al.*, 2015; Tabrez Khan *et al.*, 2013; Mallevre *et al.*, 2016) including *P. aeruginosa* and *S. aureus* (Ahmed *et al.*, 2013). Although many published studies have investigated Ag and ZnO in combination, the majority have focussed on planktonic cells (You *et al.*, 2011; Liu *et al.*, 2009; Hernández-Sierra *et al.*, 2008).

The findings from this investigation have demonstrated the antimicrobial efficacy of ZnO and Ag NP suspensions on biofilms of *P. aeruginosa* and *S. aureus*, with a lower concentration of 8/12 µg/ml of ZnO/Ag NP suspensions effective on *S. aureus* biofilms compared to 32/25 µg/ml of ZnO/Ag NP suspensions effective on *P. aeruginosa* biofilms; a 99.99% and 99.98% reduction for *S. aureus* and *P. aeruginosa* was obtained respectively (Table 4.2a and b). A 24-hour treatment was required in order to have a significant ($p \leq 0.05$) inhibitory effect (Table 4.4). The efficacy of these concentrations are further confirmed in live/dead assays in Figure 4.5 and SEM images in Figure 4.4. A higher concentration of ZnO/Ag NP suspension was required for *P. aeruginosa* biofilms, possibly due to Gram-negative bacteria having an outer membrane (Tong & McIntosh, 2004), which is absent in Gram-positive bacteria, therefore requiring a larger concentration of an antimicrobial agent to take effect. In general, Gram-negative bacteria are known to possess greater resistance to antimicrobials in comparison to Gram-positive bacteria (Silhavy *et al.*, 2010) which correlates with the findings in this investigation. Nevertheless, both combinations gave a reduction of $\geq 3 \log_{(10)}$. In the wider context, this combination could be useful against other Gram-positive and Gram-negative bacteria, in applications such as wipes for surface disinfection or even a spray so long as an equal dose of metal and metal oxide NPs are delivered.

Various authors have researched the combination of Ag and ZnO in terms of its antimicrobial efficacy but only on vegetative cells and not biofilms (Karunakaran *et al.*, 2011b, 2011a; Amornpitoksuk *et al.*, 2012; Jafari *et al.*, 2011). The lowest inhibitory combination of Ag and ZnO NP in a suspension providing a log reduction $\geq 3 \log_{(10)}$ was 32/25 µg/ml and 8/12 µg/ml of ZnO/Ag NP suspensions for *P. aeruginosa* and *S. aureus* biofilms respectively (Table 4.2 and b), where both combinations had an additive effect *P. aeruginosa* and *S. aureus* (Table 4.2a and b). This demonstrates that the total effect of Ag and ZnO in combination is equal to the total effect exhibited by both when not in combination. It would be expected that in combination, its antimicrobial effect would actually increase due to the pathways of antimicrobial action they both use for bacterial inhibition. Interaction of Ag NP with bacterial cells can cause DNA damage, leakage of cytoplasmic content therefore prevention of replication (Chen *et al.*, 2011) and Ag^{+} can inhibit enzymes containing thiol groups (Matsumura *et al.*, 2003). Zn^{2+} from ZnO NPs can form ROS, permanently damaging the cell membrane of bacteria, DNA and mitochondria (Dwivedi *et al.*, 2014). Many studies solely testing combinations of metal and metal oxide NPs have not determined the FIC index, however investigating the synergistic effect of Ag NPs and cefmetazole indicated an additive effect against *Neisseria gonorrhoeae* (Li *et al.*, 2013), and Ag NPs with streptomycin, kanamycin, ampiclox and polymyxin B were all additive against a range of Gram- positive and negative bacteria (Jain *et al.*, 2009). The combination of two metal and metal oxide NPs had a lower MBRC in comparison to when used individually. Using either Ag or ZnO alone would require a higher concentration to take effect as opposed to a combination of Ag and ZnO (Table 4.1, 4.2a and b), which is beneficial in terms of lower toxicity, cost effectiveness as well as reduced resistance. The combination of Ag and ZnO NPs together increase the antimicrobial activity exerted on the bacteria as the photocatalytic ability of ZnO and Ag NPs is improved, increasing its oxidation and reduction capability, inhibiting bacterial growth (Yang *et al.*, 2006).

Even though studies have proposed that Ag NPs inherently deliver toxicity, the majority of studies have shown that it is the ionic form that provides the antimicrobial action (Hsueh *et al.*, 2015). Kääriäinen *et al.* (2013) stated that the antibacterial of ZnO thin films on the biofilm formation of *E. coli* was due to Zn^{2+} ions, similar to findings by Franklin *et al.* (2007), Xia *et al.* (2008), Shalumon *et al.* (2011) and Kumar *et al.* (2012). Significant ($p \leq 0.05$) antimicrobial activity of Ag and ZnO thin films for the prevention of *P. aeruginosa* and *S. aureus* biofilm formation in were observed in Chapter 5 after 48 hours, owing to the release of ions from the thin films.

There is a sustained release of Ag^{+} and Zn^{2+} ions from thin film surfaces (Monteiro *et al.*, 2009), therefore requires more time to release a sufficient ion concentration for antimicrobial activity. In a suspension, a high concentration of Ag^{+}/Zn^{2+} ions are available instantly in the aqueous phase to interact with the cells, therefore there is greater interaction quicker. Kumar *et al.* (2005) stated that the reduced antimicrobial action of Ag-based antimicrobial fillers in polyamide against *S. aureus, E. coli* and *C. albicans* was due to inadequate release of Ag^{+} ions. This reinforces the fact that it is the ion release from coatings that is vital for antimicrobial activity.

When conducting qPCR, it would have been expected that the biofilm genes *icaC, ebpS,* and *fnbB* studied would have been down regulated due to the reduction of biofilm formation by ZnO/Ag NP suspensions as confirmed by live/dead assays (Figure 4.5) and SEM images (Figure 4.4). After analysing the effect of ZnO/Ag NP suspensions using viable counts, the combinatory NP suspension has proven to be antimicrobial against *P. aeruginosa* (32/25 µg/ml ZnO/Ag NP) and *S. aureus* (8/12 µg/ml ZnO/Ag NP) biofilms with significant $\log_{(10)}$ reductions within the acceptance criteria of ≥ 3 $\log_{(10)}$ set in this study (Table 4.2a and b). This correlates to the antimicrobial activity of the suspensions seen in the SEM and CLSM images (Figure 4.4 and 4.5). The 'stacking' behaviour of biofilms was observed in the live/dead assays, particularly with the untreated biofilms (Figure 4.5). SEM images support reductions observed as the rupturing of the biofilms and distortion of the cells post treatment can be seen, therefore affected the further development of the biofilm (Figure 4.4c and d). EDX images show the presence of Ag and Zn

elements in the biofilm, suggesting the adherence of the NPs to the biofilm (Figure 4.4e-h). The integrity of cells in the SEM images obtained in Figure 5.4a-d of *S. aureus* and *P. aeruginosa* biofilms on ZnO and Ag coated surfaces resemble the cells of untreated biofilms of *S. aureus* and *P. aeruginosa* on PC coupons in Figure 4.4a and b. This demonstrates the reduced inability of Ag and ZnO coated surfaces to prevent biofilm formation in comparison to NP suspensions as they are comparable to biofilms formed on untreated PC coupons. CLSM images confirmed that the effect of the NP suspension is not only limited to the surface of the biofilms, but throughout the whole biofilm as dead (red) cells can be seen throughout the top, middle and bottom portions (Figure 4.5a-h). The ion release over 24 hours was monitored using the AAS. The results suggested that the antimicrobial activity was mainly due to Ag^{+} ions, as Ag^{+} ions were quenching Zn^{2+} (Table 4.5). For example, at 32/12 µg/ml of ZnO/Ag NPs, initially, 3.58 and 0.18 mg/l of Zn^{2+} and Ag^{+} ions respectively were present, whereas in combination, the Zn^{2+} ions reduced to 0.93 mg/l, whereas Ag^{+} ions remained at a similar concentration (Table 4.5). Matai *et al.* (2014) found an increase in Zn^{2+} ion concentrations with increment between 6 and 24 hours from Ag-ZnO nanocomposites, and for Ag^{+} ion release between 6 and 12 hours when ion concentration was determined using the AAS. For future studies, it may be beneficial to monitor ion release at a range of time intervals to identify the time at which ion release peaks.

7.3 To determine the effect of thin layer coating of metal and metal oxide NPs.

The use of antimicrobial surfaces has evolved into a topic of great scientific interest, particularly in light of the vastly reported cases of *P. aeruginosa* (Souli *et al.*, 2013) and *S. aureus* (Page *et al.*, 2009).

Self-disinfecting surfaces with metal and metal oxides with innate antimicrobial characteristics provide antibiofilm activity for lengthy time periods (Humphreys, 2014). Coated surfaces prevent

the adhesion of bacterial cells to a surface after 48 hours (Table 5.1). Findings of this investigation suggest that Ag and ZnO thin films provide a statistically significant ($p \leq 0.05$) reduction of 98.47% and 97.78% for Ag and ZnO thin films respectively for *S. aureus* and 96.13% and 96.28% for Ag and ZnO thin films respectively for *P. aeruginosa* after 48 hours of formation, demonstrating that 48 hours or longer is sufficient to exert an antimicrobial effect. Although a statistically significant reduction has been shown for a 48 hour treatment of *S. aureus* and *P. aeruginosa* biofilms with Ag and ZnO coated surfaces in comparison to the control, $<3 \log_{(10)}$ reduction has been observed which is much lower in comparison to the reduction by ZnO/Ag NP suspensions ($\geq 3 \log_{(10)}$). A 24 hour formation of *P. aeruginosa* and *S. aureus* biofilms on Ag and ZnO coatings show an inhibitory effect of only a 38.01% and 46.98% reduction for Ag and ZnO coatings respectively for *P. aeruginosa,* and a 40.54% and 20.46% reduction for Ag and ZnO coatings respectively for *S. aureus* which is much lower than the inhibitory effect at 48 hours (Table 5.1). Conversely, a 24 hour treatment of biofilms of *S. aureus* (8/12 µg/ml ZnO/Ag NP suspension) and *P. aeruginosa* (32/25 µg/ml ZnO/Ag NP suspension) gave a 3.91 $\log_{(10)}$ and 3.77 $\log_{(10)}$ reduction for *S. aureus* and *P. aeruginosa* respectively (Table 4.2a and b).

The gradual ion release from Ag (Reidy *et al.,* 2013) and ZnO when attached to a surface could be having a limited effect on the antimicrobial effect on the bacterial cells. Virulence factors leading to antimicrobial resistance are able to withstand the antimicrobial effect from the ions in smaller quantities as opposed to metal and metal oxide NP suspensions which provide an instant maximum dose to a mature biofilm formed in CDC biofilm reactor (Petrochenko *et al.,* 2014). ZnO forms Zn^{2+} due to its instability in solution and these ions are able to penetrate into the cell membrane of bacteria, causing disruption of metal-ion homeostasis in the cell, and exhibit toxicity when concentrations are high (Outten & O'Halloran, 2001). The percentage reductions were slightly greater for Ag (98.47%) and ZnO (97.78%) coated samples against *S. aureus* in comparison to *P. aeruginosa* (Table 5.1). Similarly, slightly enhanced antimicrobial efficacy for 8/12 µg/ml of ZnO/Ag NP combination suspensions (Table 4.2a and b) against *S. aureus* was

observed with a reduction of 3.91 $\log_{(10)}$, whereas a 32/25 µg/ml of ZnO/Ag NP gave a 3.77 $\log_{(10)}$ reduction against *P. aeruginosa*. The lower efficacy of Ag and ZnO suspensions and thin film coatings against *P. aeruginosa* could due the shielding effect of the outer membrane present only in Gram-negative bacteria (Araújo *et al.*, 2011). Kääriäinen *et al.* (2013) studied the prevention of *E. coli* adherence on ZnO thin films, with only a 99.7-99.5% reduction. This was lower than the required reduction of >99.9%, owing to Zn^{2+} ion release and not due to photocatalytic activity (Kääriäinen *et al.*, 2013).

Even though lower $\log_{(10)}$ reductions were observed for coated surfaces in comparison to metal and metal oxide NP suspensions, coated surfaces or surfaces impregnated with an antimicrobial metal or metal oxide could be beneficial in the healthcare sector to prevent colonisation of nosocomial related bacteria and provide a sustained release of ions, although greater understanding and further development would be required.

According to the BS EN 13697:2001, in order for a disinfectant to be classed as an antimicrobial, a minimum of a 4 $\log_{(10)}$ reduction in ≤5 mins is required for bacterial cells (British Standards Institute, 2001). There is no standard in place solely for biofilms, even though most organisms reside in a biofilm form (Penesyan *et al.*, 2015). Differences in physiological characteristics of sessile and planktonic cells means that a standard designed for planktonic cells cannot be applicable to biofilms (Rollet *et al.*, 2009). Although a 4 $\log_{(10)}$ reduction in 5 mins has not been achieved in the present research, the results gained in this investigation against *P. aeruginosa* and *S. aureus* biofilms do demonstrate the potential for Ag and ZnO thin film coated surfaces and 8/12 and 32/25 µg/ml of ZnO/Ag NP suspension for *S. aureus* and *P. aeruginosa* biofilms respectively, to be further developed into antimicrobial products.

7.4 Future Work

Future research branching from this project would include further investigation into mechanisms of action of the metal/metal oxide NPs such as looking at the energy and adenosine triphosphate (ATP) levels affected in biofilms post treatment with the combination of ZnO/Ag NP suspension. Despite the difficulties faced during RNA extraction, other approaches of obtaining RNA and using alternative kits or methods would be trialled. In order for ZnO/Ag NP in suspension to be considered as a commercial product in the healthcare arena or used as part of a formula, the versatility of the suspension should be evaluated by testing its efficacy against other nosocomial pathogens - including *K. pneumoniae* (Bock *et al.*, 2016), vancomycin resistant *S. aureus*, and *C. difficle* (Ali *et al.*, 2016) and carbapenem resistant organisms (CRO) (Wang et al., 2016a)- as biofilms occur as multispecies biofilms rather than single species, this needs to be taken into consideration.

Thin film coatings have only recently begun to be explored widely for their antimicrobial use and research has mainly focused on Ag thin film coatings. It would be beneficial to explore the combined effect of sputtered Ag and ZnO thin films to observe whether an enhanced antimicrobial effect is exerted against biofilms. Furthermore, impregnation of Ag and ZnO in combination could be an interesting area of research, to observe if its antimicrobial effect overtime periods longer than 48 hours and thus its robustness as an application. Due to antimicrobial thin film coatings aiming to prevent the initial stages of biofilm formation, coating the inside of taps to prevent the persistence of *P. aeruginosa* biofilms and contamination of water systems, with antimicrobial coatings of Ag and ZnO, could be explored in order to prevent outbreaks such as those recently reported in Northern Ireland where *P. aeruginosa* caused the morality of four babies (Walker *et al.*, 2013).

It is paramount to consider if concentrations of 32/25 µg/ml and 8/12 µg/ml of ZnO/Ag NP suspensions are toxic to humans and the environment. Factors such as skin irritation for

disinfectant applications is vital as well as eye irritation, especially for a product in a spray from. Previously, high toxicity levels of phenolic agents in disinfectants have been reported, yet they are still being used in developing countries due to the low costs associated (Singh *et al.*, 2012). Ag has been reported to result in lung inflammation (Sung *et al.*, 2009) and very high concentrations of ZnO have shown to target liver cells in humans, providing cellular toxicity (Sharma *et al.*, 2012). Thorough investigation of such toxicity factors is necessary before any further development of a potential product.

7.5 Conclusion

In conclusion, the work from this study has demonstrated the ability of Ag and ZnO in suspension to treat biofilms and provide significant $\log_{(10)}$ reductions. Using a three step approach, Ag and ZnO were chosen for use in combination which enabled a lower concentration of both NPs to be used, even though only an additive effect was observed. A combination of 32/25 µg/ml of ZnO/Ag NPs was also effective against a multispecies biofilm of *P. aeruginosa* and *S. aureus*. Biofilm reduction of clinical isolates of *P. aeruginosa* (32/25 µg/ml of ZnO/Ag NPs) and MRSA (8/12 µg/ml of ZnO/Ag NPs) was also observed, showing its promise as an antimicrobial against biofilms. Results from this study have shown that there is potential that Ag and ZnO NPs in combination could be used as part of a formula for a disinfectant for the healthcare arenas. Thin film coatings showed limited capability for preventing biofilm formation. With further research into other methods of coating, it may be possible to increase the efficacy of NP thin film coating, enabling potential usage on hospital touch surfaces such as door handles, bed rails or even the inside of taps. With the increase in antimicrobial resistance in biofilms, prevalence of biofilms in the healthcare arena and the continuation in numbers of mortality rates from HCAIs, the combination of Ag and ZnO NPs could be part of a potential solution for decontaminating the healthcare environment.

References

Abbanat, D., Shang, W., Amsler, K., Santoro, C., Baum, E., Crespo-Carbone, S. & Lynch, A.S. (2014) Evaluation of the *in vitro* activities of ceftobiprole and comparators in staphylococcal colony or microtitre plate biofilm assays. *International Journal of Antimicrobial Agents*, 43, pp. 32–39.

Abdallah, M., Benoliel, C., Drider, D., Dhulster, P. & Chihib, N.E. (2014) Biofilm formation and persistence on abiotic surfaces in the context of food and medical environments. *Archives of Microbiology*, 196, pp. 453–472.

Abdel Rahim, K.A.A. & Ali Mohamed, A.M. (2015) Bactericidal and antibiotic synergistic effect of nanosilver against methicillin-resistant *Staphylococcus aureus*. *Jundishapur Journal of Microbiology*, 8, pp. e25867.

Abdulkareem, E.H., Memarzadeh, K., Allaker, R.P., Huang, J., Pratten, J. & Spratt, D. (2015) Anti-biofilm activity of zinc oxide and hydroxyapatite nanoparticles as dental implant coating materials. *Journal of Dentistry*, 43, pp. 1462–1469.

Abee, T., Kovács, Á.T., Kuipers, O.P., van der Veen, S., Kovács, A.T., Kuipers, O.P. & van der Veen, S. (2011) Biofilm formation and dispersal in Gram-positive bacteria. *Current Opinion in Biotechnology*, 22, pp. 172–179.

Abreu, A., Tavares, R., Borges, A., Mergulhão, F. & Simões, M. (2013) Current and emergent strategies for disinfection of hospital environments. *Journal of Antimicrobial Chemotherapy*, 68, pp. 2718–2732.

de Abreu, P.M., Farias, P.G., Paiva, G.S., Almeida, A.M. & Morais, P.V. (2014) Persistence of microbial communities including *Pseudomonas aeruginosa* in a hospital environment: a potential health hazard. *BMC Microbiology*, 14, pp. 118.

Adams, H., Winston, M.T., Heersink, J., Buckingham-Meyer, K.A., Costerton, J.W. & Stoodley, P. (2002) Development of a laboratory model to assess the removal of biofilm from interproximal spaces by powered tooth brushing. *American Journal of Dentistry*, 15 Spec No, pp. 12B – 17B.

Adukwu, E.C., Allen, S.C. & Phillips, C.A. (2015) A comparison of the sensitivity of four *Staphylococcus aureus* isolates to two chlorine-based disinfectants and an eco-friendly commercially available cleaning agent. *International Journal of Environmental Health Research*, 25, pp. 115–125.

Aggarwal, S., Poppele, E.H. & Hozalski, R.M. (2010) Development and testing of a novel microcantilever technique for measuring the cohesive strength of intact biofilms. *Biotechnology and Bioengineering*, 105, pp. 924–934.

Agostinho, A., James, G., Wazni, O., Citron, M. & Wilkoff, B.D. (2009) Inhibition of *Staphylococcus aureus* biofilms by a novel antibacterial envelope for use with implantable cardiac devices. *Clinical and Translational Science*, 2, pp. 193–198.

Ahamed, M., Alhadlaq, H.A., Khan, M.A.M., Karuppiah, P. & Al-Dhabi, N.A. (2014) Synthesis, characterization, and antimicrobial activity of copper oxide nanoparticles. *Journal of Nanomaterials*, 2014, pp. 17.

Ahmad, A., Khan, A., Samber, N. & Manzoor, N. (2014) Antimicrobial activity of *Mentha piperita* essential oil in combination with silver ions. *Synergy*, 1, pp. 92–98.

Ahmed, S., Ahmad, M., Swami, B.L. & Ikram, S. (2015) Plants extract mediated synthesis of silver nanoparticles for antimicrobial applications: A green expertise. *Journal of Advanced Research*, 7, pp. 17–28.

Ahmed, Z., Saeed Khan, S. & Khan, M. (2013) *In vitro* trials of some antimicrobial combinations against *Staphylococcus aureus* and *Pseudomonas aeruginosa*. *Saudi Journal of Biological Sciences*, 20, pp. 79–83.

Akhil, K., Chandran, P. & Sudheer Khan, S. (2015) Influence of humic acid on the stability and bacterial toxicity of zinc oxide nanoparticles in water. *Journal of Photochemistry and Photobiology B: Biology*, 153, pp. 289–295.

Ali, L., Khambaty, F. & Diachenko, G. (2006) Investigating the suitability of the Calgary Biofilm Device for assessing the antimicrobial efficacy of new agents. *Bioresource Technology*, 97, pp. 1887–1893.

Ali, S., Muzslay, M., Bruce, M., Jeanes, A., Moore, G. & Wilson, A.P.R. (2016) Efficacy of two hydrogen peroxide vapour aerial decontamination systems for enhanced disinfection of meticillin-resistant *Staphylococcus aureus*, *Klebsiella pneumoniae* and *Clostridium difficile* in single isolation rooms. *The Journal of Hospital Infection*, 93, pp. 70–77.

Allaker, R.P. (2010) The use of nanoparticles to control oral biofilm formation. *Journal of Dental Research*, 89, pp. 1175–1186.

Almatroudi, A., Gosbell, I.B., Hu, H., Jensen, S.O., Espedido, B.A., Tahir, S., Glasbey, T.O., Legge, P., Whiteley, G., Deva, A. & Vickery, K. (2016) *Staphylococcus aureus* dry-surface biofilms are not killed by sodium hypochlorite: implications for infection control. *Journal of Hospital Infection*, 93, pp. 263–270.

Almatroudi, A., Hu, H., Deva, A., Gosbell, I.B., Jacombs, A., Jensen, S.O., Whiteley, G., Glasbey, T. & Vickery, K. (2015) A new dry-surface biofilm model: An essential tool for efficacy testing of hospital surface decontamination procedures. *Journal of Microbiological Methods*, 117, pp. 171–176.

Ambika, S. & Sundrarajan, M. (2015) Antibacterial behaviour of *Vitex negundo* extract assisted ZnO nanoparticles against pathogenic bacteria. *Journal of Photochemistry and Photobiology. B, Biology*, 146, pp. 52–57.

American Society for Testing and Materials (2012) *ASTM standard E2562: Standard Test Method for Quantification of* Pseudomonas aeruginosa *Biofilm Grown with High Shear and Continuous Flow using CDC Biofilm Reactor*. West Conshohocken: ASTM International

Amornpitoksuk, P., Suwanboon, S., Sangkanu, S., Sukhoom, A., Muensit, N. & Baltrusaitis, J. (2012) Synthesis, characterization, photocatalytic and antibacterial activities of Ag-doped ZnO powders modified with a diblock copolymer. *Powder Technology*, 219, pp. 158–164.

Anantharaman, A., Rizvi, M.S. & Sahal, D. (2010) Synergy with rifampin and kanamycin enhances potency, kill kinetics, and selectivity of de novo-designed antimicrobial peptides. *Antimicrobial Agents and Chemotherapy*, 54, pp. 1693–1699.

Anderl, J.N., Zahller, J., Roe, F. & Stewart, P.S. (2003) Role of nutrient limitation and stationary-phase existence in *Klebsiella pneumoniae* biofilm resistance to ampicillin and ciprofloxacin. *Antimicrobial Agents and Chemotherapy*, 47, pp. 1251–1256.

Ansari, M.A., Khan, H.M., Khan, A.A., Ahmad, M.K., Mahdi, A.A., Pal, R. & Cameotra, S.S.

(2014a) Interaction of silver nanoparticles with *Escherichia coli* and their cell envelope biomolecules. *Journal of Basic Microbiology*, 54, pp. 905–915.

Ansari, M.A., Khan, H.M., Khan, A.A., Cameotra, S.S. & Alzohairy, M.A. (2015) Anti-biofilm efficacy of silver nanoparticles against MRSA and MRSE isolated from wounds in a tertiary care hospital. *Indian Journal of Medical Microbiology*, 33, pp. 101–109.

Ansari, M.A., Khan, H.M., Khan, A.A., Cameotra, S.S. & Pal, R. (2013) Antibiofilm efficacy of silver nanoparticles against biofilm of extended spectrum β-lactamase isolates of *Escherichia coli* and *Klebsiella pneumoniae*. *Applied Nanoscience*, 4, pp. 859–868.

Ansari, M.A., Khan, H.M., Khan, A.A., Cameotra, S.S., Saquib, Q. & Musarrat, J. (2014b) Gum arabic capped-silver nanoparticles inhibit biofilm formation by multi-drug resistant strains of *Pseudomonas aeruginosa*. *Journal of Basic Microbiology*, 54, pp. 688–699.

Appendini, P. & Hotchkiss, J.H. (2002) Review of antimicrobial food packaging. *Innovative Food Science and Emerging Technologies*, 3, pp. 113–126.

Applerot, G., Lipovsky, A., Dror, R., Perkas, N., Nitzan, Y., Lubart, R., Gedanken, A., Appierot, G., Lipovsky, A., Dror, R., Perkas, N., Nitzan, Y., Lubart, R. & Gedanken, A. (2009) Enhanced antibacterial activity of nanocrystalline ZnO due to increased ROS-mediated cell injury. *Advanced Functional Materials*, 19, pp. 842–852.

Arakha, M., Pal, S., Samantarrai, D., Panigrahi, T.K., Mallick, B.C., Pramanik, K., Mallick, B. & Jha, S. (2015) Antimicrobial activity of iron oxide nanoparticle upon modulation of nanoparticle-bacteria interface. *Scientific Reports*, 5, pp. 14813.

Araújo, P., Lemos, M., Mergulhão, F., Melo, L. & Simões, M. (2011) Antimicrobial resistance to disinfectants in biofilms. *Science Against Microbial Pathogens: Communicating Current Research and Technological Advances*, 3, pp. 826–834.

Arciola, C.R., Baldassarri, L. & Montanaro, L. (2001) Presence of *icaA* and *icaD* genes and slime production in a collection of staphylococcal strains from catheter-associated infections. *Journal of Clinical Microbiology*, 39, pp. 2151–2156.

Arciola, C.R., Campoccia, D., Baldassarri, L., Donati, M.E., Pirini, V., Gamberini, S. & Montanaro, L. (2006) Detection of biofilm formation in *Staphylococcus epidermidis* from implant infections. Comparison of a PCR-method that recognizes the presence of *ica* genes with two classic phenotypic methods. *Journal of Biomedical Materials Research - Part A*, 76, pp. 425–430.

Arciola, C.R., Campoccia, D., Ravaioli, S. & Montanaro, L. (2015) Polysaccharide intercellular adhesin in biofilm: structural and regulatory aspects. *Frontiers in Cellular and Infection Microbiology*, 5, pp. 7.

Arora, S., Jain, J., Rajwade, J.M. & Paknikar, K.M. (2008) Cellular responses induced by silver nanoparticles: *In vitro* studies. *Toxicology letters*, 179, pp. 93–100.

Aruoja, V., Dubourguier, H.-C., Kasemets, K. & Kahru, A. (2009) Toxicity of nanoparticles of CuO, ZnO and TiO_2 to microalgae *Pseudokirchneriella subcapitata*. *The Science of the Total Environment*, 407, pp. 1461–1468.

Atshan, S.S., Shamsudin, M.N., Karunanidhi, A., van Belkum, A., Lung, L.T.T., Sekawi, Z., Nathan, J.J., Ling, K.H., Seng, J.S.C., Ali, A.M., Abduljaleel, S.A. & Hamat, R.A. (2013) Quantitative PCR analysis of genes expressed during biofilm development of methicillin resistant *Staphylococcus aureus* (MRSA). *Infection, Genetics and Evolution*, 18, pp. 106–112.

Atshan, S.S., Shamsudin, M.N., Lung, L.T.T., Ling, K.H., Sekawi, Z., Pei, C.P. & Ghaznavi-Rad, E. (2012) Improved method for the isolation of RNA from bacteria refractory to disruption, including *S. aureus* producing biofilm. *Gene*, 494, pp. 219–224.

Augustin, M., Ali-Vehmas, T. & Atroshi, F. (2004) Assessment of enzymatic cleaning agents and disinfectants against bacterial biofilms. *Journal of Pharmacy and Pharmaceutical Sciences*, 7, pp. 55–64.

Ayliffe, G.A.J., Collins, B.J., Babb, J.R., Lowbury, E.J.L. & Newsom, S.W.B. (1974) *Pseudomonas aeruginosa* in hospital sinks. *The Lancet*, 304, pp. 578–581.

Azam, A., Ahmed, A.S., Oves, M., Khan, M.S., Habib, S.S. & Memic, A. (2012a) Antimicrobial activity of metal oxide nanoparticles against Gram-positive and Gram-negative bacteria: a comparative study. *International Journal of Nanomedicine*, 7, pp. 6003–6009.

Azam, A., Ahmed, A.S., Oves, M., Khan, M.S. & Memic, A. (2012b) Size-dependent antimicrobial properties of CuO nanoparticles against Gram-positive and negative bacterial strains. *International Journal of Nanomedicine*, 7, pp. 3527.

El Badawy, A.M., Silva, R.G., Morris, B., Scheckel, K.G., Suidan, M.T. & Tolaymat, T.M. (2011) Surface charge-dependent toxicity of silver nanoparticles. *Environmental Science and Technology*, 45, pp. 283–287.

Bader, M.S. (2006) *Staphylococcus aureus* bacteremia in older adults: predictors of 7-day mortality and infection with a methicillin-resistant strain. *Infection Control and Hospital Epidemiology*, 27, pp. 1219–1225.

Bae, E., Park, H.J., Lee, J., Kim, Y., Yoon, J., Park, K., Choi, K. & Yi, J. (2010) Bacterial cytotoxicity of the silver nanoparticle related to physicochemical metrics and agglomeration properties. *Environmental Toxicology and Chemistry*, 29, pp. 2154–2160.

Bae, E., Park, H.J., Yoon, J., Kim, Y., Choi, K. & Yi, J. (2011) Bacterial uptake of silver nanoparticles in the presence of humic acid and $AgNO_3$. *Korean Journal of Chemical Engineering*, 28, pp. 267–271.

Baghal Asghari, F., Nikaeen, M. & Mirhendi, H. (2013) Rapid monitoring of *Pseudomonas aeruginosa* in hospital water systems: a key priority in prevention of nosocomial infection. *FEMS microbiology letters*, 343, pp. 77–81.

Bahrami, K., Nazari, P., Nabavi, M., Golkar, M., Almasirad, A., Shahverdi, A.R. & Shahverdi, A.R. (2014) Hydroxyl capped silver-gold alloy nanoparticles: characterization and their combination effect with different antibiotics against *Staphylococcus aureus*. *Nanomedicine Journal*, 1, pp. 155–161.

Bailón-Sánchez, M.E., Baca, P., Ruiz-Linares, M. & Ferrer-Luque, C.M. (2014) Antibacterial and anti-biofilm activity of AH plus with chlorhexidine and cetrimide. *Journal of Endodontics*, 40, pp. 977–981.

Baker, J., Sitthisak, S., Sengupta, M., Johnson, M., Jayaswal, R.K. & Morrissey, J.A. (2010) Copper stress induces a global stress response in *Staphylococcus aureus* and represses sae and agr expression and biofilm formation. *Applied and Environmental Microbiology*, 76, pp. 150–160.

Bandeira, M., Carvalho, P.A., Duarte, A. & Jordao, L. (2015) Bacterial biofilms, antibiotic resistance and healthcare-associated infections: a dangerous connection. *Microscopy and Microanalysis*, 21, pp. 38–39.

Barbadoro, P., Labricciosa, F.M., Recanatini, C., Gori, G., Tirabassi, F., Martini, E., Gioia, M.G.,

D'Errico, M.M. & Prospero, E. (2015) Catheter-associated urinary tract infection: Role of the setting of catheter insertion. *American Journal of Infection Control*, 43, pp. 707–710.

Barber, K.E., Smith, J.R., Ireland, C.E., Boles, B.R., Rose, W.E. & Rybak, M.J. (2015) Evaluation of ceftaroline alone and in combination against biofilm-producing methicillin-resistant *Staphylococcus aureus* with reduced susceptibility to daptomycin and vancomycin in an *in vitro* pharmacokinetic/pharmacodynamic model. *Antimicrobial Agents and Chemotherapy*, 59, pp. 4497–4503.

Barken, K.B., Pamp, S.J., Yang, L., Gjermansen, M., Bertrand, J.J., Klausen, M., Givskov, M., Whitchurch, C.B., Engel, J.N. & Tolker-Nielsen, T. (2008) Roles of type IV pili, flagellum-mediated motility and extracellular DNA in the formation of mature multicellular structures in *Pseudomonas aeruginosa* biofilms. *Environmental Microbiology*, 10, pp. 2331–2343.

Bayoudh, S., Othmane, A., Bettaieb, F., Bakhrouf, A., Ouada, H. Ben & Ponsonnet, L. (2006) Quantification of the adhesion free energy between bacteria and hydrophobic and hydrophilic substrata. *Materials Science and Engineering: C*, 26, pp. 300–305.

Bayoudh, S., Othmane, A., Ponsonnet, L. & Ben Ouada, H. (2008) Electrical detection and characterization of bacterial adhesion using electrochemical impedance spectroscopy-based flow chamber. *Colloids and Surfaces A: Physicochemical and Engineering Aspects*, 318, pp. 291–300.

Beceiro, A., Tomás, M. & Bou, G. (2013) Antimicrobial resistance and virulence: a successful or deleterious association in the bacterial world? *Clinical Microbiology Reviews*, 26, pp. 185–230.

Beenken, K.E., Dunman, P.M., McAleese, F., Macapagal, D., Murphy, E., Projan, S.J., Blevins, J.S. & Smeltzer, M.S. (2004) Global gene expression in *Staphylococcus aureus* biofilms. *Journal of Bacteriology*, 186, pp. 4665–4684.

Behnke, S. & Camper, A.K. (2012) Chlorine dioxide disinfection of single and dual species biofilms, detached biofilm and planktonic cells. *Biofouling*, 28, pp. 635–647.

Behnke, S., Parker, A.E., Woodall, D. & Camper, A.K. (2011) Comparing the chlorine disinfection of detached biofilm clusters with those of sessile biofilms and planktonic cells in single- and dual-species cultures. *Applied and Environmental Microbiology*, 77, pp. 7176–7184.

Belas, R. (2014) Biofilms, flagella, and mechanosensing of surfaces by bacteria. *Trends in Microbiology*, 22, pp. 517–527.

Beloin, C., Michaelis, K., Lindner, K., Landini, P., Hacker, J., Ghigo, J.M. & Dobrindt, U. (2006) The transcriptional antiterminator RfaH represses biofilm formation in *Escherichia coli*. *Journal of Bacteriology*, 188, pp. 1316–1331.

Bera, R.K., Mandal, S.M. & Raj, C.R. (2014) Antimicrobial activity of fluorescent Ag nanoparticles. *Letters in Applied Microbiology*, 58, pp. 520–526.

Besinis, A., De Peralta, T. & Handy, R.D. (2014) The antibacterial effects of silver, titanium dioxide and silica dioxide nanoparticles compared to the dental disinfectant chlorhexidine on *Streptococcus mutans* using a suite of bioassays. *Nanotoxicology*, 8, pp. 1–16.

Big, C. & Malani, P.N. (2010) *Staphylococcus aureus* bloodstream infections in older adults: Clinical outcomes and risk factors for in-hospital mortality. *Journal of the American Geriatrics Society*, 58, pp. 300–305.

Biosurface Technologies Corporation (2010) [Online] *CDC Biofilm Reactor*. 2010. Available

from:http://www.biofilms.biz/wp-content/uploads/2010/12/web-CDC-InfoPricing-2010.pdf [Accessed: 21 April 2016].

Bjarnsholt, T. (2013) The role of bacterial biofilms in chronic infections. *APMIS*, 121, pp. 1–58.

Blanc, D.S., Gomes Magalhaes, B., Abdelbary, M., Prod'hom, G., Greub, G., Wasserfallen, J.B., Genoud, P., Zanetti, G. & Senn, L. (2016) Hand soap contamination by *Pseudomonas aeruginosa* in a tertiary care hospital: no evidence of impact on patients. *The Journal of Hospital Infection*, 93, pp. 63–67.

Blau, H., Mussaffi, H., Mei Zahav, M., Prais, D., Livne, M., Czitron, B.M. & Cohen, H.A. (2007) Microbial contamination of nebulizers in the home treatment of cystic fibrosis. *Child: Care, Health and Development*, 33, pp. 491–495.

Blindauer, C.A., Harrison, M.D., Parkinson, J.A., Robinson, A.K., Cavet, J.S., Robinson, N.J. & Sadler, P.J. (2001) A metallothionein containing a zinc finger within a four-metal cluster protects a bacterium from zinc toxicity. *Proceedings of the National Academy of Sciences of the United States of America*, 98, pp. 9593–9598.

Bock, L.J., Wand, M.E. & Sutton, J.M. (2016) Varying activity of chlorhexidine-based disinfectants against *Klebsiella pneumoniae* clinical isolates and adapted strains. *Journal of Hospital Infection*, 93, pp. 42–48.

Bohinc, K., Dražić, G., Abram, A., Jevšnik, M., Jeršek, B., Nipič, D., Kurinčič, M. & Raspor, P. (2016) Metal surface characteristics dictate bacterial adhesion capacity. *International Journal of Adhesion and Adhesives*, 68, pp. 39–46.

Boles, B.R. & Horswill, A.R. (2008) Agr-mediated dispersal of *Staphylococcus aureus* biofilms. *PLoS Pathogens*, 4, pp. e1000052.

Boles, B.R., Thoendel, M. & Singh, P.K. (2005) Rhamnolipids mediate detachment of *Pseudomonas aeruginosa* from biofilms. *Molecular Microbiology*, 57, pp. 1210–1223.

Di Bonaventura, G., Piccolomini, R., Paludi, D., D'Orio, V., Vergara, A., Conter, M. & Ianieri, A. (2008) Influence of temperature on biofilm formation by *Listeria monocytogenes* on various food-contact surfaces: Relationship with motility and cell surface hydrophobicity. *Journal of Applied Microbiology*, 104, pp. 1552–1561.

Bondarenko, O., Ivask, A., Käkinen, A., Kurvet, I. & Kahru, A. (2013) Particle-cell contact enhances antibacterial activity of silver nanoparticles. *PLoS one*, 8, pp. e64060.

Bonez, P.C., Dos Santos Alves, C.F., Dalmolin, T.V., Agertt, V.A., Mizdal, C.R., Flores, V. da C., Marques, J.B., Santos, R.C.V. & Anraku de Campos, M.M. (2013) Chlorhexidine activity against bacterial biofilms. *American Journal of Infection Control*, 41, pp. e119–e122.

Boyce, J.M., Havill, N.L., Otter, J.A., McDonald, L.C., Adams, N.M.T., Cooper, T., Thompson, A., Wiggs, L., Killgore, G., Tauman, A. & Noble-Wang, J. (2008) Impact of hydrogen peroxide vapor room decontamination on *Clostridium difficile* environmental contamination and transmission in a healthcare setting. *Infection Control and Hospital Epidemiology*, 29, pp. 723–729.

Brady, M.J., Lisay, C.M., Yurkovetskiy, A. V. & Sawan, S.P. (2003) Persistent silver disinfectant for the environmental control of pathogenic bacteria. *American Journal of Infection Control*, 31, pp. 208–214.

Brady, R.A., Leid, J.G., Camper, A.K., Costerton, J.W. & Shirtliff, M.E. (2006) Identification of *Staphylococcus aureus* proteins recognized by the antibody-mediated immune response to

a biofilm infection. *Infection and Immunity*, 74, pp. 3415–3426.

Brayner, R., Ferrari-Iliou, R., Brivois, N., Djediat, S., Benedetti, M.F. & Fiévet, F. (2006) Toxicological impact studies based on *Escherichia coli* bacteria in ultrafine ZnO nanoparticles colloidal medium. *Nano Letters*, 6, pp. 866–870.

Breathnach, A.S., Cubbon, M.D., Karunaharan, R.N., Pope, C.F. & Planche, T.D. (2012) Multidrug-resistant *Pseudomonas aeruginosa* outbreaks in two hospitals: association with contaminated hospital waste-water systems. *The Journal of Hospital Infection*, 82, pp. 19–24.

British Standards Institute (2001) *BS EN 13697:2001 - Chemical disinfectants and antiseptics. Quantitative non-porous surface test for the evaluation of bactericidal and/or fungicidal activity of chemical disinfectants used in food, industrial, domestic and institutional areas. Test method*. London: BSI

Bronner, S., Monteil, H. & Prévost, G. (2004) Regulation of virulence determinants in *Staphylococcus aureus*: Complexity and applications. *FEMS Microbiology Reviews*, 28, pp. 183–200.

Brown, L., Wolf, J.M., Prados-Rosales, R. & Casadevall, A. (2015) Through the wall: extracellular vesicles in Gram-positive bacteria, mycobacteria and fungi. *Nature Reviews. Microbiology*, 13, pp. 620–630.

Buckingham-Meyer, K., Goeres, D.M. & Hamilton, M.A. (2007) Comparative evaluation of biofilm disinfectant efficacy tests. *Journal of Microbiological Methods*, 70, pp. 236–244.

Buckingham-Meyer, K., Heersink, J., Pitts, B., Rayner, J. & Werner, E. (2003) Alternative biofilm growth reactors. In: Hamilton, M. *et al*. (eds.). *The Biofilm Laboratory: Step-by-step Protocols for Experimental Design, Analysis, and Data Interpretation*. Bozeman: Cytergy Publishing. pp. 31–51.

Burmølle, M., Webb, J.S., Rao, D., Hansen, L.H., Sørensen, S.J. & Kjelleberg, S. (2006) Enhanced biofilm formation and increased resistance to antimicrobial agents and bacterial invasion are caused by synergistic interactions in multispecies biofilms. *Applied and Environmental Microbiology*, 72, pp. 3916–3923.

Busscher, H.J. & Van Der Mei, H.C. (2006) Microbial adhesion in flow displacement systems. *Clinical Microbiology Reviews*, 19, pp. 127–141.

Bustin, S.A., Benes, V., Nolan, T. & Pfaffl, M.W. (2005) Quantitative real-time RT-PCR-a perspective. *Journal of molecular endocrinology*, 34, pp. 597–601.

Buzea, C., Pacheco, I.I. & Robbie, K. (2007) Nanomaterials and nanoparticles: sources and toxicity. *Biointerphases*, 2, pp. MR17–R71.

Campbell, C.D., Chapman, S.J., Cameron, C.M., Davidson, M.S. & Pottts, J.M. (2003) A rapid microtiter plate method to measure carbon dioxide evolved from carbon substrate amendments so as to determine the physiological profiles of soil microbial communities by using whole soil. *Applied and Environmental Microbiology*, 69, pp. 3593–3599.

Carling, P.C., Parry, M.F. & Von Beheren, S.M. (2008) Identifying opportunities to enhance environmental cleaning in 23 acute care hospitals . *Infection Control and Hospital Epidemiology*, 29, pp. 1–7.

Carvalho, I., Henriques, M., Oliveira, J.C., Alves, C.F.A., Piedade, A.P. & Sandra, C. (2013) Influence of surface features on the adhesion of *Staphylococcus epidermidis* to Ag–TiCN thin films. *Science and Technology of Advanced Materials*, 14, pp. 35009.

Casey, A.L., Adams, D., Karpanen, T.J., Lambert, P. a, Cookson, B.D., Nightingale, P., Miruszenko, L., Shillam, R., Christian, P. & Elliott, T.S.J. (2010) Role of copper in reducing hospital environment contamination. *The Journal of Hospital Infection*, 74, pp. 72–77.

Cassone, M. & Otvos, L. (2010) Synergy among antibacterial peptides and between peptides and small-molecule antibiotics. *Expert Review of Anti-infective Therapy*, 8, pp. 703–716.

Centre for Disease Control (2008) *Guideline for Disinfection and Sterilization in Healthcare Facilities*. Atlanta: CDC

Cha, J.O., Yoo, J. Il, Yoo, J.S., Chung, H.S., Park, S.H., Kim, H.S., Lee, Y.S. & Chung, G.T. (2013) Investigation of biofilm formation and its association with the molecular and clinical characteristics of methicillin-resistant *Staphylococcus aureus*. *Osong Public Health and Research Perspectives*, 4, pp. 225–232.

Chaieb, K., Mahdouani, K. & Bakhrouf, A. (2005) Detection of *icaA* and *icaD* loci by polymerase chain reaction and biofilm formation by *Staphylococcus epidermidis* isolated from dialysate and needles in a dialysis unit. *The Journal of Hospital Infection*, 61, pp. 225–230.

Chandra, J., Kuhn, D.M., Mukherjee, P.K., Hoyer, L.L., McCormick, T. & Ghannoum, M.A. (2001) Biofilm formation by the fungal pathogen *Candida albicans*: Development, architecture, and drug resistance. *Journal of Bacteriology*, 183, pp. 5385–5394.

Chavant, P., Gaillard-Martinie, B., Talon, R., Hébraud, M. & Bernardi, T. (2007) A new device for rapid evaluation of biofilm formation potential by bacteria. *Journal of Microbiological Methods*, 68, pp. 605–612.

Chen, C.W., Hsu, C.Y., Lai, S.M., Syu, W.J., Wang, T.Y. & Lai, P.S. (2014) Metal nanobullets for multidrug resistant bacteria and biofilms. *Advanced Drug Delivery Reviews*, 78, pp. 88–104.

Chen, M., Yang, Z., Wu, H., Pan, X., Xie, X. & Wu, C. (2011) Antimicrobial activity and the mechanism of silver nanoparticle thermosensitive gel. *International Journal of Nanomedicine*, 6, pp. 2873–2877.

Chen, M.J., Zhang, Z. & Bott, T.R. (2005) Effects of operating conditions on the adhesive strength of *Pseudomonas fluorescens* biofilms in tubes. *Colloids and Surfaces B: Biointerfaces*, 43, pp. 61–71.

Chen, X. & Schluesener, H.J. (2008) Nanosilver: A nanoproduct in medical application. *Toxicology Letters*, 176, pp. 1–12.

Cho, K.H., Park, J.E., Osaka, T. & Park, S.G. (2005) The study of antimicrobial activity and preservative effects of nanosilver ingredient. *Electrochimica Acta*, 51, pp. 956–960.

Choi, O. & Hu, Z. (2008) Size dependent and reactive oxygen species related nanosilver toxicity to nitrifying bacteria. *Environmental Science & Technology*, 42, pp. 4583–4588.

Chou, W.L., Yu, D.G. & Yang, M.C. (2005) The preparation and characterization of silver-loading cellulose acetate hollow fiber membrane for water treatment. *Polymers for Advanced Technologies*, 16, pp. 600–607.

Christensen, G.D., Simpson, W.A., Younger, J.J., Baddour, L.M., Barrett, F.F., Melton, D.M. & Beachey, E.H. (1985) Adherence of coagulase-negative staphylococci to plastic tissue culture plates: a quantitative model for the adherence of staphylococci to medical devices. *Journal of Clinical Microbiology*, 22, pp. 996–1006.

Chuanchuen, R., Karkhoff-Schweizer, R.R. & Schweizer, H.P. (2003) High-level triclosan

resistance in *Pseudomonas aeruginosa* is solely a result of efflux. *American Journal of Infection Control*, 31, pp. 124–127.

Di Ciccio, P., Vergara, A., Festino, A.R., Paludi, D., Zanardi, E., Ghidini, S. & Ianieri, A. (2015) Biofilm formation by *Staphylococcus aureus* on food contact surfaces: Relationship with temperature and cell surface hydrophobicity. *Food Control*, 50, pp. 930–936.

Claro, T., O'Reilly, M., Daniels, S. & Humphreys, H. (2015) Surface microbial contamination in hospitals: A pilot study on methods of sampling and the use of proposed microbiologic standards. *American Journal of Infection Control*, 43, pp. 1000–1002.

Coenye, T. & Nelis, H.J. (2010) *In vitro* and *in vivo* model systems to study microbial biofilm formation. *Journal of Microbiological Methods*, 83, pp. 89–105.

Colvin, K.M., Irie, Y., Tart, C.S., Urbano, R., Whitney, J.C., Ryder, C., Howell, P.L., Wozniak, D.J. & Parsek, M.R. (2012) The Pel and Psl polysaccharides provide *Pseudomonas aeruginosa* structural redundancy within the biofilm matrix. *Environmental Microbiology*, 14, pp. 1913–1928.

Combarros, R.G., Collado, S. & Díaz, M. (2016) Toxicity of titanium dioxide nanoparticles on *Pseudomonas putida*. *Water Research*, 90, pp. 378–386.

Condell, O., Iversen, C., Cooney, S., Power, K.A., Walsh, C., Burgess, C. & Fanning, S. (2012) Efficacy of biocides used in the modern food industry to control *Salmonella enterica*, and links between biocide tolerance and resistance to clinically relevant antimicrobial compounds. *Applied and Environmental Microbiology*, 78, pp. 3087–3097.

Conrad, J.C., Gibiansky, M.L., Jin, F., Gordon, V.D., Motto, D.A., Mathewson, M.A., Stopka, W.G., Zelasko, D.C., Shrout, J.D. & Wong, G.C.L. (2011) Flagella and pili-mediated near-surface single-cell motility mechanisms in *P. aeruginosa*. *Biophysical Journal*, 100, pp. 1608–1616.

Cooke, J., Alexander, K., Charani, E., Hand, K., Hills, T., Howard, P., Jamieson, C., Lawson, W., Richardson, J. & Wade, P. (2010) Antimicrobial stewardship: an evidence-based, antimicrobial self-assessment toolkit (ASAT) for acute hospitals. *The Journal of Antimicrobial Chemotherapy*, 65, pp. 2669–2673.

Cooke, J., Stephens, P., Ashiru-Oredope, D., Johnson, A.P., Livermore, D.M. & Sharland, M. (2014) Antibacterial usage in English NHS hospitals as part of a national Antimicrobial Stewardship Programme. *Public Health*, 128, pp. 6–10.

Costa, D., Bousseau, A., Thevenot, S., Dufour, X., Laland, C., Burucoa, C. & Castel, O. (2015) Nosocomial outbreak of *Pseudomonas aeruginosa* associated with a drinking water fountain. *The Journal of Hospital Infection*, 91, pp. 271–274.

Crémet, L., Corvec, S., Batard, E., Auger, M., Lopez, I., Pagniez, F., Dauvergne, S. & Caroff, N. (2013) Comparison of three methods to study biofilm formation by clinical strains of *Escherichia coli*. *Diagnostic Microbiology and Infectious Disease*, 75, pp. 252–255.

Crivaro, V., Di Popolo, A., Caprio, A., Lambiase, A., Di Resta, M., Borriello, T., Scarcella, A., Triassi, M. & Zarrilli, R. (2009) *Pseudomonas aeruginosa* in a neonatal intensive care unit: molecular epidemiology and infection control measures. *BMC Infectious Diseases*, 9, pp. 70.

Cucarella, C., Solano, C., Valle, J., Amorena, B., Lasa, I. & Penadés, J.R. (2001) Bap, a *Staphylococcus aureus* surface protein involved in biofilm formation. *Journal of Bacteriology*, 183, pp. 2888–2896.

Cuervo, G., Gasch, O., Shaw, E., Camoez, M., Domínguez, M.Á., Padilla, B., Pintado, V., Almirante, B., Lepe, J.A., López-Medrano, F., Ruiz de Gopegui, E., Martínez, J.A., Montejo, J.M., Perez-Nadales, E., Arnáiz, A., Goenaga, M.Á., Benito, N., Horcajada, J.P., Rodríguez-Baño, J. & Pujol, M. (2016) Clinical characteristics, treatment and outcomes of MRSA bacteraemia in the elderly. *The Journal of Infection*, 72, pp. 309–316.

Curtin, J.J. & Donlan, R.M. (2006) Using bacteriophages to reduce formation of catheter-associated biofilms by *Staphylococcus epidermidis*. *Antimicrobial Agents and Chemotherapy*, 50, pp. 1268–1275.

Dancer, S.J., White, L.F., Lamb, J., Girvan, E.K. & Robertson, C. (2009) Measuring the effect of enhanced cleaning in a UK hospital: a prospective cross-over study. *BMC Medicine*, 7, pp. 28.

Das, D., Nath, B.C., Phukon, P. & Dolui, S.K. (2013) Synthesis and evaluation of antioxidant and antibacterial behavior of CuO nanoparticles. *Colloids and Surfaces B: Biointerfaces*, 101, pp. 430–433.

Davenport, E.K., Call, D.R. & Beyenal, H. (2014) Differential protection from tobramycin by extracellular polymeric substances from *Acinetobacter baumannii* and *Staphylococcus aureus* biofilms. *Antimicrobial Agents and Chemotherapy*, 58, pp. 4755–4761.

Davey, M.E. & O'Toole, G.A. (2000) Microbial biofilms: from ecology to molecular genetics. *Microbiology and Molecular Biology Reviews*, 64, pp. 847–867.

David, M.Z. & Daum, R.S. (2010) Community-associated methicillin-*resistant Staphylococcus aureus*: epidemiology and clinical consequences of an emerging epidemic. *Clinical microbiology reviews*, 23, pp. 616–687.

Department of Health (2008a) *Clean, safe care: reducing infections and saving lives*. London: Department of Health

Department of Health (2006) *Essential steps to safe, clean care: reducing healthcare-associated infections*. London: Department of Health

Department of Health (2007) *Saving Lives: reducing infection, delivering clean and safe care*. London: Department of Health

Department of Health (2008b) *The Health and Social Care Act 2008: code of practice on the prevention and control of infections and related guidance*. London: Department of Health

Department of Health (2013) *UK 5 year antimicrobial resistance strategy 2013 to 2018*. London: Department of Health

Department of Health (2012) *Water sources and potential Pseudomonas aeruginosa contamination of taps and water systems: Advice for Augmented Care Units*. London: Department of Health

Department of Health Advisory Committee on antimicrobial resistance and healthcare associated infection (ARHAI) (2011) *Antimicrobial stewardship: Start smart - then focus*. London: Public Health England

Department of Health and the Health Protection Agency (2008) *Clostridium difficile infection: how to deal with the problem*. London: Public Health England and Department of Health

DeVasConCellos, P., Bose, S., Beyenal, H., Bandyopadhyay, A. & Zirkle, L.G. (2012) Antimicrobial particulate silver coatings on stainless steel implants for fracture management. *Materials Science and Engineering: C*, 32, pp. 1112–1120.

Dice, B., Stoodley, P., Buchinsky, F., Metha, N., Ehrlich, G.D. & Hu, F.Z. (2009) Biofilm formation by *ica*-positive and *ica*-negative strains of *Staphylococcus epidermidis in vitro*. *Biofouling*, 25, pp. 367–375.

Dizaj, S.M., Lotfipour, F., Barzegar-Jalali, M., Zarrintan, M.H. & Adibkia, K. (2014) Antimicrobial activity of the metals and metal oxide nanoparticles. *Materials Science and Engineering: C*, 44, pp. 278–284.

Djurišić, A.B., Leung, Y.H., Ng, A.M.C., Xu, X.Y., Lee, P.K.H., Degger, N. & Wu, R.S.S. (2015) Toxicity of metal oxide nanoparticles: Mechanisms, characterization, and avoiding experimental artefacts. *Small*, 11, pp. 26–44.

Doan, L., Forrest, H., Fakis, A., Craig, J., Claxton, L. & Khare, M. (2012) Clinical and cost effectiveness of eight disinfection methods for terminal disinfection of hospital isolation rooms contaminated with *Clostridium difficile* 027. *The Journal of Hospital Infection*, 82, pp. 114–121.

Dobrucka, R. & Długaszewska, J. (2016) Biosynthesis and antibacterial activity of ZnO nanoparticles using *Trifolium pratense* flower extract. *Saudi Journal of Biological Sciences*, 23, pp. 517–523.

Donlan, R.M. (2001) Biofilms and device-associated infections. *Emerging Infectious Diseases*, 7, pp. 277–281.

Donlan, R.M. (2002) Biofilms: microbial life on surfaces. *Emerging Infectious Diseases*, 8, pp. 881–890.

Donlan, R.M., Piede, J.A., Heyes, C.D., Sanii, L., Murga, R., Edmonds, P., El-Sayed, I. & El-Sayed, M.A. (2004) Model system for growing and quantifying *Streptococcus pneumoniae* biofilms *in situ* and in real time. *Applied and Environmental Microbiology*, 70, pp. 4980–4988.

Dosler, S. & Karaaslan, E. (2014) Inhibition and destruction of *Pseudomonas aeruginosa* biofilms by antibiotics and antimicrobial peptides. *Peptides*, 62, pp. 32–37.

Dosunmu, E., Chaudhari, A.A., Singh, S.R., Dennis, V.A. & Pillai, S.R. (2015) Silver-coated carbon nanotubes downregulate the expression of *Pseudomonas aeruginosa* virulence genes: a potential mechanism for their antimicrobial effect. *International Journal of Nanomedicine*, 10, pp. 5025–5034.

Dunman, P.M., Murphy, E., Haney, S., Palacios, D., Tucker-Kellogg, G., Wu, S., Brown, E.L., Zagursky, R.J., Shlaes, D. & Projan, S.J. (2001) Transcription profiling-based identification of *Staphylococcus aureus* genes regulated by the agr and/or sarA loci. *Journal of Bacteriology*, 183, pp. 7341–7353.

Dunne, W.M. (2002) Bacterial adhesion: Seen any good biofilms lately? *Clinical Microbiology Reviews*, 15, pp. 155–166.

Durairaj, R., Amirulhusni, A.N., Palanisamy, N.K., Mohd-Zain, Z. & Ping, L.J. (2012) Antibacterial effect of silver nanoparticles on multi drug resistant *Pseudomonas aeruginosa*. *World Academy of Science, Engineering and Technology*, 6, pp. 210–213.

Durán, N., Durán, M., de Jesus, M.B., Seabra, A.B., Fávaro, W.J. & Nakazato, G. (2015) Silver nanoparticles: A new view on mechanistic aspects on antimicrobial activity. *Nanomedicine: Nanotechnology, Biology and Medicine*, 12, pp. 789–799.

Durán, N., Marcato, P.D., Alves, O.L., Souza, G.I.H. De & Esposito, E. (2005) Mechanistic aspects of biosynthesis of silver nanoparticles by several *Fusarium oxysporum* strains.

Journal of nanobiotechnology, 3, pp. 8.

Durán, N., Marcato, P.D., Conti, R. De, Alves, O.L., Costa, F.T.M. & Brocchi, M. (2010) Potential use of silver nanoparticles on pathogenic bacteria, their toxicity and possible mechanisms of action. *Journal of the Brazilian Chemical Society*, 21, pp. 949–959.

Dwivedi, S., Wahab, R., Khan, F., Mishra, Y.K., Musarrat, J. & Al-Khedhairy, A.A. (2014) Reactive oxygen species mediated bacterial biofilm inhibition via zinc oxide nanoparticles and their statistical determination. *PloS one*, 9, pp. e111289.

Eckmanns, T., Oppert, M., Martin, M., Amorosa, R., Zuschneid, I., Frei, U., Rüden, H. & Weist, K. (2008) An outbreak of hospital-acquired *Pseudomonas aeruginosa* infection caused by contaminated bottled water in intensive care units. *Clinical Microbiology and Infection*, 14, pp. 454–458.

Egger, S., Lehmann, R.P., Height, M.J., Loessner, M.J. & Schuppler, M. (2009) Antimicrobial properties of a novel silver-silica nanocomposite material. *Applied and Environmental Microbiology*, 75, pp. 2973–2976.

Elhassan, M.M., Ozbak, H.A., Hemeg, H.A., Elmekki, M.A. & Ahmed, L.M. (2015) Absence of the *mec A* gene in methicillin resistant *Staphylococcus aureus* isolated from different clinical specimens in Shendi City, Sudan. *BioMed Research International*, 2015, pp. 5.

Emami-Karvani, Z. & Chehrazi, P. (2012) Antibacterial activity of ZnO nanoparticle on Gram-positive and Gram-negative bacteria. *African Journal of Microbiology Research*, 5, pp. 5–10.

Espinal, P., Marti, S. & Vila, J. (2012) Effect of biofilm formation on the survival of *Acinetobacter baumannii* on dry surfaces. *Journal of Hospital Infection*, 80, pp. 56–60.

Eyre, D.W., Golubchik, T., Gordon, N.C., Bowden, R., Piazza, P., Batty, E.M., Ip, C.L.C., Wilson, D.J., Didelot, X., O'Connor, L., Lay, R., Buck, D., Kearns, A.M., Shaw, A., Paul, J., Wilcox, M.H., Donnelly, P.J., Peto, T.E.A., Walker, A.S. & Crook, D.W. (2012) A pilot study of rapid benchtop sequencing of *Staphylococcus aureus* and *Clostridium difficile* for outbreak detection and surveillance. *BMJ Open*, 2, pp. e001124.

Fang, M., Chen, J.-H.H., Xu, X.-L.L., Yang, P.-H.H. & Hildebrand, H.F. (2015) Antibacterial activities of inorganic agents on six bacteria associated with oral infections by two susceptibility tests. *International Journal of Antimicrobial Agents*, 27, pp. 513–517.

Fayaz, A.M., Balaji, K., Girilal, M., Yadav, R., Kalaichelvan, P.T. & Venketesan, R. (2010) Biogenic synthesis of silver nanoparticles and their synergistic effect with antibiotics: a study against Gram-positive and Gram-negative bacteria. *Nanomedicine : Nanotechnology, Biology and Medicine*, 6, pp. 103–109.

Feng, G., Cheng, Y., Wang, S.-Y., Borca-Tasciuc, D.A., Worobo, R.W. & Moraru, C.I. (2015) Bacterial attachment and biofilm formation on surfaces are reduced by small-diameter nanoscale pores: how small is small enough? *Npj Biofilms And Microbiomes*, 1, pp. 15022.

Feng, Q.L., Wu, J., Chen, G.Q., Cui, F.Z., Kim, T.N. & Kim, J.O. (2000) A mechanistic study of the antibacterial effect of silver ions on *Escherichia coli* and *Staphylococcus aureus*. *Journal of Biomedical Materials Research*, 52, pp. 662–668.

Feris, K., Otto, C., Tinker, J., Wingett, D., Punnoose, A., Thurber, A., Kongara, M., Sabetian, M., Quinn, B., Hanna, C. & Pink, D. (2010) Electrostatic interactions affect nanoparticle-mediated toxicity to Gram-negative bacterium *Pseudomonas aeruginosa* PAO1. *Langmuir*, 26, pp. 4429–4436.

Ferreira, C., Pereira, A.M., Melo, L.F. & Simões, M. (2010) Advances in industrial biofilm control with micro-nanotechnology. *Current Research, Technology and Education Topics in Applied Microbiology and Microbial Biotechnology*, 2, pp. 845–854.

Firouzabadi, F.B., Noori, M., Edalatpanah, Y. & Mirhosseini, M. (2014) ZnO nanoparticle suspensions containing citric acid as antimicrobial to control *Listeria monocytogenes*, *Escherichia coli*, *Staphylococcus aureus* and *Bacillus cereus* in mango juice. *Food Control*, 42, pp. 310–314.

Flemming, H.C., Neu, T.R. & Wozniak, D.J. (2007) The EPS matrix: The 'House of Biofilm Cells'. *Journal of Bacteriology*, 189, pp. 7945–7947.

Flemming, H.C. & Wingender, J. (2010) The biofilm matrix. *Nature reviews. Microbiology*, 8, pp. 623–633.

França, A., Melo, L.D. & Cerca, N. (2011) Comparison of RNA extraction methods from biofilm samples of *Staphylococcus epidermidis*. *BMC Research Notes*, 4, pp. 572.

Franklin, N.M., Rogers, N.J., Apte, S.C., Batley, G.E., Gadd, G.E. & Casey, P.S. (2007) Comparative toxicity of nanoparticulate ZnO, bulk ZnO, and $ZnCl_2$ to a freshwater microalga (*Pseudokirchneriella subcapitata*): The importance of particle solubility. *Environmental Science & Technology*, 41, pp. 8484–8490.

French, G.L., Otter, J.A., Shannon, K.P., Adams, N.M.T., Watling, D. & Parks, M.J. (2004) Tackling contamination of the hospital environment by methicillin-resistant *Staphylococcus aureus* (MRSA): a comparison between conventional terminal cleaning and hydrogen peroxide vapour decontamination. *The Journal of Hospital Infection*, 57, pp. 31–37.

Furno, F., Morley, K.S., Wong, B., Sharp, B.L., Arnold, P.L., Howdle, S.M., Bayston, R., Brown, P.D., Winship, P.D. & Reid, H.J. (2004) Silver nanoparticles and polymeric medical devices: a new approach to prevention of infection? *The Journal of Antimicrobial Chemotherapy*, 54, pp. 1019–1024.

Fux, C.A., Costerton, J.W., Stewart, P.S. & Stoodley, P. (2005) Survival strategies of infectious biofilms. *Trends in Microbiology*, 13, pp. 34–40.

Gaddy, J.A. & Actis, L.A. (2009) Regulation of *Acinetobacter baumannii* biofilm formation. *Future Microbiology*, 4, pp. 273–278.

Ganeshnarayan, K., Shah, S.M., Libera, M.R., Santostefano, A. & Kaplan, J.B. (2009) Poly-*N*-acetylglucosamine matrix polysaccharide impedes fluid convection and transport of the cationic surfactant cetylpyridinium chloride through bacterial biofilms. *Applied and Environmental Microbiology*, 75, pp. 1308–1314.

Garrett, T.R., Bhakoo, M. & Zhang, Z. (2008) Bacterial adhesion and biofilms on surfaces. *Progress in Natural Science*, 18, pp. 1049–1056.

Gaynes, R. & Edwards, J.R. (2005) Overview of nosocomial infections caused by Gram-negative bacilli. *Clinical Infectious Diseases*, 41, pp. 848–854.

Geng, J. & Henry, N. (2011) Short time-scale bacterial adhesion dynamics. *Advances in Experimental Medicine and Biology*, 715, pp. 315–331.

Gerstel, U. & Romling, U. (2001) Oxygen tension and nutrient starvation are major signals that regulate agfD promoter activity and expression of the multicellular morphotype in *Salmonella typhimurium*. *Environmental Microbiology*, 3, pp. 638–648.

Ghafoor, A., Hay, I.D. & Rehm, B.H.A. (2011) Role of exopolysaccharides in *Pseudomonas*

aeruginosa biofilm formation and architecture. *Applied and Environmental Microbiology*, 77, pp. 5238–5246.

Ghasemian, A., Najar Peerayeh, S., Bakhshi, B. & Mirzaee, M. (2015) The microbial surface components recognizing adhesive matrix molecules (MSCRAMMs) genes among clinical isolates of *Staphylococcus aureus* from hospitalized children. *Iranian Journal of Pathology*, 10, pp. 258–264.

Ghosh, S., Goudar, V.S., Padmalekha, K.G., Bhat, S. V, Indi, S.S. & Vasan, H.N. (2012) ZnO/Ag nanohybrid: synthesis, characterization, synergistic antibacterial activity and its mechanism. *RSC Advances*, 2, pp. 930–940.

Gielda, L.M. & DiRita, V.J. (2012) Zinc competition among the intestinal microbiota. *MBio*, 3, pp. e00171–12.

Gilbert, P., Allison, D.G. & McBain, A.J. (2002) Biofilms *in vitro* and *in vivo*: do singular mechanisms imply cross-resistance? *Journal of Applied Microbiology*, 92, pp. 98S – 110S.

Gittard, S.D., Perfect, J.R., Monteiro-Riviere, N.A., Wei, W., Jin, C. & Narayan, R.J. (2009) Assessing the antimicrobial activity of zinc oxide thin films using disk diffusion and biofilm reactor. *Applied Surface Science*, 255, pp. 5806–5811.

Goeres, D.M., Hamilton, M.A., Beck, N.A., Buckingham-Meyer, K., Hilyard, J.D., Loetterle, L.R., Lorenz, L.A., Walker, D.K. & Stewart, P.S. (2009) A method for growing a biofilm under low shear at the air-liquid interface using the drip flow biofilm reactor. *Nature Protocols*, 4, pp. 783–788.

Goeres, D.M., Loetterle, L.R., Hamilton, M.A., Murga, R., Kirby, D.W. & Donlan, R.M. (2005) Statistical assessment of a laboratory method for growing biofilms. *Microbiology*, 151, pp. 757–762.

Goldenberg, S.D., Patel, A., Tucker, D. & French, G.L. (2012) Lack of enhanced effect of a chlorine dioxide-based cleaning regimen on environmental contamination with *Clostridium difficile* spores. *Journal of Hospital Infection*, 82, pp. 64–67.

Gomes, F., Teixeira, P., Ceri, H. & Oliveira, R. (2012) Evaluation of antimicrobial activity of certain combinations of antibiotics against *in vitro Staphylococcus epidermidis* biofilms. *The Indian Journal of Medical Research*, 135, pp. 542–547.

Goodman, E., Platt, R., Bass, R., Onderdonk, A., Yokoe, D. & Huang, S. (2008) Impact of an environmental cleaning intervention on the presence of methicillin-resistant *Staphylococcus aureus* and vancomycin resistant *Enterococci* on surfaces in intensive care unit rooms. *Infection Control & Hospital Epidemiology*, 29, pp. 593–599.

Götz, F. (2002) Staphylococcus and biofilms. *Molecular Microbiology*, 43, pp. 1367–1378.

Gross, R., Hauer, B., Otto, K. & Schmid, A. (2007) Microbial biofilms: New catalysts for maximizing productivity of long-term biotransformations. *Biotechnology and Bioengineering*, 98, pp. 1123–1134.

Guerrero, D.M., Nerandzic, M.M., Jury, L.A., Jinno, S., Chang, S. & Donskey, C.J. (2012) Acquisition of spores on gloved hands after contact with the skin of patients with *Clostridium difficile* infection and with environmental surfaces in their rooms. *American Journal of Infection Control*, 40, pp. 556–558.

Gupta, K., Marques, C.N.H., Petrova, O.E. & Sauer, K. (2013) Antimicrobial tolerance of

Pseudomonas aeruginosa biofilms is activated during an early developmental stage and requires the two-component hybrid SagS. *Journal of Bacteriology*, 195, pp. 4975–4987.

Gurunathan, S., Han, J.W., Kwon, D.N. & Kim, J.H. (2014) Enhanced antibacterial and anti-biofilm activities of silver nanoparticles against Gram-negative and Gram-positive bacteria. *Nanoscale Research Letters*, 9, pp. 373.

Gurunathan, S., Lee, K.J., Kalishwaralal, K., Sheikpranbabu, S., Vaidyanathan, R. & Eom, S.H. (2009) Antiangiogenic properties of silver nanoparticles. *Biomaterials*, 30, pp. 6341–6350.

Guzman, M., Dille, J. & Godet, S. (2012) Synthesis and antibacterial activity of silver nanoparticles against Gram-positive and Gram-negative bacteria. *Nanomedicine : Nanotechnology, Biology and Medicine*, 8, pp. 37–45.

Habimana, O., Semião, A.J.C. & Casey, E. (2014) The role of cell-surface interactions in bacterial initial adhesion and consequent biofilm formation on nanofiltration/reverse osmosis membranes. *Journal of Membrane Science*, 454, pp. 82–96.

Hadi, R., Vickery, K., Deva, A. & Charlton, T. (2010) Biofilm removal by medical device cleaners: comparison of two bioreactor detection assays. *Journal of Hospital Infection*, 74, pp. 160–167.

Hancock, V., Witsø, I.L. & Klemm, P. (2011) Biofilm formation as a function of adhesin, growth medium, substratum and strain type. *International Journal of Medical Microbiology*, 301, pp. 570–576.

Hanh, T.T., Thu, N.T., Hien, N.Q., An, P.N., Loan, T.T.K. & Hoa, P.T. (2016) Preparation of silver nanoparticles fabrics against multidrug-resistant bacteria. *Radiation Physics and Chemistry*, 121, pp. 87–92.

Harmsen, M., Yang, L., Pamp, S.J. & Tolker-Nielsen, T. (2010) An update on *Pseudomonas aeruginosa* biofilm formation, tolerance, and dispersal. *FEMS Immunology and Medical Microbiology*, 59, pp. 253–268.

Harris, S.R., Cartwright, E.J.P., Török, M.E., Holden, M.T.G., Brown, N.M., Ogilvy-Stuart, A.L., Ellington, M.J., Quail, M.A., Bentley, S.D., Parkhill, J. & Peacock, S.J. (2013) Whole-genome sequencing for analysis of an outbreak of meticillin-resistant *Staphylococcus aureus*:A descriptive study. *The Lancet. Infectious Diseases*, 13, pp. 130–136.

Hassan, M.S., Amna, T., Yang, O.B., El-Newehy, M.H., Al-Deyab, S.S. & Khil, M.S. (2012) Smart copper oxide nanocrystals: synthesis, characterization, electrochemical and potent antibacterial activity. *Colloids and Surfaces B: Biointerfaces*, 97, pp. 201–206.

Hassani Sangani, M., Nakhaei Moghaddam, M. & Forghanifard, M.M. (2015) Inhibitory effect of zinc oxide nanoparticles on *Pseudomonas aeruginosa* biofilm formation. *Nanomedicine Journal*, 2, pp. 121–128.

Hayden, M.K., Blom, D.W., Lyle, E.A., Moore, C.G. & Weinstein, R.A. (2008) Risk of hand or glove contamination after contact with patients colonized with vancomycin-resistant *Enterococcus* or the colonized patients' environment. *Infection Control and Hospital Epidemiology*, 29, pp. 149–154.

Health Protection Agency (2012) *English National Point Prevalence Survey on Healthcare-associated Infections and Antimicrobial Use, 2011: Preliminary Data*. London: Health Protection Agency

Heersink, J. & Goeres, D. (2003) Reactor design considerations. In: Hamilton, M. *et al.* (eds.). *The Biofilm Laboratory: Step-by-step Protocols for Experimental Design, Analysis, and*

Data Interpretation. Bozeman: Cytergy Publishing, pp. 13–15.

Heilmann, C. (2011) Adhesion mechanisms of staphylococci. *Advances in Experimental Medicine and Biology*, 715, pp. 105–123.

Heinlaan, M., Ivask, A., Blinova, I., Dubourguier, H.C. & Kahru, A. (2008) Toxicity of nanosized and bulk ZnO, CuO and TiO_2 to bacteria *Vibrio fischeri* and crustaceans *Daphnia magna* and *Thamnocephalus platyurus*. *Chemosphere*, 71, pp. 1308–1316.

Hensley, B.J. & Monson, J.R.T. (2015) Hospital-acquired infections. *Surgery (Oxford)*, 33, pp. 528–533.

Hernández-Sierra, J.F., Ruiz, F., Pena, D.C.C., Martínez-Gutiérrez, F., Martínez, A.E., Guillén, A. de J.P., Tapia-Pérez, H. & Castañón, G.M. (2008) The antimicrobial sensitivity of *Streptococcus mutans* to nanoparticles of silver, zinc oxide, and gold. *Nanomedicine : Nanotechnology, Biology and Medicine*, 4, pp. 237–240.

Hivatec Laboratory (2016) *Thin Film Deposition*. [Online]. Available from: http://hivatec.ca/consulting-design/thin-film-deposition/ [Accessed: 19 May 2016].

Holt, K.B. & Bard, A.J. (2005) Interaction of silver(I) ions with the respiratory chain of *Escherichia coli*: an electrochemical and scanning electrochemical microscopy study of the antimicrobial mechanism of micromolar Ag^+. *Biochemistry*, 44, pp. 13214–13223.

Honraet, K., Goetghebeur, E. & Nelis, H.J. (2005) Comparison of three assays for the quantification of *Candida* biomass in suspension and CDC reactor grown biofilms. *Journal of Microbiological Methods*, 63, pp. 287–295.

Howden, B.P., Peleg, A.Y. & Stinear, T.P. (2014) The evolution of vancomycin intermediate *Staphylococcus aureus* (VISA) and heterogenous-VISA. *Infection, Genetics and Evolution*, 21, pp. 575–582.

Hsueh, Y.H., Lin, K.S., Ke, W.J., Hsieh, C. Te, Chiang, C.L., Tzou, D.Y. & Liu, S.T. (2015) The antimicrobial properties of silver nanoparticles in *Bacillus subtilis* are mediated by released Ag^+ ions. *PloS one*, 10, pp. e0144306.

Hu, H., Johani, K., Gosbell, I.B., Jacombs, A.S.W., Almatroudi, A., Whiteley, G.S., Deva, A.K., Jensen, S. & Vickery, K. (2015) Intensive care unit environmental surfaces are contaminated by multidrug-resistant bacteria in biofilms: combined results of conventional culture, pyrosequencing, scanning electron microscopy, and confocal laser microscopy. *The Journal of Hospital Infection*, 91, pp. 35–44.

Huang, R., Mehta, S., Weed, D. & Price, C.S. (2006) Methicillin-resistant *Staphylococcus aureus* survival on hospital fomites. *Infection Control and Hospital Epidemiology*, 27, pp. 1267–1269.

Huang, Z., Zheng, X., Yan, D., Yin, G., Liao, X., Kang, Y., Yao, Y., Huang, D. & Hao, B. (2008) Toxicological effect of ZnO nanoparticles based on bacteria. *Langmuir*, 24, pp. 4140–4144.

Humphreys, H. (2014) Self-disinfecting and microbiocide-impregnated surfaces and fabrics: What potential in interrupting the spread of healthcare-associated infection? *Clinical Infectious Diseases*, 58, pp. 848–853.

Humphreys, H., Newcombe, R.G., Enstone, J., Smyth, E.T.M., McIlvenny, G., Davies, E. & Spencer, R. (2010) Four country healthcare-associated infection prevalence survey: pneumonia and lower respiratory tract infections. *The Journal of Hospital Infection*, 74, pp. 266–270.

Hunt, S.M., Werner, E.M., Huang, B., Hamilton, M.A. & Stewart, P.S. (2004) Hypothesis for the role of nutrient starvation in biofilm detachment. *Applied and Environmental Microbiology*, 70, pp. 7418–7425.

Huslage, K., Rutala, W.A., Sickbert-Bennett, E. & Weber, D.J. (2010) A quantitative approach to defining 'high-touch' surfaces in hospitals. *Infection Control and Hospital Epidemiology*, 31, pp. 850–853.

Ibrahim, H.M.M. (2015) Green synthesis and characterization of silver nanoparticles using banana peel extract and their antimicrobial activity against representative microorganisms. *Journal of Radiation Research and Applied Sciences*, 8, pp. 265–275.

Imamura, Y., Chandra, J., Mukherjee, P.K., Lattif, A.A., Szczotka-Flynn, L.B., Pearlman, E., Lass, J.H., O'Donnell, K. & Ghannoum, M.A. (2008) *Fusarium* and *Candida albicans* biofilms on soft contact lenses: Model development, influence of lens type, and susceptibility to lens care solutions. *Antimicrobial Agents and Chemotherapy*, 52, pp. 171–182.

Impellitteri, C.A., Tolaymat, T.M. & Scheckel, K.G. (2009) The speciation of silver nanoparticles in antimicrobial fabric before and after exposure to a hypochlorite/detergent solution. *Journal of Environmental Quality*, 38, pp. 1528–1530.

Ingle, A., Gade, A., Pierrat, S., Sonnichsen, C. & Rai, M. (2008) Mycosynthesis of silver nanoparticles using the fungus *Fusarium acuminatum* and its activity against some human pathogenic bacteria. *Current Nanoscience*, 4, pp. 141–144.

Integrated DNA Technologies (2011) *A Basic Polymerase Chain Reaction Protocol*. 2011 [Online]. Available from: https://www.idtdna.com/pages/docs/educational-resources/a-basic-pcr-protocol.pdf?sfvrsn=5 [Accessed: 21 May 2016].

Irzh, A., Genish, I., Klein, L., Solovyov, L.A. & Gedanken, A. (2010) Synthesis of ZnO and Zn nanoparticles in microwave plasma and their deposition on glass slides. *Langmuir*, 26, pp. 5976–5984.

Ito, A., Taniuchi, A., May, T., Kawata, K. & Okabe, S. (2009) Increased antibiotic resistance of *Escherichia coli* in mature biofilms. *Applied and Environmental Microbiology*, 75, pp. 4093–4100.

Ivanova, E.P., Truong, V.K., Wang, J.Y., Bemdt, C.C., Jones, R.T., Yusuf, I.I., Peake, I., Schmidt, H.W., Fluke, C., Barnes, D. & Crawford, R.J. (2010) Impact of nanoscale roughness of titanium thin film surfaces on bacterial retention. *Langmuir*, 26, pp. 1973–1982.

Ivask, A., Elbadawy, A., Kaweeteerawat, C., Boren, D., Fischer, H., Ji, Z., Chang, C.H., Liu, R., Tolaymat, T., Telesca, D., Zink, J.I., Cohen, Y., Holden, P.A. & Godwin, H.A. (2014) Toxicity mechanisms in *Escherichia coli* vary for silver nanoparticles and differ from ionic silver. *ACS Nano*, 8, pp. 374–386.

Izano, E.A., Amarante, M.A., Kher, W.B. & Kaplan, J.B. (2008) Differential roles of poly-*N*-acetylglucosamine surface polysaccharide and extracellular DNA in *Staphylococcus aureus* and *Staphylococcus epidermidis* biofilms. *Applied and Environmental Microbiology*, 74, pp. 470–476.

Jadhav, S., Gaikwad, S., Nimse, M. & Rajbhoj, A. (2011) Copper oxide nanoparticles: synthesis, characterization and their antibacterial activity. *Journal of Cluster Science*, 22, pp. 121–129.

Jafari, A., Ghane, M. & Arastoo, S. (2011) Synergistic antibacterial effects of nano zinc oxide combined with silver nanocrystals. *African Journal of Microbiology Research*, 5, pp. 5465–

5473.

Jain, J., Arora, S., Rajwade, J.M., Omray, P., Khandelwal, S. & Paknikar, K.M. (2009) Silver nanoparticles in therapeutics: development of an antimicrobial gel formulation for topical use. *Molecular Pharmaceutics*, 6, pp. 1388–1401.

Jakobsen, T.H., van Gennip, M., Phipps, R.K., Shanmugham, M.S., Christensen, L.D., Alhede, M., Skindersoe, M.E., Rasmussen, T.B., Friedrich, K., Uthe, F., Jensen, P.Ø., Moser, C., Nielsen, K.F., Eberl, L., Larsen, T.O., Tanner, D., Høiby, N., Bjarnsholt, T. & Givskov, M. (2012) Ajoene, a sulfur-rich molecule from garlic, inhibits genes controlled by quorum sensing. *Antimicrobial Agents and Chemotherapy*, 56, pp. 2314–2325.

Janaki, A.C., Sailatha, E. & Gunasekaran, S. (2015) Synthesis, characteristics and antimicrobial activity of ZnO nanoparticles. *Spectrochimica Acta Part A: Molecular and Biomolecular Spectroscopy*, 144, pp. 17–22.

Jansson, T., Clare-Salzler, Z.J., Zaveri, T.D., Mehta, S., Dolgova, N. V, Chu, B.-H., Ren, F. & Keselowsky, B.G. (2012) Antibacterial effects of zinc oxide nanorod surfaces. *Journal of Nanoscience and Nanotechnology*, 12, pp. 7132–7138.

Jayaseelan, C., Rahuman, A.A., Kirthi, A.V., Marimuthu, S., Santhoshkumar, T., Bagavan, A., Gaurav, K., Karthik, L. & Rao, K.V.B. (2012) Novel microbial route to synthesize ZnO nanoparticles using *Aeromonas hydrophila* and their activity against pathogenic bacteria and fungi. *Spectrochimica Acta Part A: Molecular and Biomolecular Spectroscopy*, 90, pp. 78–84.

Jefferies, J.M.C., Cooper, T., Yam, T. & Clarke, S.C. (2012) *Pseudomonas aeruginosa* outbreaks in the neonatal intensive care unit - a systematic review of risk factors and environmental sources. *Journal of Medical Microbiology*, 61, pp. 1052–1061.

Jefferson, K.K. (2004) What drives bacteria to produce a biofilm? *FEMS Microbiology Letters*, 236, pp. 163–173.

Jeong, S.H., Yeo, S.Y. & Yi, S.C. (2005) The effect of filler particle size on the antibacterial properties of compounded polymer/silver fibers. *Journal of Materials Science*, 40, pp. 5407–5411.

Jevons, M.P. (1961) 'Celbenin'-resistant Staphylococci. *British Medical Journal*, 1, pp. 124–125.

Jiang, X., Yu, T., Jiang, X., Zhang, W., Zhang, L. & Ma, J. (2014) Emergence of plasmid-mediated quinolone resistance genes in clinical isolates of *Acinetobacter baumannii* and *Pseudomonas aeruginosa* in Henan, China. *Diagnostic Microbiology and Infectious Disease*, 79, pp. 381–383.

Jin, T. & He, Y. (2011) Antibacterial activities of magnesium oxide (MgO) nanoparticles against foodborne pathogens. *Journal of Nanoparticle Research*, 13, pp. 6877–6885.

Jo, M.R., Bae, S.H., Go, M.R., Kim, H.J., Hwang, Y.G. & Choi, S.J. (2015) Toxicity and biokinetics of colloidal gold nanoparticles. *Nanomaterials*, 5, pp. 835–850.

Jo, Y.K., Kim, B.H. & Jung, G. (2009) Antifungal activity of silver ions and nanoparticles on phytopathogenic fungi. *Plant Disease*, 93, pp. 1037–1043.

Jones, N., Ray, B., Ranjit, K.T. & Manna, A.C. (2008) Antibacterial activity of ZnO nanoparticle suspensions on a broad spectrum of microorganisms. *FEMS Microbiology Letters*, 279, pp. 71–76.

Junttila, S., Lim, K.J. & Rudd, S. (2009) Optimization and comparison of different methods for

RNA isolation for cDNA library construction from the reindeer lichen *Cladonia rangiferina*. *BMC Research Notes*, 2, pp. 204.

Jyoti, K., Baunthiyal, M. & Singh, A. (2015) Characterization of silver nanoparticles synthesized using *Urtica dioica* Linn. leaves and their synergistic effects with antibiotics. *Journal of Radiation Research and Applied Sciences*, pp. 1–11.

Kääriäinen, M.L., Weiss, C.K., Ritz, S., Pütz, S., Cameron, D.C., Mailänder, V. & Landfester, K. (2013) Zinc release from atomic layer deposited zinc oxide thin films and its antibacterial effect on *Escherichia coli*. *Applied Surface Science*, 287, pp. 375–380.

Kaito, C. & Sekimizu, K. (2007) Colony spreading in *Staphylococcus aureus*. *Journal of Bacteriology*, 189, pp. 2553–2557.

Kalishwaralal, K., BarathManiKanth, S., Pandian, S.R.K., Deepak, V. & Gurunathan, S. (2010) Silver nanoparticles impede the biofilm formation by *Pseudomonas aeruginosa* and *Staphylococcus epidermidis*. *Colloids and Surfaces. B: Biointerfaces*, 79, pp. 340–344.

Kaplan, J.B. (2010) Biofilm dispersal: Mechanisms, clinical implications, and potential therapeutic uses. *Journal of Dental Research*, 89, pp. 205–218.

Kaplan, J.B., Ragunath, C., Ramasubbu, N. & Fine, D.H. (2003) Detachment of *Actinobacillus actinomycetemcomitans* biofilm cells by an endogenous β-hexosaminidase activity. *Journal of Bacteriology*, 185, pp. 4693–4698.

Kaplan, J.B., Ragunath, C., Velliyagounder, K., Fine, D.H. & Ramasubbu, N. (2004) Enzymatic detachment of *Staphylococcus epidermidis* biofilms. *Antimicrobial Agents and Chemotherapy*, 48, pp. 2633–2636.

Karatan, E. & Watnick, P. (2009) Signals, regulatory networks, and materials that build and break bacterial biofilms. *Microbiology and Molecular Biology Reviews*, 73, pp. 310–347.

Karpanen, T.J., Worthington, T., Hendry, E.R., Conway, B.R. & Lambert, P.A. (2008) Antimicrobial efficacy of chlorhexidine digluconate alone and in combination with eucalyptus oil, tea tree oil and thymol against planktonic and biofilm cultures of *Staphylococcus epidermidis*. *Journal of Antimicrobial Chemotherapy*, 62, pp. 1031–1036.

Karunakaran, C., Rajeswari, V. & Gomathisankar, P. (2011a) Combustion synthesis of ZnO and Ag-doped ZnO and their bactericidal and photocatalytic activities. *Superlattices and Microstructures*, 50, pp. 234–241.

Karunakaran, C., Rajeswari, V. & Gomathisankar, P. (2011b) Optical, electrical, photocatalytic, and bactericidal properties of microwave synthesized nanocrystalline Ag–ZnO and ZnO. *Solid State Sciences*, 13, pp. 923–928.

Katsikogianni, M. & Missirlis, Y.F. (2004) Concise review of mechanisms of bacterial adhesion to biomaterials and of techniques used in estimating bacteria-material interactions. *European Cells & Materials*, 8, pp. 37–57.

Kawahara, K., Tsuruda, K., Morishita, M. & Uchida, M. (2000) Antibacterial effect of silver-zeolite on oral bacteria under anaerobic conditions. *Dental Materials*, 16, pp. 452–455.

Kerr, K.G. & Snelling, A.M. (2009) *Pseudomonas aeruginosa*: a formidable and ever-present adversary. *Journal of Hospital Infection*, 73, pp. 338–344.

De Kievit, T.R. (2009) Quorum sensing in *Pseudomonas aeruginosa* biofilms. *Environmental Microbiology*, 11, pp. 279–288.

Kim, H.K., Thammavongsa, V., Schneewind, O. & Missiakas, D. (2012) Recurrent infections and immune evasion strategies of *Staphylococcus aureus*. *Current Opinion in Microbiology*, 15, pp. 92–99.

Kim, J.H., Kim, C.H., Hacker, J., Ziebuhr, W., Lee, B.K. & Cho, S.H. (2008) Molecular characterization of regulatory genes associated with biofilm variation in a *Staphylococcus aureus* strain. *Journal of Microbiology and Biotechnology*, 18, pp. 28–34.

Kim, J.S., Kuk, E., Yu, K.N., Kim, J.H., Park, S.J., Lee, H.J., Kim, S.H., Park, Y.K., Park, Y.H., Hwang, C.Y., Kim, Y.K., Lee, Y.S., Jeong, D.H. & Cho, M.H. (2007) Antimicrobial effects of silver nanoparticles. *Nanomedicine : Nanotechnology, Biology and Medicine*, 3, pp. 95–101.

Kim, N.H. & Rhee, M.S. (2016) Synergistic bactericidal action of phytic acid and sodium chloride against *Escherichia coli* O157:H7 cells protected by a biofilm. *International Journal of Food Microbiology*, 227, pp. 17–21.

Knezevic, P. & Petrovic, O. (2008) A colorimetric microtiter plate method for assessment of phage effect on *Pseudomonas aeruginosa* biofilm. *Journal of Microbiological Methods*, 74, pp. 114–118.

Komlos, J., Cunningham, A.B., Camper, A.K. & Sharp, R.R. (2005) Interaction of *Klebsiella oxytoca* and *Burkholderia cepacia* in dual-species batch cultures and biofilms as a function of growth rate and substrate concentration. *Microbial Ecology*, 49, pp. 114–125.

Kora, A.J. & Sashidhar, R.B. (2014) Biogenic silver nanoparticles synthesized with rhamnogalacturonan gum: Antibacterial activity, cytotoxicity and its mode of action. *Arabian Journal of Chemistry*

Köser, C.U., Holden, M.T.G., Ellington, M.J., Cartwright, E.J.P., Brown, N.M., Ogilvy-Stuart, A.L., Hsu, L.Y., Chewapreecha, C., Croucher, N.J., Harris, S.R., Sanders, M., Enright, M.C., Dougan, G., Bentley, S.D., Parkhill, J., Fraser, L.J., Betley, J.R., Schulz-Trieglaff, O.B., Smith, G.P. & Peacock, S.J. (2012) Rapid whole-genome sequencing for investigation of a neonatal MRSA outbreak. *The New England Journal of Medicine*, 366, pp. 2267–2275.

Kostenko, V., Lyczak, J., Turner, K. & Martinuzzi, R.J. (2010) Impact of silver-containing wound dressings on bacterial biofilm viability and susceptibility to antibiotics during prolonged treatment. *Antimicrobial Agents and Chemotherapy*, 54, pp. 5120–5131.

Kotb, S. & Sayed, M. (2015) Sensitivity of methicillin-resistance and methicillin-susceptible *Staphylococcus aureus* strains to some different disinfectants. *International Journal of Livestock Research*, 5, pp. 45–58.

Kovaleva, J., Degener, J.E. & van der Mei, H.C. (2010) Mimicking disinfection and drying of biofilms in contaminated endoscopes. *The Journal of Hospital Infection*, 76, pp. 345–350.

de Kraker, M.E.A., Wolkewitz, M., Davey, P.G. & Grundmann, H. (2011) Clinical impact of antimicrobial resistance in European hospitals: excess mortality and length of hospital stay related to methicillin-resistant *Staphylococcus aureus* bloodstream infections. *Antimicrobial Agents and Chemotherapy*, 55, pp. 1598–1605.

Kramer, A., Schwebke, I. & Kampf, G. (2006) How long do nosocomial pathogens persist on inanimate surfaces? A systematic review. *BMC Infectious Diseases*, 6, pp. 130.

Krishnamoorthy, V., Hiller, D.B., Ripper, R., Lin, B., Vogel, S.M., Feinstein, D.L., Oswald, S., Rothschild, L., Hensel, P., Rubinstein, I., Minshall, R. & Weinberg, G.L. (2012) Epinephrine induces rapid deterioration in pulmonary oxygen exchange in intact,

anesthetized rats. *Anesthesiology*, 117, pp. 745–754.

Krom, B.P., Cohen, J.B., McElhaney Feser, G.E. & Cihlar, R.L. (2007) Optimized candidal biofilm microtiter assay. *Journal of Microbiological Methods*, 68, pp. 421–423.

Kruk, T., Szczepanowicz, K., Stefańska, J., Socha, R.P. & Warszyński, P. (2015) Synthesis and antimicrobial activity of monodisperse copper nanoparticles. *Colloids and Surfaces B: Biointerfaces*, 128, pp. 17–22.

Kumar, A., Biswal, M., Dhaliwal, N., Mahesh, R., Appannanavar, S.B., Gautam, V., Ray, P., Gupta, A.K. & Taneja, N. (2014) Point prevalence surveys of healthcare-associated infections and use of indwelling devices and antimicrobials over three years in a tertiary care hospital in India. *The Journal of Hospital Infection*, 86, pp. 272–274.

Kumar, P.T.S., Lakshmanan, V.K., Anilkumar, T.V, Ramya, C., Reshmi, P., Unnikrishnan, A.G., Nair, S. V & Jayakumar, R. (2012) Flexible and microporous chitosan hydrogel/nano ZnO composite bandages for wound dressing: *in vitro* and *in vivo* evaluation. *ACS Applied Materials & Interfaces*, 4, pp. 2618–2629.

Kumar, R., Howdle, S. & Münstedt, H. (2005) Polyamide/silver antimicrobials: effect of filler types on the silver ion release. *Journal of Biomedical Materials Research. Part B, Applied Biomaterials*, 75, pp. 311–319.

Kwakye-Awuah, B., Williams, C., Kenward, M.A. & Radecka, I. (2008) Antimicrobial action and efficiency of silver-loaded zeolite X. *Journal of Applied Microbiology*, 104, pp. 1516–1524.

Lambert, P.A. (2002) Cellular impermeability and uptake of biocides and antibiotics in Gram-positive bacteria and mycobacteria. *Journal of Applied Microbiology*, 92, pp. 46S – 54S.

Lamfon, H., Porter, S.R., McCullough, M. & Pratten, J. (2004) Susceptibility of *Candida albicans* biofilms grown in a constant depth film fermentor to chlorhexidine, fluconazole and miconazole: a longitudinal study. *The Journal of Antimicrobial Chemotherapy*, 53, pp. 383–385.

Lara, H.H., Ayala-Núñez, N. V., Ixtepan Turrent, L. del C. & Rodríguez Padilla, C. (2009) Bactericidal effect of silver nanoparticles against multidrug-resistant bacteria. *World Journal of Microbiology and Biotechnology*, 26, pp. 615–621.

Latasa, C., Solano, C., Penadés, J.R. & Lasaa, I. (2006) Biofilm-associated proteins. *Comptes Rendus Biologies*, 329, pp. 849–857.

Latimer, J., Forbes, S. & McBain, A.J. (2012) Attenuated virulence and biofilm formation in *Staphylococcus aureus* following sublethal exposure to triclosan. *Antimicrobial Agents and Chemotherapy*, 56, pp. 3092–3100.

Lazazzera, B.A. (2005) Lessons from DNA microarray analysis: The gene expression profile of biofilms. *Current Opinion in Microbiology*, 8, pp. 222–227.

Lee, J.H., Kim, Y.G., Cho, M.H. & Lee, J. (2014a) ZnO nanoparticles inhibit *Pseudomonas aeruginosa* biofilm formation and virulence factor production. *Microbiological Research*, 169, pp. 888–896.

Lee, K.W.K., Periasamy, S., Mukherjee, M., Xie, C., Kjelleberg, S. & Rice, S.A. (2014b) Biofilm development and enhanced stress resistance of a model, mixed-species community biofilm. *The ISME Journal*, 8, pp. 894–907.

Lei, M.G., Cue, D., Roux, C.M., Dunman, P.M. & Lee, C.Y. (2011) Rsp inhibits attachment and

biofilm formation by repressing *fnbA* in *Staphylococcus aureus* MW2. *Journal of Bacteriology*, 193, pp. 5231–5241.

Lejeune, P. (2003) Contamination of abiotic surfaces: What a colonizing bacterium sees and how to blur it. *Trends in Microbiology*, 11, pp. 179–184.

Leuck, A.M., Johnson, J.R. & Dunny, G.M. (2014) A widely used *in vitro* biofilm assay has questionable clinical significance for enterococcal endocarditis. *PLoS one*, 9, pp. e107282.

Leung, C.Y., Chan, Y.C., Samaranayake, L.P. & Seneviratne, C.J. (2012) Biocide resistance of *Candida* and *Escherichia coli* biofilms is associated with higher antioxidative capacities. *Journal of Hospital Infection*, 81, pp. 79–86.

Lewis, K. (2001) Riddle of biofilm resistance. *Antimicrobial Agents and Chemotherapy*, 45, pp. 999–1007.

Li, B. & Logan, B.E. (2004) Bacterial adhesion to glass and metal-oxide surfaces. *Colloids and Surfaces B: Biointerfaces*, 36, pp. 81–90.

Li, L.H., Yen, M.Y., Ho, C.C., Wu, P., Wang, C.C., Maurya, P.K., Chen, P.S., Chen, W., Hsieh, W.Y. & Chen, H.W. (2013) Non-cytotoxic nanomaterials enhance antimicrobial activities of cefmetazole against multidrug-resistant *Neisseria gonorrhoeae*. *PLoS one*, 8, pp. e64794.

Li, M., Zhu, L. & Lin, D. (2011) Toxicity of ZnO Nanoparticles to *Escherichia coli*: Mechanism and the Influence of Medium Components. *Environmental Science & Technology*, 45, pp. 1977–1983.

Li, W.R., Xie, X.B., Shi, Q.S., Zeng, H.Y., Ou-Yang, Y.S. & Chen, Y. Ben (2010) Antibacterial activity and mechanism of silver nanoparticles on *Escherichia coli*. *Applied Microbiology and Biotechnology*, 85, pp. 1115–1122.

Li, Y., Leung, P., Yao, L., Song, Q.W. & Newton, E. (2006) Antimicrobial effect of surgical masks coated with nanoparticles. *Journal of Hospital Infection*, 62, pp. 58–63.

Liao, J. & Sauer, K. (2012) The merR-like transcriptional regulator brlR contributes to *Pseudomonas aeruginosa* biofilm tolerance. *Journal of Bacteriology*, 194, pp. 4823–4836.

Lindsay, D. & von Holy, A. (2006) Bacterial biofilms within the clinical setting: what healthcare professionals should know. *The Journal of Hospital Infection*, 64, pp. 313–325.

Lindsay, J.A. (2014) Evolution of *Staphylococcus aureus* and MRSA during outbreaks. *Infection, Genetics and Evolution*, 21, pp. 548–553.

Lindsay, J.A. (2013) Hospital-associated MRSA and antibiotic resistance-what have we learned from genomics? *International Journal of Medical Microbiology*, 303, pp. 318–323.

Lipovsky, A., Tzitrinovich, Z., Friedmann, H., Applerot, G., Gedanken, A. & Lubart, R. (2009) EPR study of visible light-induced ros generation by nanoparticles of ZnO. *Journal of Physical Chemistry C*, 113, pp. 15997–16001.

Liu, Q., Zhang, M., Fang, Z. & Rong, X. (2014) Effects of ZnO nanoparticles and microwave heating on the sterilization and product quality of vacuum-packaged Caixin. *Journal of the Science of Food and Agriculture*, 94, pp. 2547–2554.

Liu, W., Wu, Y., Wang, C., Li, H.C., Wang, T., Liao, C.Y., Cui, L., Zhou, Q.F., Yan, B. & Jiang, G.B. (2010) Impact of silver nanoparticles on human cells: effect of particle size. *Nanotoxicology*, 4, pp. 319–330.

Liu, Y., Baas, J., Peijnenburg, W.J. & Vijver, M.G. (2016) Evaluating the combined toxicity of

Cu and ZnO nanoparticles: utility of the concept of additivity and a nested experimental design. *Environmental Science & Technology*, 50, pp. 5328–5337.

Liu, Y., He, L., Mustapha, A., Li, H., Hu, Z.Q. & Lin, M. (2009) Antibacterial activities of zinc oxide nanoparticles against *Escherichia coli* O157:H7. *Journal of Applied Microbiology*, 107, pp. 1193–1201.

Liu, Y., Liang, P., Guo, L. & Lu, H. Bin (2005) Study on the adsorption behavior of heavy metal ions on nanometer TiO_2 supported on silica gel. *Acta Chimica Sinica*, 63, pp. 312–316.

Liu, Y. & Zhao, Q. (2005) Influence of surface energy of modified surfaces on bacterial adhesion. *Biophysical Chemistry*, 117, pp. 39–45.

Logeswari, P., Silambarasan, S. & Abraham, J. (2015) Synthesis of silver nanoparticles using plants extract and analysis of their antimicrobial property. *Journal of Saudi Chemical Society*, 19, pp. 311–317.

Lok, C.N., Ho, C.M., Chen, R., He, Q.Y., Yu, W.Y., Sun, H., Tam, P.K.H., Chiu, J.F. & Che, C.M. (2006) Proteomic analysis of the mode of antibacterial action of silver nanoparticles. *Journal of Proteome Research*, 5, pp. 916–924.

Lok, C.N., Ho, C.M., Chen, R., He, Q.Y., Yu, W.Y., Sun, H., Tam, P.K.H., Chiu, J.F. & Che, C.M. (2007) Silver nanoparticles: partial oxidation and antibacterial activities. *Journal of Biological Inorganic Chemistry*, 12, pp. 527–534.

Lorite, G.S., Rodrigues, C.M., de Souza, A.A., Kranz, C., Mizaikoff, B. & Cotta, M.A. (2011) The role of conditioning film formation and surface chemical changes on *Xylella fastidiosa* adhesion and biofilm evolution. *Journal of Colloid and Interface Science*, 359, pp. 289–295.

Loveday, H.P., Wilson, J.A., Kerr, K., Pitchers, R., Walker, J.T. & Browne, J. (2014) Association between healthcare water systems and *Pseudomonas aeruginosa* infections: a rapid systematic review. *The Journal of Hospital Infection*, 86, pp. 7–15.

Ludwig, W. & Schleifer, K.H. (2000) How quantitative is quantitative PCR with respect to cell counts? *Systematic and Applied Microbiology*, 23, pp. 556–562.

Lutskiy, M.-Y., Avneri-Katz, S., Zhu, N., Itsko, M., Ronen, Z., Arnusch, C.J. & Kasher, R. (2015) A microbiology-based assay for quantification of bacterial early stage biofilm formation on reverse-osmosis and nanofiltration membranes. *Separation and Purification Technology*, 141, pp. 214–220.

Ma, H., Williams, P.L. & Diamond, S.A. (2013) Ecotoxicity of manufactured ZnO nanoparticles-a review. *Environmental Pollution*, 172, pp. 76–85.

Macià, M.D., Rojo-Molinero, E. & Oliver, A. (2014) Antimicrobial susceptibility testing in biofilm growing bacteria. *Clinical Microbiology and Infection*, 20, pp. 981–990.

Mack, D., Rohde, H., Harris, L.G., Davies, A.P., Horstkotte, M.A. & Knobloch, J.K.M. (2006) Biofilm formation in medical device-related infection. *International Journal of Artificial Organs*, 29, pp. 343–359.

Mah, T.F.C. & O'Toole, G.A. (2001) Mechanisms of biofilm resistance to antimicrobial agents. *Trends in microbiology*, 9, pp. 34–39.

Majik, M.S. & Parvatkar, P.T. (2014) Next Generation Biofilm Inhibitors for Pseudomonas aeruginosa: Synthesis and Rational Design Approaches. *Current Topics in Medicinal Chemistry*, 14, pp. 81–109.

Makhluf, S., Dror, R., Nitzan, Y., Abramovich, Y., Jelinek, R. & Gedanken, A. (2005) Microwave-assisted synthesis of nanocrystalline MgO and its use as a bacteriocide. *Advanced Functional Materials*, 15, pp. 1708–1715.

Malani, P.N., Rana, M.M., Banerjee, M. & Bradley, S.F. (2008) *Staphylococcus aureus* bloodstream infections: The association between age and mortality and functional status. *Journal of the American Geriatrics Society*, 56, pp. 1485–1489.

Mallevre, F., Fernandes, T.F. & Aspray, T.J. (2016) *Pseudomonas putida* biofilm dynamics following a single pulse of silver nanoparticles. *Chemosphere*, 153, pp. 356–364.

Manian, F.A., Griesenauer, S., Senkel, D., Setzer, J.M., Doll, S.A., Perry, A.M. & Wiechens, M. (2011) Isolation of *Acinetobacter baumannii* complex and methicillin-resistant *Staphylococcus aureus* from hospital rooms following terminal cleaning and disinfection: can we do better? *Infection Control and Hospital Epidemiology*, 32, pp. 667–672.

Manke, A., Wang, L. & Rojanasakul, Y. (2013) Mechanisms of nanoparticle-induced oxidative stress and toxicity. *BioMed Research International*.2013.

Marais, F., Mehtar, S. & Chalkley, L. (2010) Antimicrobial efficacy of copper touch surfaces in reducing environmental bioburden in a South African community healthcare facility. *The Journal of Hospital Infection*, 74, pp. 80–82.

Marambio-Jones, C. & Hoek, E.M. V. (2010) A review of the antibacterial effects of silver nanomaterials and potential implications for human health and the environment. *Journal of Nanoparticle Research*, 12, pp. 1531–1551.

Matai, I., Sachdev, A., Dubey, P., Kumar, S.U., Bhushan, B. & Gopinath, P. (2014) Antibacterial activity and mechanism of Ag-ZnO nanocomposite on *S. aureus* and GFP-expressing antibiotic resistant *E. coli*. *Colloids and surfaces. B, Biointerfaces*, 115, pp. 359–367.

Matsukawa, M. & Greenberg, E.P. (2004) Putative exopolysaccharide synthesis genes influence *Pseudomonas aeruginosa* biofilm development. *Journal of Bacteriology*, 186, pp. 4449–4456.

Matsumura, Y., Yoshikata, K., Kunisaki, S. & Tsuchido, T. (2003) Mode of bactericidal action of silver zeolite and its comparison with that of silver nitrate. *Applied and Environmental Microbiology*, 69, pp. 4278–4281.

Maukonen, J., Mättö, J., Wirtanen, G., Raaska, L., Mattila-Sandholm, T. & Saarela, M. (2003) Methodologies for the characterization of microbes in industrial environments: A review. *Journal of Industrial Microbiology and Biotechnology*, 30, pp. 327–356.

McCourt, J., O'Halloran, D.P., McCarthy, H., O'Gara, J.P. & Geoghegan, J.A. (2014) Fibronectin-binding proteins are required for biofilm formation by community-associated methicillin-resistant *Staphylococcus aureus* strain LAC. *FEMS Microbiology Letters*, 353, pp. 157–164.

McDougald, D., Rice, S.A., Barraud, N., Steinberg, P.D. & Kjelleberg, S. (2011) Should we stay or should we go: mechanisms and ecological consequences for biofilm dispersal. *Nature Reviews Microbiology*, 10, pp. 39–50.

Meireles, A., L Goncalves, A., B Gomes, I., Chaves Simoes, L. & Simoes, M. (2015) Methods to study microbial adhesion on abiotic surfaces. *AIMS Bioengineering*, 2, pp. 297–309.

Melo, L.D., Palombo, R.R., Petri, D.F.S., Bruns, M., Pereira, E.M. a & Carmona-Ribeiro, A.M. (2011) Structure-activity relationship for quaternary ammonium compounds hybridized with poly(methyl methacrylate). *ACS Applied Materials & Interfaces*, 3, pp. 1933–1939.

Merghni, A., Ben Nejma, M., Dallel, I., Tobji, S., Ben Amor, A., Janel, S., Lafont, F., Aouni, M. & Mastouri, M. (2016) High potential of adhesion to biotic and abiotic surfaces by opportunistic *Staphylococcus aureus* strains isolated from orthodontic appliances. *Microbial Pathogenesis*, 91, pp. 61–67.

Mikolay, A., Huggett, S., Tikana, L., Grass, G., Braun, J. & Nies, D.H. (2010) Survival of bacteria on metallic copper surfaces in a hospital trial. *Applied Microbiology and Biotechnology*, 87, pp. 1875–1879.

Mirzaee, M., Peerayeh, S.N. & Ghasemian, A.M. (2014) Detection of *icaABCD* genes and biofilm formation in clinical isolates of methicillin resistant *Staphylococcus aureus*. *Iranian Journal of Pathology*, 9, pp. 257–262.

Mirzajani, F., Ghassempour, A., Aliahmadi, A. & Esmaeili, M.A. (2011) Antibacterial effect of silver nanoparticles on *Staphylococcus aureus*. *Research in Microbiology*, 162, pp. 542–549.

Mitik-Dineva, N., Wang, J., Mocanasu, R.C., Stoddart, P.R., Crawford, R.J. & Ivanova, E.P. (2008) Impact of nano-topography on bacterial attachment. *Biotechnology Journal*, 3, pp. 536–544.

Mitik-Dineva, N., Wang, J., Truong, V.K., Stoddart, P., Malherbe, F., Crawford, R.J. & Ivanova, E.P. (2009) *Escherichia coli*, *Pseudomonas aeruginosa*, and *Staphylococcus aureus* attachment patterns on glass surfaces with nanoscale roughness. *Current Microbiology*, 58, pp. 268–273.

Mohan Kumar, K., Mandal, B.K., Appala Naidu, E., Sinha, M., Siva Kumar, K. & Sreedhara Reddy, P. (2013) Synthesis and characterisation of flower shaped zinc oxide nanostructures and its antimicrobial activity. *Spectrochimica Acta. Part A, Molecular and Biomolecular spectroscopy*, 104, pp. 171–174.

Mohan, S., Oluwafemi, O.S., George, S.C., Jayachandran, V.P., Lewu, F.B., Songca, S.P., Kalarikkal, N. & Thomas, S. (2014) Completely green synthesis of dextrose reduced silver nanoparticles, its antimicrobial and sensing properties. *Carbohydrate Polymers*, 106, pp. 469–474.

Monds, R.D. & O'Toole, G.A. (2009) The developmental model of microbial biofilms: ten years of a paradigm up for review. *Trends in Microbiology*, 17, pp. 73–87.

Monteiro, D.R., Gorup, L.F., Takamiya, A.S., Ruvollo-Filho, A.C., de Camargo, E.R. & Barbosa, D.B. (2009) The growing importance of materials that prevent microbial adhesion: antimicrobial effect of medical devices containing silver. *International Journal of Antimicrobial Agents*, 34, pp. 103–110.

Moreira, J.M.R., Gomes, L.C., Araújo, J.D.P., Miranda, J.M., Simões, M., Melo, L.F. & Mergulhão, F.J. (2013) The effect of glucose concentration and shaking conditions on *Escherichia coli* biofilm formation in microtiter plates. *Chemical Engineering Science*, 94, pp. 192–199.

Moreno, S., Galván, E.M., Vázquez, N., Fiorilli, G. & Guido, P.A.C. (2015) Antibacterial efficacy of *Rosmarinus officinalis* phytochemicals against nosocomial multidrug-resistant bacteria grown in planktonic culture and biofilm. In: A. Méndez-Vilas (ed.). *The Battle Against Microbial Pathogens: Basic Science, Technological Advances and Educational Programs*. 1st edition. Badajoz: Formatex, pp. 3–8.

Morones, J.R., Elechiguerra, J.L., Camacho, A., Holt, K., Kouri, J.B., Ram, J.T., Yacaman, M.J., Ramírez, J.T. & Yacaman, M.J. (2005) The bactericidal effect of silver nanoparticles.

Nanotechnology, 16, pp. 2346–2353.

Morter, S., Bennet, G., Fish, J., Richards, J., Allen, D.J., Nawaz, S., Iturriza-Gómara, M., Brolly, S. & Gray, J. (2011) Norovirus in the hospital setting: Virus introduction and spread within the hospital environment. *Journal of Hospital Infection*, 77, pp. 106–112.

Mortimer, M., Kasemets, K. & Kahru, A. (2010) Toxicity of ZnO and CuO nanoparticles to ciliated protozoa *Tetrahymena thermophila*. *Toxicology*, 269, pp. 182–189.

Mowat, E., Butcher, J., Lang, S., Williams, C. & Ramage, G. (2007) Development of a simple model for studying the effects of antifungal agents on multicellular communities of *Aspergillus fumigatus*. *Journal of Medical Microbiology*, 56, pp. 1205–1212.

Mukha, I., Eremenko, G., Korchak, G. & Michienkova, A. (2010) Antibacterial action and physicochemical properties of stabilized silver and gold nanostructures on the surface of disperse silica. *Journal of Water Resource and Protection*, 02, pp. 131–136.

Mund, A., Kuttler, C., Pérez-Velázquez, J. & Hense, B.A. (2016) An age-dependent model to analyse the evolutionary stability of bacterial quorum sensing. *Journal of Theoretical Biology*, S0022-5193, pp. 00026–6.

Murugan, K., Selvanayaki, K. & Al-Sohaibani, S. (2016) Urinary catheter indwelling clinical pathogen biofilm formation, exopolysaccharide characterization and their growth influencing parameters. *Saudi Journal of Biological Sciences*, 23, pp. 150–159.

Nadworny, P.L., Wang, J., Tredget, E.E. & Burrell, R.E. (2008) Anti-inflammatory activity of nanocrystalline silver in a porcine contact dermatitis model. *Nanomedicine: Nanotechnology, Biology, and Medicine*, 4, pp. 241–251.

Nagant, C., Pitts, B., Stewart, P.S., Feng, Y., Savage, P.B. & Dehaye, J.-P. (2013) Study of the effect of antimicrobial peptide mimic, CSA-13, on an established biofilm formed by *Pseudomonas aeruginosa*. *Microbiology Open*, 2, pp. 318–325.

Nailis, H., Vandenbroucke, R., Tilleman, K., Deforce, D., Nelis, H. & Coenye, T. (2009) Monitoring *ALS1* and *ALS3* gene expression during *in vitro Candida albicans* biofilm formation under continuous flow conditions. *Mycopathologia*, 167, pp. 9–17.

Nakakido, M., Aikawa, C., Nakagawa, I. & Tsumoto, K. (2014) The staphylococcal elastin-binding protein regulates zinc-dependent growth/biofilm formation. *Journal of Biochemistry*, 156, pp. 155–162.

National Audit Office (2009) *Reducing Healthcare Associated Infections in Hospitals in England*. London: The Stationary Office

National Patient Safety Agency (2004) *Ready, steady, go! The full guide to implementing the cleanyourhands campaign in your trust*. London: National Patient Safety Agency

Naves, P., del Prado, G., Huelves, L., Gracia, M., Ruiz, V., Blanco, J., Dahbi, G., Blanco, M., del Carmen Ponte, M. & Soriano, F. (2008) Correlation between virulence factors and *in vitro* biofilm formation by *Escherichia coli* strains. *Microbial Pathogenesis*, 45, pp. 86–91.

Newitt, S., Myles, P.R., Birkin, J.A., Maskell, V., Slack, R.C.B., Nguyen-Van-Tam, J.S. & Szatkowski, L. (2015) Impact of infection control interventions on rates of *Staphylococcus aureus* bacteraemia in National Health Service acute hospitals, East Midlands, UK, using interrupted time-series analysis. *The Journal of Hospital Infection*, 90, pp. 28–37.

Nilsson, R.E., Ross, T. & Bowman, J.P. (2011) Variability in biofilm production by *Listeria monocytogenes* correlated to strain origin and growth conditions. *International Journal of*

Food Microbiology, 150, pp. 14–24.

Niu, C. & Gilbert, E.S. (2004) Colorimetric method for identifying plant essential oil components that affect biofilm formation and structure. *Applied and Environmental Microbiology*, 70, pp. 6951–6956.

Nolan, T., Hands, R.E. & Bustin, S.A. (2006) Quantification of mRNA using real-time RT-PCR. *Nature Protocols*, 1, pp. 1559–1582.

Nour, A.M., Barbour, E.K., Depint, F., Dooms, M., Niang, K., Dulac, A., Niamba, C.N., Chaaya, G. & Pouillart, P.R. (2010) Comparison of five RNA extraction methods from rabbit's blood. *Agriculture and Biology Journal of North America*, 1, pp. 448–450.

O'Flaherty, N. & Fenelon, L. (2015) The stethoscope and healthcare-associated infection: a snake in the grass or innocent bystander? *The Journal of Hospital Infection*, 91, pp. 1–7.

O'Neill, E., Pozzi, C., Houston, P., Humphreys, H., Robinson, D.A., Loughman, A., Foster, T.J. & O'Gara, J.P. (2008) A novel *Staphylococcus aureus* biofilm phenotype mediated by the fibronectin-binding proteins, FnBPA and FnBPB. *Journal of Bacteriology*, 190, pp. 3835–3850.

O'Neill, E., Pozzi, C., Houston, P., Smyth, D., Humphreys, H., Robinson, D.A. & O'Gara, J.P. (2007) Association between methicillin susceptibility and biofilm regulation in *Staphylococcus aureus* isolates from device-related infections. *Journal of Clinical Microbiology*, 45, pp. 1379–1388.

O'Toole, G.A. (2011) Microtiter dish biofilm formation assay. *Journal of Visualized Experiments*, 30, pp. 3–5.

O'Toole, G.A. & Kolter, R. (1998) Flagellar and twitching motility are necessary for *Pseudomonas aeruginosa* biofilm development. *Molecular Microbiology*, 30, pp. 295–304.

Office for National Statistics (2013) *Deaths involving MRSA - Office for National Statistics*. 2013 [Online]. Available from: http://www.ons.gov.uk/peoplepopulationandcommunity/birthsdeathsandmarriages/deaths/bulletins/deathsinvolvingmrsa/2013-08-22 [Accessed: 30 March 2016].

Oh, Y.J., Lee, N.R., Jo, W., Jung, W.K. & Lim, J.S. (2009) Effects of substrates on biofilm formation observed by atomic force microscopy. *Ultramicroscopy*, 109, pp. 874–880.

Ohira, T., Yamamoto, O., Iida, Y. & Nakagawa, Z.E. (2008) Antibacterial activity of ZnO powder with crystallographic orientation. *Journal of Materials Science: Materials in Medicine*, 19, pp. 1407–1412.

Oja, T., Blomqvist, B., Buckingham-Meyer, K., Goeres, D., Vuorela, P. & Fallarero, A. (2014) Revisiting an agar-based plate method: what the static biofilm method can offer for biofilm research. *Journal of Microbiological Methods*, 107, pp. 157–160.

Oliveira, A. & Cunha, M. (2008) Bacterial biofilms with emphasis on coagulase-negative staphylococci. *Journal of Venomous Animals and Toxins Including Tropical Diseases*, 14, pp. 572–596.

de Oliveira, M.M.M., Brugnera, D.F., do Nascimento, J.A. & Piccoli, R.H. (2012) Control of planktonic and sessile bacterial cells by essential oils. *Food and Bioproducts Processing*, 90, pp. 809–818.

Otter, J.A., Cummins, M., Ahmad, F., van Tonder, C. & Drabu, Y.J. (2007) Assessing the biological efficacy and rate of recontamination following hydrogen peroxide vapour

decontamination. *The Journal of Hospital Infection*, 67, pp. 182–188.

Otter, J.A., Yezli, S. & French, G.L. (2011) The role played by contaminated surfaces in the transmission of nosocomial pathogens. *Infection control and hospital epidemiology*, 32, pp. 687–699.

Otter, J.A., Yezli, S., Salkeld, J.A.G. & French, G.L. (2013) Evidence that contaminated surfaces contribute to the transmission of hospital pathogens and an overview of strategies to address contaminated surfaces in hospital settings. *American Journal of Infection Control*, 41, pp. S6–S11.

Otto, M. (2008) Staphylococcal biofilms. *Current Topics in Microbiology and Immunology*, 322, pp. 207–228.

Otto, M. (2010) Staphylococcus colonization of the skin and antimicrobial peptides. *Expert Review of Dermatology*, 5, pp. 183–195.

Outten, C.E. & O'Halloran, T. V (2001) Femtomolar sensitivity of metalloregulatory proteins controlling zinc homeostasis. *Science (New York)*, 292, pp. 2488–2492.

Padil, V.V.T. & Černík, M. (2013) Green synthesis of copper oxide nanoparticles using gum karaya as a biotemplate and their antibacterial application. *International Journal of Nanomedicine*, 8, pp. 889–898.

Page, K., Wilson, M. & Parkin, I.P. (2009) Antimicrobial surfaces and their potential in reducing the role of the inanimate environment in the incidence of hospital-acquired infections. *Journal of Materials Chemistry*, 19, pp. 3819.

Pal, S., Tak, Y.K. & Song, J.M. (2007) Does the antibacterial activity of silver nanoparticles depend on the shape of the nanoparticle? A study of the Gram-negative bacterium *Escherichia coli*. *Applied and Environmental Microbiology*, 73, pp. 1712–1720.

Pandiyarajan, T., Udayabhaskar, R., Vignesh, S., James, R.A. & Karthikeyan, B. (2013) Synthesis and concentration dependent antibacterial activities of CuO nanoflakes. *Materials Science & Engineering: C*, 33, pp. 2020–2024.

Paredes, J., Becerro, S., Arizti, F., Aguinaga, A., Del Pozo, J.L. & Arana, S. (2012) Real time monitoring of the impedance characteristics of Staphylococcal bacterial biofilm cultures with a modified CDC reactor system. *Biosensors & Bioelectronics*, 38, pp. 226–232.

Parikh, D. V. (2005) Antimicrobial Silver/Sodium Carboxymethyl Cotton Dressings for Burn Wounds. *Textile Research Journal*, 75, pp. 134–138.

Park, H.J., Kim, J.Y., Kim, J., Lee, J.H., Hahn, J.S., Gu, M.B. & Yoon, J. (2009) Silver-ion-mediated reactive oxygen species generation affecting bactericidal activity. *Water Research*, 43, pp. 1027–1032.

Park, H.J., Park, S., Roh, J., Kim, S., Choi, K., Yi, J., Kim, Y. & Yoon, J. (2013) Biofilm-inactivating activity of silver nanoparticles: A comparison with silver ions. *Journal of Industrial and Engineering Chemistry*, 19, pp. 614–619.

Park, J.H., Lee, J.H., Cho, M.H., Herzberg, M. & Lee, J. (2012) Acceleration of protease effect on *Staphylococcus aureus* biofilm dispersal. *FEMS Microbiology Letters*, 335, pp. 31–38.

Park, S.J., Kim, S.K., So, Y.I., Park, H.Y., Li, X.H., Yeom, D.H., Lee, M.N., Lee, B.L. & Lee, J.H. (2014) Protease IV, a quorum sensing-dependent protease of *Pseudomonas aeruginosa* modulates insect innate immunity. *Molecular Microbiology*, 94, pp. 1298–1314.

Pasquet, J., Chevalier, Y., Pelletier, J., Couval, E., Bouvier, D. & Bolzinger, M.A. (2014) The contribution of zinc ions to the antimicrobial activity of zinc oxide. *Colloids and Surfaces A: Physicochemical and Engineering Aspects*, 457, pp. 263–274.

Peacock, S.J., Moore, C.E., Justice, A., Kantzanou, M., Story, L., Mackie, K., O'Neill, G. & Day, N.P.J. (2002) Virulent combinations of adhesin and toxin genes in natural populations of *Staphylococcus aureus*. *Infection and Immunity*, 70, pp. 4987–4996.

Peeters, E., Nelis, H.J. & Coenye, T. (2008) Comparison of multiple methods for quantification of microbial biofilms grown in microtiter plates. *Journal of Microbiological Methods*, 72, pp. 157–165.

Penesyan, A., Gillings, M. & Paulsen, I.T. (2015) Antibiotic discovery: Combatting bacterial resistance in cells and in biofilm communities. *Molecules*, 20, pp. 5286–5298.

Pereira, C.A., Costa, A.C.B.P., Liporoni, P.C.S., Rego, M.A. & Jorge, A.O.C. (2016) Antibacterial activity of Baccharis dracunculifolia in planktonic cultures and biofilms of *Streptococcus mutans*. *Journal of Infection and Public Health*, 9, pp. 324–330.

Perelshtein, I., Applerot, G., Perkas, N., Wehrschuetz-Sigl, E., Hasmann, A., Guebitz, G. & Gedanken, A. (2009) CuO–cotton nanocomposite: Formation, morphology, and antibacterial activity. *Surface and Coatings Technology*, 204, pp. 54–57.

Pérez-Zárate, P., Aragón-Piña, A., Soria-Guerra, R.E., González-Amaro, A.M., Pérez-Urizar, J., Pérez-González, L.F. & Martinez-Gutierrez, F. (2015) Risk factors and biofilm detection on central venous catheters of patients attended at tertiary hospital. *Micron*, 78, pp. 33–39.

Periasamy, S., Joo, H.S., Duong, A.C., Bach, T.H.L., Tan, V.Y., Chatterjee, S.S., Cheung, G.Y.C. & Otto, M. (2012) How *Staphylococcus aureus* biofilms develop their characteristic structure. *Proceedings of the National Academy of Sciences of the United States of America*, 109, pp. 1281–1286.

Perrin, C., Briandet, R., Jubelin, G., Lejeune, P., Mandrand-Berthelot, M.A., Rodrigue, A. & Dorel, C. (2009) Nickel promotes biofilm formation by *Escherichia coli* K-12 strains that produce curli. *Applied and Environmental Microbiology*, 75, pp. 1723–1733.

Perumal, P.K., Wand, M.E., Sutton, J.M. & Bock, L.J. (2014) Evaluation of the effectiveness of hydrogen-peroxide-based disinfectants on biofilms formed by Gram-negative pathogens. *The Journal of Hospital Infection*, 87, pp. 227–233.

Petrochenko, P.E., Zhang, Q., Bayati, R., Skoog, S.A., Phillips, K.S., Kumar, G., Narayan, R.J. & Goering, P.L. (2014) Cytotoxic evaluation of nanostructured zinc oxide (ZnO) thin films and leachates. *Toxicology in vitro*, 28, pp. 1144–1152.

Pitten, F.-A., Werner, H.-P. & Kramer, A. (2003) A standardized test to assess the impact of different organic challenges on the antimicrobial activity of antiseptics. *Journal of Hospital Infection*, 55, pp. 108–115.

Pittet, D., Allegranzi, B., Sax, H., Dharan, S., Pessoa-Silva, C.L., Donaldson, L. & Boyce, J.M. (2006) Evidence-based model for hand transmission during patient care and the role of improved practices. *The Lancet. Infectious diseases*, 6, pp. 641–652.

Pitts, B., Hamilton, M.A., Zelver, N. & Stewart, P.S. (2003) A microtiter-plate screening method for biofilm disinfection and removal. *Journal of Microbiological Methods*, 54, pp. 269–276.

Pourmand, M.R., Shahidi, K., Nazari, P., Moosavian, S.M., Samadi, N., Pourmand, G. & Shahverdi, A.R. (2013) The different antibacterial impact of silver nanoparticles against *Legionella pneumophila* compared to other microorganisms. *Journal of Sciences, Islamic*

Republic of Iran, 24, pp. 313–319.

Prabhu, S. & Poulose, E.K. (2012) Silver nanoparticles: Mechanism of antimicrobial action, synthesis, medical applications, and toxicity effects. *International Nano Letters*, 2, pp. 32.

Prakash, P., Gnanaprakasam, P., Emmanuel, R., Arokiyaraj, S. & Saravanan, M. (2013) Green synthesis of silver nanoparticles from leaf extract of *Mimusops elengi*, Linn. for enhanced antibacterial activity against multi drug resistant clinical isolates. *Colloids and Surfaces B: Biointerfaces*, 108, pp. 255–259.

Premanathan, M., Karthikeyan, K., Jeyasubramanian, K. & Manivannan, G. (2011) Selective toxicity of ZnO nanoparticles toward Gram-positive bacteria and cancer cells by apoptosis through lipid peroxidation. *Nanomedicine: Nanotechnology, Biology and Medicine*, 7, pp. 184–192.

De Prijck, K., Nelis, H. & Coenye, T. (2007) Efficacy of silver-releasing rubber for the prevention of *Pseudomonas aeruginosa* biofilm formation in water. *Biofouling*, 23, pp. 405–411.

De Prijck, K., De Smet, N., Rymarczyk-Machal, M., Van Driessche, G., Devreese, B., Coenye, T., Schacht, E. & Nelis, H.J. (2010) *Candida albicans* biofilm formation on peptide functionalized polydimethylsiloxane. *Biofouling*, 26, pp. 269–275.

Prüß, B.M., Besemann, C., Denton, A. & Wolfe, A.J. (2006) A complex transcription network controls the early stages of biofilm development by *Escherichia coli*. *Journal of Bacteriology*, 188, pp. 3731–3739.

Public Health England (2015a) *Annual Epidemiological Commentary: Mandatory MRSA, MSSA and E. coli bacteraemia and C. difficile infection data, 2014/15*. London: Public Health England

Public Health England (2015b) *Surveillance of Pseudomonas and Stenotrophomonas species causing bacteraemia in England, Wales and Northern Ireland: 2014*. London: Public Health England

Radzig, M.A., Nadtochenko, V.A., Koksharova, O.A., Kiwi, J., Lipasova, V.A. & Khmel, I.A. (2013) Antibacterial effects of silver nanoparticles on Gram-negative bacteria: influence on the growth and biofilms formation, mechanisms of action. *Colloids and surfaces B: Biointerfaces*, 102, pp. 300–306.

Raghupathi, K.R., Koodali, R.T. & Manna, A.C. (2011) Size-dependent bacterial growth inhibition and mechanism of antibacterial activity of zinc oxide nanoparticles. *Langmuir*, 27, pp. 4020–4028.

Rai, M., Yadav, A. & Gade, A. (2009) Silver nanoparticles as a new generation of antimicrobials. *Biotechnology Advances*, 27, pp. 76–83.

Rai, R. & Bai, J. (2011) Nanoparticles and their potential application as antimicrobials. In: A. Mendez-Vilas (ed.). *Science Against Microbial Pathogens: Communicating Current Research and Technologies Advances*. Badajoz: Formatex, pp. 197–209.

Rajdev, S., Mulla, S. & Kumar, A. (2015) Evaluation of efficacy of commonly used disinfectants in bacterial biofilms of clinical bacterial isolates from medical devices from NICU & MICU of tertiary care hospital. *Journal of Patient Safety & Infection Control*, 3, pp. 50–51.

Rajesh, S., Dharanishanthi, V. & Kanna, A.V. (2014) Antibacterial mechanism of biogenic silver nanoparticles of *Lactobacillus acidophilus*. *Journal of Experimental Nanoscience*, 10, pp. 1143–1152.

Rajeshkumar, S. & Malarkodi, C. (2014) *In vitro* antibacterial activity and mechanism of silver nanoparticles against foodborne pathogens. *Bioinorganic Chemistry and Applications*, 2014, pp. 1–10.

Randle, J., Arthur, A. & Vaughan, N. (2010) Twenty-four-hour observational study of hospital hand hygiene compliance. *The Journal of Hospital Infection*, 76, pp. 252–255.

Ray, P.C., Yu, H. & Fu, P.P. (2009) Toxicity and environmental risks of nanomaterials: challenges and future needs. *Journal of Environmental Science and Health. Part C.*, 27, pp. 1–35.

Reidy, B., Haase, A., Luch, A., Dawson, K.A. & Lynch, I. (2013) Mechanisms of silver nanoparticle release, transformation and toxicity: A critical review of current knowledge and recommendations for future studies and applications. *Materials*, 6, pp. 2295–2350.

Reisner, A., Krogfelt, K.A., Klein, B.M., Zechner, E.L. & Molin, S. (2006) *In vitro* biofilm formation of commensal and pathogenic *Escherichia coli* strains: impact of environmental and genetic factors. *Journal of Bacteriology*, 188, pp. 3572–3581.

Ren, G., Hu, D., Cheng, E.W.C., Vargas-Reus, M.A., Reip, P. & Allaker, R.P. (2009) Characterisation of copper oxide nanoparticles for antimicrobial applications. *International Journal of Antimicrobial Agents*, 33, pp. 587–590.

Rendueles, O., Kaplan, J.B. & Ghigo, J.M. (2013) Antibiofilm polysaccharides. *Environmental Microbiology*, 15, pp. 334–346.

Renner, L.D. & Weibel, D.B. (2011) Physicochemical regulation of biofilm formation. *MRS Bulletin*, 36, pp. 347–355.

Resch, A., Leicht, S., Saric, M., Pásztor, L., Jakob, A., Götz, F. & Nordheim, A. (2006) Comparative proteome analysis of *Staphylococcus aureus* biofilm and planktonic cells and correlation with transcriptome profiling. *Proteomics*, 6, pp. 1867–1877.

Resch, A., Rosenstein, R., Nerz, C., Go, F. & Götz, F. (2005) Differential gene expression profiling of *Staphylococcus aureus* cultivated under biofilm and planktonic conditions. *Applied and Environmental Microbiology*, 71, pp. 2663–2676.

Rich, J.O., Leathers, T.D., Nunnally, M.S. & Bischoff, K.M. (2011) Rapid evaluation of the antibiotic susceptibility of fuel ethanol contaminant biofilms. *Bioresource Technology*, 102, pp. 1124–1130.

Richards, J.J. & Melander, C. (2009) Controlling bacterial biofilms. *ChemBioChem*, 10, pp. 2287–2294.

Rogers, J. V., Parkinson, C. V., Choi, Y.W., Speshock, J.L. & Hussain, S.M. (2008) A preliminary assessment of silver nanoparticle inhibition of monkeypox virus plaque formation. *Nanoscale Research Letters*, 3, pp. 129–133.

Rogers, S.A., Huigens, R.W., Cavanagh, J. & Melander, C. (2010) Synergistic effects between conventional antibiotics and 2-aminoimidazole-derived antibiofilm agents. *Antimicrobial Agents and Chemotherapy*, 54, pp. 2112–2118.

Rohde, H., Burandt, E.C., Siemssen, N., Frommelt, L., Burdelski, C., Wurster, S., Scherpe, S., Davies, A.P., Harris, L.G., Horstkotte, M.A., Knobloch, J.K.M.M., Ragunath, C., Kaplan, J.B. & Mack, D. (2007) Polysaccharide intercellular adhesin or protein factors in biofilm accumulation of *Staphylococcus epidermidis* and *Staphylococcus aureus* isolated from prosthetic hip and knee joint infections. *Biomaterials*, 28, pp. 1711–1720.

Rohde, H., Frankenberger, S., Zähringer, U. & Mack, D. (2010) Structure, function and contribution of polysaccharide intercellular adhesin (PIA) to *Staphylococcus epidermidis* biofilm formation and pathogenesis of biomaterial-associated infections. *European Journal of Cell Biology*, 89, pp. 103–111.

Rollet, C., Gal, L. & Guzzo, J. (2009) Biofilm-detached cells, a transition from a sessile to a planktonic phenotype: a comparative study of adhesion and physiological characteristics in *Pseudomonas aeruginosa*. *FEMS Microbiology Letters*, 290, pp. 135–142.

Rump, L. V, Asamoah, B. & Gonzalez-Escalona, N. (2010) Comparison of commercial RNA extraction kits for preparation of DNA-free total RNA from Salmonella cells. *BMC Research Notes*, 3, pp. 211.

Rupp, M.E., Fitzgerald, T., Marion, N., Helget, V., Puumala, S., Anderson, J.R. & Fey, P.D. (2004) Effect of silver-coated urinary catheters: Efficacy, cost-effectiveness, and antimicrobial resistance. *American Journal of Infection Control*, 32, pp. 445–450.

Rutala, W.A. & Weber, D.J. (2011) Are room decontamination units needed to prevent transmission of environmental pathogens? *Infection Control and Hospital Epidemiology*, 32, pp. 743–747.

Rutala, W.A. & Weber, D.J. (2016) Monitoring and improving the effectiveness of surface cleaning and disinfection. *American Journal of Infection Control*, 44, pp. e69–e76.

Rutala, W.A. & Weber, D.J. (2001) New disinfection and sterilization methods. *Emerging Infectious Diseases*, 7, pp. 348–353.

Rutala, W.A. & Weber, D.J. (2014) Selection of the ideal disinfectant. *Infection Control and Hospital Epidemiology*, 35, pp. 855–865.

Rutherford, S.T. & Bassler, B.L. (2012) Bacterial quorum sensing: its role in virulence and possibilities for its control. *Cold Spring Harbor Perspectives in Medicine*, 2, pp. a012427.

SACAR (2007) Appendix 2 Specialist advisory committee on antimicrobial resistance (SACAR) antimicrobial framework. *Journal of Antimicrobial Chemotherapy*, 60, pp. i87–i90.

Sadeghi, B., Garmaroudi, F.S., Hashemi, M., Nezhad, H.R., Nasrollahi, A., Ardalan, S. & Ardalan, S. (2012) Comparison of the anti-bacterial activity on the nanosilver shapes: Nanoparticles, nanorods and nanoplates. *Advanced Powder Technology*, 23, pp. 22–26.

El Saeed, A.M., El-Fattah, M.A. & Azzam, A.M. (2015) Synthesis of ZnO nanoparticles and studying its influence on the antimicrobial, anticorrosion and mechanical behavior of polyurethane composite for surface coating. *Dyes and Pigments*, 121, pp. 282–289.

Sakoulas, G., Moellering, R.C. & Eliopoulos, G.M. (2006) Adaptation of methicillin-resistant *Staphylococcus aureus* in the face of vancomycin therapy. *Clinical Infectious Diseases*, 1, pp. S40–S50.

Sakuragi, Y. & Kolter, R. (2007) Quorum-sensing regulation of the biofilm matrix genes (pel) of *Pseudomonas aeruginosa*. *Journal of Bacteriology*, 189, pp. 5383–5386.

Saldaña, Z., Xicohtencatl-Cortes, J., Avelino, F., Phillips, A.D., Kaper, J.B., Puente, J.L. & Girón, J.A. (2009) Synergistic role of curli and cellulose in cell adherence and biofilm formation of attaching and effacing *Escherichia coli* and identification of Fis as a negative regulator of curli. *Environmental Microbiology*, 11, pp. 992–1006.

Samberg, M.E., Orndorff, P.E. & Monteiro-Riviere, N.A. (2011) Antibacterial efficacy of silver nanoparticles of different sizes, surface conditions and synthesis methods. *Nanotoxicology*,

5, pp. 244–253.

Samuel, U. & Guggenbichler, J.P. (2004) Prevention of catheter-related infections: The potential of a new nano-silver impregnated catheter. *International Journal of Antimicrobial Agents*, 23, pp. S75–S78.

Sandberg, M., Määttänen, A., Peltonen, J., Vuorela, P.M. & Fallarero, A. (2008) Automating a 96-well microtitre plate model for *Staphylococcus aureus* biofilms: an approach to screening of natural antimicrobial compounds. *International journal of antimicrobial agents*, 32, pp. 233–240.

Santiago-Vázquez, L.Z., Ranzer, L.K. & Kerr, R.G. (2006) Comparison of two total RNA extraction protocols using the marine gorgonian coral *Pseudopterogorgia elisabethae* and its symbiont *Symbiodinium* sp. *Electronic Journal of Biotechnology*, 9, pp. 598–603.

Dos Santos, C.A., Seckler, M.M., Ingle, A.P., Gupta, I., Galdiero, S., Galdiero, M., Gade, A. & Rai, M. (2014) Silver nanoparticles: Therapeutical uses, toxicity, and safety issues. *Journal of Pharmaceutical Sciences*, 103, pp. 1931–1944.

Saraf, R. (2013) Cost effective and monodispersed zinc oxide nanoparticles synthesis and their characterization. *International Journal of Advances in Applied Sciences*, 2, pp. 85–88.

Sarkar, A., Raji, A., Garaween, G., Soge, O., Rey-Ladino, J., Al-Kattan, W., Shibl, A. & Senok, A. (2016) Antimicrobial resistance and virulence markers in methicillin sensitive *Staphylococcus aureus* isolates associated with nasal colonization. *Microbial Pathogenesis*, 93, pp. 8–12.

Sauer, K. (2003) The genomics and proteomics of biofilm formation. *Genome Biology*, 4, pp. 219.

Sauer, K., Camper, A.K., Ehrlich, G.D., Costerton, J.W. & Davies, D.G. (2002) *Pseudomonas aeruginosa* displays multiple phenotypes during development as a biofilm. *Journal of Bacteriology*, 184, pp. 1140–1154.

Sauer, K., Cullen, M.C., Rickard, A.H., Zeef, L.A.H., Davies, D.G. & Gilbert, P. (2004) Characterization of nutrient-induced dispersion in *Pseudomonas aeruginosa* PAO1 biofilm. *Journal of Bacteriology*, 186, pp. 7312–7326.

Sawai, J. (2003) Quantitative evaluation of antibacterial activities of metallic oxide powders (ZnO, MgO and CaO) by conductimetric assay. *Journal of Microbiological Methods*, 54, pp. 177–182.

Schleheck, D., Barraud, N., Klebensberger, J., Webb, J.S., McDougald, D., Rice, S.A. & Kjelleberg, S. (2009) *Pseudomonas aeruginosa* PAO1 preferentially grows as aggregates in liquid batch cultures and disperses upon starvation. *PLoS one*, 4, pp. e5513.

Schwering, M., Song, J., Louie, M., Turner, R.J. & Ceri, H. (2013) Multi-species biofilms defined from drinking water microorganisms provide increased protection against chlorine disinfection. *Biofouling*, 29, pp. 917–928.

Seil, J.T. & Webster, T.J. (2012) Antimicrobial applications of nanotechnology: methods and literature. *International Journal of Nanomedicine*, 7, pp. 2767–2781.

Seo, Y.S., Lee, D.Y., Rayamahji, N., Kang, M.L. & Yoo, H.S. (2008) Biofilm-forming associated genotypic and phenotypic characteristics of *Staphylococcus* spp. isolated from animals and air. *Research in Veterinary Science*, 85, pp. 433–438.

Shah, S.N., Ali, S.I., Ali, S.R., Naeem, M., Bibi, Y., Ali, S.R., Raza, S.M., Khan, Y. & Sherwani, S.K. (2016) Synthesis and characterization of zinc oxide nanoparticles for antibacterial

applications. *Journal of Basic and Applied Sciences*, 12, pp. 205–210.

Shalumon, K.T., Anulekha, K.H., Nair, S. V, Nair, S. V, Chennazhi, K.P. & Jayakumar, R. (2011) Sodium alginate/poly(vinyl alcohol)/nano ZnO composite nanofibers for antibacterial wound dressings. *International Journal of Biological Macromolecules*, 49, pp. 247–254.

Sharma, B.K., Saha, A., Rahaman, L., Bhattacharjee, S. & Tribedi, P. (2015) Silver inhibits the biofilm formation of *Pseudomonas aeruginosa*. *Advances in Microbiology*, 05, pp. 677–685.

Sharma, V., Anderson, D. & Dhawan, A. (2012) Zinc oxide nanoparticles induce oxidative DNA damage and ROS-triggered mitochondria mediated apoptosis in human liver cells (HepG2). *Apoptosis*, 17, pp. 852–870.

Sheldon, A.T. (2005) Antiseptic 'resistance': real or perceived threat? *Clinical Infectious Diseases*, 40, pp. 1650–1656.

Shen, Y., Stojicic, S. & Haapasalo, M. (2011) Antimicrobial efficacy of chlorhexidine against bacteria in biofilms at different stages of development. *Journal of Endodontics*, 37, pp. 657–661.

Shin, S.H., Ye, M.K., Kim, H.S. & Kang, H.S. (2007) The effects of nano-silver on the proliferation and cytokine expression by peripheral blood mononuclear cells. *International Immunopharmacology*, 7, pp. 1813–1818.

Silhavy, T.J., Kahne, D. & Walker, S. (2010) The bacterial cell envelope. *Cold Spring Harbor Perspectives in Biology*, 2, pp. a000414.

Silva, S., Negri, M., Henriques, M., Oliveira, R., Williams, D. & Azeredo, J. (2010) Silicone colonization by non-*Candida albicans* Candida species in the presence of urine. *Journal of Medical Microbiology*, 59, pp. 747–754.

Simões, M., Simões, L.C., Cleto, S., Machado, I., Pereira, M.O. & Vieira, M.J. (2007) Antimicrobial mechanisms of ortho-phthalaldehyde action. *Journal of Basic Microbiology*, 47, pp. 230–242.

Sinde, E. & Carballo, J. (2000) Attachment of *Salmonella* spp. and *Listeria monocytogenes* to stainless steel, rubber and polytetrafluorethylene: the influence of free energy and the effect of commercial sanitizers. *Food Microbiology*, 17, pp. 439–447.

Singh, M., Sharma, R., Gupta, P.K., Rana, J.K., Sharma, M. & Taneja, N. (2012) Comparative efficacy evaluation of disinfectants routinely used in hospital practice: India. *Indian Journal of Critical Care Medicine*, 16, pp. 123–129.

Sirelkhatim, A., Mahmud, S., Seeni, A., Kaus, N.H.M., Ann, L.C., Bakhori, S.K.M., Hasan, H. & Mohamad, D. (2015) Review on Zinc Oxide Nanoparticles: Antibacterial Activity and Toxicity Mechanism. *Nano Micro Letters*, 7, pp. 219–242.

Skinner-Nemec, K.A., Nichols, N.N. & Leathers, T.D. (2007) Biofilm formation by bacterial contaminants of fuel ethanol production. *Biotechnology Letters*, 29, pp. 379–383.

Skyberg, J.A., Siek, K.E., Doetkott, C. & Nolan, L.K. (2007) Biofilm formation by avian *Escherichia coli* in relation to media, source and phylogeny. *Journal of Applied Microbiology*, 102, pp. 548–554.

Smith, K. & Hunter, I.S. (2008) Efficacy of common hospital biocides with biofilms of multi-drug resistant clinical isolates. *Journal of Medical Microbiology*, 57, pp. 966–973.

Sondi, I. & Salopek-Sondi, B. (2004) Silver nanoparticles as antimicrobial agent: A case study on *E. coli* as a model for Gram-negative bacteria. *Journal of Colloid and Interface Science*, 275, pp. 177–182.

Song, H.Y., Ko, K.K., Oh, I.H. & Lee, B.T. (2006) Fabrication of silver nanoparticles and their antimicrobial mechanisms. *European Cells & Materials*, 11, pp. 58.

Sotiriou, G.A. & Pratsinis, S.E. (2010) Antibacterial activity of nanosilver ions and particles. *Environmental Science & Technology*, 44, pp. 5649–5654.

Souli, M., Galani, I., Plachouras, D., Panagea, T., Armaganidis, A., Petrikkos, G. & Giamarellou, H. (2013) Antimicrobial activity of copper surfaces against carbapenemase-producing contemporary Gram-negative clinical isolates. *The Journal of Antimicrobial Chemotherapy*, 68, pp. 852–857.

Spoering, A. & Lewis, K. (2001) Biofilms and planktonic Cells of *Pseudomonas aeruginosa* have similar resistance to killing by antimicrobials. *Journal of Bacteriology*, 183, pp. 6746–6751.

Steinberg, N. & Kolodkin-Gal, I. (2015) The matrix reloaded: Probing the extracellular matrix synchronizes bacterial communities. *Journal of Bacteriology*, 197, pp. 02516–14.

Stepanović, S., Djukić, V., Djordjević, V. & Djukić, S. (2003) Influence of the incubation atmosphere on the production of biofilm by staphylococci. *Clinical Microbiology and Infection*, 9, pp. 955–958.

Stepanović, S., Vuković, D., Dakić, I., Savić, B. & Švabić-Vlahović, M. (2000) A modified microtiter-plate test for quantification of staphylococcal biofilm formation. *Journal of Microbiological Methods*, 40, pp. 175–179.

Stewart, P.S.S., Rayner, J., Roe, F. & Rees, W.M.M. (2001) Biofilm penetration and disinfection efficacy of alkaline hypochlorite and chlorosulfamates. *Journal of Applied Microbiology*, 91, pp. 525–532.

Stiefel, U., Cadnum, J.L., Eckstein, B.C., Guerrero, D.M., Tima, M.A. & Donskey, C.J. (2011) Contamination of hands with methicillin-resistant *Staphylococcus aureus* after contact with environmental surfaces and after contact with the skin of colonized patients. *Infection Control and Hospital Epidemiology*, 32, pp. 185–187.

Stoimenov, P.K., Klinger, R.L., Marchin, G.L. & Klabunde, K.J. (2002) Metal oxide nanoparticles as bactericidal agents. *Langmuir*, 18, pp. 6679–6686.

Stoodley, P., Cargo, R., Rupp, C.J., Wilson, S. & Klapper, I. (2002a) Biofilm material properties as related to shear-induced deformation and detachment phenomena. *Journal of Industrial Microbiology and Biotechnology*, 29, pp. 361–367.

Stoodley, P., Sauer, K., Davies, D.G. & Costerton, J.W. (2002b) Biofilms as complex differentiated communities. *Annual Review of Microbiology*, 56, pp. 187–209.

Stranak, V., Wulff, H., Rebl, H., Zietz, C., Arndt, K., Bogdanowicz, R., Nebe, B., Bader, R., Podbielski, A., Hubicka, Z. & Hippler, R. (2011) Deposition of thin titanium–copper films with antimicrobial effect by advanced magnetron sputtering methods. *Materials Science and Engineering: C*, 31, pp. 1512–1519.

Subramanian, B., Anu Priya, K., Thanka Rajan, S., Dhandapani, P. & Jayachandran, M. (2014) Antimicrobial activity of sputtered nanocrystalline CuO impregnated fabrics. *Materials Letters*, 128, pp. 1–4.

Sueke, H., Kaye, S.B., Neal, T., Hall, A., Tuft, S. & Parry, C.M. (2010) An *in vitro* investigation

of synergy or antagonism between antimicrobial combinations against isolates from bacterial keratitis. *Investigative Ophthalmology & Visual Science*, 51, pp. 4151–4155.

Sun, F., Qu, F., Ling, Y., Mao, P., Xia, P., Chen, H. & Zhou, D. (2013) Biofilm-associated infections: antibiotic resistance and novel therapeutic strategies. *Future Microbiology*, 8, pp. 877–886.

Sung, J.H., Ji, J.H., Park, J.D., Yoon, J.U., Kim, D.S., Jeon, K.S., Song, M.Y., Jeong, J., Han, B.S., Han, J.H., Chung, Y.H., Chang, H.K., Lee, J.H., Cho, M.H., Kelman, B.J. & Yu, I.J. (2009) Subchronic inhalation toxicity of silver nanoparticles. *Toxicological Sciences*, 108, pp. 452–461.

Sung, K., Khan, S.A., Nawaz, M.S. & Khan, A.A. (2003) A simple and efficient Triton X-100 boiling and chloroform extraction method of RNA isolation from Gram-positive and Gram-negative bacteria. *FEMS Microbiology Letters*, 229, pp. 97–101.

Sungkaworn, T., Triampo, W., Nalakarn, P., Triampo, D., Tang, I.M. & Lenbury, Y. (2007) The effects of TiO_2 nanoparticles on tumor cell colonies: fractal dimension and morphological properties. *International Journal of Biological and Life Sciences*, 2, pp. 67–74.

Szczuka, E., Urbańska, K., Pietryka, M. & Kaznowski, A. (2013) Biofilm density and detection of biofilm-producing genes in methicillin-resistant *Staphylococcus aureus* strains. *Folia Microbiologica*, 58, pp. 47–52.

Szunyogová, E., Mudroňová, D., Györyová, K., Nemcová, R., Kovářová, J. & Piknová-Findoráková, L. (2007) The physicochemical and biological properties of zinc(II) complexes. *Journal of Thermal Analysis and Calorimetry*, 88, pp. 355–361.

Tabrez Khan, S., Ahamed, M., Al-Khedhairy, A. & Musarrat, J. (2013) Biocidal effect of copper and zinc oxide nanoparticles on human oral microbiome and biofilm formation. *Materials Letters*, 97, pp. 67–70.

Tajeddin, E., Rashidan, M., Razaghi, M., Javadi, S.S.S., Sherafat, S.J., Alebouyeh, M., Sarbazi, M.R., Mansouri, N. & Zali, M.R. (2016) The role of the intensive care unit environment and health-care workers in the transmission of bacteria associated with hospital acquired infections. *Journal of Infection and Public Health*, 9, pp. 13–23.

Talari, M.K., Abdul Majeed, A.B., Tripathi, D.K. & Tripathy, M. (2012) Synthesis, characterization and antimicrobial investigation of mechanochemically processed silver doped ZnO nanoparticles. *Chemical & Pharmaceutical Bulletin*, 60, pp. 818–824.

Taylor, P.L., Omotoso, O., Wiskel, J.B., Mitlin, D. & Burrell, R.E. (2005) Impact of heat on nanocrystalline silver dressings: Part II: Physical properties. *Biomaterials*, 26, pp. 7230–7240.

Teitzel, G.M. & Parsek, M.R. (2003) Heavy metal resistance of biofilm and planktonic *Pseudomonas aeruginosa*. *Applied and Environmental Microbiology*, 69, pp. 2313–2320.

Tenover, F.C., Gorwitz, R.J. & Fischetti, V.A. (2006) Gram-positive pathogens. *ASM Press*, 119, pp. S3–S10.

Thuptimdang, P., Limpiyakorn, T., McEvoy, J., Prüß, B.M. & Khan, E. (2015) Effect of silver nanoparticles on Pseudomonas putida biofilms at different stages of maturity. *Journal of Hazardous Materials*, 290, pp. 127–133.

Tiller, J.C., Liao, C.J., Lewis, K. & Klibanov, a M. (2001) Designing surfaces that kill bacteria on contact. *Proceedings of the National Academy of Sciences of the United States of America*, 98, pp. 5981–5985.

Tong, J. & McIntosh, T.J. (2004) Structure of supported bilayers composed of lipopolysaccharides and bacterial phospholipids: raft formation and implications for bacterial resistance. *Biophysical Journal*, 86, pp. 3759–3771.

Toole, G.O., Kaplan, H. & Kolter, R. (2000) Biofilm Formation as microbial development. *Annual Review of Microbiology*, 50, pp. 49–79.

Toté, K., Berghe, D. Vanden, Maes, L. & Cos, P. (2008) A new colorimetric microtitre model for the detection of *Staphylococcus aureus* biofilms. *Letters in Applied Microbiology*, 46, pp. 249–254.

Toté, K., Horemans, T., Vanden Berghe, D., Maes, L. & Cos, P. (2010) Inhibitory effect of biocides on the viable masses and matrices of *Staphylococcus aureus* and *Pseudomonas aeruginosa* biofilms. *Applied and Environmental Microbiology*, 76, pp. 3135–3142.

Trautmann, M., Bauer, C., Schumann, C., Hahn, P., Höher, M., Haller, M. & Lepper, P.M. (2006) Common RAPD pattern of *Pseudomonas aeruginosa* from patients and tap water in a medical intensive care unit. *International Journal of Hygiene and Environmental Health*, 209, pp. 325–331.

Trautmann, M., Halder, S., Lepper, P.M. & Exner, M. (2009) Reservoirs of *Pseudomonas aeruginosa* in the intensive care unit. The role of tap water as a source of infection. *Bundesgesundheitsblatt, Gesundheitsforschung, Gesundheitsschutz*, 52, pp. 339–344.

Trautmann, M., Lepper, P.M. & Haller, M. (2005) Ecology of *Pseudomonas aeruginosa* in the intensive care unit and the evolving role of water outlets as a reservoir of the organism. *American Journal of Infection Controll*, 33, pp. S41–S49.

Tremblay, Y.D.N., Caron, V., Blondeau, A., Messier, S. & Jacques, M. (2014) Biofilm formation by coagulase-negative staphylococci: impact on the efficacy of antimicrobials and disinfectants commonly used on dairy farms. *Veterinary Microbiology*, 172, pp. 511–518.

Truong, V.K., Lapovok, R., Estrin, Y.S., Rundell, S., Wang, J.Y., Fluke, C.J., Crawford, R.J. & Ivanova, E.P. (2010) The influence of nano-scale surface roughness on bacterial adhesion to ultrafine-grained titanium. *Biomaterials*, 31, pp. 3674–3683.

Truong, V.K., Rundell, S., Lapovok, R., Estrin, Y., Wang, J.Y., Berndt, C.C., Barnes, D.G., Fluke, C.J., Crawford, R.J. & Ivanova, E.P. (2009) Effect of ultrafine-grained titanium surfaces on adhesion of bacteria. *Applied Microbiology and Biotechnology*, 83, pp. 925–937.

Ulkür, E., Oncul, O., Karagoz, H., Yeniz, E. & Celiköz, B. (2005) Comparison of silver-coated dressing (Acticoat™), chlorhexidine acetate 0.5% (Bactigrass®), and fusidic acid 2% (Fucidin®) for topical antibacterial effect in methicillin-resistant Staphylococci-contaminated, full-skin thickness rat burn wounds. *Burns*, 31, pp. 874–877.

Umar, A., Rahman, M.M., Al-Hajry, A. & Hahn, Y.-B. (2009) Enzymatic glucose biosensor based on flower-shaped copper oxide nanostructures composed of thin nanosheets. *Electrochemistry Communications*, 11, pp. 278–281.

Umscheid, C.A., Agarwal, R.K. & Brennan, P.J. (2010) Updating the guideline development methodology of the Healthcare Infection Control Practices Advisory Committee (HICPAC). *American Journal of Infection Control*, 38, pp. 264–273.

Uppuluri, P., Dinakaran, H., Thomas, D.P., Chaturvedi, A.K. & Lopez-Ribot, J.L. (2009) Characteristics of *Candida albicans* biofilms grown in a synthetic urine medium. *Journal of Clinical Microbiology*, 47, pp. 4078–4083.

Usman, M.S., El Zowalaty, M.E., Shameli, K., Zainuddin, N., Salama, M. & Ibrahim, N.A. (2013)

Synthesis, characterization, and antimicrobial properties of copper nanoparticles. *International Journal of Nanomedicine*, 8, pp. 4467–4479.

Vadillo-Rodríguez, V., Busscher, H.J., Norde, W., De Vries, J. & Van Der Mei, H.C. (2004) Atomic force microscopic corroboration of bond aging for adhesion of *Streptococcus thermophilus* to solid substrata. *Journal of Colloid and Interface Science*, 278, pp. 251–254.

Valiev, R.Z., Semenova, I.P., Latysh, V. V., Rack, H., Lowe, T.C., Petruzelka, J., Dluhos, L., Hrusak, D. & Sochova, J. (2008) Nanostructured titanium for biomedical applications. *Advanced Engineering Materials*, 10, pp. B15–B17.

Vandecasteele, S.J., Peetermans, W.E., Merckx, R.., Rijnders, B.J.A. & Van Eldere, J. (2003) Reliability of the *ica*, *aap* and *atlE* genes in the discrimination between invasive, colonizing and contaminant *Staphylococcus epidermidis* isolates in the diagnosis of catheter-related infections. *Clinical Microbiology and Infection*, 9, pp. 114–119.

Vazquez, V., Liang, X., Horndahl, J.K., Ganesh, V.K., Smeds, E., Foster, T.J. & Hook, M. (2011) Fibronigen is a ligand for the S. aureus MSCRAMM Bbp (Bone sialoprotein-binding protein). *The Journal of Biological Chemistry*, 286, pp. 29797–29805.

Velázquez-Velázquez, J.L., Santos-Flores, A., Araujo-Meléndez, J., Sánchez-Sánchez, R., Velasquillo, C., González, C., Martínez-Castañon, G. & Martinez-Gutierrez, F. (2015) Anti-biofilm and cytotoxicity activity of impregnated dressings with silver nanoparticles. *Materials Science & Engineering: C*, 49, pp. 604–611.

Vickery, K., Deva, A., Jacombs, A., Allan, J., Valente, P. & Gosbell, I.B. (2012) Presence of biofilm containing viable multiresistant organisms despite terminal cleaning on clinical surfaces in an intensive care unit. *Journal of Hospital Infection*, 80, pp. 52–55.

Vickery, K., Pajkos, A. & Cossart, Y. (2004) Removal of biofilm from endoscopes: Evaluation of detergent efficiency. *American Journal of Infection Control*, 32, pp. 170–176.

Vidic, J., Stankic, S., Haque, F., Ciric, D., Le Goffic, R., Vidy, A., Jupille, J. & Delmas, B. (2013) Selective antibacterial effects of mixed ZnMgO nanoparticles. *Journal of Nanoparticle Research*, 15, pp. 1595.

Wagenvoort, J.H.T., Sluijsmans, W. & Penders, R.J.R. (2000) Better environmental survival of outbreak vs. sporadic MRSA isolates. *Journal of Hospital Infection*, 45, pp. 231–234.

Walkenhorst, W.F., Sundrud, J.N. & Laviolette, J.M. (2014) Additivity and synergy between an antimicrobial peptide and inhibitory ions. *Biochimica et Biophysica Acta*, 1838, pp. 2234–2242.

Walker, J. & Moore, G. (2014) *Pseudomonas aeruginosa* in hospital water systems: Biofilms, guidelines, and practicalities. *Journal of Hospital Infection*, 89, pp. 324–327.

Walker, J.T.T., Jhutty, A., Parks, S., Willis, C., Copley, V., Turton, J.F.F., Hoffman, P.N.N. & Bennett, A.M.M. (2013) Investigation of healthcare-acquired infections associated with *Pseudomonas aeruginosa* biofilms in taps in neonatal units in Northern Ireland. *Journal of Hospital Infection*, 86, pp. 16–23.

Wand, M.E., Bock, L.J., Turton, J.F., Nugent, P.G. & Mark Sutton, J. (2012) *Acinetobacter baumannii* virulence is enhanced in *Galleria mellonella* following biofilm adaptation. *Journal of Medical Microbiology*, 61, pp. 470–477.

Wang, B., Li, B., Liang, Y., Li, J., Gao, L., Chen, L., Duan, K. & Shen, L. (2016a) Pleiotropic effects of temperature-regulated 2-OH-lauroytransferase (PA0011) on *Pseudomonas aeruginosa* antibiotic resistance, virulence and type III secretion system. *Microbial*

pathogenesis, 91, pp. 5–17.

Wang, B., Zhang, Y., Mao, Z., Yu, D. & Gao, C. (2014a) Toxicity of ZnO nanoparticles to macrophages due to cell uptake and intracellular release of zinc ions. *Journal of Nanoscience and Nanotechnology*, 14, pp. 5688–5696.

Wang, D., Gao, Y., Lin, Z., Yao, Z. & Zhang, W. (2014b) The joint effects on *Photobacterium phosphoreum* of metal oxide nanoparticles and their most likely coexisting chemicals in the environment. *Aquatic Toxicology*, 154, pp. 200–206.

Wang, D., Lin, Z., Wang, T., Yao, Z., Qin, M., Zheng, S. & Lu, W. (2016b) Where does the toxicity of metal oxide nanoparticles come from: The nanoparticles, the ions, or a combination of both? *Journal of Hazardous Materials*, 308, pp. 328–334.

Wang, M.C., Tseng, C.C., Wu, A.B., Huang, J.J., Sheu, B.S. & Wu, J.J. (2009) Different roles of host and bacterial factors in *Escherichia coli* extra-intestinal infections. *Clinical Microbiology and Infection*, 15, pp. 372–379.

Weber, D.J. & Rutala, W.A. (2013) Understanding and preventing transmission of healthcare-associated pathogens due to the contaminated hospital environment. *Infection Control and Hospital Epidemiology*, 34, pp. 449–452.

Wessels, S. & Ingmer, H. (2013) Modes of action of three disinfectant active substances: a review. *Regulatory Toxicology and Pharmacology*, 67, pp. 456–467.

Wilks, S.A., Michels, H. & Keevil, C.W. (2005) The survival of *Escherichia coli* O157 on a range of metal surfaces. *International Journal of Food Microbiology*, 105, pp. 445–454.

Williams, D.L. & Bloebaum, R.D. (2010) Observing the biofilm matrix of *Staphylococcus epidermidis* ATCC 35984 grown using the CDC biofilm reactor. *Microscopy and Microanalysis*, 16, pp. 143–152.

Winstanley, C., O'Brien, S. & Brockhurst, M.A. (2016) *Pseudomonas aeruginosa* evolutionary adaptation and diversification in cystic fibrosis chronic lung infections. *Trends in Microbiology*, 24, pp. 327–337.

Wise, J. (2012) Three babies die in pseudomonas outbreak at Belfast neonatal unit. *British Medical Journal*, 344, pp. e592.

Wojcieszak, D., Kaczmarek, D., Antosiak, A., Mazur, M., Rybak, Z., Rusak, A., Osekowska, M., Poniedzialek, A., Gamian, A. & Szponar, B. (2015) Influence of Cu-Ti thin film surface properties on antimicrobial activity and viability of living cells. *Materials Science & Engineering: C*, 56, pp. 48–56.

Wong, H.S., Townsend, K.M., Fenwick, S.G., Maker, G., Trengove, R.D. & O'Handley, R.M. (2010) Comparative susceptibility of *Salmonella Typhimurium* biofilms of different ages to disinfectants. *Biofouling*, 26, pp. 859–864.

Wood, T.K., Hong, S.H. & Ma, Q. (2011) Engineering biofilm formation and dispersal. *Trends in Biotechnology*, 29, pp. 87–94.

World Health Organisation (2014) *Antimicrobial resistance: global report on surveillance*. Geneva: World Health Organisation

World Health Organization (2002) *Prevention of hospital-acquired infections: A pratical guide.* Geneva: World Health Organisation

Worthington, R.J. & Melander, C. (2013) Combination approaches to combat multidrug-resistant

bacteria. *Trends in Biotechnology*, 31, pp. 177–184.

Wroblewska, M.M., Sawicka-Grzelak, A., Marchel, H., Luczak, M. & Sivan, A. (2008) Biofilm production by clinical strains of *Acinetobacter baumannii* isolated from patients hospitalized in two tertiary care hospitals. *FEMS Immunology and Medical Microbiology*, 53, pp. 140–144.

Wu, H.Q., Wei, X.W., Shao, M.W., Gu, J.S. & Qu, M.Z. (2002) Synthesis of copper oxide nanoparticles using carbon nanotubes as templates. *Chemical Physics Letters*, 364, pp. 152–156.

Wu, X., Held, K., Zheng, C., Staudinger, B.J., Chavez, J.D., Weisbrod, C.R., Eng, J.K., Singh, P.K., Manoil, C. & Bruce, J.E. (2015a) Dynamic proteome response of *Pseudomonas aeruginosa* to tobramycin antibiotic treatment. *Molecular & Cellular Proteomics*, 14, pp. 2126–2137.

Wu, X., Santos, R.R. & Fink-Gremmels, J. (2015b) Cadmium modulates biofilm formation by *Staphylococcus epidermidis*. *International Journal of Environmental Research and Public Health*, 12, pp. 2878–2894.

Wyszogrodzka, G., Marszałek, B., Gil, B. & Dorożyński, P. (2016) Metal-organic frameworks: mechanisms of antibacterial action and potential applications. *Drug Discovery Today*, 21, pp. 1009–1018.

Xia, T., Kovochich, M., Liong, M., Mädler, L., Gilbert, B., Shi, H., Yeh, J.I., Zink, J.I. & Nel, A.E. (2008) Comparison of the mechanism of toxicity of zinc oxide and cerium oxide nanoparticles based on dissolution and oxidative stress properties. *ACS Nano*, 2, pp. 2121–2134.

Xing, M., Shen, F., Liu, L., Chen, Z., Guo, N., Wang, X., Wang, W., Zhang, K., Wu, X., Li, Y., Sun, S. & Yu, L. (2012) Antimicrobial efficacy of the alkaloid harmaline alone and in combination with chlorhexidine digluconate against clinical isolates of *Staphylococcus aureus* grown in planktonic and biofilm cultures. *Letters in Applied Microbiology*, 54, pp. 475–482.

Yamamoto, O. (2001) Influence of particle size on the antibacterial activity of zinc oxide. *International Journal of Inorganic Materials*, 3, pp. 643–646.

Yamamoto, O., Nakakoshi, K., Sasamoto, T., Nakagawa, H. & Miura, K. (2001) Adsorption and growth inhibition of bacteria on carbon materials containing zinc oxide. *Carbon*, 39, pp. 1643–1651.

Yang, L., Hu, Y., Liu, Y., Zhang, J., Ulstrup, J. & Molin, S. (2011a) Distinct roles of extracellular polymeric substances in *Pseudomonas aeruginosa* biofilm development. *Environmental Microbiology*, 13, pp. 1705–1717.

Yang, L., Liu, Y., Wu, H., Hóiby, N., Molin, S. & Song, Z. (2011b) Current understanding of multi-species biofilms. *International Journal of Oral Science*, 3, pp. 74–81.

Yang, L., Mao, J., Zhang, X., Xue, T., Hou, T., Wang, L. & Tu, M. (2006) Preparation and characteristics of Ag/nano-ZnO composite antimicrobial agent. *Nanosciences*, 11, pp. 44–48.

Yang, L., Nilsson, M., Gjermansen, M., Givskov, M. & Tolker-Nielsen, T. (2009a) Pyoverdine and PQS mediated subpopulation interactions involved in *Pseudomonas aeruginosa* biofilm formation. *Molecular Microbiology*, 74, pp. 1380–1392.

Yang, S., Hay, I.D., Cameron, D.R., Speir, M., Cui, B., Su, F., Peleg, A.Y., Lithgow, T., Deighton,

M.A. & Qu, Y. (2015) Antibiotic regimen based on population analysis of residing persister cells eradicates *Staphylococcus epidermidis* biofilms. *Scientific Reports*, 5, pp. 18578.

Yang, S., Wang, C., Chen, L. & Chen, S. (2010) Facile dicyandiamide-mediated fabrication of well-defined CuO hollow microspheres and their catalytic application. *Materials Chemistry and Physics*, 120, pp. 296–301.

Yang, W., Shen, C., Ji, Q., An, H., Wang, J., Liu, Q. & Zhang, Z. (2009b) Food storage material silver nanoparticles interfere with DNA replication fidelity and bind with DNA. *Nanotechnology*, 20, pp. 085102.

Yazdani, R., Oshaghi, M., Havayi, A., Pishva, E., Salehi, R., Sadeghizadeh, M. & Foroohesh, H. (2006) Detection of *icaAD* gene and biofilm formation in *Staphylococcus aureus* isolates from wound infections. *Iranian Journal of Public Health*, 35, pp. 25–28.

Yezli, S. & Otter, J.A. (2012) Does the discovery of biofilms on dry hospital environmental surfaces change the way we think about hospital disinfection? *The Journal of Hospital Infection*, 81, pp. 293–294.

Yıldırım, Ö.A., Unalan, H.E. & Durucan, C. (2013) Highly Efficient Room Temperature Synthesis of Silver-Doped Zinc Oxide (ZnO:Ag) Nanoparticles: Structural, Optical, and Photocatalytic Properties. *Journal of the American Ceramic Society*, 96, pp. 766–773.

Yoon, K.-Y., Hoon Byeon, J., Park, J.-H. & Hwang, J. (2007) Susceptibility constants of *Escherichia coli* and *Bacillus subtilis* to silver and copper nanoparticles. *The Science of the total environment*, 373, pp. 572–575.

Yoshino, Y., Makino, T., Katayama, Y. & Hata, T. (2000) Optimization of zinc oxide thin film for surface acoustic wave filters by radio frequency sputtering. *Vacuum*, 59, pp. 538–545.

You, J., Zhang, Y. & Hu, Z. (2011) Bacteria and bacteriophage inactivation by silver and zinc oxide nanoparticles. *Colloids and Surfaces B: Biointerfaces*, 85, pp. 161–167.

Young, B.C., Golubchik, T., Batty, E.M., Fung, R., Larner-Svensson, H., Votintseva, A.A., Miller, R.R., Godwin, H., Knox, K., Everitt, R.G., Iqbal, Z., Rimmer, A.J., Cule, M., Ip, C.L., Didelot, X., Harding, R.M., Donnelly, P., Peto, T.E., Crook, D.W., Bowden, R. & Wilson, D.J. (2012) Evolutionary dynamics of *Staphylococcus aureus* during progression from carriage to disease. *Proceedings of the National Academy of Sciences*, 109, pp. 4550–4555.

Yu, J.X. & Li, T.H. (2011) Distinct biological effects of different nanoparticles commonly used in cosmetics and medicine coatings. *Cell & Bioscience*, 1, pp. 19.

Yu, T., Cheong, F.-C. & Sow, C.-H. (2004) The manipulation and assembly of CuO nanorods with line optical tweezers. *Nanotechnology*, 15, pp. 1732–1736.

Yuan Gao & Cranston, R. (2008) Recent advances in antimicrobial treatments of textiles. *Textile Research Journal*, 78, pp. 60–72.

Yuan, Z., Li, J., Cui, L., Xu, B., Zhang, H. & Yu, C.P. (2013) Interaction of silver nanoparticles with pure nitrifying bacteria. *Chemosphere*, 90, pp. 1404–1411.

Yuranova, T., Rincon, A.G., Bozzi, A., Parra, S., Pulgarin, C., Albers, P. & Kiwi, J. (2003) Antibacterial textiles prepared by RF-plasma and vacuum-UV mediated deposition of silver. *Journal of Photochemistry and Photobiology A: Chemistry*, 161, pp. 27–34.

Zarpellon, M.N., Gales, A.C., Sasaki, A.L., Selhorst, G.J., Menegucci, T.C., Cardoso, C.L., Garcia, L.B. & Tognim, M.C.B. (2015) Survival of vancomycin-intermediate

Staphylococcus aureus on hospital surfaces. *Journal of Hospital Infection*, 90, pp. 347–350.

Zhang, H. & Chen, G. (2009) Potent antibacterial activities of Ag/TiO_2 nanocomposite powders synthesized by a one-pot sol-gel method. *Environmental Science & Technology*, 43, pp. 2905–2910.

Zhang, L., Ding, Y., Povey, M. & York, D. (2008) ZnO nanofluids-A potential antibacterial agent. *Progress in Natural Science*, 18, pp. 939–944.

Zhang, L., Jiang, Y., Ding, Y., Povey, M. & York, D. (2007) Investigation into the antibacterial behaviour of suspensions of ZnO nanoparticles (ZnO nanofluids). *Journal of Nanoparticle Research*, 9, pp. 479–489.

Zhou, Z., Liu, J. & Chu, L. (2005) Preparation and antibacterial effect of doped tetra-needle like ZnO whiskers. *Materials Science Forum*, 486-487, pp. 77–80.

Zinjarde, S. (2012) Bio-inspired nanomaterials and their applications as antimicrobial agents. *Chronicles of Young Scientists*, 3, pp. 74–81.

Zuniga, E., Melville, P.A., Saidenberg, A.B.S., Laes, M.A., Gonsales, F.F., Salaberry, S.R.S., Gregori, F., Brandão, P.E., Dos Santos, F.G.B., Lincopan, N.E. & Benites, N.R. (2015) Occurrence of genes coding for MSCRAMM and biofilm-associated protein Bap in *Staphylococcus* spp. isolated from bovine subclinical mastitis and relationship with somatic cell counts. *Microbial Pathogenesis*, 89, pp. 1–6.

Appendices

Explore

Case Processing Summary

	Cases					
	Valid		Missing		Total	
	N	Percent	N	Percent	N	Percent
Data	72	100.0%	0	0.0%	72	100.0%

Descriptives

			Statistic	Std. Error
Data	Mean		7.4621	.04887
	95% Confidence Interval for Mean	Lower Bound	7.3646	
		Upper Bound	7.5595	
	5% Trimmed Mean		7.4512	
	Median		7.3850	
	Variance		.172	
	Std. Deviation		.41468	
	Minimum		7.00	
	Maximum		8.17	
	Range		1.17	
	Interquartile Range		.81	
	Skewness		.249	.283
	Kurtosis		-1.667	.559

Tests of Normality

	Kolmogorov-Smirnov[a]			Shapiro-Wilk		
	Statistic	df	Sig.	Statistic	df	Sig.
Data	.261	72	.000	.823	72	.000

a. Lilliefors Significance Correction

Data

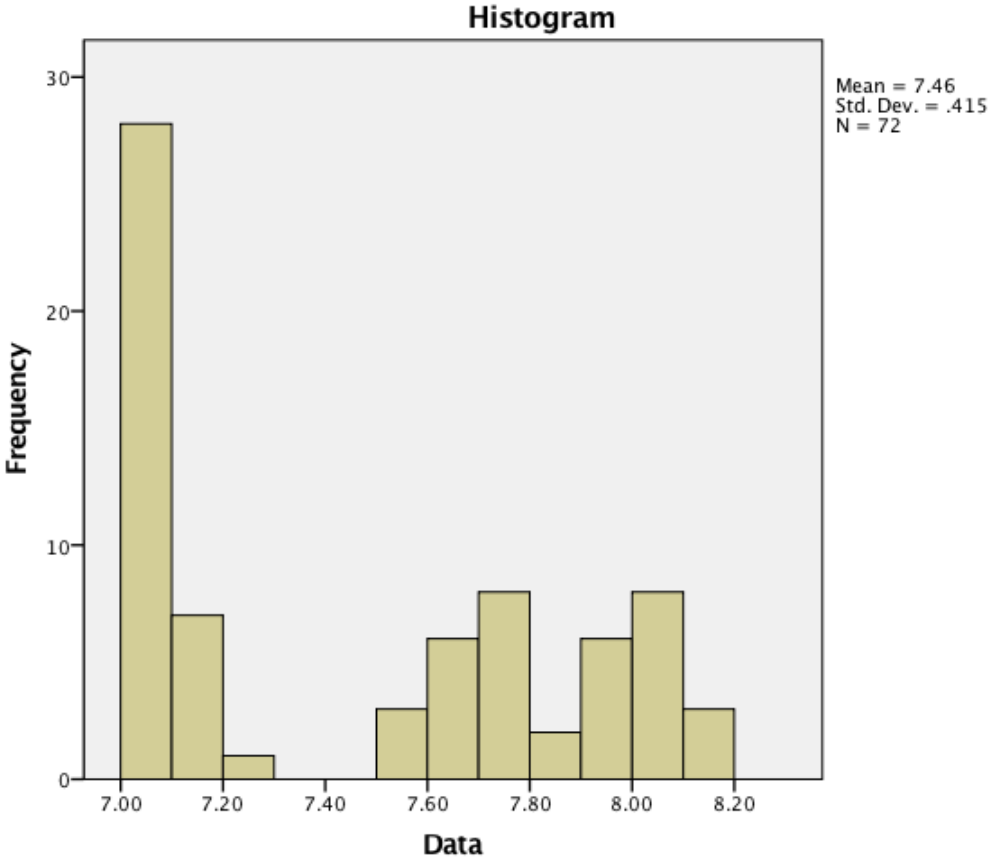

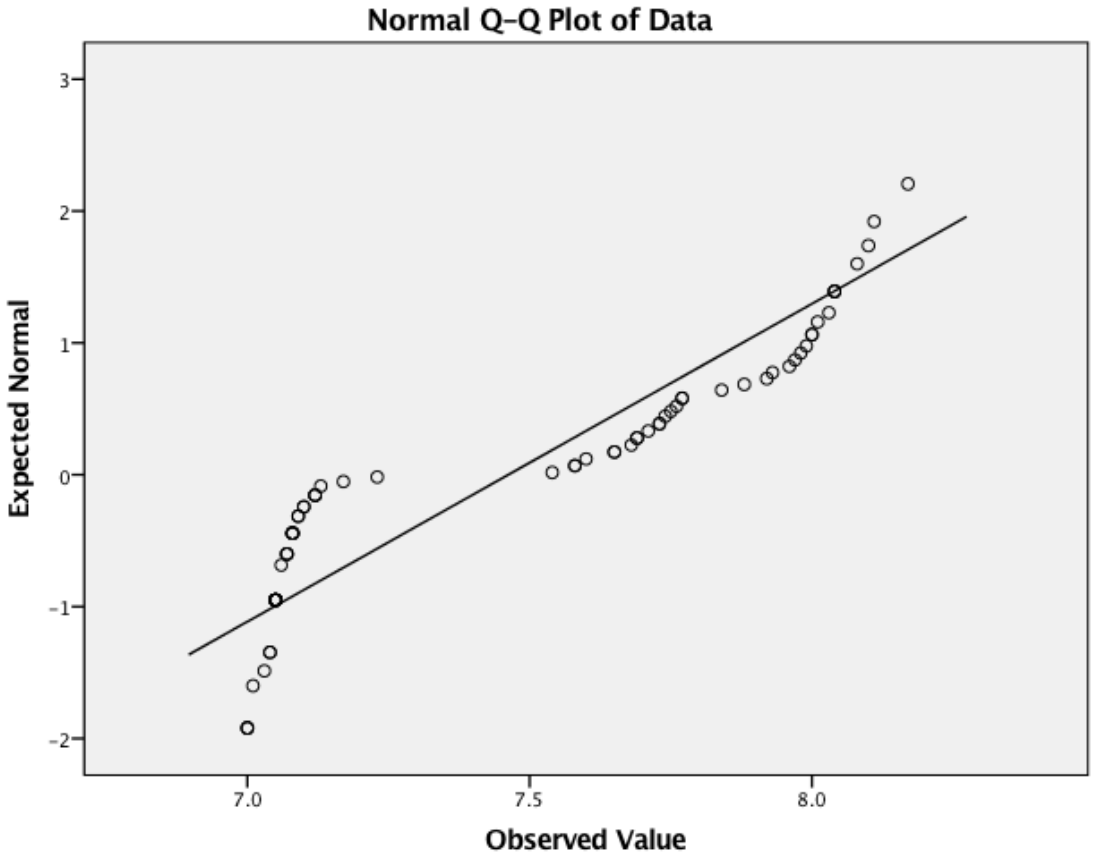
Normal Q-Q Plot of Data
Expected Normal
3
2
1
0
-1
-2
7.0
7.5
8.0
Observed Value

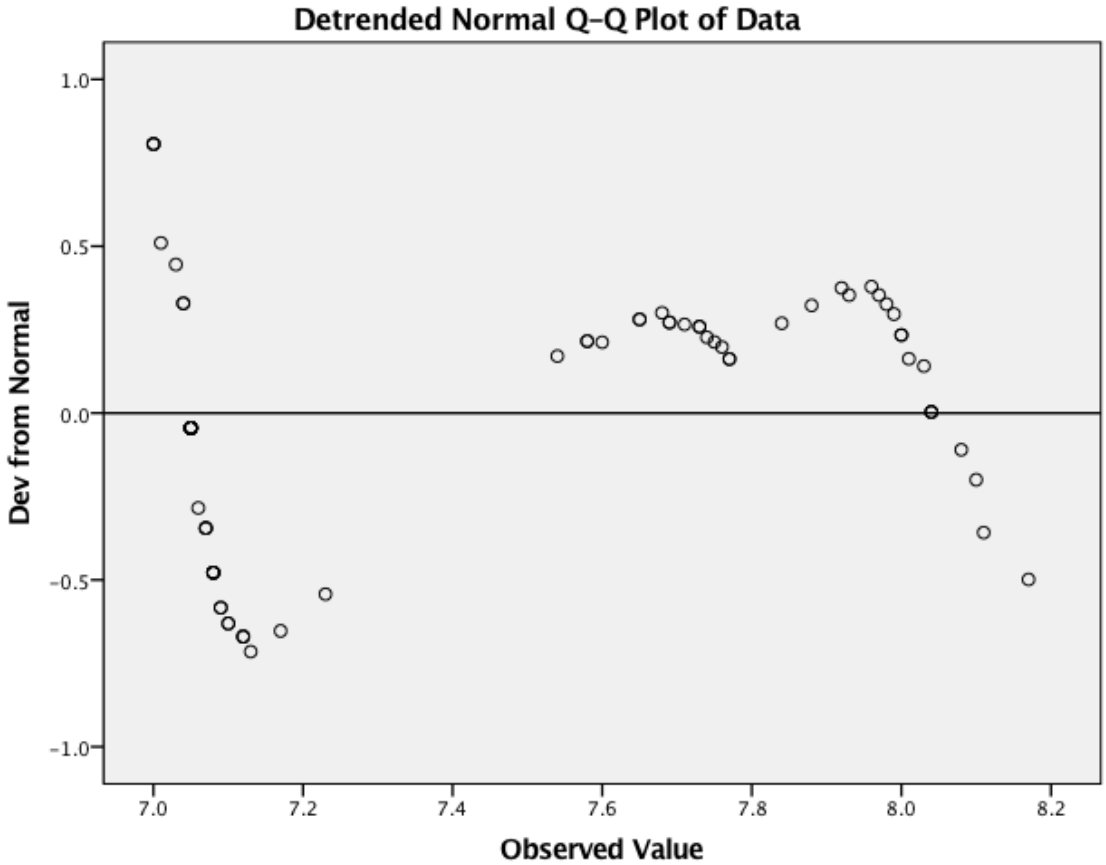
Detrended Normal Q-Q Plot of Data
Dev from Normal
1.0
0.5
0.0
-0.5
-1.0
7.0
7.2
7.4
7.6
7.8
8.0
8.2
Observed Value

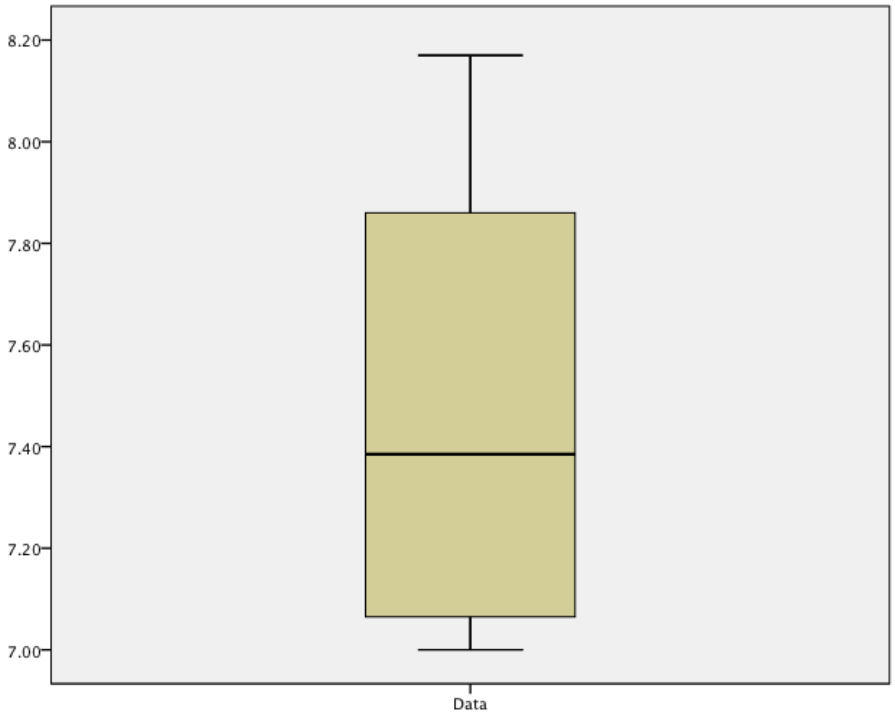

NPar Tests

Mann-Whitney Test

Ranks

	Group	N	Mean Rank	Sum of Ranks
Data	PA Pl	18	18.69	336.50
	PA SS	18	18.31	329.50
	Total	36		

Test Statistics[a]

	Data
Mann-Whitney U	158.500
Wilcoxon W	329.500
Z	-.111
Asymp. Sig. (2-tailed)	.912
Exact Sig. [2*(1-tailed Sig.)]	.913[b]

a. Grouping Variable: Group

b. Not corrected for ties.

NPar Tests

Mann-Whitney Test

Ranks

	Group	N	Mean Rank	Sum of Ranks
Data	SA Pl	18	21.47	386.50
	SA SS	18	15.53	279.50
	Total	36		

Test Statistics[a]

	Data
Mann-Whitney U	108.500
Wilcoxon W	279.500
Z	-1.715
Asymp. Sig. (2-tailed)	.086
Exact Sig. [2*(1-tailed Sig.)]	.091[b]

a. Grouping Variable: Group

b. Not corrected for ties.

Silicon Wafer Cleaning

The samples were bomb cleaned with 50% H_2O_2 and 50% sulphuric acid. The sample is ultrasonicated for 2 mins in 18 MΩ deionised water. This was repeated 5 times. The sample is then dipped in to buffered hydrofluoric acid (HF) (Fisher Electronic Grade) in a H_2O:HF=10:1 mixture. The sample is ultrasonicated for 2 mins in 18 MΩ deionised water again and this was repeated a further 5 times. The samples were spin dried at 3000 rpm under nitrogen for 30 seconds and left for 15 mins to bake in the air at 100°C.

Publications Associated With Thesis

Publications

SfAM Summer Conference-Edinburgh, 2012: Comparison of reproducibility of a static and a continuous flow method for the formation of *Staphylococcus aureus* and *Pseudomonas aeruginosa* biofilms.

Antibiotic Alternatives for the New Millenium-London, 2014: Comparison of the antibacterial effect of silver and zinc oxide in solution and on coated surfaces.

SfAM Summer Conference-Dublin, 2015: Comparison of the antibacterial effect of silver and zinc oxide in solution and on coated surfaces on biofilms.